EPFL

Thèse n° 10 582

Variability is the rule: Neurophysiology and contextual visual processing in schizophrenia

Présentée le 14 juin 2024

Faculté des sciences de la vie
Laboratoire de psychophysique
Programme doctoral en neurosciences

pour l'obtention du grade de Docteur ès Sciences

par

Dario Alejandro GORDILLO LOPEZ

Acceptée sur proposition du jury

Prof. M. Mathis, présidente du jury
Prof. M. Herzog, directeur de thèse
Prof. N. Langer, rapporteur
Prof. B. Keane, rapporteur
Prof. D. Van De Ville, rapporteur

École polytechnique fédérale de Lausanne

2024

Acknowledgments

I would like to thank my supervisor, Michael Herzog, for his immense support during these almost five years in Lausanne. Thanks to all my jury members, Prof. Mackenzie Mathis, Prof. Dimitri Van De Ville, Prof. Nicolas Langer, and Prof. Brian Keane for their rigorousity and great ideas. To Prof. Carmen Sandi for her valuable evaluation of my yearly progress. Thanks for devoting a part of your time to listening to me saying many things, often too fast.

I would like also to thank every single person that I have met in Lausanne. To every single person I have played football with on the terrains up in Les Marronniers, Bus 1 (or 21, but goes from the other way), arrêt Stade Olympique. To every single person I have played music with in the undergrounds of la Borde, esplanade, or the fitness club. I hope I have shown you my love with more than words, or even solely with words, which often works too. To my football friends, I hope I have shown you my love with assists, and to my music friends, I hope I have shown you my love through my devotedness. To my family for being always present in my mind, and to a person who appeared at the right moment. You all know who you are, and if you read this and you know who that other person is, and this other person has not read this, tell them.

Llámame, y si no contesto, te devuelvo la llamada, o mándame un mensaje. Intento ser un buen amigo, casi nunca estoy en las buenas.

What comes in the next pages, is just a small part of what these years have been.

Résumé

Traditionnellement, les études en recherche sur la schizophrénie s'appuient sur un seul paradigme expérimental. Les résultats montrent généralement une différence significative entre les patients et les groupes de contrôle. Les études ultérieures visent à décrire le mécanisme anormal sous-jacent aux niveaux génétique et neurobiologique. Bien que cette approche ait permis d'énormes avancées dans le domaine, les recherches des vingt dernières années suggèrent qu'elle ne capture peut-être pas entièrement la complexité de la schizophrénie. De nouvelles méthodologies de recherche sont nécessaires pour examiner systématiquement la nature complexe du trouble. Ici, j'ai utilisé l'électroencéphalogramme (EEG) en état de repos et des paradigmes visuels pour explorer la complexité de la neurophysiologie et du traitement visuel contextuel dans la schizophrénie.

Initialement, je démontre que diverses caractéristiques extraites de l'EEG en état de repos, telles que la puissance de la bande bêta ou les mesures de connectivité, présentent de faibles corrélations entre elles, malgré des différences significatives de groupe entre patients et contrôles. Je montre que certaines de ces caractéristiques restent remarquablement stables sur plusieurs années, ce qui indique que l'erreur de mesure ne peut pas expliquer entièrement ces faibles corrélations et que la variabilité pourrait refléter des différences réelles chez les patients. Ces résultats soulèvent des questions cruciales sur la nature et l'interprétation des résultats significatifs en recherche sur la schizophrénie et plaident en faveur de méthodologies de recherche qui examinent systématiquement un large éventail de caractéristiques. De plus, je présente des résultats d'EEG et de comportement suggérant que ce problème s'étend à des domaines au-delà de la recherche sur la schizophrénie. Je propose différents scénarios pour expliquer ces résultats déroutants et suggère des stratégies pour faire face à cette grande variabilité.

De plus, je présente des résultats comportementaux utilisant des expériences de *visual (un)crowding* [(dé)encombrement] pour sonder la vision contextuelle dans la schizophrénie. Dans ces expériences, le traitement d'une cible visuelle est influencé par la présence d'autres objets autour. Je démontre que, dans différentes variantes de ce paradigme, les mêmes patients ont montré à la fois un traitement contextuel intact et déficient par rapport aux

contrôles, soulevant ainsi des questions sur la généralisabilité des résultats obtenus en utilisant un seul paradigme expérimental pour étudier les mécanismes généraux. En outre, je fournis des preuves neurophysiologiques d'altérations dans les processus de codage prédictif dans la schizophrénie, suggérant ainsi une contribution potentielle à des altérations de la vision contextuelle et d'autres aspects complexes de la perception et de la psychopathologie chez les patients.

Mots-clés

Schizophrénie, EEG, état de repos, complexité, vision, traitement contextuel, stabilité, codage prédictif, variabilité

Abstract

Traditionally, studies in schizophrenia research employ a single experimental paradigm. The results typically demonstrate a significant difference between patients and controls. Subsequent studies aim to describe the underlying abnormal mechanism at the genetic and neurobiological levels. While this approach has driven tremendous advancements in the field, research over the past twenty years suggests that it may not entirely capture the complexity of schizophrenia. New research methodologies are needed to systematically investigate the intricate nature of the disorder. Here, I utilized resting-state electroencephalogram (EEG) and visual paradigms to delve into the complexity of neurophysiology and contextual visual processing in schizophrenia.

Initially, I demonstrate that various features extracted from resting-state EEG, such as beta band power or connectivity measures, exhibit weak correlations with each other, despite significant group differences between patients and controls. I show that some of these features remain remarkably stable over several years, indicating that measurement error cannot entirely account for these low correlations and that variability might reflect genuine individual differences. These findings raise critical questions about the nature and interpretation of significant results in schizophrenia research and advocate for research methodologies that systematically examine a large range of features. Furthermore, I present EEG and behavioral results suggesting that this issue extends to fields beyond schizophrenia research. I propose different scenarios to explain these puzzling results and suggest strategies to cope with this vast variability.

Additionally, I present behavioral results using visual (un)crowding experiments to probe contextual vision in schizophrenia. In (un)crowding, the processing of a visual target is influenced by flankers. I demonstrate that in variations of this paradigm, the same patients exhibited intact and deficient contextual processing compared to controls, raising questions about the generalizability of results obtained using a single experimental paradigm to investigate general abnormal mechanisms. Moreover, I provide neurophysiological evidence for alterations in predictive coding processes in schizophrenia, potentially contributing to

alterations in contextual vision and other complex aspects of perception and psychopathology in patients.

Keywords

Schizophrenia, EEG, resting-state, complexity, vision, contextual processing, stability, predictive coding, variability

List of publications

Peer-reviewed publications

- Gordillo, D.*, da Cruz, J. R.*, Chkonia, E., Lin, W.-H., Favrod, O., Brand, A., Figueiredo, P., Roinishvili, M., & Herzog, M. H. (2023). The EEG multiverse of schizophrenia. *Cerebral Cortex*, 33(7), 3816–3826. https://doi.org/10.1093/cercor/bhac309
- Gordillo, D., da Cruz, J. R., Moreno, D., Garobbio, S., & Herzog, M. H. (2023). Do we really measure what we think we are measuring? *iScience*, 26, 106017. https://doi.org/10.1016/j.isci.2023.106017
- Choung, O. H., Gordillo, D., Roinishvili, M., Brand, A., Herzog, M. H., & Chkonia, E. (2022). Intact and deficient contextual processing in schizophrenia patients. *Schizophrenia Research: Cognition*, 30, 100265. https://doi.org/10.1016/j.scog.2022.100265

Preprints

- Alamia, A. *, Gordillo, D. *, Chkonia, E., Roinishvili, M., Cappe, C., & Herzog, M. H. (2023). Oscillatory traveling waves reveal predictive coding abnormalities in schizophrenia. *BioRxiv*, 2023.10.09.561490. https://doi.org/10.1101/2023.10.09.561490

* denotes equal contribution

Table of contents

Chapter 1. Introduction

1.1. The complexity of schizophrenia

The past two decades have seen remarkable progress in understanding the biology of schizophrenia, led by technological advancements and large-scale collaborative efforts. For example, breakthroughs in genetics have allowed scientists to analyze the genomes of thousands of patients, offering insights into candidate biological pathways for the illness (Ripke et al., 2014; Singh et al., 2022; Trubetskoy et al., 2022). Similarly, the aggregation and meta-analysis of neuroimaging data from numerous patient cohorts have facilitated the study of brain alterations with high statistical power (Kelly et al., 2018; Van Erp et al., 2016, 2018). Moreover, the availability of computational tools has led to the development of machine learning and biophysical models, allowing the classification and modeling of neural circuits potentially involved in schizophrenia (Cortes-Briones et al., 2022; Fogelson et al., 2014; Huys et al., 2016; Stephan & Mathys, 2014). These examples represent only a fraction of the strides made in the field.

While these advancements have significantly enhanced our understanding of schizophrenia, they also highlight its complexity. Genetic studies have shown that schizophrenia is a highly polygenic disorder, lacking clear-cut genetic signatures, despite a heritability of close to 80% (Burmeister et al., 2008; Sullivan et al., 2003). Neuroimaging meta-analyses have shown that brain abnormalities in schizophrenia are highly heterogeneous, affecting a broad range of brain structures, and present to a different extent in different patients (Van Erp et al., 2018). For instance, the effect size for cortical thickness differences between patients and controls was d=0.53, corresponding to a discriminability of approximately 60% between groups only. Additionally, patients with schizophrenia exhibit a large spectrum of deficits besides brain and behavioral ones, including those in the immunological (Cullen et al., 2019; Horváth & Mirnics, 2014) or cardiometabolic (So et al., 2019; Strawbridge et al., 2021) systems, among others. These findings raise questions on how the understanding of a particular deficit can shed light on other deficits. Furthermore, given the substantial variability of deficits among patients, it becomes crucial to effectively address this heterogeneity to identify the main aspects of schizophrenia.

1.2. From *deep* to *shallow* rooting in schizophrenia research

Traditionally, studies in schizophrenia research employ a single experimental paradigm. The results often show a clear-cut difference in patients compared to healthy controls. Subsequent studies then delve into the underlying cognitive, neural, and genetic abnormal mechanisms. I refer to this approach as the *deep rooting* approach.

Importantly, examining single deficits can offer insights into abnormal mechanisms, and this may have potential implications for treatment and prevention. For instance, cognitive deficits have a profound impact on the quality of life and social outcomes in patients (Eack & Newhill, 2007; Green et al., 2015). Therefore, as treatments often do not effectively improve such deficits (Howes et al., 2024; Nielsen et al., 2015), a thorough investigation of the underlying mechanisms becomes crucial. Furthermore, analyzing single deficits may aid in identifying endophenotypes, i.e., paradigms targeting genetic risk factors, which can summarize the complex genetic architecture of the disorder through simple tests (Braff et al., 2006; Gottesman & Gould, 2003). There are several examples of those excellent tests (Allen et al., 2009; Chkonia, Roinishvili, Makhatadze, et al., 2010; da Cruz et al., 2020). Hence, the *deep rooting* approach has led to tremendous advancements in the field and holds the potential to offer new insights, but there are limitations. This approach implicitly assumes that the deficit being studied represents a crucial aspect of schizophrenia. However, this assumption may not always hold.

The limitations of the classic approach are highlighted by studies that have examined multiple paradigms in patients. For example, Price and colleagues (2006) analyzed four EEG paradigms in patients with schizophrenia and healthy controls. Although there were significant group differences between patients and controls, correlations between the paradigms were weak. Moreover, combining these paradigms improved the classification accuracy between patients and controls, suggesting that each paradigm captures different aspects of schizophrenia. Similarly, Seidman and colleagues (2015) correlated a battery of 15 paradigms targeting neurophysiological and cognitive functioning in patients. Cognitive paradigms showed high correlations, but neurophysiological measures were largely uncorrelated in patients. This suggests that there might be several underlying factors related to deficits in schizophrenia. Hence, focusing on single deficits may have its limitations. Additionally, Braff and colleagues

(2007) reported weak correlations between two EEG paradigms in patients, despite significant group differences between patients and controls. These findings highlight that results obtained through a single paradigm might be less broadly explanatory than assumed.

To effectively address this heterogeneity, a *shallow rooting* approach might become necessary. In this approach, outputs from a variety of paradigms can be systematically compared and also potentially combined. The aforementioned studies are in line with this approach. This may facilitate the identification and examination of general abnormal mechanisms targeted by different paradigms. Moreover, this approach can aid in the development of multivariate models to enhance classification or prediction, for example, of clinical outcomes. This approach is more in line with the widely acknowledged heterogeneous nature of schizophrenia, which is characterized by a collection of symptoms and impairments. Therefore, describing schizophrenia through a collection of paradigms and test outcomes might provide a more representative view of the illness.

1.3. Schizophrenia and contextual processing

Patients with schizophrenia exhibit a variety of psychotic symptoms as well as cognitive and perceptual deficits (Barch & Ceaser, 2012; Tandon et al., 2009). This diverse psychopathology relies on alterations in a broad range of brain structures and functions, which is in line with genetic and neuroimaging studies (Kelly et al., 2018; Trubetskoy et al., 2022; Van Erp et al., 2018). Being schizophrenia a plausibly "whole-brain" illness, assessments of the visual system are of prime interest in schizophrenia research because approximately one-third of the cortex is dedicated to visual processing, and vision entails a wide range of feedback and feedforward computations (Rolls et al., 2023; Van Essen, 2003). Therefore, signatures of schizophrenia will likely be identified through the employment of visual paradigms (Diamond et al., 2022).

Visual impairments are central to cognitive and social functioning deficits in schizophrenia, (Javitt, 2009; Silverstein & Keane, 2011b). For instance, it has been proposed that patients abnormally integrate basic visual features into complex structures, resulting in aberrant visual perception that may in turn contribute to psychopathology (Silverstein & Keane, 2011a). Context plays a crucial role in this integration of visual information.

Numerous studies suggest that patients with schizophrenia process contextual visual information differently from controls (Seymour et al., 2013; Silverstein & Keane, 2011a; Tibber et al., 2013). For example, patients have been shown to be less susceptible to some visual illusions (Keane et al., 2013; Sanders et al., 2013; Uhlhaas et al., 2006), indicating reduced reliance on contextual information. However, other studies reported higher susceptibility to visual illusions in patients (Chen et al., 2008; Kantrowitz et al., 2009) or even no differences, compared to controls (Grzeczkowski et al., 2018; Kaliuzhna et al., 2019). Hence, results are mixed.

Contextual processing is also investigated through visual (un)crowding experiments (Herzog et al., 2015) wherein target perception is modulated by different flanker configurations (Herzog et al., 2016; Pelli & Tillman, 2008). Results again are mixed, with some studies showing that target processing in patients was less affected by flankers (Robol et al., 2013), whereas other studies showed that patients were more affected or even not affected, compared to controls (Roinishvili et al., 2015). Thus, understanding which factors contribute to these mixed results is crucial for elucidating the mechanisms of contextual vision.

To explain this range of contextual effects in schizophrenia, predictive coding (PC) has been proposed as a candidate framework. PC proposes that the brain generates predictions about sensory information and adjusts these predictions according to the differences between the expected and incoming sensory inputs (Colombo & Seriès, 2012; Huang & Rao, 2011; Vilares & Kording, 2011). It has been proposed that patients with schizophrenia dysfunctionally adjust those predictions (Friston, 2005; Sterzer et al., 2018). For instance, resistance to visual illusions and also vivid sensory hallucinations have often been explained as a failure to attenuate signals from sensory cortices in patients (Weilnhammer et al., 2020). However, it has also been proposed that patients generate stronger predictions which exert greater influence on perception than sensory information, contributing to aberrancies in perception and positive symptoms (Corlett et al., 2009, 2019; Friston, 2005; Sterzer et al., 2018). These contrasting views demonstrate that PC processes might be more intricate than initially thought.

Indeed, it has been proposed that there might be several levels of predictive processing, and alterations at those different levels might contribute to different phenomena in schizophrenia (Corlett et al., 2019; Sterzer et al., 2018). Hence, PC might be a rather hierarchical process. For instance, abnormalities in lower levels of PC might contribute to basic sensory processing

impairments, while alterations at higher levels might be involved in more complex phenomena such as sensory hallucinations or delusions. Hence, experimentally investigating these hypothetical levels of predictive processing in patients with schizophrenia will provide further insights into the underlying mechanisms and how they contribute to clinical symptoms and perceptual alterations in patients.

1.4. Variability and measurement error

In the complex sciences, each branch relies on tests designed to target the crucial aspects of the field. Traditionally, these tests yield significant differences between intervention and control conditions or significantly predict other relevant variables. Numerous studies are then conducted with the test because it is assumed that those significant results come with substantial explanatory power for the phenomena under study. However, recent studies have shown that tests thought to target similar underlying mechanisms often exhibit weak correlations with each other, i.e., construct validity is limited. Schizophrenia research is just one example of this issue, which extends to fields including aging research (Garobbio et al., 2022), vision science (Cappe et al., 2014; Cretenoud et al., 2019; Goodbourn et al., 2012), and psychology (Eisenberg et al., 2019). For instance, in vision science, different tests assessing basic visual functions have shown weak correlations, despite significant test-retest reliability (Bosten et al., 2017; Cappe et al., 2014; Cretenoud et al., 2019). Notably, some of these tests demonstrate often remarkable stability even over several years (Garobbio et al., 2024), suggesting that measurement error alone cannot fully account for the observed low correlations.

These results might seem unexpected, but they align well with basic statistical principles. Cohen proposed cutoff values of 0.1, 0.3, and 0.5 to categorize weak, medium, and strong correlations (Cohen, 1988), a criterion widely accepted in psychology and other fields. Gignac and Szodorai (2016) suggested revising these cutoffs due to the limited number of studies meeting the criteria for a high correlation, proposing new cutoff values of 0.1, 0.2, and 0.3. However, even a *strong* correlation of $r = 0.5$ leaves 75% of the variance unexplained. Similarly, for case-control studies, a *large* Cohen's *d* of 0.8 corresponds to a discriminability of 65% only, i.e., 35% of cases are left unexplained. Achieving 80% of explained variance requires a Cohen's

d of 1.68, which is extremely rare. Thus, even with large effect sizes (let alone *statistically significant* results), substantial explanatory power is not guaranteed. Lowering cutoff values could even potentially make the situation worse in some cases. Therefore, when each study explains a small part of the variance, it is not surprising that results from different studies do not correlate strongly.

Another explanation is that research methodologies in fields such as biology and human neuroscience have often overlooked complexity. For example, the variability observed in the data might reflect genuine variability among individuals, making it challenging to reduce findings to general mechanisms since uncorrelated tests may point to different ones. *Shallow rooting* approaches can be advantageous in such cases, as they delineate research scenarios across a broad spectrum of paradigms and measurements. Within this space composed of many test outcomes, latent factors may potentially explain more variability in the data compared to single variables. Overall, systematically analyzing these scenarios is crucial for advancing scientific progress. In this thesis, I have taken a step forward in this direction.

1.5. Outline of the thesis

This thesis comprises five studies to which I contributed during my PhD. Chapters 2 and 3 detail two studies where I examined the complexity of neurophysiology in schizophrenia. In Chapters 4 and 5, studies of contextual visual processing and predictive coding in schizophrenia are presented. Chapter 6 presents an extensive analysis of a public database, highlighting the variability of results obtained through different analysis methods. In Chapter 7, I will discuss these studies and propose potential future research directions. Chapters 2, 4, 5, and 6 contain the manuscripts themselves, while Chapter 3 presents preliminary results and methods. Below, I summarize each chapter. The references for Chapters 1 and 7 are presented at the end of the document. Chapters 2 to 6 each contain its reference list.

Summary of Chapter 2: The EEG multiverse of schizophrenia

There is a variety of methods to analyze resting-state EEG data, including EEG microstates and connectivity techniques, which quantify certain properties of brain functioning. Some of these methods have been employed in schizophrenia research, often revealing significant group

differences between patients and controls. This suggests that the method being employed targets a key function related to schizophrenia. Subsequent studies aim to understand the neural and genetic mechanisms underlying these group differences and their relation to psychopathology. Importantly, most of these studies typically utilize one method.

In Chapter 2, I present a study wherein the resting-state EEG of 121 patients with schizophrenia and 75 healthy controls were analyzed using multiple analysis methods, through which we extracted 194 EEG features (e.g., detrended fluctuation exponents in alpha band, beta-band power) from the very same EEG data. Group comparisons were conducted for each EEG feature to identify those potentially targeting aspects related to schizophrenia. Next, we correlated the features showing a significant group difference to understand to what extent they tap into a common underlying mechanism of schizophrenia.

We identified 69 features showing significant group differences between patients and controls. Effect sizes ranged from medium to large, suggesting that potentially important aspects of the disorder were targeted by the features. Notably, many of these 69 features had been reported as abnormal in patients with schizophrenia in previous studies, including detrended fluctuation exponents in the alpha and beta bands, and EEG microstates temporal parameters, suggesting that these previously reported findings are robust and reproducible. Surprisingly, our correlation analysis revealed generally weak correlations among the 69 EEG features (***Figure 1***). These findings were further corroborated through multivariate and disattenuated correlations.

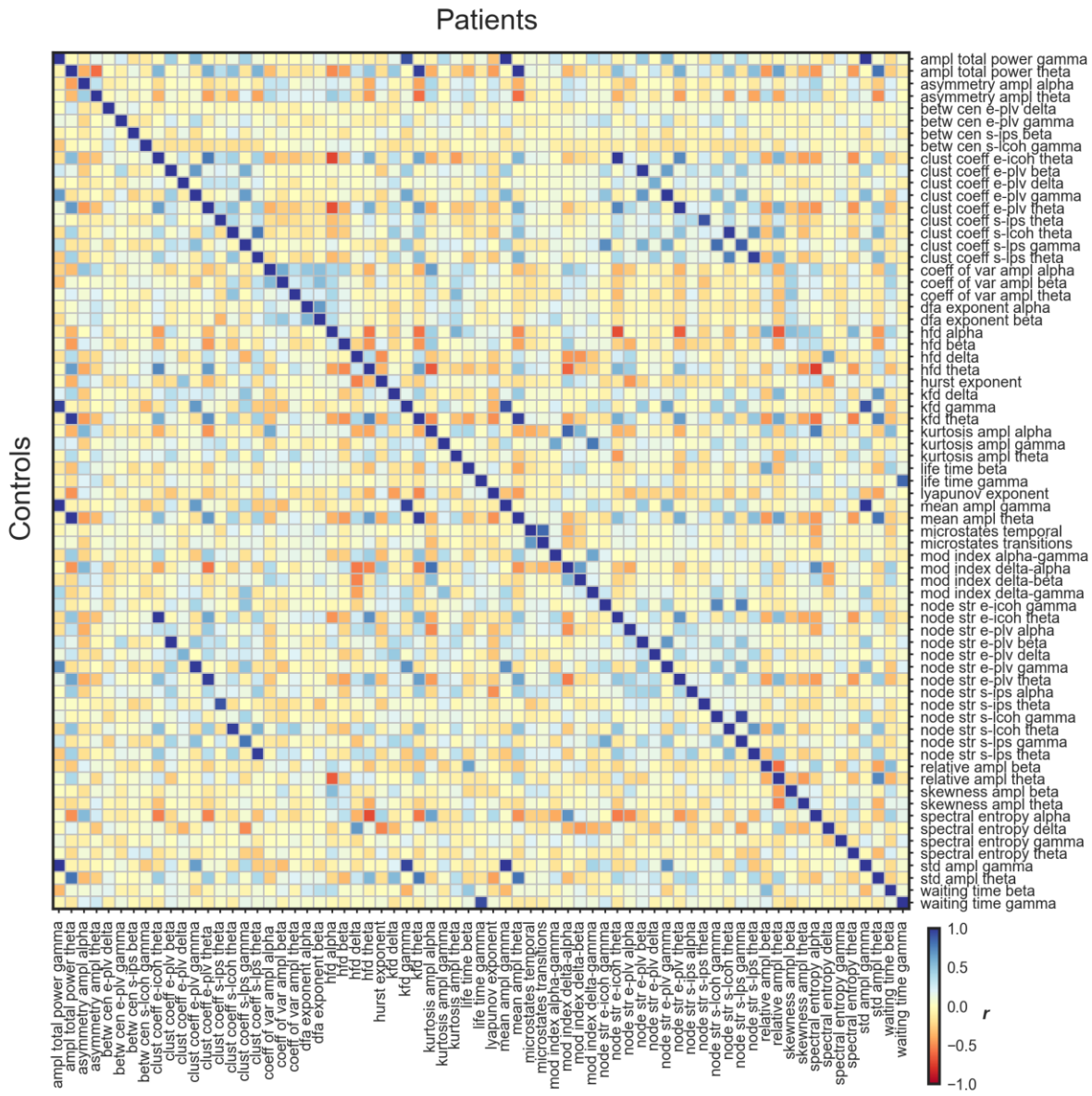

Figure 1. Pairwise correlations between the 69 EEG features demonstrating significant group differences between patients with schizophrenia (upper triangle) and healthy controls (lower triangle). As a representative variable for each feature for this correlation analysis, we selected the electrode, brain region (for features obtained in the source space), or microstate parameter/transition showing the largest effect size in the group comparison, i.e., the variable with better discriminability between groups. Strong blue or red colors represent strong correlations, while yellow colors indicate correlation values close to zero.

Our findings raise critical considerations regarding the nature and interpretation of significant results in schizophrenia research. The low correlations suggest that even if a significant group difference is found, this might not necessarily indicate that the EEG feature has significant explanatory power for the illness, as deficits in one feature do not predict deficits in another feature. While high measurement error might be one explanation for these results, we found

that similar features, such as those in the same frequency bands or obtained through similar algorithms, correlated more strongly, suggesting that test retests might be adequate. Another explanation may be that the features are sensitive to comorbidities or idiosyncrasies, contributing to the variance, and provoking the low correlations. Finally, schizophrenia may be a highly heterogeneous disorder at the neurophysiological level, with each feature pointing to a different aspect. Investigating these scenarios would lead to key insights into the complexity of neurophysiology in schizophrenia.

Summary of Chapter 3: Stability assessment of resting-state EEG in schizophrenia

In Chapter 3, I present preliminary findings from a stability evaluation of resting-state EEG. These findings are based on data collected from a cohort of 40 patients with schizophrenia and 27 healthy controls. These participants underwent EEG recordings approximately four years after their initial involvement in the study described in Chapter 2.

The main goal was to assess the stability of EEG features showing group differences between patients with schizophrenia and controls. This evaluation aimed to determine whether the low correlations observed in Chapter 2, could be attributed to measurement error or poor properties of the EEG features. If EEG features demonstrate high reliability even after several years, it would suggest their robustness and potential relevance in targeting abnormal mechanisms of the illness. Moreover, this may also help identify stable features for further correlation analyses. Importantly, we capitalized on recent analytical advancements to enhance the signal-to-noise ratio of the EEG features. For example, instead of using canonical frequency bands, such as the 8 to 12 Hz range for the alpha band, we determined individual-specific frequency bands based on spectral peak information for each subject, among other improvements in analysis techniques detailed in Chapter 3.

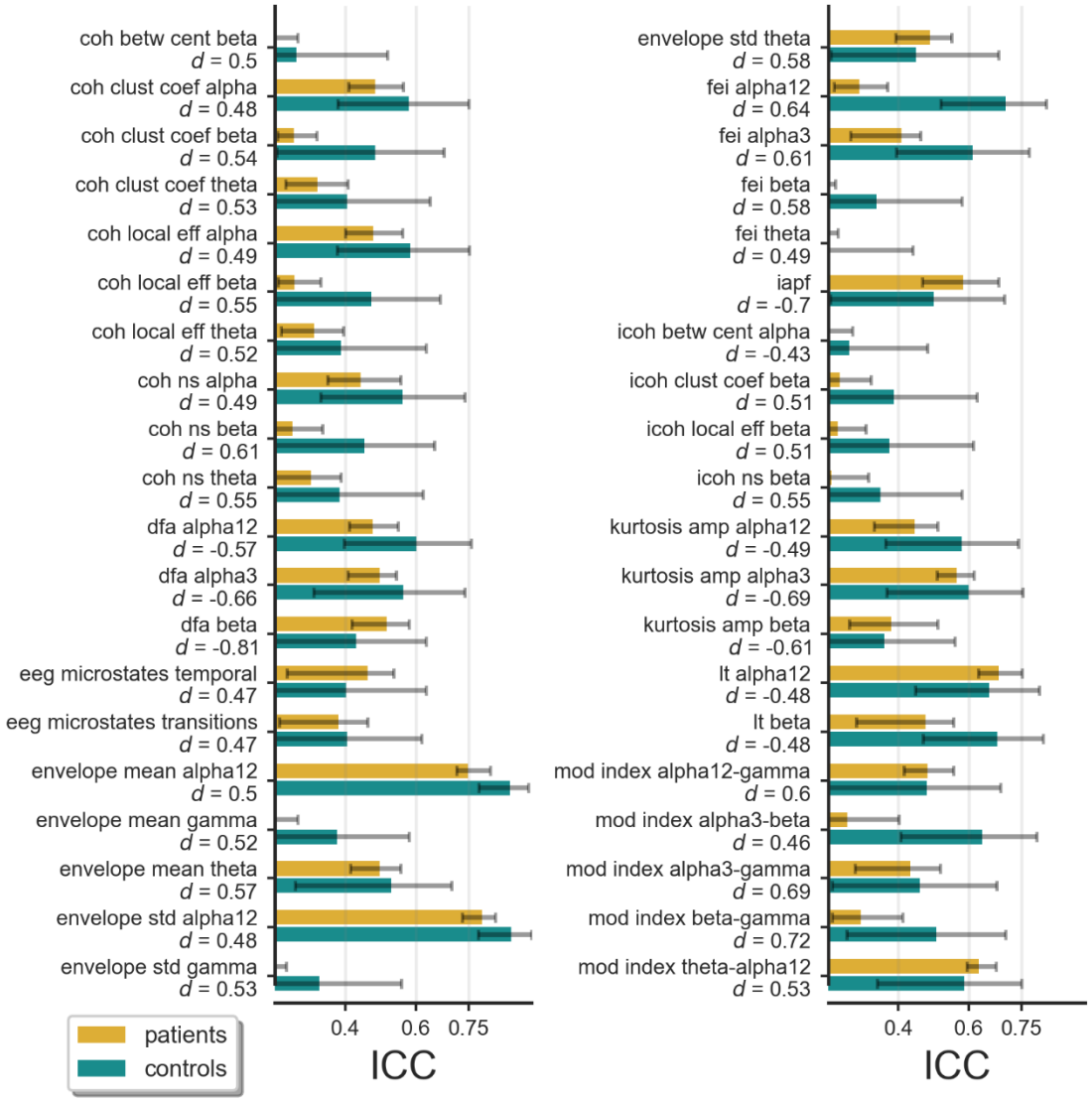

Figure 2. Intraclass correlation coefficients (ICC) of 40 out of 82 EEG features demonstrating a significant group difference between patients with schizophrenia and controls. Group difference analyses were conducted using a sample comprising 135 patients with schizophrenia and 92 healthy controls. Stability was assessed separately for each group. Below the names of the EEG features, we display the highest effect size, e.g., across electrodes, observed in the group comparisons using each EEG feature. Confidence intervals represent the 25th and 75th percentiles of ICC values across electrodes, brain regions, or microstate parameters/transitions.

Our preliminary findings reveal many features exhibiting adequate stability both in patients and controls (***Figure 2, 3***). This suggests that these highly stable features may, to a large extent, mirror underlying mechanisms for the illness rather than idiosyncratic aspects. Further work is needed to fully understand the nature of these findings and their implications for neurophysiological studies in schizophrenia research.

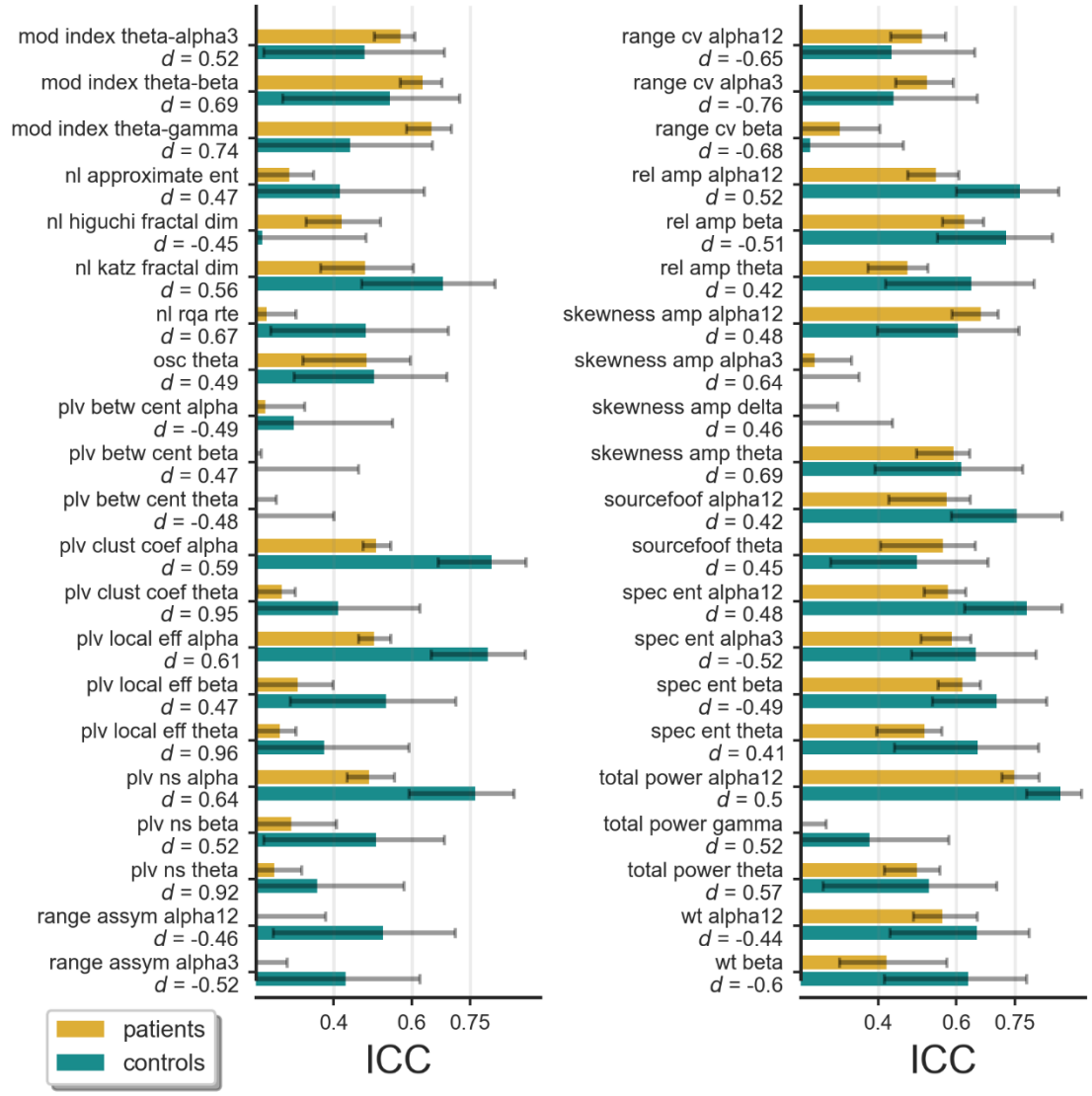

Figure 3. Intraclass correlation coefficients (ICC) of 42 (not presented in ***Figure 2***) out of 82 EEG features demonstrating a significant group difference between patients with schizophrenia and controls. Below the names of the EEG features, we display the highest effect size, e.g., across electrodes, observed in the group comparisons using each EEG feature. Confidence intervals represent the 25th and 75th percentiles of ICC values across electrodes or brain regions.

Summary of Chapter 4: Intact and deficient contextual processing in schizophrenia:

Contextual vision studies in patients with schizophrenia have yielded mixed results. Various factors such as attentional or motivational effects in patients, false positives, and differences in the paradigms and underlying mechanisms may contribute to these conflicting results.

In Chapter 4, I present a study where we utilized visual (un)crowding as a method to delve into contextual visual processing in schizophrenia. In (un)crowding, the processing of a target is

modulated by flankers. This paradigm allowed us to systematically investigate both facilitating and deteriorating contextual effects across flanker configurations. There are advantages to this specific paradigm. For example, by examining both deteriorating and facilitating effects, we can mitigate the influence of reduced attention in patients. Additionally, as the same group of patients performed all conditions, we can assess whether changes in the spatial arrangement of the stimuli yield consistent results. Furthermore, contextual effects are examined relative to a *target-only* condition which is generally missing in other paradigms such as visual illusions. We conducted two experiments.

In Experiment 1, participants had to discriminate a target presented among six different flanker configurations. We found intact contextual processing in patients (***Figure 4***).

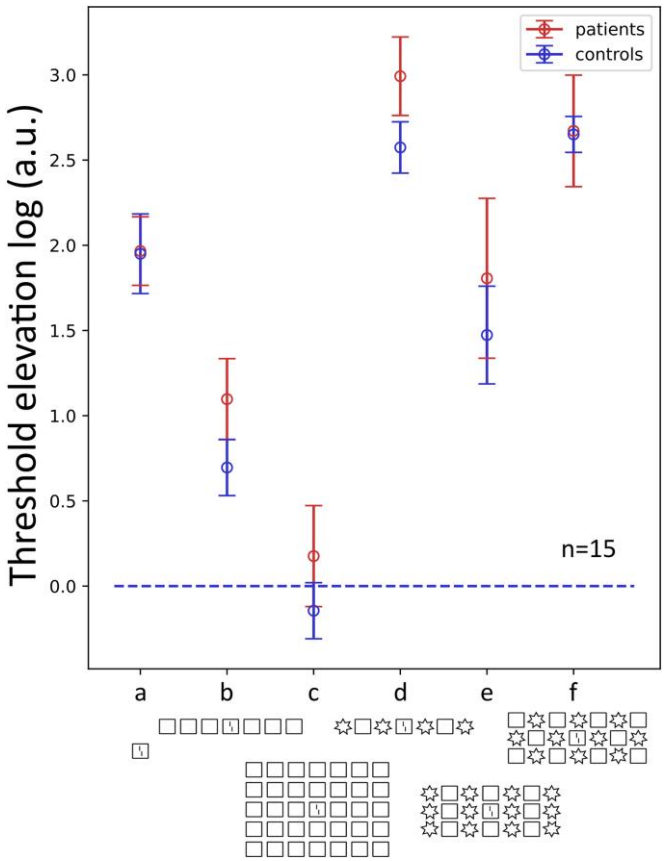

Figure 4. Experiment 1 detailed in Chapter 4. Mean threshold elevations, i.e., threshold relative to the target-only condition, for six configurations of flankers. Error bars represent the standard error of the mean. Larger threshold elevation values represent reduced performance (more contextual effects), while lower values represent better performance (less contextual effects). Patients with schizophrenia and healthy controls show similar contextual effects across flanker configurations.

In Experiment 2, we examined two flanker configurations - one leading to crowding and the other to uncrowding. Stimuli were presented for six different durations. We expected that

performance would increase with stimulus duration, particularly for the uncrowding condition, as recurrent processing, may come into play. This improvement was indeed observed in both groups, yet to a much lesser extent in patients (***Figure 5***) indicating that patients had impaired contextual processing.

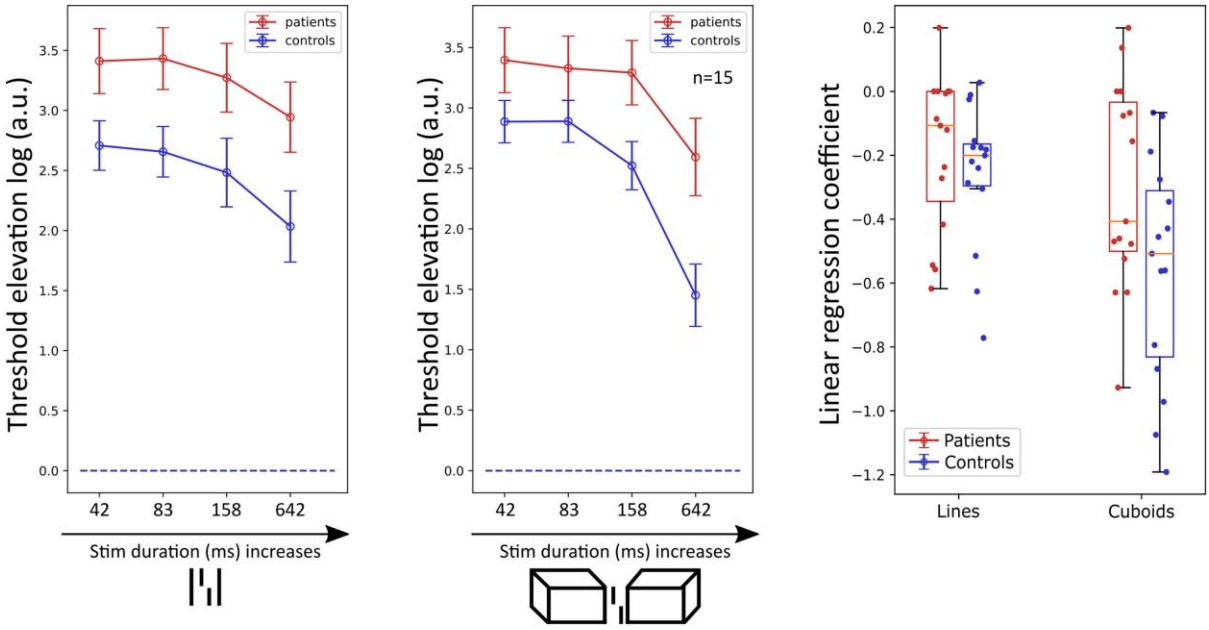

Figure 5. Experiment 2 detailed in Chapter 4. The leftmost and middle panels show mean threshold elevations, i.e., thresholds relative to the target-only condition. Error bars represent the standard error of the mean. In the rightmost panel, beta coefficients for linear regression are presented for each participant. Coefficients close to zero indicate that performance did not change across stimulus durations.

We propose that mixed results in contextual vision studies might be partly due to differences in stimuli and specific aspects of the paradigm since we found that the very same patients exhibited intact and deficient contextual processing in variations of the same (un)crowding paradigm. These results also might question the presence of general contextual processing deficits in patients, since such deficits should not depend so strongly on the paradigms. Therefore, we propose that to substantiate claims about abnormal mechanisms, it is essential to verify them using more than one paradigm.

Summary of Chapter 5: Oscillatory traveling waves reveal predictive coding abnormalities in schizophrenia:

Predictive coding (PC) proposes that sensory inputs are compared with prior expectations, with subsequent adjustments made based on the disparities in this comparison. Patients with schizophrenia have been proposed to dysfunctionally adjust prior expectations, leading to aberrancies in perception and potentially also clinical symptoms. Most evidence for alterations in PC processes comes from behavioral paradigms. In Chapter 5, I present neurophysiological evidence for PC alterations in schizophrenia.

We analyzed EEG data from both resting state and a visual backward masking (VBM) paradigm using the method of oscillatory traveling waves. To quantify oscillatory traveling waves, neural activity along the central midline of electrodes is analyzed to probe how oscillations travel from occipital to frontal areas, i.e., forward traveling waves (FW), and vice versa, i.e., top-down, backward traveling waves (BW). Waves in the alpha band have been proposed to reflect different components of predictive processing, including prior precision for BW, and prediction errors for FW (***Figure 6***).

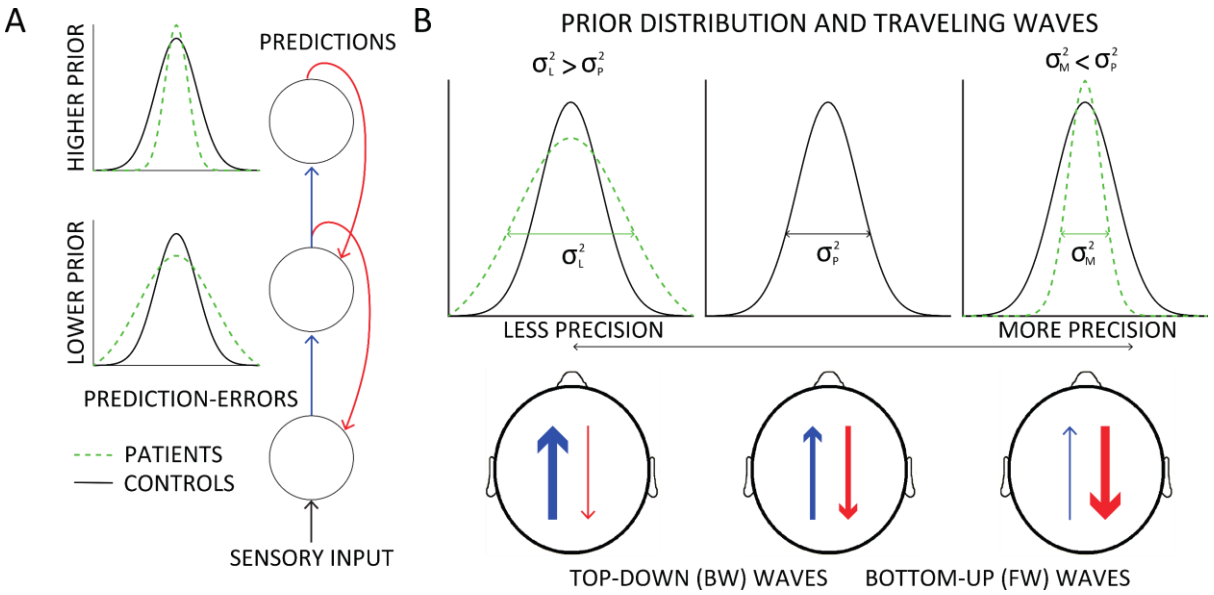

Figure 6. Predictive coding and traveling waves. A) Predictive coding (PC) processes are often formulated in Bayesian terms, wherein prior distributions generate predictions that are in turn compared with sensory inputs (i.e., the likelihood). The priors are adjusted based on the prediction errors. B) Considering traveling waves as probes for PC processes (Alamia & VanRullen, 2019), forward (FW) and backward waves (BW) would represent predictions and prediction errors. More precise priors would generate stronger predictions resulting in increased

BW, whereas less precise priors would generate inaccurate predictions resulting in higher prediction errors and therefore stronger FW.

We observed that for the resting-state data, patients with schizophrenia demonstrated higher BW and lower FW in the alpha band compared to controls, suggesting that there might be more precision in higher-order priors in patients (***Figure 7B***). During VBM, however, FW in the alpha band were enhanced in the patients, suggesting that sensory information was more strongly weighted, indicating alterations in lower-level priors (***Figure 7C, D***).

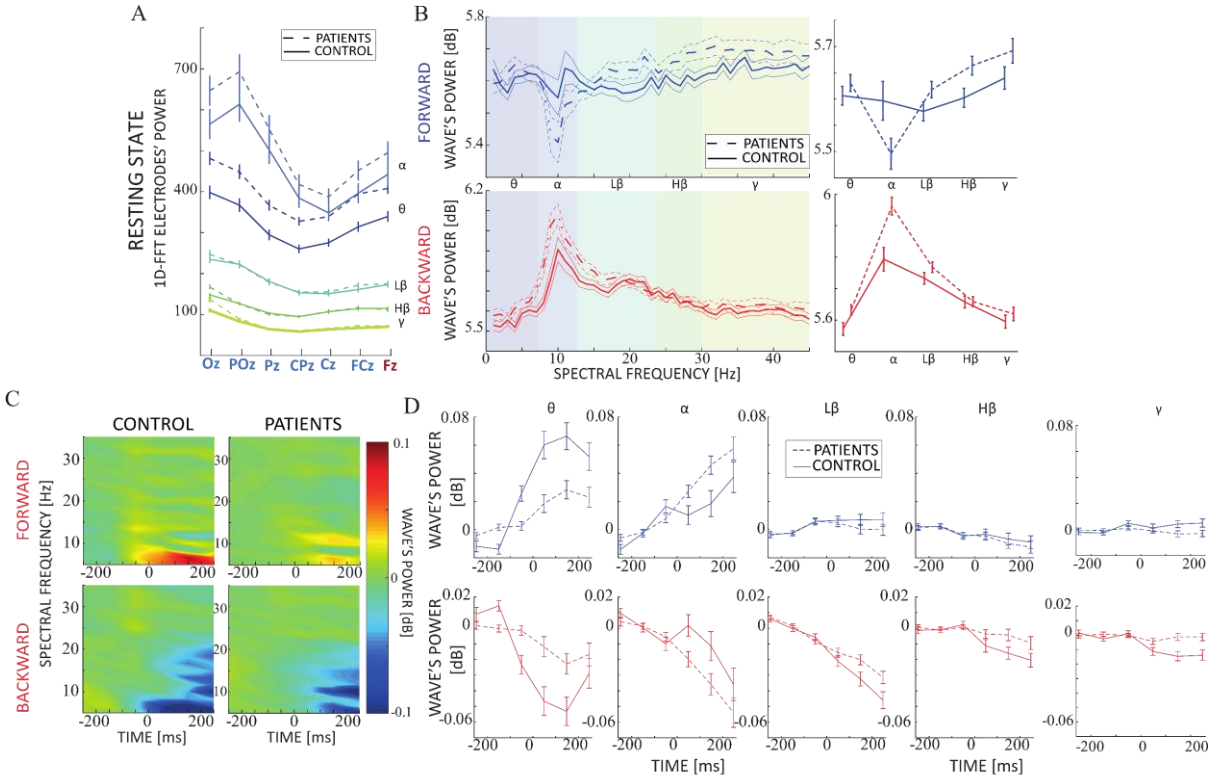

Figure 7. Traveling waves during resting-state and a visual backward masking task. A) Power for each frequency band (each indicated by a different color) and electrode for patients with schizophrenia and controls in the resting-state dataset. B) Spectra for forward and backward waves in the resting-state database, along with the mean of each frequency band (rightmost panel). C) Spectrogram of baseline-corrected forward and backward waves for the visual backward masking (VBM) dataset. D) Mean values of baseline-corrected forward and backward waves for each frequency band. The x-axis represents time in milliseconds. All error bars represent the standard error of the mean.

Our findings support hierarchical-specific accounts for PC, suggesting that there might plausibly be multiple levels of predictive processing, relying on priors located across these different levels. This is suggested by the distinct patterns of traveling waves observed at resting-state and during visual stimulation. Importantly, it is proposed that different levels of

predictive processing may give rise to different phenomena, ranging from basic sensory alterations to more complex manifestations such as psychotic symptoms. Further studies investigating how dysfunctions at different levels contribute to clinical symptoms and perceptual alterations in schizophrenia would provide insights into candidate mechanisms underlying the phenomenology and psychopathology in patients.

Summary of Chapter 6: Do we really measure what we think we are measuring?

In resting-state EEG research, various EEG features have been proposed to reflect brain mechanisms involved in cognitive functioning. These links are often established through correlations, demonstrating that variability in EEG features relates to variability in cognitive paradigms. Additionally, researchers frequently investigate the neural correlates of age-related decline in brain functioning by comparing EEG features between older and younger adults.

In Chapter 6, I present an extensive analysis of a database containing resting-state EEG and behavioral performance in a battery of six tasks from 138 younger and 63 older adults. From the resting-state EEG data, we extracted 175 EEG features using a range of analysis methods, while 12 behavioral variables were extracted from the battery of cognitive tests. Our primary objectives were twofold: first, to identify EEG features correlating with cognitive variables, and second, to investigate age-related aspects of neurophysiology by identifying EEG features that were able to classify older from younger adults.

First, to identify associations between EEG and cognitive variables we correlated each EEG feature with each behavioral variable. Second, group comparisons between older and younger adults were conducted for each EEG feature to identify features sensitive to age-related aspects of neurophysiology. Following these analyses, pairwise correlations were conducted with the features showing either significant correlations with a behavioral variable or significant group differences, aiming to understand whether all these significant results align with a common mechanism.

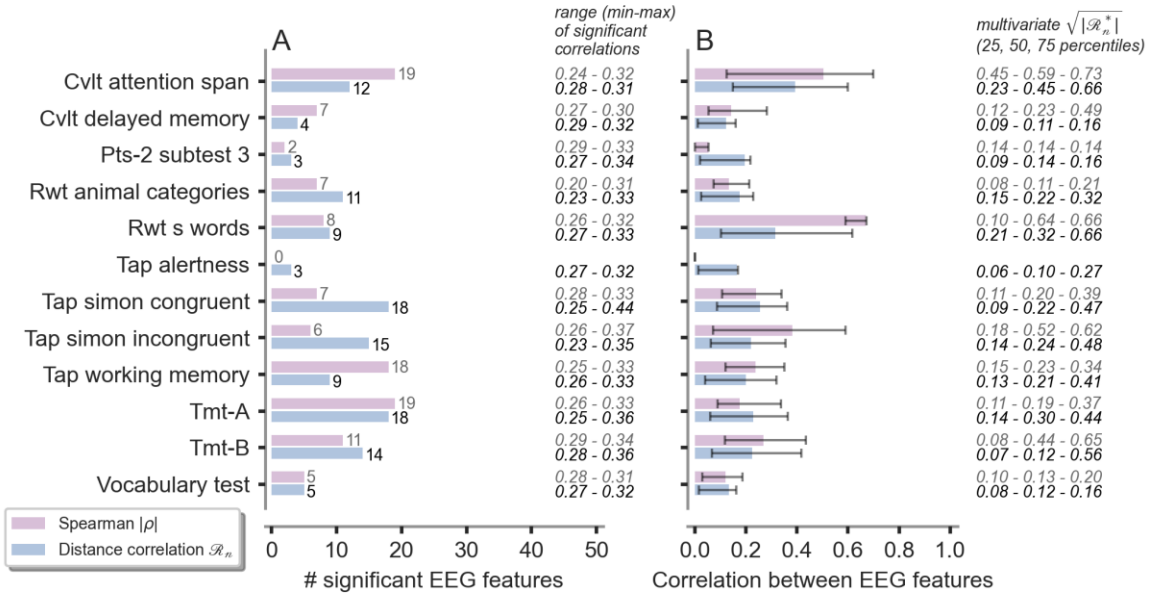

Figure 8. Results for the correlation analyses between each EEG feature and behavioral variable for younger adults. A) Number of EEG features that correlated significantly to each cognitive variable. The range (min-max) of significant Spearman and distance correlations are indicated on the right side of the panel B) We pairwise correlated the EEG features showing significant correlations with each behavioral variable and indicate here the median Spearman and distance correlation (CI indicates the 25th and 75th percentiles). Higher values would indicate that EEG features target similar aspects of the behavioral variable. Multivariate distance correlations (ranging from 0 to 1) were also calculated between EEG features showing a significant correlation with each behavioral variable. Multivariate correlations allow us to consider all electrodes, brain regions, and microstate parameters of each EEG feature. We reported the 25th, 50th, and 75th percentiles of these multivariate correlations on the right side of the panel.

We identified 109 significant relationships between EEG features and cognitive variables for younger adults using Spearman correlations (***Figure 8A***). These features were obtained using various analysis methods, including connectivity, spectral power, and temporal autocorrelations (see ***Figure 9*** for an example). However, although there was generally more than one feature correlating significantly with the same cognitive variable, we observed in most cases either weak or medium correlations between these EEG features (***Figure 8B***).

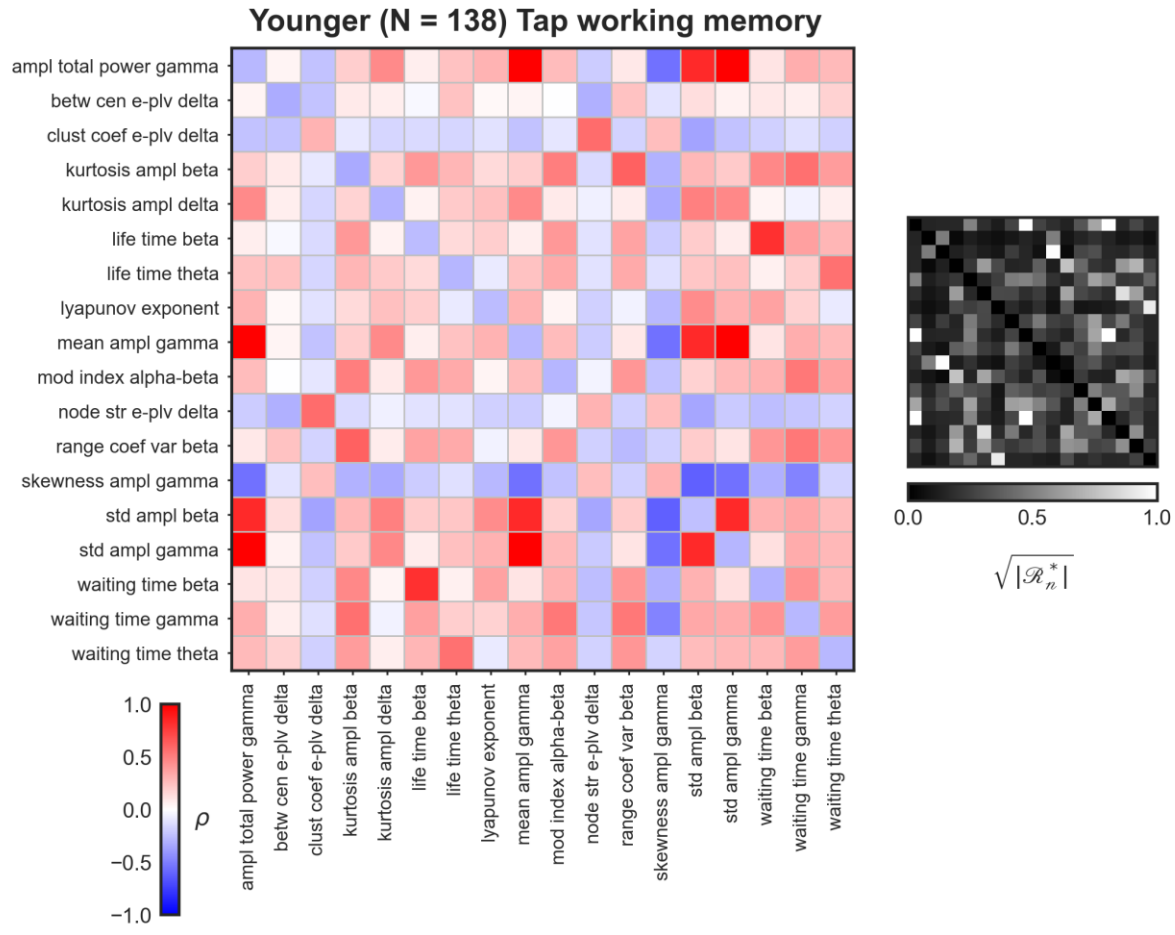

Figure 9. Example of the relationship between a range of EEG features and a behavioral variable measuring working memory performance. There are several EEG features, extracted from very different methods, which show significant correlations with the variable, yet, correlations are not always strong between EEG features. Therefore, different EEG features may target a different function potentially involved in behavioral performance. The main diagonal contains the maximum Spearman correlation of the EEG feature with the cognitive variable (since EEG features are composed of several electrodes, brain regions, or microstate parameters). On the right side, we show the pairwise multivariate distance correlations between the EEG features (with all its variables). In this multivariate analysis, all variables of the EEG features are employed for the pairwise correlation analyses.

Additionally, we identified 108 EEG features that exhibited significant differences between older and younger adults. The correlations were again not very strong between the EEG features. Similar features were however highly correlated, which was also supported by principal component analysis.

We demonstrate that using the very same database, a large range of significant associations between EEG features and cognitive variables can be established. However, these results do not necessarily point to a common mechanism, since EEG features were not always strongly

correlated with each other. In a complementary analysis, we found that employing latent dimensions of EEG features enhanced predictive power for certain cognitive variables. This suggests the presence of multiple mechanisms at play, each potentially targeted by a different EEG feature. Therefore, our findings advocate for the use of more than one EEG feature when investigating the neural correlates of cognitive functions.

Similarly, for the features demonstrating differences between groups, we found that while pairwise correlations were not strong, there were latent dimensions of features that explained a significant amount of the variance. Thus, further analyses of those latent dimensions may potentially reveal age-related brain mechanisms.

Overall, our findings suggest that results from studies employing a single EEG feature may fall short of explaining behavioral differences. Sets of features, rather than single features, may provide a more accurate representation of complex mechanisms. Complementing *deep* with *shallow rooting* approaches may provide deeper insights into neurophysiology.

Chapter 2. The EEG multiverse of schizophrenia

Dario Gordillo [1,†], Janir Ramos da Cruz [1,2,3,†], Eka Chkonia [4,5], Wei-Hsiang Lin [1], Ophélie Favrod[1], Andreas Brand[1], Patrícia Figueiredo [2], Maya Roinishvili[5,6], Michael H. Herzog [1]

[1] Laboratory of Psychophysics, Brain Mind Institute, School of Life Sciences, École Polytechnique Fédérale de Lausanne (EPFL), CH-1015 Lausanne, Switzerland,

[2] Institute for Systems and Robotics – Lisboa, Department of Bioengineering, Instituto Superior Técnico, Universidade de Lisboa,1049-001 Lisbon, Portugal,

[3] Wyss Center for Bio and Neuroengineering, CH-1202 Geneva, Switzerland,

[4] Department of Psychiatry, Tbilisi State Medical University (TSMU), 0186 Tbilisi, Georgia,

[5] Institute of Cognitive Neurosciences, Free University of Tbilisi, 0159 Tbilisi, Georgia,

[6] Laboratory of Vision Physiology, Ivane Beritashvili Centre of Experimental Biomedicine, 0160 Tbilisi, Georgia

† Dario Gordillo and Janir Ramos da Cruz contributed equally to this work.

Postprint of the article published in *Cerebral Cortex*

Full citation: Gordillo, D.*, da Cruz, J. R.*, Chkonia, E., Lin, W.-H., Favrod, O., Brand, A., Figueiredo, P., Roinishvili, M., & Herzog, M. H. (2023). The EEG multiverse of schizophrenia. *Cerebral Cortex*, 33(7), 3816–3826. https://doi.org/10.1093/cercor/bhac309

Detailed personal contribution: I performed statistical and analyses and contributed to the extraction of EEG features alongside Janir Ramos da Cruz and Wei-Hsiang Lin. Additionally, I wrote the manuscript with Janir Ramos da Cruz and the contribution of the other authors. I revised the manuscript with the contribution of the other authors.

Abstract

Research on schizophrenia typically focuses on one paradigm for which clear-cut differences between patients and controls are established. Great efforts are made to understand the underlying genetical, neurophysiological, and cognitive mechanisms, which eventually may explain the clinical outcome. One tacit assumption of these “deep rooting” approaches is that paradigms tap into common and representative aspects of the disorder. Here, we analyzed the resting-state electroencephalogram (EEG) of 121 schizophrenia patients and 75 controls. Using

multiple signal processing methods, we extracted 194 EEG features. Sixty-nine out of the 194 EEG features showed a significant difference between patients and controls, indicating that these features detect an important aspect of schizophrenia. Surprisingly, the correlations between these features were very low. We discuss several explanations to our results and propose that complementing "deep" with "shallow" rooting approaches might help in understanding the underlying mechanisms of the disorder.

Introduction

Schizophrenia patients show strong abnormalities in many domains, including personality, cognition, perception, and even immunology. In many experimental paradigms, the differences between patients and controls have large effect sizes, indicating that important aspects of the disease are detected. This provokes two questions: What do these abnormalities have in common, and how representative are they of the disease? For example, patients exhibit strong deficits in cognition, such as in working memory tasks (Meyer-Lindenberg et al. 2001), which are attributed to the abnormalities of cortico-cerebellar-thalamic-cortical circuits (Andreasen et al. 1998). Patients show also diminished skin flushing with the niacin skin test (Rybakowski and Weterle 1991), which is attributed to dysfunctional phospholipase A2 arachidonic acid signaling (Messamore 2012). How do the working memory deficits correspond to deficits in skin functioning? Very few studies have correlated deficits with each other (Toomey et al. 1998; Braff et al. 2006, 2007; Price et al. 2006; Dickinson et al. 2011; Seidman et al. 2015). The Consortium on the Genetics of Schizophrenia studied neurocognitive and neurophysiological abnormalities in schizophrenia patients with a battery of 15 paradigms (Seidman et al. 2015). They found that neurocognitive measures shared a significant amount of variance, while neurophysiological measures were almost entirely independent. Price et al. (2006) studied four candidate electrophysiological endophenotypes of schizophrenia (mismatch negativity, P50, P300, and antisaccades). Even though patients and their family members showed deficits in each of these endophenotypes, the features were largely uncorrelated.

Here, we took another road. Instead of comparing different paradigms, we analyzed the very same data of the very same patients and controls with different electroencephalogram (EEG)

analysis methods, including many that have shown atypical patterns in patients (Kim et al. 2000; Boutros et al. 2008; Uhlhaas and Singer 2010; Nikulin et al. 2012; Sun et al. 2014; Andreou et al. 2015; Di Lorenzo et al. 2015; da Cruz et al. 2020a). Data were recorded from a 5-min resting-state session during which the participants did nothing else than relaxing. Many of the resting-state EEG features we extracted are thought to reflect brain mechanisms linked to important aspects of the disorder. For example, schizophrenia patients exhibit reduced long-range temporal correlations (LRTC) in the alpha and beta frequency bands (Nikulin et al. 2012) suggested to reflect excessive switching of neuronal states. Patients also have shown atypical patterns in the dynamics of the EEG microstates classes C and D (Rieger et al. 2016; da Cruz et al. 2020a), which were proposed to correspond to imbalances in attentional and information processing. Schizophrenia patients have shown increased power in the delta, theta, and beta frequency bands (Venables et al. 2009). Increased beta power was suggested to reflect cortical hyperexcitability, and increased power in the delta and theta bands were proposed to relate to atypical dopaminergic function, to name a few examples. All these results, individually, suggest that each EEG feature captures important aspects of schizophrenia. But how representative are these abnormalities of the disorder? Does a patient showing abnormal microstate dynamics also show deficits in LRTC or in other EEG features?

Aiming to shed light on this EEG "multiverse" of schizophrenia, we analyzed the resting-state EEG data of 121 schizophrenia patients and 75 healthy controls with multiple methods. We extracted 194 EEG features, such as time-domain features, frequency-domain, and connectivity features both in electrode and source space, and nonlinear dynamical features. Then, we correlated the features that showed significant group differences to evaluate how these abnormalities/deficits relate to each other. We also examined whether these EEG features show adequate predictive power to clinical scales measuring key symptoms of schizophrenia.

Materials and methods

Participants

Two groups of participants joined the experiment: schizophrenia patients (n = 121) and healthy controls (n = 75). All participants took part in a battery of tests comprising perceptual and

cognitive tasks as well as EEG recordings. Data of 101 patients and 75 controls have already been published in different contexts (Favrod et al. 2018; da Cruz et al. 2020a, 2020b; Garobbio et al. 2021). Patients were recruited from the Tbilisi Mental Health Hospital or the psycho-social rehabilitation center. Patients were invited to participate in the study when they had recovered sufficiently from an acute psychotic episode. Thirty-five were inpatients and 86 were outpatients. Patients were diagnosed using the Diagnostic and Statistical Manual of Mental Disorders Fourth Edition (DSM-IV) by means of an interview based on the Structured Clinical Interview for DSM-IV, Clinical Version, information from staff, and study of patients' records. Psychopathology of patients was assessed by an experienced psychiatrist using the Scale for the Assessment of Negative Symptoms (SANS) and the Scale for the Assessment of Positive Symptoms (SAPS). Out of the 121 patients, 106 were receiving neuroleptic medication. Chlorpromazine (CPZ) equivalents are indicated in Table 1. Controls were recruited from the general population in Tbilisi, aiming to match the patients' demographics as closely as possible. All controls were free from psychiatric axis I disorders and had no family history of psychosis. General exclusion criteria were alcohol or drug abuse, severe neurological incidents or diagnoses, developmental disorders (autism spectrum disorder or intellectual disability), or other somatic mind-altering illnesses, which were assessed through interview by certified psychiatrists. All participants were no older than 55 years. Group characteristics are presented in Table 1. All participants signed informed consent and were informed that they could quit the experiment at any time. All procedures complied with the Declaration of Helsinki (except for preregistration) and were approved by the Ethical Committee of the Institute of Postgraduate Medical Education and Continuous Professional Development (Georgia); protocol number: 09/07; title: "Genetic polymorphisms and early information processing in schizophrenia."

Table 1. Group average statistics (± standard deviation).

	Patients	Controls	Statistics
Gender (F/M)	22/99	39/36	$\chi^2(1) = 24.702$, $p = 6.690e\text{-}7$[a]
Age (years)	35.8 ± 9.2	35.1 ± 7.7	$t(194) = 0.519$, $p = 0.604$[b]
Education (years)	13.3 ± 2.6	15.1 ± 2.9	$t(194) = -4.418$, $p = 1.657e\text{-}5$[b]
Handedness (L/R)	6/115	4/71	$\chi^2(1) = 0.013$, $p = 0.908$[a]

Illness duration (years)	10.8 ± 8.7		
SANS	10.1 ± 5.2		
SAPS	8.6 ± 3.2		
CPZ equivalent[c]	561.1 ± 389.4		
[a]Pearson's chi-squared test [b]Two-sided independent samples *t*-test [c]Average CPZ equivalents calculated over the 106 Patients receiving neuroleptic medication			

EEG recording and data processing

Participants were sitting in a dim lit room. They were instructed to keep their eyes closed and to relax for 5 min. Resting-state EEG was recorded using a BioSemi Active Two Mk2 system (Biosemi B.V., The Netherlands) with 64 Ag-AgCl sintered active electrodes referenced to the common mode sense electrode. The recording sampling rate was 2,048 Hz. Offline data were downsampled to 256 Hz and were preprocessed using an automatic pipeline (da Cruz et al. 2018). Preprocessed EEG data were analyzed using multiple signal processing methods in the electrode and source space. In total, 194 EEG features were extracted (see Supplementary Table 1). Out of the 194 EEG features, 50 were obtained in the source space and 144 in the electrode space. For source space analysis, we defined 80 brain regions (40 per hemisphere) according to the AAL atlas (see Supplementary Table 2). See Supplementary Methods for a detailed description of the analysis methods.

Group comparisons

We compared patients' and controls' scores for each of the 194 EEG features. For each of the J variables (i.e. 64 electrodes, 80 brain regions, or 12 microstate parameters, depending on the number of variables of each EEG feature) of a given feature, we performed a two-way ANCOVA, with Group (patients and controls) and Gender (male and female) as factors and with Education as a covariate. The *P*-values for the effect of Group were corrected for J comparisons using false discovery rate (FDR; with an error rate of 5%). Group effects' η^2 were converted to Cohen's *d*.

Pearson, partial least squares, and distance correlations

First, for each EEG feature that contained at least one variable showing a significant difference between patients and controls (after correcting for multiple comparisons), we selected the variable (i.e. electrode, brain region, or microstate parameter) with the biggest effect size to be the representative variable for that feature. Then, for patients and controls separately, we computed pairwise Pearson correlations between the representative variables of each significant EEG feature. As a complementary analysis, we computed Pearson correlations between the first principal components of the EEG features showing significant group differences for patients and controls separately. Second, to quantify the overall relationship, i.e. the amount of shared information, between pairs of multivariate EEG features, we used partial least squares correlation (PLSC). PLSC generalizes correlations between two variables to two matrices (Tucker 1958; McIntosh et al. 1996). The shared information can be quantified as the inertia common to the 2 features (Krishnan et al. 2011). The statistical significance of the inertia was assessed using a permutation test (McIntosh et al. 2004; Abdi and Williams 2013). The inertia values were normalized. Hence, the normalized inertias ($\mathfrak{I}_{relative}$) ranged from 0 (the two EEG features are completely unrelated) to 1 (the two EEG features contain the same information). PLSC analysis was done for patients and controls separately. Finally, for patients and controls separately, we quantified the relationship between pairs of multivariate EEG features using distance correlations (Székely and Rizzo 2013). Distance correlations are close to 0 if the multivariate features are unrelated and are close to 1 if features are strongly related. See Supplementary Methods for details.

Regression and classification analyses

To evaluate whether EEG features predict the psychopathology scores (SAPS and SANS) adequately, we used elastic net regression models (Zou and Hastie 2005). Elastic nets can handle regression problems where the number of predictors is relatively large compared to the number of samples as well as multicollinearity (i.e. the predictors are not linearly independent) by combining the l_1 and l_2 penalties to achieve regularization. For each of the 194 EEG features (with all its variables), we built 2 regression models, one to predict SAPS scores and one to predict SANS scores. We performed 20 repetitions of a 3-fold nested cross-validation procedure. First, one third of the data (1-fold) was left out for validation (test set),

while the remaining data (2-folds; train set) were used to find the optimal parameters, namely the amount of penalization and the compromise between l_1 and l_2 penalties, using 3-fold cross-validation. The model with the parameters leading to best performance in the train set was tested on the left-out data (test set). The entire procedure was repeated 20 times, with different allocations of the patients in the train and test sets. Using the same crossvalidation procedure, i.e. 20 repetitions of a 3-fold cross-validation, we also evaluated predictive performance using a nonlinear random forest regression model, setting the maximum depth of the tree to 10 and the number of trees to 100. Random forests are meta estimators that average several decision trees trained on subsets of the dataset to improve accuracy and to avoid overfitting. Prediction performance was calculated using the coefficient of determination (R^2) and the root-mean-squared error (RMSE). The distribution of the prediction performance values was obtained from the 60 aggregated RMSE and R^2 across repetitions of the procedure. Further, we evaluated the classification performance of the EEG features, i.e. we aimed to discriminate between patients and controls using penalized logistic regression. Accuracy (ACC) and area under the curve (AUC) were obtained using a training procedure consisting of 100 repetitions of a 3-fold cross-validation method. First, 33% of the data were separated as the testing set, and the remaining 67%, i.e. training set, were used to estimate the amount of penalization (l_1 norm, 10 values between $e^{-4}$and e^{4}) using 3-fold cross validation. The model giving the best fit on the training set was tested on the left out 33% of the data and the classification ACC and AUC were estimated. The entire procedure was repeated for 100 times, allocating the participants differently at each iteration, and the values of ACC and AUC were aggregated. The mean ACC and AUC were obtained for each EEG feature. To identify the features that classified patients and controls significantly, we repeated the above-mentioned procedure for 1,000 times and aggregated the ACC and AUC values. We assigned different EEG feature values to different participants at each repetition (random label permutation). The mean AUCs obtained in the previous step were compared to the null distribution of 1,000 AUC values and a P-value was obtained. The P-value indicated the probability of a value of AUC obtained from random label permutation to be larger than that obtained from the original data. We declare that the features were significant if the value was <5%.

Results

Multiple EEG features reveal significant group effects and classification performance

For 121 patients (22 females, 35.8±9.2 years old, 13.3±2.6 years of education) and 75 age-matched healthy controls (39 females, 35.1±7.7 years old, 15.1±2.9 years of education; Table 1), we extracted, in total, 194 features from the resting-state EEG recordings, including time-domain, frequency-domain, connectivity, and nonlinear dynamical features (Supplementary Table 1). Among the 194 EEG features, 69 (35.57%) showed significant differences between patients and controls with medium to large effect sizes (Cohen's *d* varied from 0.463 to 1.037, Fig. 1). Patients showed significantly reduced values in 24 out of the 69 EEG features, revealing significant group differences (illustrated as negative effect size in Fig. 1). Patients exhibited significantly higher values than controls in 45 EEG features.

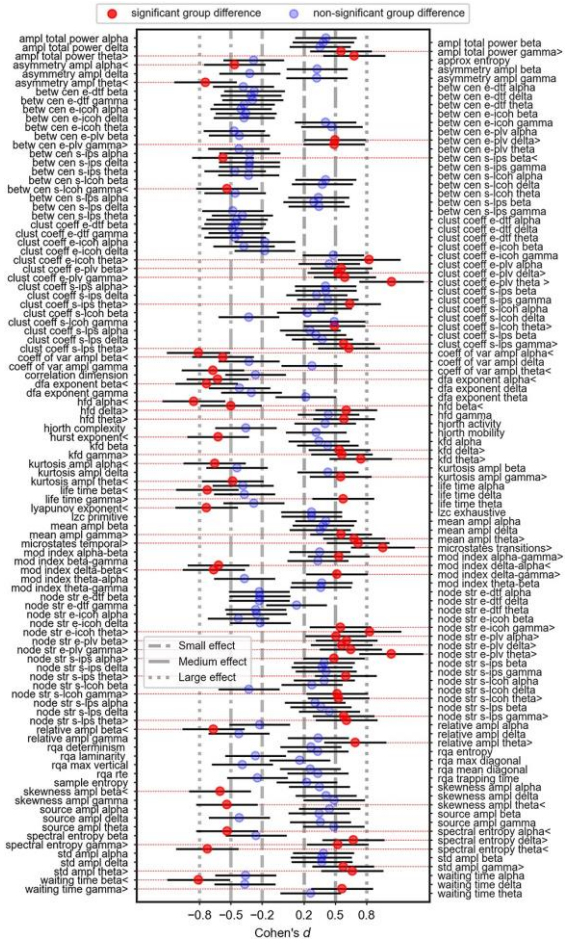

Fig. 1. Effect size (Cohen's *d*) of the group differences between patients and controls for each of the 194 EEG features. We took the values of the electrode, brain region, or microstate parameter, with the largest effect size according to Cohen's *d* (η^2 values were converted to Cohen's *d*) to be the representative variable for each feature.

Significant group differences, after correction for multiple comparisons (using FDR), are depicted in red, with dotted red horizontal lines serving as a guide to their labels. > and< were added to the feature labels to indicate if patients had significantly higher or lower values than controls, respectively. The non-significant effects are shown in blue. Error bars represent 95% confidence intervals. A list with the abbreviations and the corresponding name of each feature is presented in Supplementary Table 1.

Using cross validated classification analysis, we found 91 EEG features with a significant AUC performance compared to the null models. The AUC values of the EEG features with significant classification performance ranged between 0.610 and 0.848 for the training sets and between 0.523 and 0.715 for the testing sets. The classification accuracies of the significant EEG features ranged between 0.691 and 0.873 for the training sets and between 0.590 and 0.736 for the testing sets. Out of the 69 EEG features, which showed a significant effect in the group comparison using ANCOVA, 57 features also showed a significant classification performance (Supplementary Table 3).

Correlations between EEG features

To evaluate to what extent features that showed significant group differences are sensitive to the same aspects of the disorder, we computed Pearson's correlations between pairs of features (Fig. 2). As the representative variable for each feature, we took the values of the electrode, brain region, or microstate parameter which showed the largest group difference according to Cohen's *d* (Fig. 1). Surprisingly, we found that, in the patients group, only 36.49% of the pairwise correlations were significant at a level of 0.05 (without correcting for multiple comparisons). For the control group, only 26.73% of the correlations were significant. Since significance depends on the sample size, here, we focus on the magnitude of the correlation coefficients (r-values). In general, the magnitudes of the r-values were very low in both patients (0.055, 0.122, and 0.251 for the 25th, 50th, and 75th percentiles, respectively) and controls (0.059, 0.129, and 0.242 for the 25th, 50th, and 75th percentiles, respectively; Fig. 2). Strong correlations were found mainly for pairs of very closely related features (Supplementary Tables 4 and 5), such as between waiting-time statistics of gamma bursts ("waiting time gamma") and life-time statistics of gamma bursts ("life time gamma"; r = 0.836 and r = 0.926 in patients and controls, respectively). Similar results were found when, instead of the variable showing the largest group difference, we selected the first principal component as the representative variable of each EEG feature showing a significant group difference between

patients and controls. The r-values were low in both patients (0.060, 0.152, and 0.313 for the 25th, 50th, and 75th percentiles, respectively) and controls (0.059, 0.135, and 0.264 for the 25th, 50th, and 75th percentiles, respectively). Similar results were found using disattenuated r-values (see Supplementary Results). Interestingly, when we put together all variables from all EEG features, 13,112 variables in total, and we corrected for multiple comparisons using Holm method, we found 272 variables from 16 EEG features which showed significant differences (see Supplementary Table 6). When we correlated these 16 EEG features, selecting the variable showing the largest effect as the representative variable, we found that correlations were stronger in patients (0.163, 0.317, and 0.454 for the 25th, 50th, and 75th percentiles, respectively) than in controls (0.088, 0.164, and 0.302 for the 25th, 50th, and 75th percentiles, respectively). Potentially, these features might be interesting for future investigations.

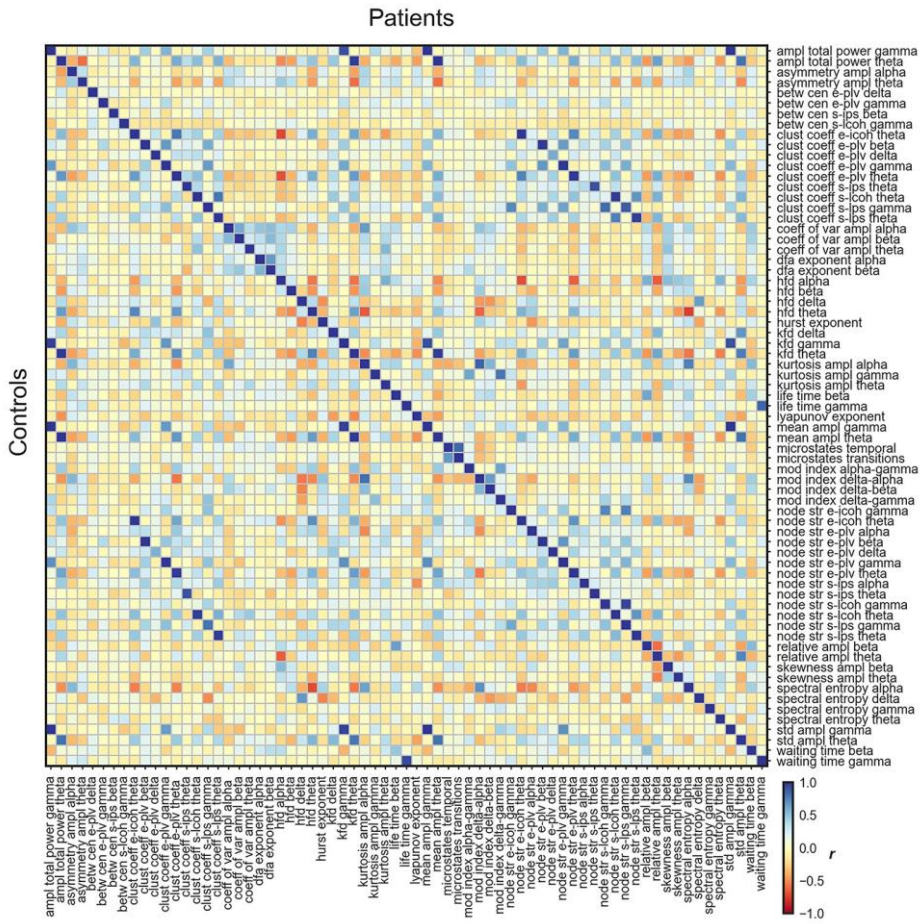

Fig. 2. Pairwise correlations between the 69 EEG features which showed significant group differences between patients and controls. Patients' r-values are presented in the upper triangle and controls' r-values are shown in the lower triangle. Strong negative and positive r-values are depicted in red and blue, respectively, and r-values around 0 in yellow. For each feature, we used the values of the electrode, brain region, or microstate parameter

which showed the largest effect size as the representative variable for the correlations. A list with the abbreviations and corresponding name of each feature is shown in Supplementary Table 1.

To quantify the overall shared information between pairs of EEG features, which showed significant group differences, by taking not only variables with the largest effect size into account but all variables of the features, we used PLSC and distance correlations. For the patients, 55.92% of the pairwise inertias were significant (without correcting for multiple comparisons) and for controls, 40.28%. In general, relative inertias were not very high in both patients (0.254, 0.329, and 0.409 for the 25th, 50th, and 75th percentiles, respectively) and controls (0.305, 0.387, and 0.472 for the 25th, 50th, and 75th percentiles, respectively; Fig. 3). As in the Pearson's correlation results, features that showed strong associations were mainly similar features, such as the same network statistics for different connectivity measures in the theta band, for example, at the electrode level: clustering coefficient connectivity estimated with the phase locking value ("clust coeff e-plv theta") and with the imaginary part of coherence ("clust coeff e-icoh theta"; $\mathfrak{I}_{relative}$= 0.804 and $\mathfrak{I}_{relative}$= 0.826, in patients and controls, respectively). Distance correlations show similar results. The distance correlation values were low in both patients (0.096, 0.189, and 0.329 for the 25th, 50th, and 75th percentiles, respectively) and controls (0.102, 0.168, and 0.303 for the 25th, 50th, and 75th percentiles, respectively). For the patients, 61.59% of the pairwise distance correlations were significant and 47.02% of the pairwise distance correlations were significant for controls (without correction for multiple comparisons). Disattenuated values were stronger for relative inertias, whereas for distance correlations, the values were not strong (see Supplementary Results).

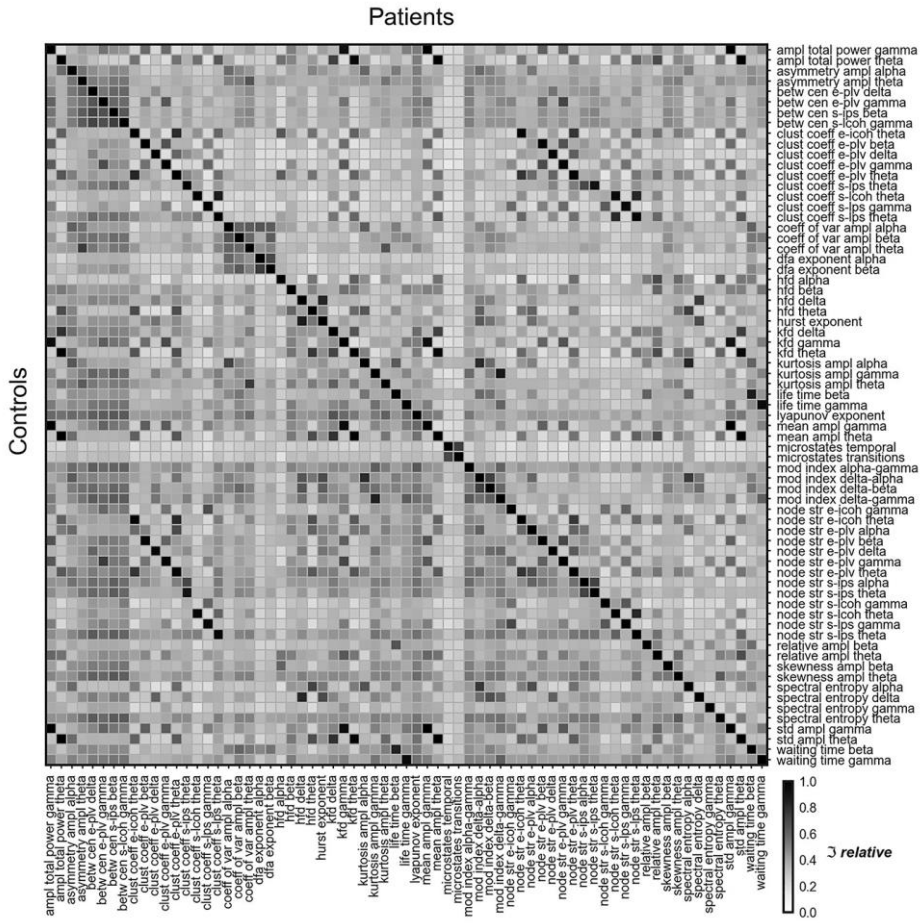

Fig. 3. Shared information between the 69 EEG features which showed significant group differences, as measured by the relative inertia ($\Im_{relative}$) computed with PLSC. The relative inertia ranges from 0 (the two features are completely unrelated) to 1 (the two features' values move together by the exact same percentage). Patients' relative inertias are presented in the upper triangle, and controls' relative inertias are shown in the lower triangle. A list with the abbreviations and corresponding name of each feature is shown in Supplementary Table 1.

Prediction of psychopathology scores

We evaluated whether EEG features were adequate predictors of psychopathology scores determined by the Scale for the Assessment of Positive Symptoms (SAPS) and the Scale for the Assessment of Negative Symptoms (SANS), which target positive (hallucinations, delusions, bizarre behavior, and positive formal thought disorder) and negative (affective flattening, alogia, apathy, anhedonia, and attention) symptoms, respectively. All 194 EEG features exhibited very weak out-of-sample predictive ability to both the SANS and SAPS scores. Results were very similar for both the linear (i.e., elastic net) and nonlinear (i.e., random forest) models. See Supplementary Table 7 and Supplementary Table 8 for details.

Discussion

Traditionally, most studies in schizophrenia research focus on a single experimental paradigm and analysis method, which shows significant differences between patients and controls. Extensive research with the paradigm tries to derive the underlying genetic and neurophysiological causes of the disorder. This approach has been quite successful in the formulation of hypotheses, such as the dopamine hypothesis (Howes and Kapur 2009), the social brain hypothesis (Burns 2006), the glutamate hypothesis (Hu et al. 2015), or the dysconnection hypothesis (Friston et al. 2016), just to name a few.

Here, we took a different road and examined to what extent abnormalities, quantified by different EEG features, correlate with each other. Many of the investigated features were previously linked to different abnormalities of brain processes in schizophrenia. Here, we reproduced many of these results, such as imbalance in microstates dynamics (Rieger et al. 2016; da Cruz et al. 2020a), decreased LRTC in the alpha and beta bands (Nikulin et al. 2012), decreased life time and waiting time in the beta band (Sun et al. 2014), increased spectral amplitude in the theta band (Boutros et al. 2008), increased connectivity in the theta band at the source level (Andreou et al. 2015; Di Lorenzo et al. 2015), and decreased Lyapunov exponent (Kim et al. 2000), among others. With our systematic analysis, we also found abnormalities in EEG features, which, to the best of our knowledge, have not been reported yet, namely, delta-phase gamma-amplitude coupling, range EEG coefficient of variation and asymmetry in the theta and alpha bands, etc. In some way, deeper analysis of each feature may have warranted an in-depth study and a potential publication. However, we did not want to elaborate on these methods individually because we wanted to understand how all EEG features relate to each other in their entirety.

The surprising insight from our analysis is that, even though we are probing the same signals from the same participants, we found only weak correlations between the 69 significant features. The only strong correlations we found were between features that are similar from the outset, thereby resembling test-retests. This suggests that, even though each EEG feature reveals clear-cut and reproducible differences between patients and controls, none of the features is truly representative for the disease. Hence, the traditional approach of focusing on a single experimental paradigm and analysis method has its limitations. These results remind

us that schizophrenia is indeed a very heterogeneous disease, a well-known fact, which is however not always taken seriously enough because, as mentioned above, most research tries to find the one or a few causes of schizophrenia within one well-described paradigm by digging as deep as possible into the underlying neurophysiological and genetic mechanisms. In analogy to botany, one may call these approaches "deep rooting" approaches.

There can be several reasons why we did not find strong correlations between EEG features even though they show clear-cut group effects. First, test re-test reliability may be low. However, similar EEG features showed strong correlations. Second, EEG features show clear-cut group differences, but variance in the patients and controls is low, leading to low correlations, the well-known reliability paradox (Hedge et al. 2018). However, variance is high, particularly, in the schizophrenia patients. Third, it may be that the linear and nonlinear methods we used are blind to more complex structures. Fourth, EEG features pick up disease-related and, to a substantial amount, also disease-unrelated aspects. When different EEG features tap into different of these disease-unrelated mechanisms, correlations may be low. For example, one EEG feature may strongly depend on the level of fatigue and another one on cardiac functions, which may be both intact in the patients. In this case, variance may be high in both populations but correlations may be low. We cannot determine to what extent this scenario holds true in our study. Fifth, schizophrenia is a heterogeneous disease and different EEG features tap into different aspects of the disease.

Particularly the fifth scenario suggests to complement "deep rooting" approaches with "shallow rooting" approaches, representing schizophrenia within a high-dimensional space, where many tests and analysis outcomes are used instead of one. In this respect, low correlations between tests are a wanted feature because different aspects of the disease are targeted—as long as the tests do not measure mainly disease-unrelated aspects. Tests should ideally have large effect sizes, low mutual correlations, and a "flat" factor structure. Whether this is possible is an open question and depends very much on the underlying causes of schizophrenia.

Current machine learning approaches are well within this spirit (Yang et al. 2010; Mothi et al. 2019; Phang et al. 2020; Morgan et al. 2021). For example, Clementz et al. (2016) analyzed 9 variables, including evoked EEG variables, with k-means clustering. Three clusters were found, which, however, did not correspond to DSM psychosis categories. Using sparse canonical

correlation analysis, a bundle of neuroimaging features showed strong links to lifestyle and demographic variables in schizophrenia and bipolar disorder patients (Moser et al. 2018). Future research will tell what we gain from "shallow rooting" approaches. The gain will strongly depend on the complexity of the disease.

Within a multifactorial framework, there are several possible scenarios of complexity. Our results show that there cannot be one cause. However, on the lowest complexity level, there may be a few independent causes, which were not found yet. Given the heterogeneity of the disease, including abnormalities in the cognitive (Andreasen et al. 1998), but also the skin functioning domain (Messamore 2012), the causes need to be on a rather general level, likely subcellular, present in all human functioning. On a medium complexity level, schizophrenia may be an approximatively "additive" disease, where many small abnormalities add up to severe symptoms. For example, the many single-nucleotide polymorphisms (SNPs) involved in schizophrenia may each contribute a little (Schizophrenia Working Group of the Psychiatric Genomics Consortium 2014). In an even more complex scenario, schizophrenia is a disease where many causes act in a truly combinatorial manner, i.e. focusing on a single or a few causes is of no avail. One needs always to take all causes into account, which may be impossible because such approaches require impossible sample sizes. For example, only certain combinations of redundant functions, each coming with at least two variants, cause the disease. If one function is upregulated and another one is downregulated in an individual, there are no abnormalities. Deficits manifest only when all or most functions are either up- or down-regulated. In such a combinatorial scenario, it would be difficult to find the underlying causes since each variant itself does not lead to a deficit; only certain combinations do.

Our study has several limitations. There are demographic differences between patients and controls, which might affect our group comparisons. However, we attempted to minimize these demographic effects by using education as a covariate and gender as factor in the analyses. Similarly, we cannot exclude effects of medication in our results. Nonetheless, we find similar patterns of correlations between EEG features, i.e. weak associations, in both patients and controls, suggesting that if there is an effect of medication, it is small. Further, our sample size is relatively small for achieving reliable estimates of predictive power (Schnack and Kahn 2016; Varoquaux 2018; Poldrack et al. 2020). Importantly, during resting-state EEG recordings, participants might be differently engaged into different aspects of cognitive

processing. However, the group effects revealed by the 69 EEG features indicate that there is abnormal processing even if the patients would engage differently into different aspects of cognition. Moreover, task-based EEG features also do not correlate strongly (Braff et al. 2006; Price et al. 2006; Seidman et al. 2015). In the healthy control group, the low correlations are only partly surprising since we do not know to what extent different EEG features tap into similar mechanisms, which is contrary to the patient group for which we know that the features are related to processing abnormalities. Still, it is surprising that so few features correlate in the control group as well and how similar the correlations look in patients and controls.

Our results and the complexity of the disease may explain a deep mystery in schizophrenia research. Schizophrenia has an estimated heritability of 70%–85% (Burmeister et al. 2008). For example, the chance to also suffer from schizophrenia for monozygotic twins is about 33% when the partner twin has the disease (Hilker et al. 2018). Furthermore, about 0.25%–0.75% people of a population suffer from schizophrenia and related psychotic disorders (Kessler et al. 2005; Saha et al. 2005; Moreno-Küstner et al. 2018). These values are rather stable across cultures (Simeone et al. 2015). Given that schizophrenia patients have less offspring (Bassett et al. 1996; Avila et al. 2001; Keller and Miller 2006; MacCabe et al. 2009), this provokes the question why schizophrenia has not been extinguished during the course of evolution (Keller and Miller 2006; Liu et al. 2019). In the above-mentioned combinatorial scenario with many redundant functions, this may simply happen because evolution operates on the individual SNP level and not on the combinatorial one. As long as most of the population shows average functioning, there will be no change of the allele distributions. In the additive scenario, evolution may extinct harmful alleles, of which each constitutes only a little risk, very slowly and these may be replaced by harmful de novo mutations (Keller and Miller 2006). To what extent such considerations hold true will be shown by “shallow rooting” approaches using a plethora of paradigms and a multiverse of analysis methods.

Acknowledgements

We would like to thank Marc Repnow for his comments and Ben Lönnqvist for proofreading the manuscript. M.H.H., E.C., A.B., and M.R. designed the research; M.R. and E.C. performed the research; J.R.d.C., D.G., W.-H.L., and O.F. analyzed the data; J.R.d.C., D.G., O.F. A.B., P.F.,

and M.H.H. wrote the paper. The codes that support the findings of this study are available upon request. The authors declare no competing interests.

Funding

This work was partially funded by the Fundação para a Ciência e a Tecnologia under grant FCT PD/BD/105785/2014 and the National Centre of Competence in Research (NCCR) Synapsy financed by the Swiss National Science Foundation under grant 51NF40-185897.

Conflict of interest statement: None declared.

References

Abdi H, Williams LJ. Partial least squares methods: Partial least squares correlation and partial least square regression. In: Reisfeld B, Mayeno AN, editors. *Computational toxicology. Methods in molecular biology*. Totowa (NJ): Humana Press; 2013. pp. 549–579

Andreasen NC, Paradiso S, O'Leary DS. "Cognitive dysmetria" as an integrative theory of schizophrenia: A dysfunction in cortical-subcortical-cerebellar circuitry? *Schizophr Bull*. 1998:24:203–218.

Andreou C, Leicht G, Nolte G, Polomac N, Moritz S, Karow A, Hanganu-Opatz IL, Engel AK, Mulert C. Resting-state theta-band connectivity and verbal memory in schizophrenia and in the high-risk state. *Schizophr Res*. 2015:161:299–307.

Avila M, Thaker G, Adami H. Genetic epidemiology and schizophrenia: a study of reproductive fitness. *Schizophr Res*. 2001:47:233–241.

Bassett AS, Bury A, Hodgkinson KA, Honer WG. Reproductive fitness in familial schizophrenia. *Schizophr Res*. 1996:21:151–160.

Boutros NN, Arfken C, Galderisi S, Warrick J, Pratt G, Iacono W. The status of spectral EEG abnormality as a diagnostic test for schizophrenia. *Schizophr Res*. 2008:99:225–237.

Braff DL, Freedman R, Schork NJ, Gottesman II. Deconstructing schizophrenia: an overview of the use of endophenotypes in order to understand a complex disorder. *Schizophr Bull*. 2006:33:21–32.

Braff DL, Light GA, Swerdlow NR. Prepulse inhibition and P50 suppression are both deficient but not correlated in schizophrenia patients. *Biol Psychiatry*. 2007:61:1204–1207.

Burmeister M, McInnis MG, Zöllner S. Psychiatric genetics: progress amid controversy. *Nat Rev Genet*. 2008:9:527–540.

Burns J. The social brain hypothesis of schizophrenia. *World Psychiatry Off J World Psychiatr Assoc WPA*. 2006:5:77–81.

Clementz BA, Sweeney JA, Hamm JP, Ivleva EI, Ethridge LE, Pearlson GD, Keshavan MS, Tamminga CA. Identification of distinct psychosis biotypes using brain-based biomarkers. *Am J Psychiatry*. 2016:173:373–384.

da Cruz JR, Chicherov V, Herzog MH, Figueiredo P. An automatic pre-processing pipeline for EEG analysis (APP) based on robust statistics. *Clin Neurophysiol*. 2018:129:1427–1437.

da Cruz JR, Favrod O, Roinishvili M, Chkonia E, Brand A, Mohr C, Figueiredo P, Herzog MH. EEG microstates are a candidate endophenotype for schizophrenia. *Nat Commun*. 2020a:11:3089.

da Cruz JR, Shaqiri A, Roinishvili M, Favrod O, Chkonia E, Brand A, Figueiredo P, Herzog MH. Neural compensation mechanisms of siblings of schizophrenia patients as revealed by high-density EEG. *Schizophr Bull*. 2020b:46:1009–1018.

Di Lorenzo G, Daverio A, Ferrentino F, Santarnecchi E, Ciabattini F, Monaco L, Lisi G, Barone Y, Di Lorenzo C, Niolu C, et al. Altered resting-state EEG source functional connectivity in schizophrenia: the effect of illness duration. *Front Hum Neurosci*. 2015:9:234.

Dickinson D, Goldberg TE, Gold JM, Elvevag B, Weinberger DR. Cognitive factor structure and invariance in people with schizophrenia, their unaffected siblings, and controls. *Schizophr Bull*. 2011:37:1157–1167.

Favrod O, Roinishvili M, da Cruz JR, Brand A, Okruashvili M, Gamkrelidze T, Figueiredo P, Herzog MH, Chkonia E, Shaqiri A. Electrophysiological correlates of visual backward masking in patients with first episode psychosis. *Psychiatry Res Neuroimaging*. 2018:282:64–72.

Friston K, Brown HR, Siemerkus J, Stephan KE. The dysconnection hypothesis (2016). *Schizophr Res*. 2016:176:83–94.

Garobbio S, Roinishvili M, Favrod O, da Cruz JR, Chkonia E, Brand A, Herzog MH. Electrophysiological correlates of visual backward masking in patients with bipolar disorder. *Psychiatry Res Neuroimaging*. 2021:307:111206.

Hedge C, Powell G, Sumner P. The reliability paradox: why robust cognitive tasks do not produce reliable individual differences. *Behav Res Methods*. 2018:50:1166–1186.

Hilker R, Helenius D, Fagerlund B, Skytthe A, Christensen K, Werge TM, Nordentoft M, Glenthøj B. Heritability of schizophrenia and schizophrenia spectrum based on the nationwide Danish twin register. *Biol Psychiatry*. 2018:83:492–498.

Howes OD, Kapur S. The dopamine hypothesis of schizophrenia: version III—the final common pathway. *Schizophr Bull*. 2009:35:549–562.

Hu W, MacDonald ML, Elswick DE, Sweet RA. The glutamate hypothesis of schizophrenia: evidence from human brain tissue studies: glutamate system and schizophrenia. *Ann N Y Acad Sci*. 2015:1338:38–57.

Keller MC, Miller G. Resolving the paradox of common, harmful, heritable mental disorders: Which evolutionary genetic models work best? *Behav Brain Sci*. 2006:29:385–404.

Kessler RC, Birnbaum H, Demler O, Falloon IRH, Gagnon E, Guyer M, Howes MJ, Kendler KS, Shi L, Walters E, et al. The prevalence and correlates of nonaffective psychosis in the National Comorbidity Survey Replication (NCS-R). *Biol Psychiatry*. 2005:58:668–676.

Kim D-J, Jeong J, Chae J-H, Park S, Yong Kim S, Jin Go H, Paik I-H, Kim K-S, Choi B. An estimation of the first positive Lyapunov exponent of the EEG in patients with schizophrenia. *Psychiatry Res Neuroimaging*. 2000:98:177–189.

Krishnan A, Williams LJ, McIntosh AR, Abdi H. Partial least squares (PLS) methods for neuroimaging: a tutorial and review. *NeuroImage*. 2011:56:455–475.

Liu C, Everall I, Pantelis C, Bousman C. Interrogating the evolutionary paradox of schizophrenia: a novel framework and evidence supporting recent negative selection of schizophrenia risk alleles. *Front Genet*. 2019:10:389.

MacCabe JH, Koupil I, Leon DA. Lifetime reproductive output over two generations in patients with psychosis and their unaffected siblings: the Uppsala 1915–1929 Birth Cohort Multigenerational study. *Psychol Med*. 2009:39:1667.

McIntosh AR, Bookstein FL, Haxby JV, Grady CL. Spatial pattern analysis of functional brain images using partial least squares. *NeuroImage*. 1996:3:143–157.

McIntosh AR, Chau WK, Protzner AB. Spatiotemporal analysis of event-related fMRI data using partial least squares. *NeuroImage*. 2004:23:764–775.

Messamore E. Niacin subsensitivity is associated with functional impairment in schizophrenia. *Schizophr Res*. 2012:137:180–184.

Meyer-Lindenberg A, Poline J-B, Kohn PD, Holt JL, Egan MF, Weinberger DR, Berman KF. Evidence for abnormal cortical functional connectivity during working memory in schizophrenia. *Am J Psychiatry*. 2001:158:1809–1817.

Moreno-Küstner B, Martín C, Pastor L. Prevalence of psychotic disorders and its association with methodological issues. A systematic review and meta-analyses. *PLoS One*. 2018:13:e0195687.

Morgan SE, Young J, Patel AX, Whitaker KJ, Scarpazza C, van Amelsvoort T, Marcelis M, van Os J, Donohoe G, Mothersill D, et al. Functional magnetic resonance imaging connectivity accurately distinguishes cases with psychotic disorders from healthy controls, based on cortical features associated with brain network development. *Biol Psychiatry Cogn Neurosci Neuroimaging*. 2021:6:1125–1134.

Moser DA, Doucet GE, Lee WH, Rasgon A, Krinsky H, Leibu E, Ing A, Schumann G, Rasgon N, Frangou S. Multivariate associations among behavioral, clinical, and multimodal imaging phenotypes in patients with psychosis. *JAMA Psychiatry*. 2018:75:386.

Mothi SS, Sudarshan M, Tandon N, Tamminga C, Pearlson G, Sweeney J, Clementz B, Keshavan MS. Machine learning improved classification of psychoses using clinical and biological stratification: update from the bipolar-schizophrenia network for intermediate phenotypes (B-SNIP). *Schizophr Res*. 2019:214:60–69.

Nikulin VV, Jönsson EG, Brismar T. Attenuation of long-range temporal correlations in the amplitude dynamics of alpha and beta neuronal oscillations in patients with schizophrenia. *NeuroImage*. 2012:61:162–169.

Phang C-R, Noman F, Hussain H, Ting C-M, Ombao H. A multi-domain connectome convolutional neural network for identifying schizophrenia from EEG connectivity patterns. *IEEE J Biomed Health Inform*. 2020:24:1333–1343.

Poldrack RA, Huckins G, Varoquaux G. Establishment of best practices for evidence for prediction: a review. *JAMA Psychiatry*. 2020:77:534.

Price GW, Michie PT, Johnston J, Innes-Brown H, Kent A, Clissa P, Jablensky AV. A multivariate electrophysiological endophenotype, from a unitary cohort, shows greater research utility than any single feature in the Western Australian family study of schizophrenia. *Biol Psychiatry*. 2006:60:1–10.

Rieger K, Diaz Hernandez L, Baenninger A, Koenig T. 15 years of microstate research in schizophrenia—Where are we? A meta-analysis. *Front Psychiatry*. 2016:7:22.

Rybakowski J, Weterle R. Niacin test in schizophrenia and affective illness. *Biol Psychiatry*. 1991:29:834–836.

Saha S, Chant D, Welham J, McGrath J. A systematic review of the prevalence of schizophrenia. *PLoS Med*. 2005:2:e141.

Schizophrenia Working Group of the Psychiatric Genomics Consortium. Biological insights from 108 schizophrenia-associated genetic loci. *Nature*. 2014:511:421–427.

Schnack HG, Kahn RS. Detecting neuroimaging biomarkers for psychiatric disorders: sample size matters. *Front Psychiatry*. 2016:7:50.

Seidman LJ, Hellemann G, Nuechterlein KH, Greenwood TA, Braff DL, Cadenhead KS, Calkins ME, Freedman R, Gur RE, Gur RC, et al. Factor structure and heritability of endophenotypes in schizophrenia: findings from the Consortium On The Genetics of Schizophrenia (COGS-1). *Schizophr Res*. 2015:163:73–79.

Simeone JC, Ward AJ, Rotella P, Collins J, Windisch R. An evaluation of variation in published estimates of schizophrenia prevalence from 1990–2013: a systematic literature review. *BMC Psychiatry*. 2015:15:193.

Sun J, Tang Y, Lim KO, Wang J, Tong S, Li H, He B. Abnormal dynamics of EEG oscillations in schizophrenia patients on multiple time scales. *IEEE Trans Biomed Eng*. 2014:61:1756–1764.

Székely GJ, Rizzo ML. The distance correlation t -test of independence in high dimension. *J Multivar Anal*. 2013:117:193–213.

Toomey R, Faraone SV, Seidman LJ, Kremen WS, Pepple JR, Tsuang MT. Association of neuropsychological vulnerability markers in relatives of schizophrenic patients. *Schizophr Res*. 1998:31:89–98.

Tucker LR. An inter-battery method of factor analysis. *Psychometrika*. 1958:23:111–136.

Uhlhaas PJ, Singer W. Abnormal neural oscillations and synchrony in schizophrenia. *Nat Rev Neurosci*. 2010:11:100–113.

Varoquaux G. Cross-validation failure: small sample sizes lead to large error bars. *NeuroImage*. 2018:180:68–77.

Venables NC, Bernat EM, Sponheim SR. Genetic and disorder-specific aspects of resting state EEG abnormalities in schizophrenia. *Schizophr Bull*. 2009:35:826–839.

Yang H, Liu J, Sui J, Pearlson G, Calhoun VD. A hybrid machine learning method for fusing fMRI and genetic data: combining both improves classification of schizophrenia. *Front Hum Neurosci*. 2010:4:192.

Zou H, Hastie T. Regularization and variable selection via the elastic net. *J R Stat Soc Ser B Stat Methodol*. 2005:67:301–320.

Chapter 3. Stability assessment of resting-state EEG in schizophrenia

Dario Gordillo [1], Eka Chkonia [2,3], Andreas Brand[1], Maya Roinishvili [3,4], Michael H. Herzog [1]

[1] Laboratory of Psychophysics, Brain Mind Institute, School of Life Sciences, École Polytechnique Fédérale de Lausanne (EPFL), CH-1015 Lausanne, Switzerland,

[2] Department of Psychiatry, Tbilisi State Medical University (TSMU), 0186 Tbilisi, Georgia,

[3] Institute of Cognitive Neurosciences, Free University of Tbilisi, 0159 Tbilisi, Georgia,

[4] Laboratory of Vision Physiology, Ivane Beritashvili Centre of Experimental Biomedicine, 0160 Tbilisi, Georgia

This section presents preliminary results of an ongoing project examining the stability of resting-state EEG features in patients with schizophrenia.

Preliminary Results

We identified 82 out of 148 EEG features that showed a significant difference between patients with schizophrenia and healthy controls. This comparison was conducted using a sample of 135 patients with schizophrenia and 92 healthy controls (see Table 1). Importantly, some of the EEG features included in this study were not considered in Gordillo et al. (2023). For example, we defined spectral and frequency features in six frequency bands instead of five. Detailed information regarding the EEG analyses is presented in the Methods section. Furthermore, due to the larger sample size in the present study, we had increased statistical power to detect features showing group differences. The effect sizes (Cohen's *d*) for the EEG features demonstrating significant differences between groups ranged from 0.41 to 0.96.

Stability assessment

The stability of EEG features was assessed using a retest sample comprising 40 patients with schizophrenia and 27 healthy controls. Resting-state EEG data were recorded after an average of 4.461 (±1.543) years for patients and 4.745 (±1.56) years for healthy controls (for details, see Table 2). For each variable (electrode, brain region, or microstate parameter/transition), we calculated the intraclass correlation coefficient (ICC) and Spearman correlation.

Additionally, we computed multivariate distance correlations considering the entire set of variables for each EEG feature. This analysis was conducted separately for each group.

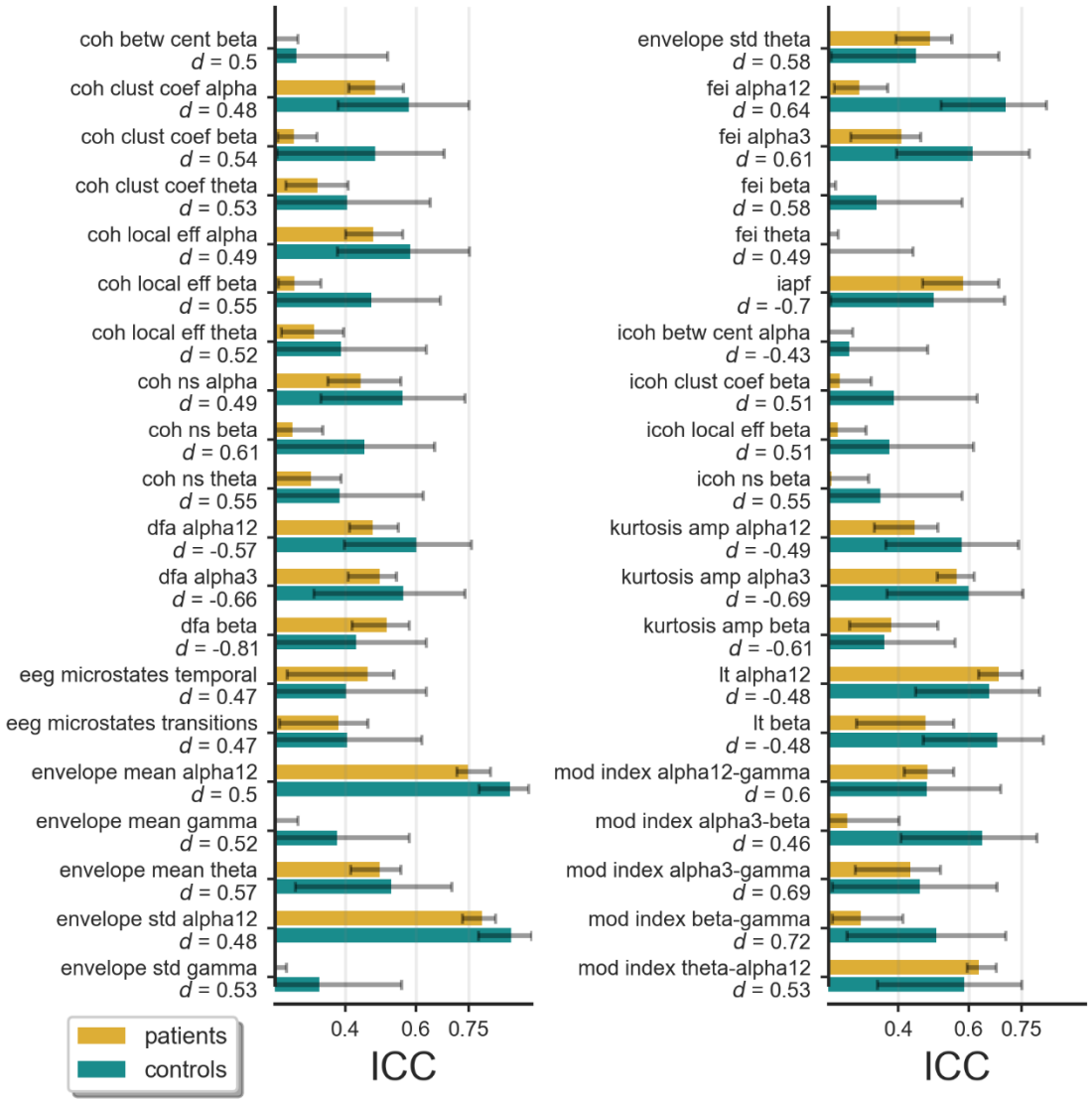

Figure 1. Intraclass correlation coefficients (ICC) of 40 out of 82 EEG features demonstrating a significant group difference between patients with schizophrenia and controls. Group difference analyses were conducted using the sample described in Table 1, comprising 135 patients with schizophrenia and 92 healthy controls. Stability was assessed separately for each group. Below the names of the EEG features, we display the maximum effect size observed in the group difference analysis. Confidence intervals represent the 25th and 75th percentiles of ICC values across electrodes, brain regions, or microstate parameters/transitions.

In the patient group, out of the 82 EEG features showing differences between groups, 36 exhibited (median) ICC values below 0.4, indicating poor reliabilities. Additionally, 36 features showed fair reliabilities, with ICC values ranging between 0.4 and 0.59. Nine features demonstrated good reliabilities, with ICC values between 0.6 and 0.75, while only one feature, specifically the envelope standard deviation in the alpha 12 band, exhibited excellent reliability

with an ICC value above 0.75. For the control group, 22 EEG features showed poor reliabilities, 35 exhibited fair reliabilities, 16 demonstrated good reliabilities, and 9 exhibited excellent reliabilities, all out of the 82 EEG features showing differences between groups.

In patients with schizophrenia, the 25th, 50th, and 75th percentiles of the (median) Spearman correlations across the 82 EEG features showing group differences were 0.28, 0.45, and 0.55, respectively. For controls, the corresponding percentile values were 0.40, 0.51, and 0.65. For multivariate distance correlations, which range from 0 to 1, the 25th, 50th, and 75th percentiles for patients were 0.64, 0.70, and 0.77, respectively. For controls, the corresponding percentiles were 0.72, 0.78, and 0.86.

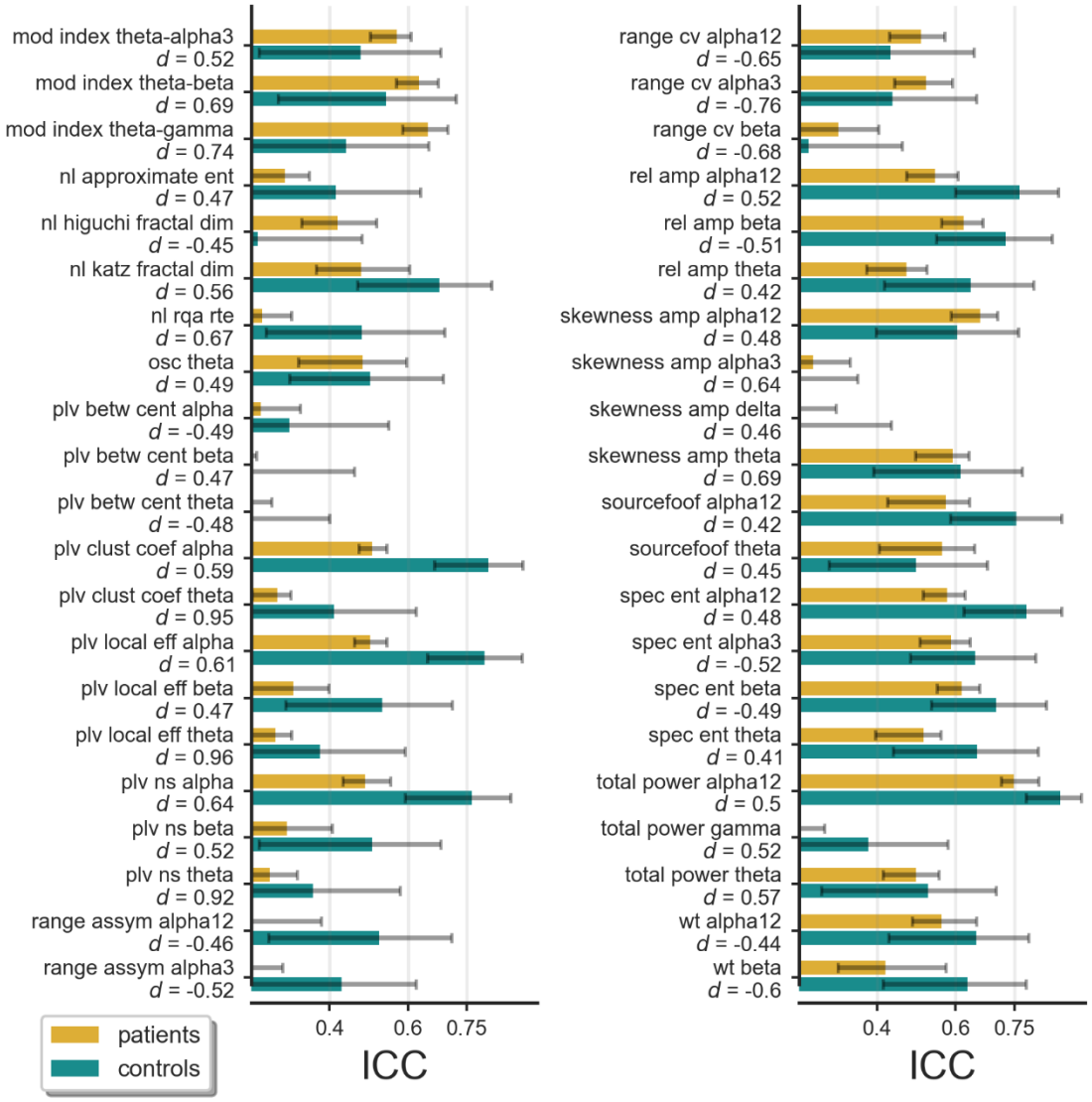

Figure 2. Intraclass correlation coefficients (ICC) of 42 (not presented in Figure 1) out of 82 EEG features demonstrating a significant group difference between patients with schizophrenia and controls. Group difference analyses were conducted using the sample described in Table 1, comprising 135 patients with schizophrenia and

92 healthy controls. Stability was assessed separately for each group. Below the names of the EEG features, we display the maximum effect size observed in the group difference analysis. Confidence intervals represent the 25th and 75th percentiles of ICC values across electrodes, brain regions, or microstate parameters/transitions.

Methods

Participants

Patients with schizophrenia were recruited from the Tbilisi Mental Health Hospital or the psycho-social rehabilitation center. They were invited to participate in the experiments after recovering from an acute episode. Diagnosis of schizophrenia was conducted according to the Diagnostic and Statistical Manual of Mental Disorders Fourth Edition (DSM-IV) criteria. This diagnosis was established through an interview based on the Structured Clinical Interview for DSM-IV, Clinical Version, along with information from staff and a review of patients' records. Psychopathology in patients was assessed using the Scale for the Assessment of Negative Symptoms (SANS) and the Scale for the Assessment of Positive Symptoms (SAPS).

Control participants were recruited from the general population in Tbilisi, Georgia, with the aim of matching patients' demographics as closely as possible. Controls were eligible to participate if they did not have any psychiatric axis I disorders and had no family history of psychosis. General exclusion criteria included alcohol or drug abuse, severe neurological incidents or diagnoses, developmental disorders (such as autism spectrum disorder or intellectual disability), or other somatic mind-altering conditions.

All participants provided informed consent and were informed of their right to withdraw from the experiment at any time. The study procedures were conducted in compliance with the Declaration of Helsinki (except for pre-registration) and were approved by the Ethical Committee of the Institute of Postgraduate Medical Education and Continuous Professional Development in Georgia (Protocol number: 09/07; Title: "Genetic polymorphisms and early information processing in schizophrenia").

Recording time 1

We present data from 135 patients with schizophrenia and 92 healthy controls. Previously published data included 121 patients with schizophrenia and 75 healthy controls (Gordillo, da

Cruz, Chkonia, et al., 2023). All participants underwent a battery of behavioral paradigms and resting-state EEG recordings. Among the 135 patients, 121 were receiving neuroleptic medication, with Chlorpromazine (CPZ) equivalents indicated in Table 1. There were 40 inpatients and 95 outpatients. The maximum age for patients was up to 55 years, while for controls, it was up to 62 years. Detailed group characteristics are provided in Table 1.

Recording time 2

Resting-state EEG data were collected from 40 patients with schizophrenia and 27 healthy controls after an average of 4.461 years (±1.543 SD) for patients (range: 1.99 - 9.96 years) and 4.745 years (±1.56 SD) for healthy controls (range: 2.675 - 10.563 years). Details regarding the sample characteristics are provided in Table 2. Psychopathology in patients was re-assessed using SANS and SAPS. At recording time 1, four patients were receiving neuroleptic medication but not at recording time 2, while three patients were not receiving medication at recording time 1 but were receiving medication at recording time 2. Additionally, thirty-one patients were receiving medication at both recording moments.

Table 1. Group average statistics of all subjects recorded at time 1

	Patients	Controls	Statistics
Sex (F/M)	27/108	44/48	$\chi^2(1) = 18.436$, $p = 1.757e\text{-}5$[b]
Age (years)	36.2 ± 9.2	36.7 ± 9.3	$t(225) = -0.359$, $p = 0.720$[c]
Education (years)	13.3 ± 2.6	15.3 ± 3.0	$t(225) = -5.341$, $p = 2.260e\text{-}7$[c]
Handedness (L/R)	6/129	5/87	$\chi^2(1) = 0.001$, $p = 0.979$[b]
Illness duration (years)	11.3 ± 8.5		
SANS	10.4 ± 5.3		
SAPS	8.5 ± 3.2		
CPZ equivalent[a]	579.4 ± 395.0		

SANS - Scale for the Assessment of Negative Symptoms, SAPS - Scale for Assessment of Positive, CPZ - chlorpromazine

[a]Average CPZ equivalents calculated over the 121 patients receiving neuroleptic medication

[b]Pearson's chi-squared test

[c]Two-sided independent samples *t*-test

Table 2. Group average statistics of subjects with two recordings

	Patients 1	Patients 2	Statistics Patients	Controls 1	Controls 2	Statistics Controls
Sex (F/M)	5/35	5/35		7/20	7/20	
Age (years)	37.2 ± 9.6	41.4 ± 9.7	$t(39) = 16.393$, $p = 4.344e\text{-}19$[b]	33.7 ± 7.8	38.1 ± 7.9	$t(26) = 12.952$, $p = 7.585e\text{-}13$[b]
Handedness (L/R)	3/37	3/37		2/25	2/25	
Illness duration (years)	13.7 ± 8.9	18.2 ± 9.3	$t(39) = 13.355$, $p = 3.942e\text{-}16$[b]			
SANS	10.1 ± 5.1	11.1 ± 5.3	$t(39) = 1.542$, $p = 0.131$[b]; $rho=0.713$, $p = 2.403e\text{-}7$[c]			
SAPS	8.2 ± 3.2	8.2 ± 2.7	$t(39) = 0.085$, $p = 0.933$[b]; $rho=0.237$, $p = 0.141$[c]			
CPZ equivalent[a]	629.9 ± 456.7	667.2 ± 450.2	$t(30) = -0.103$, $p = 0.918$[b]; $rho=0.399$, $p = 0.028$[c]			

[a]Average CPZ equivalents calculated over 35 and 34 patients receiving neuroleptic medication at recording time 1 and 2, respectively.

[b]Paired *t*-test

[c]Spearman correlation

EEG recording and preprocessing

Participants were instructed to sit in a dimly lit room with their eyes closed and relax for 5 minutes. Resting-state EEG data were recorded using a BioSemi Active Two Mk2 system (Biosemi B.V., The Netherlands) equipped with 64 Ag-AgCl sintered active electrodes, referenced to the common mode sense electrode. The recording sampling rate was set to 2048 Hz for both recording sessions. The same recording system was utilized for both time points.

Subsequently, the data were downsampled to 256 Hz and processed using an automated pipeline (da Cruz et al., 2018). A step was included to discard time points with amplitudes exceeding ± 400uV, considering a window of ±200ms around these points. Preprocessing steps consisted of bandpass filtering in the range of 1–90 Hz, removal of powerline noise, re-referencing to the biweight estimate of the mean across all channels, identification and interpolation of bad channels using 3D spline interpolation, removal of bad EEG segments, independent component analysis for the removal of eye movement, muscular, and other artifacts related to bad channels, and re-referencing to a common average reference.

EEG analysis

Periodic and aperiodic components of power spectra

Using the Fitting Oscillations & One Over F (FOOOF) algorithm (Donoghue et al., 2020), we extracted four EEG features: the Individual Alpha Peak Frequency (IAPF), Individual Alpha Peak Power, the 1/f slope, and the 1/f offset of the power spectra. Initially, the continuous EEG data were segmented into 4-second windows with a 50% overlap, and the power spectrum was computed using the Fast Fourier Transform (FFT) and a Hanning window using the FieldTrip toolbox for MATLAB (Oostenveld et al., 2011). Subsequently, the average spectrum was analyzed using the FOOOF algorithm, enabling the identification of oscillatory peaks in the power spectra as well as non-oscillatory features.

Importantly, we utilized the IAPF to define individualized frequency bands based on recent research and recommendations (Babiloni et al., 2020; Popov et al., 2023). Specifically, six frequency bands were determined: delta (1 – [IAPF-6 Hz]), theta ([IAPF-6 Hz] – [IAPF-4 Hz]), alpha1/2 ([IAPF-4 Hz] - IAPF), alpha3 (IAPF – [IAPF+2 Hz]), beta ([IAPF+2 Hz] - 30 Hz), and gamma (30 Hz to 40 Hz). From the oscillatory spectra, we also derived power values in the theta, alpha1/2, alpha3, and beta bands.

Temporal correlations

Temporal correlations were assessed for the delta, theta, alpha1/2, alpha3, and beta frequency bands, as the delta and gamma bands did not exhibit strong oscillations with the FOOOF analysis. We computed both long-range (> 1 second) temporal correlations (LRTC) and short-term (~< 1 second) autocorrelations of EEG oscillations. To calculate LRTC, we employed

detrended fluctuation analysis (DFA), whereas short-term autocorrelations were determined using the life and waiting times algorithm. In both analyses, we utilized the amplitude envelopes of the band-pass filtered EEG signals instead of the raw time series, focusing on how the amplitude of the oscillations changes over time. The amplitude envelopes were derived using the Hilbert transform.

DFA

To conduct detrended fluctuation analysis (DFA), we initially defined 20 window sizes ranging from 1 to 25 seconds, distributed logarithmically. At each window size, we detrended the integrated amplitude envelope and computed the variance, known as the fluctuation function. We employed 50% overlapping windows to augment the number of windows and, consequently, the signal-to-noise ratios. Subsequently, for each window size, we calculated the average fluctuation function across the overlapping windows. A line was fitted to these average fluctuation functions in a logarithmic scale. The slope of this fitted line determined the scaling exponent.

Life and waiting times

Life and waiting times analysis quantifies characteristics of the duration of oscillation bursts. To determine the onset and end of oscillation bursts, we relied on a threshold derived from the median amplitude envelope. Subsequently, we obtained distributions for life and waiting times, representing the durations of bursts above or below the threshold for the entire signal length. We then calculated the 95th percentile of these distributions for each electrode, which was subsequently utilized for further analysis.

Functional excitation inhibition ratio

Functional excitation/inhibition ratios (fE/I) were devised as proxies for the E/I balance of brain networks that demonstrate critical dynamics (Bruining et al., 2020). Initially, the amplitude envelopes of the time series were computed using the Hilbert transform and segmented into 80% overlapping 5-second windows. Subsequently, the amplitude envelope for each window was integrated and divided by the mean amplitude. The resulting amplitude-normalized data were detrended, and the standard deviation was computed to yield a normalized fluctuation function. The fE/I was calculated as one minus the Pearson correlation between the amplitude

and normalized fluctuation functions across all windows. Notably, only electrodes exhibiting a DFA exponent above 0.6 were included in the fE/I analysis.

Source analysis

For source analyses, including the generation of connectivity matrices as described in the Connectivity analysis section, we closely followed the methods outlined by Popov et al. (2023). Utilizing the headmodel provided in https://www.fieldtriptoolbox.org/tutorial/networkanalysis_eeg/, we implemented a parcellation scheme comprising 24 brain regions (12 per hemisphere) based on the Desikan-Killiani atlas (Desikan et al., 2006). This identical parcellation scheme was employed in a previous study (Popov et al., 2023). Opting for a smaller number of parcels may potentially enhance signal-to-noise ratios compared to larger parcellations, given the low spatial resolution of EEG. The single-dipole leadfields within each brain parcel were concatenated. Next, we generated time-series data for each brain region through principal component analysis (PCA). These source time series were then subjected to spectral analysis from 1 to 40 Hz and analyzed using the FOOOF algorithm to quantify source oscillatory power within each frequency band. Specifically, we obtained source spectral power in the theta, alpha1/2, alpha3, and beta frequency bands.

Connectivity analysis

EEG connectivity analyses were conducted in both electrode and source space using the FieldTrip toolbox. In electrode space, we employed the phase-locking value and imaginary coherence algorithms. Before connectivity analysis in the electrode space, scalp current densities were derived using the spline method. For source connectivity analysis, we utilized only the imaginary coherence algorithm. Source time series were estimated using the linearly constrained minimum variance beamforming algorithm (LCMV).

Connectivity analyses were focused specifically at the peak of the alpha frequency, as well as in the beta and theta bands. The resulting functional connectivity matrices were analyzed using the brain connectivity toolbox (BCT). Four network measures were derived: node strength, clustering coefficient, local efficiency, and betweenness centrality.

Nonlinear features

We extracted 19 full-band nonlinear and entropy features for each electrode. These features included sample entropy, permutation entropy, approximate entropy, Katz fractal dimension, Higuchi fractal dimension, Hjorth parameters (activity, mobility, and complexity), Lempel-Ziv complexity, correlation dimension, Lyapunov exponents, as well as recurrence quantification analysis features (determinism, mean diagonal length, entropy, laminarity, trapping time, recurrence time entropy, and maximum vertical time length).

To calculate these features, EEG data were initially segmented into 4-second time windows. Each measure was then computed within each window and subsequently averaged. Detailed procedures for obtaining these features have been outlined in (Gordillo, da Cruz, Moreno, et al., 2023).

EEG microstates

First, the continuous EEG data underwent bandpass filtering between 2 and 20 Hz, a common frequency band used across studies (Tarailis et al., 2023). The initial step of the microstate analysis involved identifying a set of representative topographic maps for each subject. Only topographic maps at global field power (GFP) peaks were considered for analysis due to their higher signal-to-noise ratios. A modified k-means procedure was then applied to these maps, repeated 100 times, and the solution with the highest explained variance was retained. The optimal number of clusters was determined using cross-validation, with cluster centers ranging from 4 to 7.

Subsequently, individual maps were concatenated and subjected to another modified k-means procedure, repeated 500 times, with the number of clusters again ranging from 4 to 7. The representative maps for the back-fitting procedures were obtained from a large sample comprising 135 patients and 92 controls. Notably, both patients and controls were included together to obtain these representative maps, aligning with recent recommendations (Murphy et al., 2024).

The obtained maps were backfitted to the bandpass-filtered data, and the resulting fitted microstate sequence was smoothed using the 'windowed' option with default parameters in the microstates EEGLAB toolbox (Poulsen et al., 2018). From this analysis, we derived

microstate duration, time coverage, global explained variance, and occurrence as temporal parameters, along with pairwise transition probabilities.

Spectral and amplitude features

The subsequent analyses were conducted separately for each of the six individualized frequency bands defined previously.

Statistics of amplitude envelopes

The electrode time series were initially divided into 4-second segments, and each analysis was performed on each segment before averaging across segments. Five statistical descriptors of the distribution of the signal and amplitude envelopes were computed. Amplitude envelopes were derived using the Hilbert transform. The descriptors included the mean and standard deviation of the amplitude envelopes, kurtosis, skewness, and total power of the signals. Additionally, peak-to-peak asymmetries were calculated using the range-EEG analysis method.

Spectral entropies and relative amplitudes

To derive these features, the continuous EEG data were initially segmented into 4-second windows with a 50% overlap, and the power spectrum was computed using fast Fourier transform (FFT) with a Hanning window. Subsequently, the average spectrum for each electrode was examined. Relative amplitudes were determined by computing the ratio between the sum of the power spectrum values within the bounds of the frequency band of interest and the sum of the power spectrum values of the full-band signal. Spectral entropy was computed as Shannon's entropy of the ratio between the normalized power spectrum in the frequency band under analysis and the normalized power spectrum of the full-band signal.

Phase-amplitude coupling

Cross-frequency couplings were assessed using the modulation index. Initially, electrode time series were partitioned into non-overlapping segments lasting 4 seconds each and were then filtered into the theta, alpha1/2, alpha3, beta, and gamma bands, utilizing the individualized frequency bands determined based on the Individual Alpha Peak Frequency (IAPF) (refer to Periodic and aperiodic components of power spectra). Subsequently, nine cross-frequency interactions were defined: Theta phase with alpha1/2, alpha3, beta, and gamma amplitudes;

alpha1/2 phase with beta and gamma amplitudes; alpha3 phase with beta and gamma amplitudes; and beta phase with gamma amplitudes. To compute these interactions, the phase and amplitude time series were derived using the instantaneous phase and amplitudes obtained through the Hilbert transform. Phase values were discretized into 18 bins (ranging from -180 to 180 degrees), and the mean amplitude value for each bin (of the modulated frequency band) was computed. Kullback-Leibler (KL) divergence was then employed to measure the disparity between uniformly distributed amplitudes across bin phase values (indicating no couplings) and the actual data. The average KL divergence across the 4-second windows was computed and utilized for subsequent analyses.

Statistical analysis

Group differences

We utilized the identical group difference analysis methodology as detailed in Gordillo et al. (2023). For each variable (i.e., electrodes, brain regions, or microstate parameters/transitions) of every EEG feature, we conducted an analysis of covariance (ANCOVA) incorporating GROUP and SEX as factors, with EDUCATION serving as a covariate, given that these characteristics displayed group differences (refer to Table 1). We corrected for multiple comparisons within each EEG feature. For instance, for EEG features in electrode space, we executed 64 ANCOVAs, and subsequently adjusted the resulting 64 P-values for the effect of GROUP using false discovery rates (FDR) with an error rate of 5%. The effect sizes η^2 of the ANCOVAs were converted to Cohen's *d*.

Stability assessment

To evaluate the stability of features, we employed intraclass correlations with model 3,1 (ICC3,1). ICC3,1 offers the advantage of considering mean differences between repeated measurements. Therefore, high ICC values not only signify higher stability of the ranks but also indicate stability of the values themselves. We calculated ICC3,1 values for each electrode separately. As EEG features comprise varying numbers of electrodes, brain regions, and microstate temporal parameters/transitions, to summarize the reliability of each feature, we reported the 25th, 50th, and 75th percentiles of the ICC values. The *intraclass_corr* function

from the *Pingouin* package was used for ICC calculation. Following previously established criteria by Cicchetti (1994), reliability was categorized as poor if values were below 0.4, fair between 0.4 and 0.59, good between 0.6 and 0.75, and excellent if above 0.75. Additionally, we assessed stability using Spearman and multivariate distance correlations. The latter allowed us to evaluate stability by considering all variables of the EEG features. For this purpose, we utilized the *distance_correlation* function from the *dcor* package for Python.

References

Babiloni, C., Barry, R. J., Başar, E., Blinowska, K. J., Cichocki, A., Drinkenburg, W. H. I. M., Klimesch, W., Knight, R. T., Lopes da Silva, F., Nunez, P., Oostenveld, R., Jeong, J., Pascual-Marqui, R., Valdes-Sosa, P., & Hallett, M. (2020). International Federation of Clinical Neurophysiology (IFCN) – EEG research workgroup: Recommendations on frequency and topographic analysis of resting state EEG rhythms. Part 1: Applications in clinical research studies. *Clinical Neurophysiology*, *131*(1), 285–307. https://doi.org/10.1016/j.clinph.2019.06.234

Bruining, H., Hardstone, R., Juarez-Martinez, E. L., Sprengers, J., Avramiea, A.-E., Simpraga, S., Houtman, S. J., Poil, S.-S., Dallares, E., Palva, S., Oranje, B., Matias Palva, J., Mansvelder, H. D., & Linkenkaer-Hansen, K. (2020). Measurement of excitation-inhibition ratio in autism spectrum disorder using critical brain dynamics. *Scientific Reports*, *10*(1), 9195. https://doi.org/10.1038/s41598-020-65500-4

Cicchetti, D. V. (1994). Guidelines, criteria, and rules of thumb for evaluating normed and standardized assessment instruments in psychology. *Psychological Assessment*, *6*(4), 284–290. https://doi.org/10.1037/1040-3590.6.4.284

da Cruz, J. R., Chicherov, V., Herzog, M. H., & Figueiredo, P. (2018). An automatic pre-processing pipeline for EEG analysis (APP) based on robust statistics. *Clinical Neurophysiology*, *129*(7), 1427–1437. https://doi.org/10.1016/j.clinph.2018.04.600

Desikan, R. S., Ségonne, F., Fischl, B., Quinn, B. T., Dickerson, B. C., Blacker, D., Buckner, R. L., Dale, A. M., Maguire, R. P., Hyman, B. T., Albert, M. S., & Killiany, R. J. (2006). An automated labeling system for subdividing the human cerebral cortex on MRI scans into gyral based regions of interest. *NeuroImage*, *31*(3), 968–980. https://doi.org/10.1016/j.neuroimage.2006.01.021

Donoghue, T., Haller, M., Peterson, E. J., Varma, P., Sebastian, P., Gao, R., Noto, T., Lara, A. H., Wallis, J. D., Knight, R. T., Shestyuk, A., & Voytek, B. (2020). Parameterizing neural power spectra into periodic and aperiodic components. *Nature Neuroscience*, *23*(12), 1655–1665. https://doi.org/10.1038/s41593-020-00744-x

Gordillo, D., da Cruz, J. R., Chkonia, E., Lin, W.-H., Favrod, O., Brand, A., Figueiredo, P., Roinishvili, M., & Herzog, M. H. (2023). The EEG multiverse of schizophrenia. *Cerebral Cortex*, *33*(7), 3816–3826. https://doi.org/10.1093/cercor/bhac309

Gordillo, D., da Cruz, J. R., Moreno, D., Garobbio, S., & Herzog, M. H. (2023). Do we really measure what we think we are measuring? *iScience*, *26*(2), 106017. https://doi.org/10.1016/j.isci.2023.106017

Murphy, M., Wang, J., Jiang, C., Wang, L. A., Kozhemiako, N., Wang, Y., the GRINS Consortium, Wang, J., Jiang, C., Gai, G., Zou, K., Wang, Z., Yu, X., Wang, G., Tan, S., Murphy, M., Hall, M. H., Zhu, W., Zhou, Z., … Purcell, S. M. (2024). A Potential Source of Bias in Group-Level EEG Microstate Analysis. *Brain Topography*, *37*(2), 232–242. https://doi.org/10.1007/s10548-023-00992-7

Oostenveld, R., Fries, P., Maris, E., & Schoffelen, J.-M. (2011). FieldTrip: Open Source Software for Advanced Analysis of MEG, EEG, and Invasive Electrophysiological Data. *Computational Intelligence and Neuroscience*, *2011*, 1–9. https://doi.org/10.1155/2011/156869

Popov, T., Tröndle, M., Baranczuk-Turska, Z., Pfeiffer, C., Haufe, S., & Langer, N. (2023). Test–retest reliability of resting-state EEG in young and older adults. *Psychophysiology*, *60*(7), e14268. https://doi.org/10.1111/psyp.14268

Poulsen, A. T., Pedroni, A., Langer, N., & Hansen, L. K. (2018). *Microstate EEGlab toolbox: An introductory guide*. https://doi.org/10.1101/289850

Tarailis, P., Koenig, T., Michel, C. M., & Griškova-Bulanova, I. (2023). The Functional Aspects of Resting EEG Microstates: A Systematic Review. *Brain Topography*. https://doi.org/10.1007/s10548-023-00958-9

Chapter 4. Intact and deficient contextual processing in schizophrenia patients

Oh-Hyeon Choung [a], Dario Gordillo [a], Maya Roinishvili [b,c], Andreas Brand [a], Michael H. Herzog [a], Eka Chkonia [d]

[a] Laboratory of Psychophysics, Brain Mind Institute, ´Ecole Polytechnique F´ed´erale de Lausanne (EPFL), Lausanne, Switzerland

[b] Laboratory of Vision Physiology, Ivane Beritashvili Centre of Experimental Biomedicine, Tbilisi, Georgia

[c] Institute of Cognitive Neurosciences, Free University of Tbilisi, Tbilisi, Georgia

[d] Department of Psychiatry, Tbilisi State Medical University, Tbilisi, Georgia

Postprint of the article published in *Schizophrenia Research: Cognition*

Full citation: Choung, O. H., Gordillo, D., Roinishvili, M., Brand, A., Herzog, M. H., & Chkonia, E. (2022). Intact and deficient contextual processing in schizophrenia patients. *Schizophrenia Research: Cognition*, 30, 100265. https://doi.org/10.1016/j.scog.2022.100265

Detailed personal contribution: I participated in data analysis with Oh-Hyeon Choung and contributed to the writing and revision of the manuscript.

Abstract

Schizophrenia patients are known to have deficits in contextual vision. However, results are often very mixed. In some paradigms, patients do not take the context into account and, hence, perform more veridically than healthy controls. In other paradigms, context deteriorates performance much more strongly in patients compared to healthy controls. These mixed results may be explained by differences in the paradigms as well as by small or biased samples, given the large heterogeneity of patients' deficits. Here, we show that mixed results may also come from idiosyncrasies of the stimuli used because in variants of the same visual paradigm, tested with the same participants, we found intact and deficient processing.

1. Introduction

Numerous studies have reported that schizophrenia patients have deficits in utilizing visual contextual information (Seymour et al., 2013; Tibber et al., 2013; review: Silverstein and Keane, 2011). For example, studies have shown diminished susceptibility to illusions in patients (e.g., depth inversion illusion: Keane et al., 2013; apparent motion: Sanders et al., 2013; Ebbinghaus illusion: Uhlhaas et al., 2006). However, Grzeczkowski et al. (2018), Kaliuzhna et al. (2019), Yang et al. (2013), and Tibber et al. (2013) found intact illusion perception, whereas Kantrowitz et al. (2009), Chen et al. (2008), and Frith and Friston (2013) found increased susceptibility. Results are clearly mixed (review: King et al., 2017; Notredame et al., 2014). Diminished dependency on contextual information can make perception even more veridical in schizophrenia patients. Dakin and colleagues (2005) presented a medium-contrast patch within a high-contrast surround. Controls perceived the contrast of the patch as largely lower than the true contrast, whereas schizophrenia patients reported a value closer to the true contrast, even though contrast discrimination itself has strongly deteriorated in schizophrenia patients (Must et al., 2004; Slaghuis, 1998). These results are usually explained in terms of weaker modulation of cortical responses in the primary visual cortex (Anderson et al., 2017; Seymour et al., 2013) or by biased expectations (or priors) in early visual areas (Frith and Friston, 2013). However, results are again mixed. Kaliuzhna et al. (2019) showed that perceptual judgments are rather biased in accordance with natural scenes' probability distributions.

Another example of visual contextual modulation is crowding. In crowding, target perception is largely impaired when presented together with flankers (review: Herzog et al., 2016; Levi, 2008; Pelli and Tillman, 2008; Strasburger, 2020). Schizophrenia patients showed less crowding (Kraehenmann et al., 2012; Robol et al., 2013). However, we found recently that crowding was intact or even stronger in the patients (Roinishvili et al., 2015). Hence, results are mixed here too.

In all of the above studies, context acted only uni-directionally, e.g., making perception less veridical. These results can be explained by many mechanisms, some of which are not necessarily visual, such as diminished attention to the target (e.g., Barch et al., 2012). We have recently used a “bidirectional” crowding paradigm where adding contextual elements first

deteriorated performance, but adding further elements improved performance (Chicherov and Herzog, 2015; Chicherov et al., 2014; Doerig et al., 2019; Herzog and Manassi, 2015; Herzog et al., 2015, 2016; Malania et al., 2007; Manassi et al., 2012, 2013, 2015, 2016; Saarela et al., 2009; Sayim et al., 2008, 2010, 2011; Choung et al., 2019, Choung et al., 2021; Doerig et al., 2019). With this crowding and uncrowding paradigm, patients showed almost the same performance as controls, except for an unspecific target processing deficit (Roinishvili et al., 2015). In this paradigm, next to basic vision processing, grouping and Gestalt processing are key (Bornet et al., 2021; Choung et al., 2021, Choung et al., submitted; Doerig et al., 2019; Doerig et al., 2020a; Francis et al., 2017), which seem to be intact in the patients (Favrod et al., 2022).

Hence, it remains unclear whether or not there are general contextual deficits in schizophrenia. Here, we propose that there are no general impaired mechanisms but that deficits depend strongly on idiosyncrasies of the specific stimuli.

2. Materials and methods

2.1. Participants

Seventeen schizophrenia patients and 16 age-matched unaffected participants took part in the two experiments. Patients were recruited from the Tbilisi Mental Health Center. Age and gender-matched controls were recruited from the general population in Tbilisi. Patients were diagnosed according to the Diagnostic and Statistical Manual of Mental Disorders (DSM-IV/V), based on the Structured Clinical Interview for DSM-IV/V (Clinician Version), information from the staff, and the study of the records. Psychopathology of schizophrenia was assessed by an experienced psychiatrist (EC) by the Scales for the Assessment of Negative Symptoms and Scales for the Assessment of Positive Symptoms (SANS, SAPS; Andreasen, 1984, 1989). Two schizophrenia patients and one control participant were excluded because of poor eye fixation. Hence, we retained the data of 15 participants from each group. Group characteristics are presented in Table 1. All participants had normal or corrected to normal visual acuity in the Freiburg Visual Acuity Test (FrACT), as indicated by a binocular score >1.0 (Bach, 1996). Participants gave written consent before the experiment. All experiments were conducted following the Declaration of Helsinki except for the preregistration (World Medical Association,

2013) and were approved by the local ethics committee (Tbilisi mental Health Center, independent Ethics committee, Georgia).

Table 1. Group average statistics (±SD) of patients and controls. SANS stands for Scale for the Assessment of Negative Symptoms. SAPS stands for Scale for the Assessment of Positive Symptoms. CPZ stands for chlorpromazine.

	Age	Gender (F/M)	Education (years)	Handness (L/R)	Illness duration (years)	SANS	SAPS	CPZ
Patients	39.1±9.5	5/10	13.5±3.3	1/14	15.6±8.8	7.2±3.4	8.1±2.4	421.9±265.2
Controls	38.3±8.0	5/10	14.6±2.4	0/15				

2.2. Apparatus

Stimuli were displayed on an LCD screen (ASUS VG248QE, Taipei, Taiwan; screen resolution 1920 × 1080 pixels). The room was dimly illuminated (0.5 lx). The viewing distance was 75 cm, and the participant's chin and forehead were positioned on a chin-rest. Responses were collected using hand-held push buttons. Participants' eye movements were tracked with a The Eye Tribe eye tracker (60 Hz sampling frequency, The Eye Tribe, Copenhagen, Denmark), and stimuli were displayed only when participants adequately fixated.

2.3. Stimuli

Stimuli were white (100 cd/m^2) and presented on a black background with luminance below 0.3 cd/m^2. Participants were asked to fixate on a red fixation dot (diameter of 8 arcmin, 20 cd/m^2). Stimuli were presented for 150 ms in experiment 1 and 42 ms to 642 ms in experiment 2. When no response was registered within 3 s, the trial was repeated randomly within the same block. A feedback tone was given for incorrect responses (600 Hz) and omissions (300 Hz). Vernier stimuli were composed of two vertical bars. Each bar was 40 arcmin long, 1.8 arcmin wide (anti-aliased), and separated by a 4 arcmin gap. Left/right offsets of vertical verniers were balanced within a block. Flankers were either lines, combinations of squares and stars, or cuboids. In experiment 1, the target Vernier was surrounded by one square in all conditions. Flanker configurations were composed of squares and stars. Squares were composed of 96 arcmin long lines, stars were composed of seven 38.4 arcmin long lines, and

the center-to-center distance between two flankers was 120 arcmin. In experiment 2, two vertical lines or two cuboids were presented to the left or the right of the Vernier target with a distance of 23.33 arcmin. Lines were 84 arcmin long; cuboids' width was 116.67 arcmin, height was 84 arcmin, and the oblique line's angle was 135° with a length of 47.14 arcmin.

Each configuration was presented at the center of the screen, and the fixation dot was presented at an eccentricity of 6° to the left, i.e., the stimulus was presented in the periphery. Psychophysics Toolbox was used to present the stimuli (Brainard, 1997; Kleiner et al., 2007; Pelli and Vision, 1997).

2.4. Procedures

2.4.1. General procedure

Two experiments were carried out on two days within a week. In both experiments, participants were asked to discriminate the Vernier offset direction of the lower bar compared to the upper bar. Different flanking configurations were tested 160 times in two sessions (80 trials per session). To reduce target-location uncertainty, only the target was presented alone for 150 ms at the beginning of each block. We used the PEST stair-case procedure (Taylor and Creelman, 1967). In PEST, test levels are changed step-wise based on the recent response history. The current test level is only changed when the percentage of correct responses for this test level lies, with some certainty, above or below the threshold criterion of 75 %. After 80 trials, we ended the procedure and derived the threshold from the psychometric function fitted to the data post-hoc (details in Data analysis). We randomized the order of experimental conditions across participants.

2.4.2. Experiment 1

7 flanker configurations were tested. The configurations were as follows: Vernier alone, Vernier surrounded by one square, Vernier with 7 horizontally aligned squares, Vernier with 35 squares (5 × 7 grid), Vernier with 3 squares and 4 stars, Vernier with 9 squares and 12 stars, and Vernier with 11 squares and 10 stars (Fig. 1). The 7 configurations were tested in a blockwise manner. Therefore, two sessions of 7 blocks each were tested, and all 7 configurations were tested in each session. The order of blocks within the session was randomized.

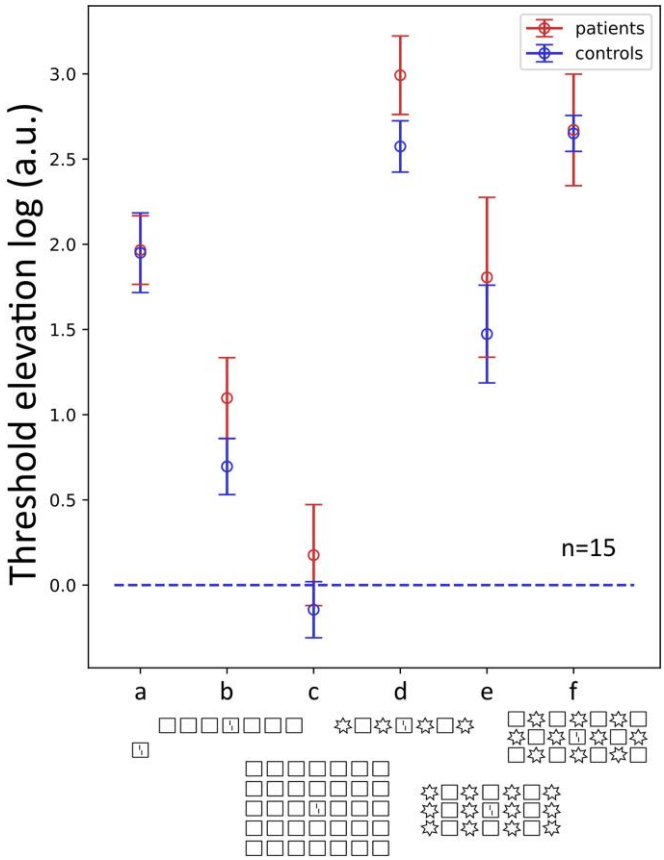

Fig. 1. Experiment 1. The y-axis shows mean of log-transformed threshold elevation (±SEM) relative to the unflanked (Vernier alone) condition (blue and red dotted lines equal to 0). Large thresholds represent poor performance (strong crowding), and low thresholds represent good performance (weak crowding). Patients and controls perform similarly. (For interpretation of the references to color in this figure legend, the reader is referred to the web version of this article.)

2.4.3. Experiment 2

Two flanker configurations (Vernier with two lines and Vernier with two cuboids) with four different stimulus durations (42 ms, 83 ms, 158 ms, and 642 ms) were tested. Each configuration was tested within a session, stimulus durations were randomized within the session. Each configuration with each stimulus duration was tested twice (80 trials each). Thus, each session was composed of 4 blocks of 80 trials, and there were 4 sessions. The experimental order was line flankers, cuboid flankers, cuboid flankers, and line flankers session.

2.5. Data analysis

We fitted a cumulative Gaussian function (psychometric function) to the data (tested levels and hit rates) and determined the vernier offset for which 75 % correct responses were reached (threshold). Psignifit 2.5 toolbox (Fründ et al., 2011) was used for the fitting. High

thresholds indicate inferior performance, and low thresholds indicate good performance. Next, we divided the threshold in each condition by the threshold in the Vernier alone condition (threshold elevation). Data were log-transformed to bring the data closer to normality. No obvious violation of normality was detected by visual inspection.

Using R (R Core Team, 2019) and lme4 package (Bates et al., 2015), we computed linear mixed-effects models (LMM) to account for dependent variables and random variations due to individual differences. The fixed and random effects are specified for each experiment (see Results for specifications of each experiment). Significance was obtained through likelihood ratio tests (χ^2) by comparing nested models. For each fitted model, using *MuMIn* package (Barton, 2020), we computed the effect size (r^2), i.e., the explained variance, when including (conditional r_c^2) and excluding (marginal r_m^2) the random effects (Johnson, 2014; Nakagawa et al., n.d.; Nakagawa and Schielzeth, 2013).

3. Results

3.1. Experiment 1. Intact (Un)crowding in schizophrenia patients

Similar to previous findings (Roinishvili et al., 2015), schizophrenia patients showed similar crowding behavior as controls. When the Vernier target was surrounded by a simple flanker (square), the target was strongly and similarly crowded in both the patient group and control group (Fig. 1a). Patients' and controls' performance improved by adding three squares on the left and right sides of the center square (7-square; Fig. 1b). By presenting the Vernier with a grid of squares (35 squares; Fig. 1c), performance improved almost to the level of the Vernier only condition (Fig. 1 dotted lines). Crowding was strong when presenting squares and stars alternatively (Fig. 1d, e, f). Overall, performance of patients and controls were comparable in all conditions.

To analyze the relation between threshold elevation and configuration depending on the two groups, we computed an LMM with the 7 flanker configurations and the 2 groups (patients and controls) as fixed effects (Fig. 1a-f). Individual participants were considered as random intercepts. We found no significant interaction between the two fixed effects (likelihood ratio test between an additive and an interaction model: $\chi^2(5) = 2.070$, $p = 0.839$). The

configurations showed clear and significant differences (configurations: $\chi^2(5) = 155.264$, $p < 0.001$), but there was no significant difference between the two groups (groups: $\chi^2(1) = 0.979$, $p = 0.322$). Although the absence of evidence is not evidence of absence, our results suggest that patients perform complex crowding tasks similarly to controls. Moreover, the difference of explained variance by the models with and without the group as a fixed effect is only 0.8 % ($r_m^2 = 0.491$, $r_m^2 = 0.483$). The detailed estimates are reported in Supp. Table 1.

3.2. Experiment 2. Deficient time-consuming processing in schizophrenia patients

As reported in previous works, grouping requires recurrent processes (Doerig et al., 2020b; Sayim et al., 2010, Sayim et al., 2014), which may be abnormal in the patients. Hence, we tested two flanker configurations with four stimulus durations. Two configurations were two lines and two cuboids (Fig. 2 left & right). Note that both flanker configurations contained the two lines next to the target Vernier. In both the control group and patient group, performance did not improve by increasing the stimulus duration for line flankers, whereas performance improved significantly by increasing the stimulus duration for cuboid flankers. However, performance improvement for the cuboid flanker condition in the patient group required more time than in the control group.

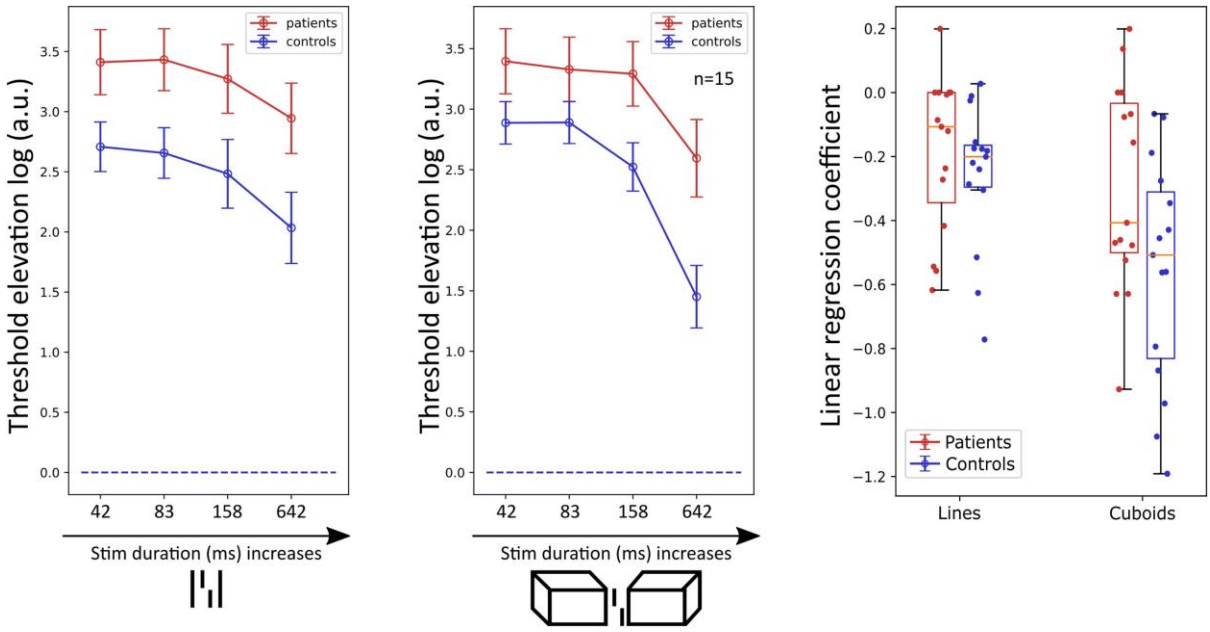

Fig. 2. Experiment 2. Left & middle, the y-axis shows mean of log-transformed threshold elevation (±SEM) relative to the unflanked (Vernier alone) condition (blue and red dotted lines equal to 0). Larger thresholds represent poor performance (strong crowding), and smaller thresholds represent good performance (weak crowding). Right, beta coefficients for linear regression of each participant. The y-axis shows the linear regression coefficient. Close-to-zero coefficient (gray dotted line) means the performance did not change by increasing the stimulus duration.

(For interpretation of the references to color in this figure legend, the reader is referred to the web version of this article.)

To analyze the effects of stimulus duration and groups on Vernier threshold elevation for each condition separately, we used an LMM with stimulus duration (42, 83, 158, 642 ms) and population groups (controls and patients) as fixed effects. Individual participants were considered as random intercepts. For line the flanker condition, we found no significant interaction between the two fixed effects (likelihood ratio test between an additive and an interaction model: $\chi^2(1) = 1.553$, $p = 0.213$). Stimulation duration showed a significant effect (stimulus duration: $\chi^2(1) = 43.784$, $p < 0.001$), whereas the population group only showed marginal significance (groups: $\chi^2(1) = 4.479$, $p = 0.034$). For the cuboid flanker condition, we found a significant interaction between the two fixed effects (likelihood ratio test between an additive and an interaction model: $\chi^2(1) = 8.559$, $p < 0.01$). Therefore, the effect of stimulus duration should be considered per group. The detailed estimates are reported in Supp. Tables 2 and 3.

To closely dissect the effect of stimulus duration per participant, we fitted individual participants' threshold elevation levels against the stimulus duration with a regression line. Then, we compared the fitted slope values between the groups. For the control group in the line flanker condition, the fitted slope values' 25^{th}, 50^{th}, and 75^{th} quantiles were −0.296, −0.201, and −0.165, respectively (r^2=0.677 ± 0.065). For the patient group in the line flanker condition, the fitted slope values' 25^{th}, 50^{th}, and 75^{th} quantiles were −0.344, −0.107, and 0.000, respectively (r^2=0.790 ± 0.068). There was no significant difference between the two groups ($t(28) = 0.848$, $p = 0.404$, $d = 0.310$). With line flankers, the performance was bad in both groups, regardless of the stimulus presentation time.

In the cuboid flanker condition, we found a group difference. For the control group, the fitted slope values' 25th, 50th, and 75th quantiles were −0.831, −0.508, and −0.311, respectively (r^2 = 0.789 ± 0.041). For the patient group, the fitted slope values' 25th, 50th, and 75th quantiles were −0.501, −0.407, and −0.034, respectively (r^2=0.733 ± 0.070). There was a significant difference between fitted slope values ($t(28) = 2.077$, $p = 0.047$, $d = 0.758$). The significant difference shows that performance improves significantly more in the control than patient group by increasing the stimulus time.

In summary, we found that, in the uncrowding condition (cuboid flanker condition), patients' performance improves less than that of control participants when increasing the stimulation duration. Thus, the data shows that patients have mainly a quantitative but not a qualitative deficit in processing the line flankers and a quantitative and qualitative deficit with the cuboid flankers.

4. Discussion

Contextual processing is often seriously impaired, and various mechanisms were proposed to explain these effects in schizophrenia; such as reduced surround suppression (Anderson et al., 2017; Seymour et al., 2013), or abnormal expectations (or priors) (Friston, 2005; Frith and Friston, 2013; Sterzer et al., 2018). However, the results are mixed. Hence, it is unclear whether or not the proposed mechanism is, indeed, at work and whether it is impaired in schizophrenia patients. Mixed results may come from biased sampling, and unspecific non-visual aspects, among others. Alternatively, there may not be one abnormal mechanism for contextual vision in general. Here, we have shown evidence for this latter hypothesis. We found that the same patients can have intact processing in one paradigm (Exp. 1, Fig. 1) but deficient processing in a variant of the very same paradigm (Exp. 2, Fig. 2). This result rules out unspecific aspects, such as diminished attention and biased sampling since the very same observers participated in all the experiments. It may well be that the small changes in the spatial layout of the crowding stimuli lead to the involvement of different mechanisms, of which only some are abnormal. Hence, claims about abnormal mechanisms should be verified with more than one paradigm. On the other hand, our results offer the opportunity to pit intact and deficient processing against each other within one paradigm and, thus, unearth specific abnormal mechanisms.

We like to mention that it is important to publish null results, such as the ones of intact processing in Fig. 1. Since patients usually perform worse than controls, a significant group difference always indicates a deficit, which may lead to the impression that patients are deficient in most paradigms. However, this is not the case.

Interestingly, patients show strong crowding (Fig. 1, a, d, f, and Fig. 2 left: line flanker) and uncrowding (Fig. 1, b, c, e, and Fig. 2 middle: cuboid flanker), similar to the control group, suggesting that complex grouping and Gestalt processing are intact. However, in Exp. 2, we found a significant difference in the time-consuming recurrent processing. Indeed, for the cuboid condition, where control participants have uncrowding with longer stimulus duration, schizophrenia patients needed longer stimulus duration to have uncrowding (cuboid condition, Fig. 2 middle). Importantly, uncrowding in patients was intact. However, the sample size is small (15 per group). Our results point to the possibility that some configurations of the stimuli might reveal clear-cut group effects, which might provide a ground for investigating putative underlying mechanisms. However, we suggest that group effects on certain configurations of stimuli might be driven by idiosyncratic aspects of the paradigm rather than by a common disease-related mechanism. We need to mention that also in Exp. 1 processing is most likely not feedforward and relies on grouping.

The results of Exp. 2 are in accordance with previous results, where specific complex processing is intact, but there is a main deficit (Brand et al., 2005; Lauffs et al., 2016; Roinishvili et al., 2015; Schütze et al., 2007). Importantly, this deficit cannot come from target processing per se because the performance in the vernier alone condition was only slightly deteriorated. What causes this general deficit remains an enigma.

CRediT authorship contribution statement

Oh-Hyeon Choung: idea and conceptualization, methodology, software, data curation, formal analysis, writing original draft and revision, visualization.

Dario Gordillo: formal analysis, writing original draft and revision, visualization.

Maya Roinishvili: idea and conceptualization, resources, data curation and collection, writing original draft.

Andreas Brand: conceptualization, writing original draft and revision.

Michael H. Herzog: idea and conceptualization, writing original draft and revision, supervision, project administration, funding acquisition.

Eka Chkonia: resources, data curation, writing original draft and revision, project administration, funding acquisition.

Declaration of competing interest

The authors (OHC, DG, MR, AB, MHH, and EC) declare no conflict of interest.

Acknowledgment

OHC, DG, MR, MHH were supported by the Swiss National Science Foundation1 (SNF) 320030_176153 "Basics of visual processing: from elements to figures" and the National Centre of Competence in Research (NCCR) Synapsy financed by the Swiss National Science Foundation under grant 51NF40-185897.

References

Anderson, E.J., Tibber, M.S., Schwarzkopf, D.S., Shergill, S.S., Fernandez-Egea, E., Rees, G., Dakin, S.C., 2017. Visual population receptive fields in people with schizophrenia have reduced inhibitory surrounds. J. Neurosci. 37 (6), 1546–1556. https://doi.org/10.1523/JNEUROSCI.3620-15.2016.

Andreasen, N.C., 1984. Scale for the assessment of positive symptoms (SAPS). University of Iowa, Iowa City.

Andreasen, N.C., 1989. Scale for the Assessment of Negative Symptoms (SANS). Br. J. Psychiatry 155 (Suppl 7), 53–58.

Bach, M., 1996. The freiburg visual acuity test—automatic measurement of visual acuity. Optom. Vis. Sci. 73 (1), 49–53.

Barch, D.M., Carter, C.S., Dakin, S.C., Gold, J., Luck, S.J., MacDonald III, A., Ragland, J. D., Silverstein, S., Strauss, M.E., 2012. The clinical translation of a measure of gain control: the contrast-contrast effect task. Schizophr. Bull. 38 (1), 135–143. https://doi.org/10.1093/schbul/sbr154.

Barton, K., 2020. MuMIn: multi-model inference. https://CRAN.R-project.org/package=MuMIn.

Bates, D., Machler, M., Bolker, B., Walker, S., 2015. Fitting linear mixed-effects models using lme4. J. Stat. Softw. 67 (1), 1–48. https://doi.org/10.18637/jss.v067.i01.

Bornet, A., Choung, O.-H., Doerig, A., Whitney, D., Herzog, M.H., Manassi, M., 2021. Global and high-level effects in crowding cannot be predicted by either high-dimensional pooling or target cueing. J. Vis. 21 (12), 10. https://doi.org/10.1167/jov.21.12.10.

Brainard, D.H., 1997. The psychophysics toolbox. Spat. Vis. 10 (4), 433–436. https://doi.org/10.1163/156856897X00357.

Brand, A., Kopmann, S., Marbach, S., Heinze, M., Herzog, M.H., 2005. Intact and deficient feature fusion in schizophrenia. Eur. Arch. Psychiatry Clin. Neurosci. 255 (6), 413–418. https://doi.org/10.1007/s00406-005-0590-x.

Chen, Y., Norton, D., Ongur, D., 2008. Altered center-surround motion inhibition in schizophrenia. Biol. Psychiatry 64 (1), 74–77. https://doi.org/10.1016/j.biopsych.2007.11.017.

Chicherov, V., Herzog, M.H., 2015. Targets but not flankers are suppressed in crowding as revealed by EEG frequency tagging. NeuroImage 119, 325–331.

Chicherov, V., Plomp, G., Herzog, M.H., 2014. Neural correlates of visual crowding. Neuroimage 93, 23–31.

Choung, O.-H., Rashal, E., Herzog, M.H., 2019. Basic gestalt laws cannot explain uncrowding. Perception 48 (CONF), 28.

Choung, O.-H., Bornet, A., Doerig, A., Herzog, M.H., 2021. Dissecting (un)crowding. J. Vis. 21 (10), 1–20. https://doi.org/10.1167/jov.21.10.10.

Choung, O.-H., Rashal, E., Kunchulia, M., Herzog, M.H., 2022. Basic Gestalt Principles Cannot Explain Uncrowding (Submitted).

Dakin, S., Carlin, P., Hemsley, D., 2005. Weak suppression of visual context in chronic schizophrenia. Curr. Biol. 15 (20), R822–R824.

Doerig, A., Bornet, A., Rosenholtz, R., Francis, G., Clarke, A.M., Herzog, M.H., 2019.

Beyond Bouma's window: how to explain global aspects of crowding? PLoS Comput. Biol. 15 (5), e1006580 https://doi.org/10.1371/journal.pcbi.1006580.

Doerig, A., Bornet, A., Choung, O.-H., Herzog, M.H., 2020. Crowding reveals fundamental differences in local vs. global processing in humans and machines. Vis.Res. 167, 39–45. https://doi.org/10.1016/j.visres.2019.12.006.

Doerig, A., Schmittwilken, L., Sayim, B., Manassi, M., Herzog, M.H., 2020. Capsule networks as recurrent models of grouping and segmentation. PLoS Comput. Biol. 16 (7), e1008017.

Favrod, O., Brand, A., Berdzenishvili, E., Chkonia, E., Akselrod, M., Wagemans, J., Herzog, M.H., Roinishvili, M., 2022. Embedded figures in schizophrenia: a main deficit but no specificity. Schizophr. Res. 28, 100227 https://doi.org/10.1016/j.scog.2021.100227.

Francis, G., Manassi, M., Herzog, M.H., 2017. Neural dynamics of grouping and segmentation explain properties of visual crowding. Psychol. Rev. 124 (4), 483–504. https://doi.org/10.1037/rev0000070.

Friston, K., 2005. A theory of cortical responses. Philos. Trans. R. Soc. B Biol. Sci. 360 (1456), 815–836. https://doi.org/10.1098/rstb.2005.1622.

Frith, C.D., Friston, K.J., 2013. False perceptions and false beliefs: Understanding schizophrenia. In: Neurosciences and the Human Person: New Perspectives on Human Activities, 121, pp. 1–15.

Fründ, I., Haenel, N.V., Wichmann, F.A., 2011. Inference for psychometric functions in the presence of nonstationary behavior. J. Vis. 11 (6), 16. https://doi.org/10.1167/11.6.16.

Grzeczkowski, L., Roinishvili, M., Chkonia, E., Brand, A., Mast, F.W., Herzog, M.H., Shaqiri, A., 2018. Is the perception of illusions abnormal in schizophrenia? Psychiatry Res. 270, 929–939. https://doi.org/10.1016/j.psychres.2018.10.063.

Herzog, M.H., Manassi, M., 2015. Uncorking the bottleneck of crowding: a fresh look at object recognition. Curr. Opin. Behav. Sci. 1, 86–93.

Herzog, M.H., Sayim, B., Chicherov, V., Manassi, M., 2015. Crowding, grouping, and object recognition: a matter of appearance. J. Vis. 15 (6), 5.

Herzog, M.H., Thunell, E., Ögmen, H., 2016. Putting low-level vision into global context: why vision cannot be reduced to basic circuits. Vis. Res. 126, 9–18. https://doi.org/10.1016/j.visres.2015.09.009.

Johnson, P.C., 2014. Extension of Nakagawa & Schielzeth's R2GLMM to random slopes models. Methods Ecol. Evol. 5 (9), 944–946. https://doi.org/10.1111/2041-210X.12225.

Kaliuzhna, M., Stein, T., Rusch, T., Sekutowicz, M., Sterzer, P., Seymour, K.J., 2019. No evidence for abnormal priors in early vision in schizophrenia. Schizophr. Res. 210, 245–254. https://doi.org/10.1016/j.schres.2018.12.027.

Kantrowitz, J.T., Butler, P.D., Schecter, I., Silipo, G., Javitt, D.C., 2009. Seeing the world dimly: the impact of early visual deficits on visual experience in schizophrenia. Schizophr. Bull. 35 (6), 1085–1094. https://doi.org/10.1093/schbul/sbp100.

Keane, B.P., Silverstein, S.M., Wang, Y., Papathomas, T.V., 2013. Reduced depth inversion illusions in schizophrenia are state-specific and occur for multiple object types and viewing conditions. J. Abnorm. Psychol. 122 (2), 506.

King, D.J., Hodgekins, J., Chouinard, P.A., Chouinard, V.-A., Sperandio, I., 2017. A review of abnormalities in the perception of visual illusions in schizophrenia. Psychon. Bull. Rev. 24 (3), 734–751. https://doi.org/10.3758/s13423-016-1168-5.

Kleiner, M., Brainard, D., Pelli, D., 2007. What's New in Psychtoolbox-3?.

Kraehenmann, R., Vollenweider, F.X., Seifritz, E., Kometer, M., 2012. Crowding deficits in the visual periphery of schizophrenia patients. PLoS ONE 7 (9), e45884. https://doi.org/10.1371/journal.pone.0045884.

Lauffs, M.M., Shaqiri, A., Brand, A., Roinishvili, M., Chkonia, E., Ögmen, H., Herzog, M. H., 2016. Local versus global and retinotopic versus non-retinotopic motion processing in schizophrenia patients. Psychiatry Res. 246, 461–465. https://doi.org/10.1016/j.psychres.2016.09.049.

Levi, D.M., 2008. Crowding—an essential bottleneck for object recognition: a mini-review. Vis. Res. 48 (5), 635–654. https://doi.org/10.1016/j.visres.2007.12.009.

Malania, M., Herzog, M.H., Westheimer, G., 2007. Grouping of contextual elements that affect vernier thresholds. J. Vis. 7 (2), 1.

Manassi, M., Sayim, B., Herzog, M.H., 2012. Grouping, pooling, and when bigger is better in visual crowding. J. Vis. 12 (10), 13.

Manassi, M., Sayim, B., Herzog, M.H., 2013. When crowding of crowding leads to uncrowding. J. Vis. 13 (13), 10.

Manassi, M., Hermens, F., Francis, G., Herzog, M.H., 2015. Release of crowding by pattern completion. J. Vis. 15 (8), 16.

Manassi, M., Lonchampt, S., Clarke, A., Herzog, M.H., 2016. What crowding can tell us about object representations. J. Vis. 16 (3), 35.

Must, A., Janka, Z., Benedek, G., K´eri, S., 2004. Reduced facilitation effect of collinear flankers on contrast detection reveals impaired lateral connectivity in the visual cortex of schizophrenia patients. Neurosci. Lett. 357 (2), 131–134. https://doi.org/10.1016/j.neulet.2003.12.046.

Nakagawa, S., Schielzeth, H., 2013. A general and simple method for obtaining R2 from generalized linear mixed-effects models. Methods Ecol. Evol. 4 (2), 133–142. https://doi.org/10.1111/j.2041-210x.2012.00261.x.

Nakagawa et al., n.d.Nakagawa, S., Johnson, P. C. D., & Schielzeth, H. (n.d.). The coefficient of determination R2 and intra-class correlation coefficient from generalized linear mixed-effects models revisited and expanded. 11.

Notredame, C.-E., Pins, D., Deneve, S., Jardri, R., 2014. What visual illusions teach us about schizophrenia. Front. Integr. Neurosci. 8. https://www.frontiersin.org/article/10.3389/fnint.2014.00063.

Pelli, D.G., Tillman, K.A., 2008. The uncrowded window of object recognition. Nat. Neurosci. 11 (10), 1129–1135. https://doi.org/10.1038/nn.2187.

Pelli, D.G., Vision, S., 1997. The VideoToolbox software for visual psychophysics: transforming numbers into movies. Spat. Vis. 10, 437–442.

R Core Team, 2019. R: A Language and Environment for Statistical Computing (Vienna, Austria). R Foundation for Statistical Computing. https://www.R-project.org/.

Robol, V., Tibber, M.S., Anderson, E.J., Bobin, T., Carlin, P., Shergill, S.S., Dakin, S.C., 2013. Reduced crowding and poor contour detection in schizophrenia are consistent with weak surround inhibition. PLoS ONE 8 (4), e60951. https://doi.org/10.1371/journal.pone.0060951.

Roinishvili, M., Cappe, C., Shaqiri, A., Brand, A., Rürup, L., Chkonia, E., Herzog, M.H., 2015. Crowding, grouping, and gain control in schizophrenia. Psychiatry Res. 226 (2-3), 441–445. https://doi.org/10.1016/j.psychres.2015.01.009.

Saarela, T.P., Sayim, B., Westheimer, G., Herzog, M.H., 2009. Global stimulus configuration modulates crowding. J. Vis. 9 (2), 5.

Sanders, L.L.O., de Millas, W., Heinz, A., Kathmann, N., Sterzer, P., 2013. Apparent motion perception in patients with paranoid schizophrenia. Eur. Arch. Psychiatry Clin. Neurosci. 263 (3), 233–239. https://doi.org/10.1007/s00406-012-0344-5.

Sayim, B., Westheimer, G., Herzog, M.H., 2008. Contrast polarity, chromaticity, and stereoscopic depth modulate contextual interactions in vernier acuity. J. Vis. 8 (8), 12.

Sayim, B., Westheimer, G., Herzog, M.H., 2010. Gestalt factors modulate basic spatial vision. Psychol. Sci. 21 (5), 641–644. https://doi.org/10.1177/0956797610368811.

Sayim, B., Westheimer, G., Herzog, M.H., 2011. Quantifying target conspicuity in contextual modulation by visual search. J. Vis. 11 (1), 6.

Sayim, B., Manassi, M., Herzog, M., 2014. How color, regularity, and good gestalt determine backward masking. J. Vis. 14 (7), 8. https://doi.org/10.1167/14.7.8.

Schütze, C., Bongard, I., Marbach, S., Brand, A., Herzog, M.H., 2007. Collinear contextual suppression in schizophrenic patients. Psychiatry Res. 150, 237–243.

Seymour, K., Stein, T., Sanders, L.L.O., Guggenmos, M., Theophil, I., Sterzer, P., 2013. Altered contextual modulation of primary visual cortex responses in schizophrenia. Neuropsychopharmacology 38 (13), 2607–2612. https://doi.org/10.1038/npp.2013.168.

Silverstein, S.M., Keane, B.P., 2011. Vision science and schizophrenia research: toward a review of the disorder editors' introduction to special section. Schizophr. Bull. 37 (4), 681–689. https://doi.org/10.1093/schbul/sbr053.

Slaghuis, W.A., 1998. Contrast sensitivity for stationary and drifting spatial frequency gratings in positive- and negative-symptom schizophrenia. J. Abnorm. Psychol. 107 (1), 49–62. https://doi.org/10.1037/0021-843X.107.1.49.

Sterzer, P., Adams, R.A., Fletcher, P., Frith, C., Lawrie, S.M., Muckli, L., Corlett, P.R., 2018. The predictive coding account of psychosis. Biol. Psychiatry 84 (9), 634–643.

Strasburger, H., 2020. Seven myths on crowding and peripheral vision. I-Perception 11 (3). https://doi.org/10.1177/2041669520913052, 2041669520913052.

Taylor, M., Creelman, C.D., 1967. PEST: efficient estimates on probability functions. J. Acoust. Soc. Am. 41 (4A), 782–787.

Tibber, M., Anderson, E., Bobin, T., Antonova, E., Seabright, A., Wright, B., Carlin, P., Shergill, S., Dakin, S., 2013. Visual surround suppression in schizophrenia. Front. Psychol. 4. https://www.frontiersin.org/article/10.3389/fpsyg.2013.00088.

Uhlhaas, P.J., Phillips, W.A., Mitchell, G., Silverstein, S.M., 2006. Perceptual grouping in disorganized schizophrenia. Psychiatry Res. 145 (2), 105–117. https://doi.org/10.1016/j.psychres.2005.10.016.

World Medical Association, 2013. World Medical Association Declaration of Helsinki: ethical principles for medical research involving human subjects. JAMA 310 (20), 2191–2194. https://doi.org/10.1001/jama.2013.281053.

Yang, E., Tadin, D., Glasser, D.M., Hong, S.W., Blake, R., Park, S., 2013. Visual context processing in schizophrenia. Clin. Psychol. Sci. 1 (1), 5–15. https://doi.org/10.1177/2167702612464618.

Chapter 5. Oscillatory traveling waves reveal predictive coding abnormalities in schizophrenia

Andrea Alamia[1,2*], Dario Gordillo[3*], Eka Chkonia[4,5], Maya Roinishvili[5,6], Celine Cappe[1] and Michael H. Herzog[3]

[1]Cerco, CNRS Université de Toulouse, Toulouse 31052 (France)

[2]Artificial and Natural Intelligence Toulouse Institute (ANITI), Toulouse (France)

[3]Laboratory of Psychophysics, Brain Mind Institute, School of Life Sciences, École Polytechnique Fédérale de Lausanne (EPFL), CH-1015 Lausanne (Switzerland)

[4]Department of Psychiatry, Tbilisi State Medical University (TSMU), 0186 Tbilisi (Georgia)

[5]Institute of Cognitive Neurosciences, Free University of Tbilisi, 0159 Tbilisi (Georgia)

[6]Laboratory of Vision Physiology, Ivane Beritashvili Centre of Experimental Biomedicine, 0160 Tbilisi (Georgia)

*Andrea Alamia and Dario Gordillo contributed equally to this work.

A previous version of this manuscript has been published as a preprint: Alamia, A. *, Gordillo, D. *, Chkonia, E., Roinishvili, M., Cappe, C., & Herzog, M. H. (2023). Oscillatory traveling waves reveal predictive coding abnormalities in schizophrenia. BioRxiv, 2023.10.09.561490. https://doi.org/10.1101/2023.10.09.561490

Detailed personal contribution: I participated in writing the manuscript alongside with Andrea Alamia and Michael Herzog, and contributed with data analysis alongside with Andrea Alamia.

Abstract

The computational mechanisms underlying psychiatric disorders are hotly debated. One hypothesis, grounded in the Bayesian predictive coding framework, proposes that schizophrenia patients have abnormalities in encoding prior beliefs about the environment, resulting in abnormal sensory inference, which can explain core aspects of the psychopathology, such as psychotic symptoms. Here, we tested this hypothesis by identifying oscillatory traveling waves as neural signatures of predictive coding. By analyzing an EEG dataset comprising 146 patients with schizophrenia and 96 healthy controls, we found that patients exhibit stronger top-down alpha-band traveling waves compared to healthy controls

during resting state, reflecting stronger priors at higher levels of the predictive processing hierarchy. Conversely, we found stronger bottom-up alpha-band waves in patients during a visual task, reflecting an alteration of lower sensory priors. These hierarchical-specific abnormalities might explain a range of symptoms and perceptual impairments observed in patients with schizophrenia within a common computational framework.

Significance

We provide novel evidence favoring the Bayesian predictive coding interpretation of schizophrenia. Relying on computational and experimental works that characterized electrophysiological correlates of predictive processes, we investigate oscillatory traveling waves in EEG data of 146 patients with schizophrenia and 96 age-matched healthy controls. Our results reveal stronger top-down alpha-band traveling waves in patients, reflecting an increase in the precision of high-level priors. On the other hand, we observed an increase in bottom-up alpha-band waves during a visual task, in line with the proposed reduction in precision of lower-level sensory priors. Our findings suggest that traveling waves' analysis is a versatile technique to probe predictive processing mechanisms in different cognitive processes. Impairments in this mechanism may underlie perceptual alterations as well as the pronounced clinical symptoms of schizophrenia.

Introduction

Schizophrenia is a severe mental disorder that affects about one percent of the world's population (McCutcheon et al., 2020). Schizophrenia is characterized by a large range of psychotic symptoms as well as by strong impairments in mental functioning, including perception, cognition, and personality.

Numerous hypotheses and mechanisms have been proposed to explain these abnormalities. One hypothesis is that schizophrenia patients dysfunctionally update their cognitive world model, usually described within the framework of Bayesian inference and predictive coding (Corlett et al., 2009; Krystal et al., 2017). According to this framework, perception combines incoming sensory evidence with prior information, i.e., beliefs about the world (figure 1A).

However, experimental evidence for this framework from behavioral studies is mixed, including studies showing that patients rely more on prior beliefs than on sensory information (Cassidy et al., 2018; Powers et al., 2017), studies which found stronger reliance on sensory information in the patients (Stuke et al., 2019; Weilnhammer et al., 2020), and even studies which found intact processing (Choung et al., 2022; Kaliuzhna et al., 2019; Tibber et al., 2013).

Basic sensory impairments and hallucinations may however rely on abnormalities at different levels of predictive processing. Hence, it has been proposed that schizophrenia patients weigh the prior information more strongly in hierarchically higher-regions, but rely more on sensory information in lower hierarchical regions (Corlett et al., 2019; Sterzer et al., 2018). These hierarchical-specific alterations in the priors would explain both impairments in basic sensory processing and also more complex phenomena such as hallucinations or delusions (Friston et al., 2016; Krystal et al., 2017), and may therefore also explain the mixed experimental results.

Here, we tested the hypothesis that there are hierarchical-specific alterations in predictive processing from a neurophysiological perspective. In recent work, it was shown that oscillatory alpha-band (8-12Hz) traveling waves are neural signatures of predictive coding (Alamia & VanRullen, 2019; Arnal & Giraud, 2012; Bastos et al., 2012, 2015; Friston, 2019; Michalareas et al., 2016). In these studies (Alamia & VanRullen, 2019; Pang et al., 2020), neural activity was measured along the central midline of electrodes (Oz-Fz) to determine how oscillations propagate as traveling waves from occipital to frontal areas (forward waves) or in the opposite direction (backward waves). Based on a model, implementing predictive coding under minimal assumptions (Alamia & VanRullen, 2019), the authors proposed that forward traveling waves encode sensory information and prediction-errors (i.e., the difference between top-down predictions and the actual activity), while backward waves carry the prior information (Rao & Ballard, 1999). A pharmacological study provided additional evidence for the relationship between traveling waves and predictive coding using a serotonergic psychedelics drug (i.e., N, N-Dimethyltryptamine, DMT; Alamia et al., 2020). According to a recently proposed hypothesis (Carhart-Harris & Friston, 2019), psychedelics act on the high-level prior distributions in the brain, decreasing their precision (defined as the inverse of the variance, figure 1B). As a consequence, there is an increase in forward waves carrying prediction-errors (figure 1B, left panel). Indeed, after the intake of DMT a decrease and an increase in the alpha-band traveling waves propagating top-down and bottom-up, respectively, was observed . Here, we used the

very same analysis to test whether patients rely more on prior beliefs than on sensory evidence during eyes-closed, resting-state EEG and a visual backward masking task. Following the Bayesian framework, we expect stronger alpha band backward waves during resting state in schizophrenia patients than in healthy controls, due to more precise high-order priors; on the other hand, we expect stronger forward alpha-band waves during a visual task, reflecting an increase in the weighting of the sensory information. (figure 1B). We analyzed a large EEG dataset comprising 146 patients with schizophrenia and 96 age-matched healthy controls.

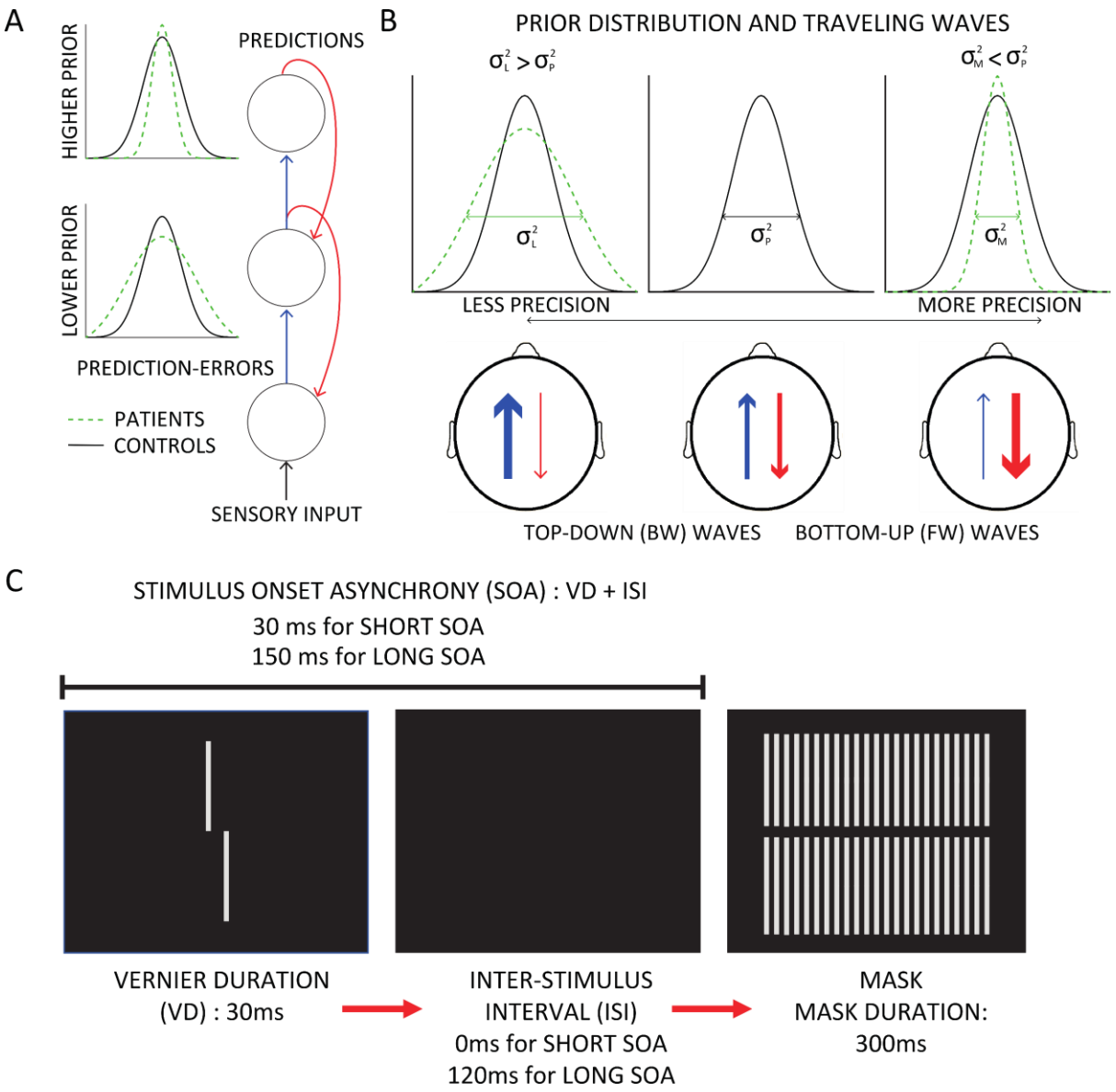

Figure 1 – Predictive coding and traveling waves. A) In the Bayesian predictive coding perspective, predictions are generated by prior distributions in higher brain regions and prediction-errors are computed to update the prior based on the sensory evidence (i.e., the likelihood). Recently, it was proposed that there are hierarchical-specific abnormalities of the priors' precision in schizophrenia. Specifically, patients have been suggested to have a better

precision in higher areas and worse precision in lower, sensory-related areas (Corlett et al., 2019). B) Considering backward (BW) and forward (FW) waves as proxies of predictions and prediction-errors, respectively (Alamia & VanRullen, 2019), one would expect different patterns of traveling waves depending on the precision of the prior: a more precise prior (rightmost panel) generates stronger predictions, and in turn stronger backward waves, whereas less precise prior information (leftmost pattern) generates inaccurate predictions, hence higher prediction-errors, reflected in stronger forward waves. C) In our experiment, the target consisted of a Vernier, i.e., two vertical lines slightly offset horizontally either to the left or right (as shown). Participants were instructed to indicate the offset direction. A grating mask was presented afterwards, making the discriminability of the offset spatially and temporally challenging.

Results

We re-analyzed EEG data from previous studies with resting state data (eyes closed; da Cruz et al., 2020; Gordillo et al., 2023) and a visual backward masking task (da Cruz, Shaqiri, et al., 2020; Garobbio et al., 2021). We quantified brain oscillations along the central electrodes' mid-line (from Oz to Fz, figure 2), as in our previous work (Alamia & VanRullen, 2019; Pang et al., 2020). We considered sliding time windows of 1 and 0.5 seconds from two different datasets, one eyes-closed resting state and one visual backward masking (VBM) task (see Methods and figure 2). First, for all time windows, we create 2D maps by stacking the signals from the seven electrodes, obtaining images with time and electrodes as axes (figure 2).

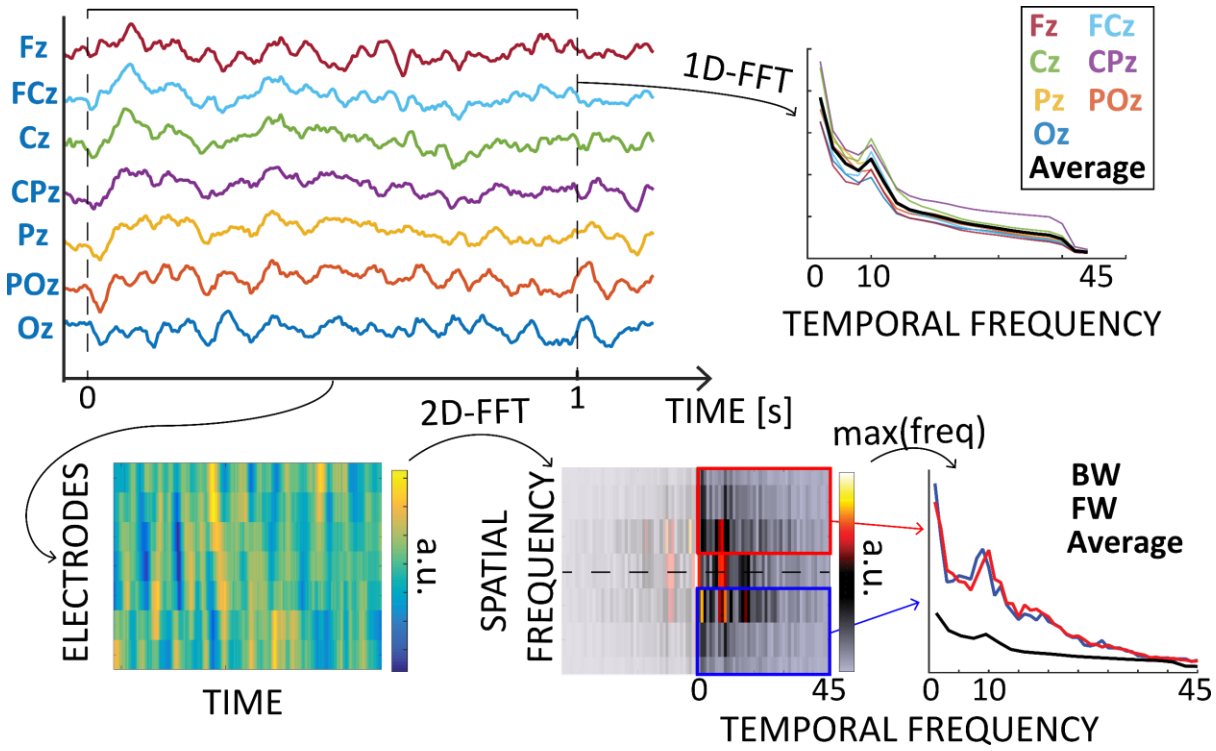

Figure 2 – Quantifying traveling waves. From a 0.5 or 1-second time window, we extract 2D maps by combining seven midline electrodes. We then compute 2D-FFT to evaluate forward (FW – in blue) and backward (BW – in red) waves, as quantified by the maximum values in the lower- and upper-right quadrants, respectively. Lastly, we computed the waves amount in decibels by using the average 1D-FFT of each electrode as a baseline (see Methods).

For each of these images, we computed 2D Fast Fourier Transform (FFT) to quantify the amount of traveling waves propagating from occipital to frontal areas and vice versa (i.e., forward or backward, respectively). To determine an appropriate baseline (see Methods), we averaged each midline electrode 1D-FFT to obtain a baseline accounting for fluctuations in the overall power unrelated to the traveling waves (i.e., without the spatial information of the electrodes). The waves' amount is expressed as a log-ratio in decibels [dB] (see Methods).

Traveling waves during rest

In both the patients (N=121) and the control group (N=75), we quantified the spectral power in five frequency bands (θ: 3Hz - 7Hz, α: 8Hz – 12 Hz, low β:13Hz – 22Hz, high β: 23Hz –30 Hz, and γ: 30Hz – 45Hz) along the midline electrodes (from Oz to Fz, see figure 2). First, we compared each electrode's spectral power between the two groups. For each frequency band, we performed Bayesian ANOVA, considering ELECTRODE and GROUP as factors (see Methods for details). As shown in figure 3A, we found a higher spectral power in the patients compared to the control group in the θ and α bands (GROUP factor $BF_{10}>>10^4$ in both frequency bands) but not in the beta- and gamma-bands. For all frequency bands, the ELECTRODE factor revealed a strong effect (all $BF_{10}>>10^{66}$). Next, we focused on the spatial component of brain oscillations by investigating differences in the spectra of traveling waves propagating forward (FW) and backward (BW). Figure 3B shows the spectra for both groups: as in our previous work (Alamia et al., 2023), in the control group, we found a typical spectral pattern with high backward waves in the α and low β (13Hz -22Hz) bands, and a flat profile in the forward waves (i.e., no difference between bands). We then compared the FW and BW spectra of the control group with those of the patients, considering the five frequency bands (θ, α, low and high β, and γ; figure 3B). We performed two-factor ANCOVAs, considering GROUP and BAND as factors and GENDER, AGE, and EDUCATION as covariates. For both FW and BW waves, we found a similar pattern of results: a very strong effect for the BAND factor ($BF_{10}>>10^{11}$ for both FW and BW waves) but mild to no effect in the GROUP factor (BW waves, $BF_{10}=7.519$; FW waves,

BF_{10}=0.514); however, in both directions, we found a very robust effect of the GROUP x BAND interaction (for both FW and BW waves BF_{10}>>400), revealing significant differences between the two groups. Concerning the covariates, there are no effects of EDUCATION or GENDER (BW waves, BF_{10}<0.4; FW waves, BF_{10}<0.8), but a small effect of AGE for the FW waves (BW waves, BF_{10}=1.968; FW waves, BF_{10}=4.684). We further analyzed these results by performing Bayesian ANOVAs for each frequency band separately, considering as factors GROUP and DIRECTION (either forward or backward).

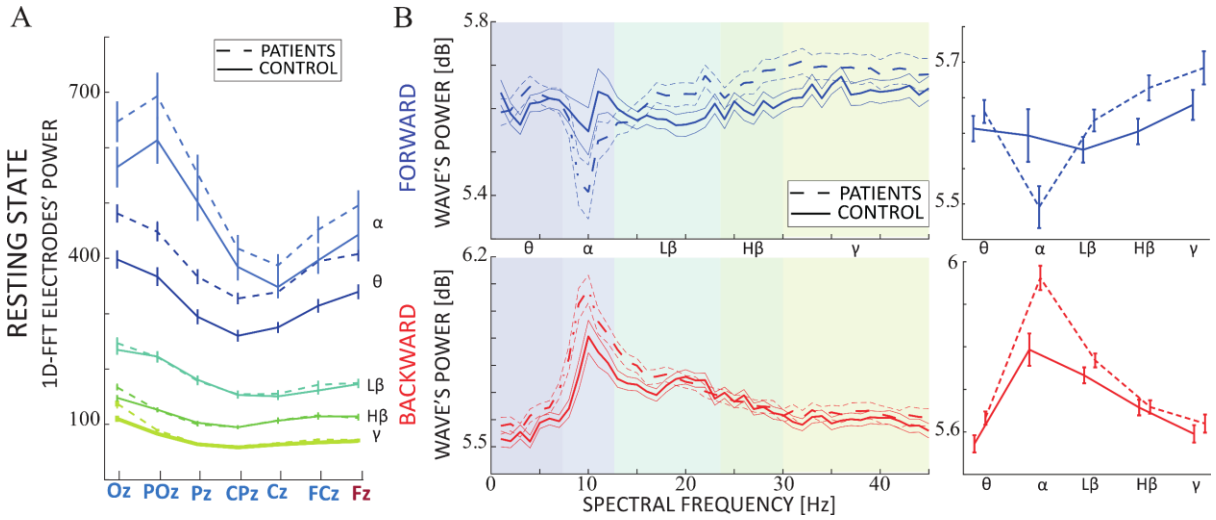

Figure 3 – Differences in traveling waves between patients and controls during rest. A) Raw power for each spectral band in the midline electrodes (x-axis) for both the patients and control group. Each color represents a different frequency band. Error bars represent standard errors. B) The left panels illustrate the spectra for both forward (blue) and backward (red) waves for the two groups; the right panels show the mean for each frequency band. Error bars represent standard errors.

Overall, the results show no difference between the groups (all frequency bands, 0.1<BF_{10}<1), and a robust effect in the DIRECTION factor for θ, low β, and γ (all BF_{10}>>10^7). However, there was a strong interaction between GROUP and DIRECTION in the α band (BF_{10}>>500), which, in line with our previous analysis, reveals distinct oscillatory dynamics between the patient and the control group. Specifically, these results confirm the difference shown in figure 3B: the most substantial effect was observed in the alpha-band (as confirmed by a larger Bayes Factor), where schizophrenia patients revealed an increase in backward waves and a decrease in forward waves.

Traveling waves for backward masking

Previous results showed that the traveling wave pattern changes drastically between resting state EEG and visual evoked activity (Pang et al., 2020). In addition, according to the proposed Bayesian framework, schizophrenia patients have less precise priors at hierarchically lower sensory areas, thus weighing more the sensory information than healthy controls (Corlett et al., 2019; Sterzer et al., 2018). Accordingly, we expect an increase in alpha-band forward waves in patients following visual stimulation, in line with the hypothesis that alpha-band forward waves reflect precision-weighted sensory information (Alamia et al., 2020; Friston, 2019). For evoked activity, we analyzed a dataset of a Visual Backward Masking (VBM) task (see Herzog et al., 2004). In VBM, a briefly presented target is followed by a mask (figure 1C). There were 4 conditions: Vernier only, Long SOA, Short SOA, and Mask only conditions. In the Vernier only condition, there was no mask, whereas in the Long SOA, and Short SOA conditions, the target Vernier was followed by a mask with either an SOA of 150 or 30 ms, respectively. The Mask only condition provides a control condition, where no target was presented.

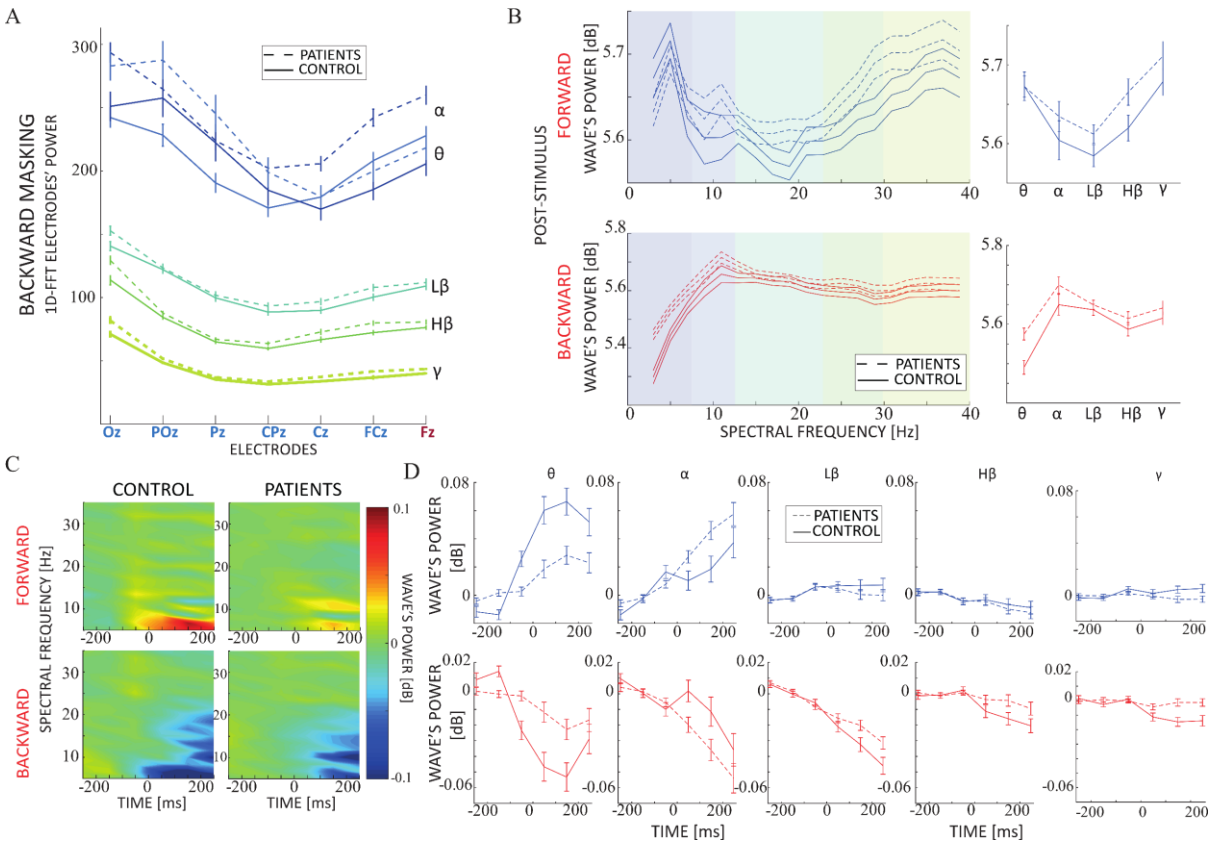

Figure 4 – Differences in traveling waves between patients and controls during visual backward masking. A) Raw power for each spectral band in the midline electrodes (x-axis), for both the patients and control group in VBM dataset. Each color represents a different frequency band. B) The left panels illustrate the spectra for both forward (blue) and backward (red) waves for the two groups; the right panels show the mean for each frequency band. C) Spectrograms representing the forward and backward waves (upper and lower panels, respectively) for the control (left) and patient (right) groups. Color-coded values are baseline corrected considering 200ms before stimulus onset (at 0ms on the x-axis). D) Mean values and standard errors for each frequency band for the patient and control groups (dashed and solid lines, respectively); the x-axis represents time in milliseconds, with stimulus onset at 0ms. Error bars represent standard errors

As in the resting state analysis, we first assessed the spectral power in each electrode separately (figure 4A). The Bayesian ANOVA, having ELECTRODE and GROUP as factors, revealed an overall higher power in the patient than in the control group in all frequency bands. As in resting state EEG, we also found a substantial effect of the ELECTRODE factor in all bands (all $BF_{10}>>10^{48}$). We then investigated the FW and BW traveling waves via two-factor ANCOVAs, with GROUP and BAND as primary factors and GENDER, AGE, and EDUCATION as covariates (figure 4B). We considered the waves after the onset of the visual stimulus before applying the baseline correction. Regarding the backward waves, we found a strong effect of BAND ($BF_{10}>10^{18}$), and moderate evidence for a difference between GROUP after the stimulus onset ($BF_{10}=8.47$) but inconclusive before ($BF_{10}=0.911$). We did not find evidence for an interactions ($BF_{10}<0.16$) or the covariates (all $0.4<BF_{10}<1.5$). These results suggest that patients have a higher amount of backward waves irrespective of the frequency band after the onset of the target. Regarding the FW waves, we observed a strong effect in the BAND factor ($BF_{10}>10^{8}$) as well as in the GROUP factor ($BF_{10}>47$). We found no evidence for the interaction ($BF_{10}<0.04$), and inconclusive evidence for the covariate variables (all $BF_{10}<1.8$). Next, we analyzed the changes in FW and BW waves with respect to the onset of the stimulus in each frequency band (i.e., applying a baseline correction computed on the 200ms before stimulus onset). In order to perform such analysis, we computed traveling waves in a time window ranging from 250ms before to 250ms after stimulus onset, with a temporal resolution of 100ms. Figure 4C illustrates the spectrogram for both forward and backward waves in both groups, whereas figure 4D gathers the same results for each frequency band separately. Considering specifically alpha- and theta-band waves, our results reveal a difference between GROUP in the forward waves (α, $BF_{10}=21.52$; θ, $BF_{10}=15.99$), but with opposite effect: patients reveal an increase in alpha-band FW after stimulus onset, and vice versa in the theta-band. Regarding the BW waves, we found evidence for a difference in the theta-band ($BF_{10}>10^{6}$) but not in the alpha-

band waves (BF_{10}=0.13). Not surprisingly, in both FW and BW waves we found an effect of the TIME factor (θ: FW, BF_{10}=145.48, BW, $BF_{10}>10^{16}$; α: FW, BF_{10}=8.12, BW, $BF_{10}>10^{14}$), and an interaction between GROUP and TIME in all conditions (BF_{10}>5 in all conditions) except in alpha BW waves (BF_{10}=0.015). Considering beta and gamma-band traveling waves, as revealed in figure 4D, we did not observe any effect in the GROUP factor (all BF_{10}<0.6) and an effect on TIME only for the BW low beta-band waves ($BF_{10}>10^{16}$), but not otherwise (all $0.1<BF_{10}<1.8$). All in all, these results confirm the prediction that the patient group show higher FW waves specifically in the alpha-band range, in line with the hypothesis that they rely more on precision-weighted sensory information.

Additionally, we investigated differences between groups in FW and BW alpha-band waves in each condition separately (i.e., *Vernier only*, *Long SOA*, *Short SOA*, and *Mask only* conditions, see above for details). As shown in supplementary figure S1, we confirm our results in all conditions except when only the mask was shown, corroborating the robustness of our results.

Correlation between the resting-state and the VBM dataset

Out of the 144 patients and 96 control participants, 119 and 75, respectively, also belonged to the resting-state dataset, thus allowing us to reveal whether oscillatory traveling waves during rest are predictive of waves occurring during backward masking, reflecting general dynamics underlying predictive processes, which are not specific to the different tasks and/or experimental design. We correlated band by band the amount of forward and backward waves in both groups (figure 5A), using Pearson correlations. In the visual backward masking dataset, we considered traveling waves before the onset of the stimulus to avoid the influence of visual processes (i.e., ERPs responses). As summarized in table 1, we found strong evidence for positive correlations between the two datasets for both forward and backward waves in all frequency bands and in both the control and the patient group.

		PATIENTS		CONTROL	
		Pearson's r	BF_{10}	Pearson's r	BF_{10}
FORWARD	θ	0.443	33457.916	0.376	30.532
	α	0.393	1775.222	0.504	4175.345
	low β	0.510	$3.781\times10^{+6}$	0.544	31240.309

	high β	0.561	$3.253\times10^{+8}$	0.589	456398.413
	γ	0.607	$3.341\times10^{+10}$	0.745	$2.941\times10^{+11}$
BACKWARD	θ	0.403	2997.128	0.390	47.777
	α	0.391	1605.222	0.535	19551.076
	low β	0.357	293.238	0.414	105.358
	high β	0.406	3670.341	0.551	45799.009
	γ	0.524	$1.170\times10^{+7}$	0.663	$9.435\times10^{+7}$

Table 1 – Coefficients of correlation between resting states and backward visual masking traveling waves.

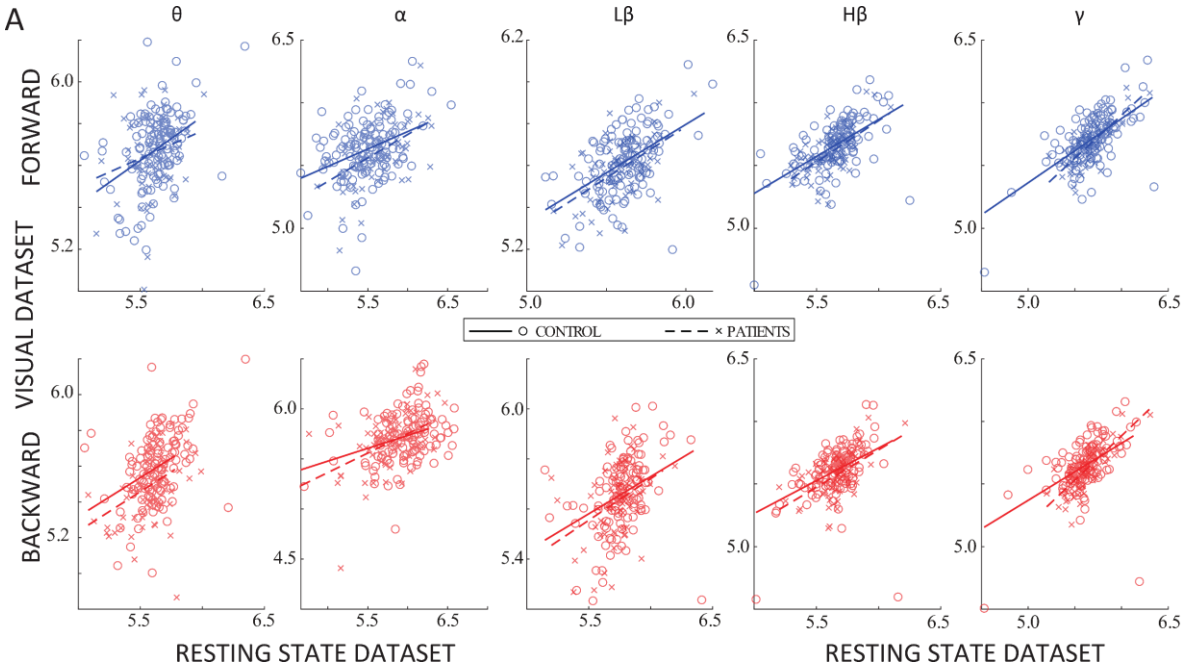

Figure 5 – Correlations between datasets. A) Each subplot shows the correlation between traveling waves in the two datasets (resting state vs. VBM task). Columns represent different frequency bands, red and blue plots indicate backward and forward waves, respectively. The fitted line indicates significant (Pearson) correlations (see results for details).

Testing the effects of medication and symptoms profile on traveling waves

To exclude potential confounds due to medication intake and to investigate whether traveling waves are associated to psychopathology in the schizophrenia patients, we correlated the amount of forward and backward waves in each frequency band with the Chlorpromazine (CPZ) equivalent dose that each patient received during the time of the recordings and with

the scores in the negative and positive symptoms assessment (SANS and SAPS, respectively). All Pearson correlations in both datasets and for all frequency bands provided evidence in favor of the null hypothesis, that is, a lack of correlation between the amount of waves and CPZ-equivalents (resting state dataset: for both FW and BW waves in all frequency band $-0.1<r<0.1$, $BF_{10}<0.19$; VBM dataset: for both FW and BW waves in all frequency band $-0.14<r<0.1$, $BF_{10}<0.22$). Second, we performed a correlation between FW and BW waves and the SANS and SAPS scores (see Methods). We did not find evidence for correlations between traveling waves and SANS or SAPS scores (for both FW and BW waves in all frequency bands, $-0.13<r<0.13$, $BF_{10}<0.23$). We obtained similar results in the VBM dataset, in which we did not find any correlation in most frequency bands ($-0.15<r<0.15$, $BF_{10}<0.3$), except for a small correlation between SAPS and BW waves in the low β ($r=0.24$, $BF_{10}=3.1$), high β bands ($r=0.26$, $BF_{10}=5.16$), and in the γ band ($r=0.26$, $BF_{10}=4.58$); and between SAPS and FW waves in the γ band ($r=0.27$, $BF_{10}=7.404$).

Discussion

Analyzing EEG recordings in patients with schizophrenia and healthy controls (da Cruz, Favrod, et al., 2020; da Cruz, Shaqiri, et al., 2020; Garobbio et al., 2021; Gordillo et al., 2023), we found direct evidence for a dysfunctional updating of beliefs about the world in schizophrenia (Fletcher & Frith, 2009). Previous studies have shown indirect evidence in favor of this interpretation (Corlett et al., 2009; Krystal et al., 2017; Ellson, 1941; Kafadar et al., 2022; Kot & Serper, 2002). In our study, we targeted abnormalities in oscillatory traveling waves, proposed to reflect the flow of information in predictive processes (Alamia et al., 2020; Alamia & VanRullen, 2019). Unlike previous work, our analysis allowed us to visualize and disentangle the different actors involved in the predictive coding process, flowing from higher to lower cortical areas, and prediction-errors, propagating in the opposite, bottom-up, direction in patients with schizophrenia and healthy controls. Our results reveal a substantial increase in top-down and a decrease in bottom-up alpha-band traveling waves in patients compared to healthy controls in the resting state dataset, and the opposite pattern of results in the visual backward masking paradigm, demonstrating that patients with schizophrenia have more precise priors (i.e., smaller variability) than healthy participants at hierarchically higher prior but less precise priors in lower sensory areas (Corlett et al., 2019; Friston, 2005; Powers et al.,

2017). Importantly, these findings describe not only the temporal but also the spatial component of brain rhythms, supporting the key idea that oscillatory dynamics are best understood when interpreted as traveling waves propagating across cortical regions, coordinating and synchronizing different brain regions (Alexander et al., 2009; Muller et al., 2018).

Our results may reconcile previously contradictory findings. Some authors proposed that positive symptoms in schizophrenia relate to abnormalities in prior expectations (Wacongne, 2016; Weilnhammer et al., 2020); on the other hand, other authors argued against this interpretation, based on indirect experimental findings, such as intact illusion perception and intact contextual processing (Choung et al., 2022; Grzeczkowski et al., 2018; Lhotka et al., 2023). To reconcile these contradicting findings, a more nuanced framework was proposed, separating priors in the lower areas from those in higher ones (Corlett et al., 2019; Sterzer et al., 2018). For example, visual illusions may rely on relatively lower-level priors, which affect visual perception specifically, whereas schizophrenia patients may have impairments in higher-level priors, involved in higher-order functions. Accordingly, schizophrenia patients proved to be more sensitive than controls to illusions involving higher-order processing, such as temporal expectations in the triple flash illusion (Norton et al., 2008), than simpler visual illusions. Our results are in line with this hypothesis. In particular, we measured traveling waves during rest and during a visual backward masking task, in which neither predictions nor sensory expectations play any substantial role (especially in resting state), suggesting that alpha-band traveling waves do not reflect specific perceptual features of the task, but rather broader brain states. This conclusion is further corroborated by the lack of difference between distinct conditions in the visual backward masking task (fig. S1).

Neural oscillations have long been studied in schizophrenia research and have been proposed to play a crucial role in coordinating neural activity, and aberrancies in their strength and synchronization may be a core pathophysiological mechanism of schizophrenia (Uhlhaas & Singer, 2006, 2010). Our findings are consistent with previous studies, in which differences between patients with schizophrenia and healthy controls have been observed in several frequency bands during resting-state (Gordillo et al., 2023; Newson & Thiagarajan, 2019) and different tasks or experimental conditions (Hirano & Uhlhaas, 2021; Javitt et al., 2018; Roach & Mathalon, 2008). For example, during resting-state, schizophrenia patients show increased

activity in the delta, theta and beta bands (Venables et al., 2009), whereas activity in the alpha and gamma bands is strongly decreased, compared to healthy controls (Knyazeva et al., 2008; Uhlhaas & Singer, 2013). Similarly, during visual processing, activity in the delta, theta and gamma bands has been shown to be reduced in schizophrenia patients (Martínez et al., 2018; Uhlhaas et al., 2006). Accordingly, our results reveal consistent differences between schizophrenia patients and healthy participants in a broad-band fashion but with a more substantial effect in the alpha-band, consistent with our hypothesis. As in our work, previous studies also related brain oscillations to predictive coding, associating prediction and prediction-error to different frequency bands (Bastos et al., 2012, 2015; Michalareas et al., 2016; Vezoli et al., 2021). Specifically, gamma oscillations (>30Hz) have been proposed to reflect local cortical processes, and besides characterizing a wide range of cognitive functions (Lundqvist et al., 2016; Zhang et al., 2012), they proved to match reliably sensory expectations and prediction errors, corroborated by the fact that the regular repetition and the unexpected omission of a stimulus respectively decrease and increase gamma oscillations' activity (Fujioka et al., 2009; Iversen et al., 2009). In agreement with our interpretation, alpha and beta band oscillations (~8-30Hz) have been related to top-down activity, carrying predictions from higher to lower brain regions (Haegens et al., 2011; Samaha et al., 2015; van Pelt et al., 2016). In our results, the relationship between top-down traveling waves and prior belief is further corroborated by a positive correlation between backward waves in the beta and gamma bands, and positive symptoms assessment (SAPS), which quantifies the symptoms related to hallucinations, delusions, and aberrancies in perception. Importantly, our study is the first one to consider oscillations as traveling waves propagating through the cortex in a forward and backward manner, thus, taking into account not only the temporal but also the spatial dimension of oscillations. It is this aspect that allowed us to reconcile the mixed findings about Bayesian predictions in schizophrenia.

All in all, our findings demonstrate that schizophrenia patients have stronger high-level priors, which elicit stronger alpha-band oscillations, and weaker low-level priors, leading to an overall dysfunctional updating of their cognitive and sensory world model. Our results provide direct evidence in favor of hierarchical-specific abnormalities in the prior of schizophrenia patients.

Methods

Participants

We present resting-state and evoked EEG data collected from two groups of participants: schizophrenia patients (N=146) and healthy controls (N=96). Resting-state EEG data were recorded for 121 schizophrenia patients and 75 healthy controls. Visual backward masking (VBM) EEG data were recorded from 144 schizophrenia patients and 96 healthy controls, with 119 schizophrenia patients and 75 healthy controls also having resting-state recordings. Previous studies have already utilized the resting-state data for 121 schizophrenia patients and 75 healthy controls (Gordillo et al., 2023), as well as the VBM EEG data for 121 schizophrenia patients and 94 healthy controls (Garobbio et al., 2021).

Schizophrenia patients were recruited from the Tbilisi Mental Health Hospital or the psycho-social rehabilitation center. Among the patients, 49 were inpatients, while 97 were outpatients. Diagnostic assessment for patients was determined using the Diagnostic and Statistical Manual of Mental Disorders Fourth Edition (DSM-IV) through interviews, information from staff, and examination of patients' records. The severity of the patient's symptoms was assessed by an experienced psychiatrist using the Scale for the Assessment of Negative Symptoms (SANS) and the Scale for the Assessment of Positive Symptoms (SAPS). Out of the 144 patients, 131 were receiving neuroleptic medication. The equivalent doses of Chlorpromazine (CPZ) are provided in Table 1.

Controls were selected from the general population in Tbilisi, aiming to closely match the demographics of the patient group. All control participants had no psychiatric axis I disorders and no family history of psychosis. Exclusion criteria included alcohol or drug abuse, severe neurological incidents or diagnoses, developmental disorders such as autism spectrum disorder or intellectual disability, or other significant somatic illnesses affecting mental functioning. These criteria were assessed through interviews conducted by certified psychiatrists. Detailed characteristics of the groups are presented in Table 1.

Before participating in the study, all individuals provided informed consent and were informed of their right to withdraw from the study at any time. The study procedures were conducted in accordance with the Declaration of Helsinki (except for preregistration) and were approved

by the Ethical Committee of the Institute of Postgraduate Medical Education and Continuous Professional Development in Georgia (protocol number: 09/07; title: "Genetic polymorphisms and early information processing in schizophrenia").

Table 1. Group statistics

	VBM patients	VBM controls	Statistics	RS patients	RS controls	Statistics
Gender (M/F)	115/29	49/47	$X^2(1)=22.108$, P<0.001[a]	22/99	39/36	$X^2(1)=24.702$, P<0.001[a]
Age (years)	35.5±9.1	35.0±8.3	t(238)=-0.393, P=0.695[b]	35.8±9.2	35.1±7.7	t(194)=-0.519, P=0.604[b]
Education (years)	13.2±2.6	15.2±2.9	t(238)=-5.432, P<0.001[b]	13.3±2.6	15.1±2.9	t(194)=4.418, P<0.001[b]
Handedness (L/R)	7/137	6/90	$X^2(1)=0.217$, P=0.641[a]	6/115	4/71	$X^2(1)=0.013$, P=0.908[a]
Illness duration (years)	10.7±8.5			10.8±8.7		
SANS	10.1±5.2			10.1±5.2		
SAPS	8.7±3.2			8.6±3.2		
CPZ equivalent	578.3±391.6			561.1±389.4		
Visual acuity	1.4±0.4	1.6±0.4	t(238)=-3.388, P<0.001[b]	1.4±0.4	1.6±0.4	t(194)=2.969, P=0.003[b]
Vernier duration*	20 [20, 50]	20[20, 20]	$X^2(1)=37.949$, P<0.001[c]	20 [20, 52.5]	20[20, 20]	$X^2(1)=28.25$, P<0.001[c]

Note: SANS, Scale for the Assessment of Negative Symptoms; SAPS, Scale for the Assessment of Positive Symptoms; CPZ, Chlorpromazine equivalents

[a] Pearson's chi-squared test

[b] Two-sided independent samples t-test

[c] Mood's median test

*Median [25th percentile, 75th percentile]; Vernier duration value is missing for one patient in both datasets

Experimental procedure

Visual backward masking

Stimuli

The stimuli consisted of two vertical line segments of 10' (arc-minutes) length with a gap of 1'. The lower bar was slightly offset either to the left or right compared to the upper bar. The offset was fixed at about 1.2'. The mask was composed of 25 verniers without offset separated by 3.33'.

Apparatus

The stimuli were displayed on a cathode ray tube screen (Siemens Fujitsu P796-1) with a refresh rate of 100 Hz. The screen resolution was 1024 x 768 pixels. Participants were seated at 3.5m from the monitor in a dimly lit room. A pixel comprised about 18'' (arc-seconds). Stimuli were white. The luminance was 100 cd/m^2 (measured with a Gretag Macbeth Eye-One Display 2 colorimeter) on a black background of < 1 cd/m^2.

Adaptive procedure

Further details of the paradigm can be found in a previous study (Herzog et al., 2004). We determined the Vernier Discrimination Threshold (VD) required for participants to achieve 75% of correct responses in identifying a vernier offset of 0.6'. Participants were required to achieve a VD shorter than 100 milliseconds. The vernier stimulus, with the individualized VD for each participant and an offset of 1.2', was presented, followed by an interstimulus interval and a mask lasting 300 milliseconds. Using a staircase procedure, we adaptively determined the target-mask stimulus onset asynchrony (SOA), calculated as the sum of VD and interstimulus interval (ISI), to achieve a performance level of 75% correct responses. This was done using Parametric Estimation by Sequential Testing (PEST). Each participant completed the test twice, and the results of the first and second tests were averaged and are presented in Table 1.

EEG experiment

ERP latencies and amplitudes vary with VD. Hence, for the EEG experiment, we maintained VDs and SOAs constant thereby using the same stimuli for all observers. We set the VD to 30 milliseconds, which corresponds to the average VD observed in previous studies involving patients (Chkonia et al., 2010; Herzog et al., 2004). Our experiment encompassed four distinct

stimulus conditions (Favrod et al., 2017, 2019; Plomp et al., 2013). In the Vernier Only condition, only the target vernier stimulus was presented. The Long SOA condition involved the presentation of the mask following the target vernier, with an SOA of 150 milliseconds. In contrast, the Short SOA condition featured the immediate presentation of the mask after the target vernier, resulting in an SOA of 30 milliseconds. The selection of SOAs for the Long SOA and Short SOA conditions was based on the mean SOAs observed in previous studies involving both schizophrenia patients and controls (Chkonia et al., 2010; Favrod et al., 2018; Herzog et al., 2004; Plomp et al., 2013). To provide a control condition, we included the Mask Only condition, wherein only the mask stimulus was presented. In this particular case, accuracy was determined by comparing the left/right offset response to a randomly chosen hypothetical offset.

Resting-state

Resting-state EEG data were recorded for 5min. Participants were seated in a dimly lit room and were instructed to close their eyes and relax during the recording.

EEG recording and preprocessing

EEG was recorded using a BioSemi Active 2 system with 64 Ag-AgCl sintered active electrodes, referenced to the common mode sense electrode. The sampling rate was 2048 Hz. Offline data were downsampled to 512 Hz and preprocessed using an automatic preprocessing pipeline (da Cruz et al., 2018). For resting-state EEG data, the preprocessing included the following steps: high-pass filtering at 1 Hz; power line noise removal (using CleanLine; www.nitrc.org/projects/cleanline); re-referencing to the bi-weight estimate of the average of all electrodes; removal and 3D spline interpolation of bad electrodes; removal of bad epochs; independent component analysis (ICA) to remove artifacts related to eye-movements, muscle activity, and bad electrodes, and removal of epochs with artifacts (1s epochs). For VBM EEG data, the preprocessing was similar to the resting-state data with the difference that a band-pass filtering between 1 and 40 Hz was performed instead of high-pass filtering at 1 Hz. VBM EEG data from 2 patients (both present in the resting-state dataset) and 2 healthy controls (1 present in the resting-state dataset) were discarded due to excessive EEG artifacts.

Traveling wave analysis

As in our previous studies (Alamia et al., 2020; Pang et al., 2020) we quantified traveling waves' propagation along seven midline electrodes, running from occipital to frontal regions (Oz, POz, Pz, CPz, Cz, FCz, Fz, as shown in figure 1). After segmenting the signal in a 1-second time window (and 500ms for the VBM dataset), we stacked the signals from the seven electrodes to create 2D maps, with time and electrodes as axes. From each map, we compute 2D-FFT transformation: importantly, the power in the lower and upper quadrants quantifies the amount of forward (FW - from occipital to frontal electrodes) and backward (BW - from frontal to occipital) waves, respectively (see figure 1). For each frequency in the 2-45Hz range, we considered the maximum values in both the upper and lower quadrant, obtaining a spectrum for both BW and FW waves, respectively. We then needed to determine a baseline to account for fluctuations in the overall power unrelated to the traveling waves. For this reason, we computed the average 1D-FFT of each midline electrode, which provides a baseline accounting for the spectral power unrelated to the traveling waves (i.e., without the spatial information obtained by combining the electrodes). We finally obtained the waves' amount in decibels [dB] as:

$$FW\ [dB] = 10 * log_{10}\left(\frac{FW}{average}\right); \quad BW\ [dB] = 10 * log_{10}\ (\frac{BW}{average}).$$

This value quantifies the total waves compared to the null distribution, thus being informative when contrasted against zero. It is important, however, to notice that this is a surface-level analysis, and it is not informative about the underlying sources. When interpreting these traveling waves results, it is also important to consider issues related to long-range connections and distortions due to scalp interference (Alexander et al., 2019; Nunez, 1974). In particular, when considering traveling waves analysis with non-invasive surface recordings (such as EEG), it is crucial to consider distortions and interference between coincident waves and limitations due to the electrode configurations (Alexander et al., 2019; Nunez, 1974, 2000). Specifically, it's possible to detect only waves shorter than the spatial length of the sensor array and waves longer than twice the distance between electrodes (due to the Nyquist criterion in space). In addition, different cortical processes may generate a similar pattern of traveling waves visible via surface recordings (Alamia & VanRullen, 2023), thus limiting the interpretation of possible underlying sources.

Statistical analyses

We analyzed frequency-band averaged traveling waves by means of Bayesian ANOVAs. In all analyses, we computed Bayes Factors (BF) as the ratio between the models testing the alternative against the null hypothesis. All BFs are denoted as BF_{10} throughout the paper. In practice, BFs provide substantial (BF>~5) or strong (BF>~10) evidence in favor of the alternative hypothesis, and low BF (BF<~0.5) suggests a lack of effect (Masson, 2011). In each dataset, we performed a Bayesian ANOVA on each electrode spectral power considering ELECTRODE (from Oz to Fz along the midline) and GROUP (patients and control) as fixed factors and SUBJECT as the random term. We also performed an ANCOVA considering GENDER, AGE, and EDUCATION as covariates, GROUP and BAND as fixed terms, and SUBJECT as random terms. Lastly, all Bayesian correlations were computed considering both Pearson and Kendall, but we reported for simplicity only Bayes Factor for the Pearson r (similar results were obtained considering Kendall correlations). We performed all analyses in JASP (Love et al., 2019), considering default uniform prior distributions.

Acknowledgments

This project was funded by the European Union under the European Union's Horizon 2020 research and innovation program (grant agreements No. 101075930 to Andrea Alamia) and the National Centre of Competence in Research (NCCR) Synapsy financed by the Swiss National Science Foundation under grant 51NF40-185897. Views and opinions expressed are however those of the author(s) only and do not necessarily reflect those of the European Union or the European Research Council (ERC). Neither the European Union nor the granting authority can be held responsible for them.

References

Alamia, A., Terral, L., d'Ambra, M. R., & VanRullen, R. (2023). Distinct roles of forward and backward alpha-band waves in spatial visual attention. *Elife*, *12*, e85035.

Alamia, A., Timmermann, C., Nutt, D. J., VanRullen, R., & Carhart-Harris, R. L. (2020). DMT alters cortical travelling waves. *eLife*, *9*, e59784. https://doi.org/10.7554/eLife.59784

Alamia, A., & VanRullen, R. (2019). Alpha oscillations and traveling waves : Signatures of predictive coding? *PLOS Biology*, *17*(10), e3000487. https://doi.org/10.1371/journal.pbio.3000487

Alamia, A., & VanRullen, R. (2023). A Traveling Waves Perspective on Temporal Binding. *Journal of Cognitive Neuroscience*, 1-9. https://doi.org/10.1162/jocn_a_02004

Alexander, D. M., Ball, T., Schulze-Bonhage, A., & Van Leeuwen, C. (2019). Large-scale cortical travelling waves predict localized future cortical signals. *PLoS Computational Biology*, *15*(11). https://doi.org/10.1371/journal.pcbi.1007316

Alexander, D. M., Flynn, G. J., Wong, W., Whitford, T. J., Harris, A. W. F., Galletly, C. A., & Silverstein, S. M. (2009). Spatio-temporal EEG waves in first episode schizophrenia. *Clinical Neurophysiology*, *120*(9), 1667-1682. https://doi.org/10.1016/j.clinph.2009.06.020

Arnal, L. H., & Giraud, A.-L. (2012). Cortical oscillations and sensory predictions. *Trends in Cognitive Sciences*, *16*(7), 390-398. https://doi.org/10.1016/j.tics.2012.05.003

Bastos, A. M., Usrey, W. M., Adams, R. A., Mangun, G. R., Fries, P., & Friston, K. J. (2012). Canonical Microcircuits for Predictive Coding. *Neuron*, *76*(4), 695-711. https://doi.org/10.1016/j.neuron.2012.10.038

Bastos, A. M., Vezoli, J., Bosman, C. A., Schoffelen, J.-M., Oostenveld, R., Dowdall, J. R., De Weerd, P., Kennedy, H., & Fries, P. (2015). Visual Areas Exert Feedforward and Feedback Influences through Distinct Frequency Channels. *Neuron*, *85*(2), 390-401. https://doi.org/10.1016/j.neuron.2014.12.018

Carhart-Harris, R. L., & Friston, K. J. (2019). REBUS and the Anarchic Brain : Toward a Unified Model of the Brain Action of Psychedelics. *Pharmacological Reviews*, *71*(3), 316-344. https://doi.org/10.1124/pr.118.017160

Cassidy, C. M., Balsam, P. D., Weinstein, J. J., Rosengard, R. J., Slifstein, M., Daw, N. D., Abi-Dargham, A., & Horga, G. (2018). A Perceptual Inference Mechanism for Hallucinations Linked to Striatal Dopamine. *Current Biology: CB*, *28*(4), 503-514.e4. https://doi.org/10.1016/j.cub.2017.12.059

Chkonia, E., Roinishvili, M., Makhatadze, N., Tsverava, L., Stroux, A., Neumann, K., Herzog, M. H., & Brand, A. (2010). The Shine-Through Masking Paradigm Is a Potential Endophenotype of Schizophrenia. *PLoS ONE*, *5*(12), e14268. https://doi.org/10.1371/journal.pone.0014268

Choung, O.-H., Gordillo, D., Roinishvili, M., Brand, A., Herzog, M. H., & Chkonia, E. (2022). Intact and deficient contextual processing in schizophrenia patients. *Schizophrenia Research: Cognition*, *30*, 100265. https://doi.org/10.1016/j.scog.2022.100265

Corlett, P. R., Frith, C. D., & Fletcher, P. C. (2009). From drugs to deprivation : A Bayesian framework for understanding models of psychosis. *Psychopharmacology*, *206*(4), 515-530. https://doi.org/10.1007/s00213-009-1561-0

Corlett, P. R., Horga, G., Fletcher, P. C., Alderson-Day, B., Schmack, K., & Powers, A. R. (2019). Hallucinations and Strong Priors. *Trends in Cognitive Sciences*, *23*(2), 114-127. https://doi.org/10.1016/j.tics.2018.12.001

da Cruz, J. R., Chicherov, V., Herzog, M. H., & Figueiredo, P. (2018). An automatic pre-processing pipeline for EEG analysis (APP) based on robust statistics. *Clinical Neurophysiology*, *129*(7), 1427-1437. https://doi.org/10.1016/j.clinph.2018.04.600

da Cruz, J. R., Favrod, O., Roinishvili, M., Chkonia, E., Brand, A., Mohr, C., Figueiredo, P., & Herzog, M. H. (2020). EEG microstates are a candidate endophenotype for schizophrenia. *Nature Communications*, *11*(1), 3089. https://doi.org/10.1038/s41467-020-16914-1

da Cruz, J. R., Shaqiri, A., Roinishvili, M., Favrod, O., Chkonia, E., Brand, A., Figueiredo, P., & Herzog, M. H. (2020). Neural Compensation Mechanisms of Siblings of Schizophrenia Patients as Revealed by High-Density EEG. *Schizophrenia Bulletin*, *46*(4), 1009-1018. https://doi.org/10.1093/schbul/sbz133

Ellson, D. G. (1941). Hallucinations produced by sensory conditioning. *Journal of Experimental Psychology*, *28*(1), 1-20. https://doi.org/10.1037/h0054167

Favrod, O., da Cruz, J. R., Roinishvili, M., Berdzenishvili, E., Brand, A., Figueiredo, P., Herzog, M. H., & Chkonia, E. (2019). Electrophysiological correlates of visual backward masking in patients with major depressive disorder. *Psychiatry Research: Neuroimaging*, *294*, 111004. https://doi.org/10.1016/j.pscychresns.2019.111004

Favrod, O., Roinishvili, M., da Cruz, J. R., Brand, A., Okruashvili, M., Gamkrelidze, T., Figueiredo, P., Herzog, M. H., Chkonia, E., & Shaqiri, A. (2018). Electrophysiological correlates of visual backward masking in patients with first episode psychosis. *Psychiatry Research: Neuroimaging*, *282*, 64-72. https://doi.org/10.1016/j.pscychresns.2018.10.008

Favrod, O., Sierro, G., Roinishvili, M., Chkonia, E., Mohr, C., Herzog, M. H., & Cappe, C. (2017). Electrophysiological correlates of visual backward masking in high schizotypic personality traits participants. *Psychiatry Research*, *254*, 251-257. https://doi.org/10.1016/j.psychres.2017.04.051

Fletcher, P. C., & Frith, C. D. (2009). Perceiving is believing : A Bayesian approach to explaining the positive symptoms of schizophrenia. *Nature Reviews Neuroscience*, *10*(1), Article 1. https://doi.org/10.1038/nrn2536

Friston, K., Brown, H. R., Siemerkus, J., & Stephan, K. E. (2016). The dysconnection hypothesis (2016). *Schizophrenia Research*, *176*(2-3), 83-94. https://doi.org/10.1016/j.schres.2016.07.014

Friston, K. J. (2005). Hallucinations and perceptual inference. *Behavioral and Brain Sciences*, *28*(6), 764-766. https://doi.org/10.1017/S0140525X05290131

Friston, K. J. (2019). Waves of prediction. *PLOS Biology*, *17*(10), e3000426. https://doi.org/10.1371/journal.pbio.3000426

Fujioka, T., Trainor, L. J., Large, E. W., & Ross, B. (2009). Beta and gamma rhythms in human auditory cortex during musical beat processing. *Annals of the New York Academy of Sciences*, *1169*, 89-92. https://doi.org/10.1111/j.1749-6632.2009.04779.x

Garobbio, S., Roinishvili, M., Favrod, O., da Cruz, J. R., Chkonia, E., Brand, A., & Herzog, M. H. (2021). Electrophysiological correlates of visual backward masking in patients with bipolar disorder. *Psychiatry Research: Neuroimaging*, *307*, 111206. https://doi.org/10.1016/j.pscychresns.2020.111206

Gordillo, D., da Cruz, J. R., Chkonia, E., Lin, W.-H., Favrod, O., Brand, A., Figueiredo, P., Roinishvili, M., & Herzog, M. H. (2023). The EEG multiverse of schizophrenia. *Cerebral Cortex*, *33*(7), 3816-3826. https://doi.org/10.1093/cercor/bhac309

Grzeczkowski, L., Roinishvili, M., Chkonia, E., Brand, A., Mast, F. W., Herzog, M. H., & Shaqiri, A. (2018). Is the perception of illusions abnormal in schizophrenia? *Psychiatry Research*, *270*, 929-939. https://doi.org/10.1016/j.psychres.2018.10.063

Haegens, S., Händel, B. F., & Jensen, O. (2011). Top-Down Controlled Alpha Band Activity in Somatosensory Areas Determines Behavioral Performance in a Discrimination Task. *Journal of Neuroscience*, *31*(14), 5197-5204. https://doi.org/10.1523/JNEUROSCI.5199-10.2011

Herzog, M. H., Kopmann, S., & Brand, A. (2004). Intact figure-ground segmentation in schizophrenia. *Psychiatry Research*, *129*(1), 55-63. https://doi.org/10.1016/j.psychres.2004.06.008

Hirano, Y., & Uhlhaas, P. J. (2021). Current findings and perspectives on aberrant neural oscillations in schizophrenia. *Psychiatry and Clinical Neurosciences*, *75*(12), 358-368. https://doi.org/10.1111/pcn.13300

Iversen, J. R., Repp, B. H., & Patel, A. D. (2009). Top-down control of rhythm perception modulates early auditory responses. *Annals of the New York Academy of Sciences*, *1169*, 58-73. https://doi.org/10.1111/j.1749-6632.2009.04579.x

Javitt, D. C., Lee, M., Kantrowitz, J. T., & Martinez, A. (2018). Mismatch negativity as a biomarker of theta band oscillatory dysfunction in schizophrenia. *Schizophrenia Research*, *191*, 51-60. https://doi.org/10.1016/j.schres.2017.06.023

Kafadar, E., Fisher, V. L., Quagan, B., Hammer, A., Jaeger, H., Mourgues, C., Thomas, R., Chen, L., Imtiaz, A., Sibarium, E., Negreira, A. M., Sarisik, E., Polisetty, V., Benrimoh, D., Sheldon, A. D., Lim, C., Mathys, C., & Powers, A. R. (2022). Conditioned Hallucinations and Prior Overweighting Are State-Sensitive Markers of Hallucination Susceptibility. *Biological Psychiatry*, *92*(10), 772-780. https://doi.org/10.1016/j.biopsych.2022.05.007

Knyazeva, M. G., Jalili, M., Meuli, R., Hasler, M., De Feo, O., & Do, K. Q. (2008). Alpha rhythm and hypofrontality in schizophrenia. *Acta Psychiatrica Scandinavica*, *118*(3), 188-199. https://doi.org/10.1111/j.1600-0447.2008.01227.x

Kot, T., & Serper, M. (2002). Increased susceptibility to auditory conditioning in hallucinating schizophrenic patients : A preliminary investigation. *The Journal of Nervous and Mental Disease*, *190*(5), 282-288. https://doi.org/10.1097/00005053-200205000-00002

Krystal, J. H., Murray, J. D., Chekroud, A. M., Corlett, P. R., Yang, G., Wang, X.-J., & Anticevic, A. (2017). Computational Psychiatry and the Challenge of Schizophrenia. *Schizophrenia Bulletin*, *43*(3), 473-475. https://doi.org/10.1093/schbul/sbx025

Lhotka, M., Ischebeck, A., Helmlinger, B., & Zaretskaya, N. (2023). No common factor for illusory percepts, but a link between pareidolia and delusion tendency : A test of predictive coding theory. *Frontiers in Psychology*, *13*, 1067985. https://doi.org/10.3389/fpsyg.2022.1067985

Love, J., Selker, R., Marsman, M., Jamil, T., Dropmann, D., Verhagen, J., Ly, A., Gronau, Q. F., Šmíra, M., Epskamp, S., Matzke, D., Wild, A., Knight, P., Rouder, J. N., Morey, R. D., & Wagenmakers, E.-J. (2019). JASP : Graphical Statistical Software for Common Statistical Designs. *Journal of Statistical Software*, *88*, 1-17. https://doi.org/10.18637/jss.v088.i02

Lundqvist, M., Rose, J., Herman, P., Brincat, S. L. L., Buschman, T. J. J., & Miller, E. K. K. (2016). Gamma and Beta Bursts Underlie Working Memory. *Neuron*, *90*(1), 152-164. https://doi.org/10.1016/j.neuron.2016.02.028

Martínez, A., Gaspar, P. A., Hillyard, S. A., Andersen, S. K., Lopez-Calderon, J., Corcoran, C. M., & Javitt, D. C. (2018). Impaired Motion Processing in Schizophrenia and the Attenuated Psychosis Syndrome : Etiological and Clinical Implications. *American Journal of Psychiatry*, *175*(12), 1243-1254. https://doi.org/10.1176/appi.ajp.2018.18010072

Masson, M. E. J. (2011). A tutorial on a practical Bayesian alternative to null-hypothesis significance testing. *Behavior Research Methods*, *43*(3), 679-690. https://doi.org/10.3758/s13428-010-0049-5

McCutcheon, R. A., Reis Marques, T., & Howes, O. D. (2020). Schizophrenia—An Overview. *JAMA Psychiatry*, *77*(2), 201-210. https://doi.org/10.1001/jamapsychiatry.2019.3360

Michalareas, G., Vezoli, J., van Pelt, S., Schoffelen, J.-M., Kennedy, H., & Fries, P. (2016). Alpha-Beta and Gamma Rhythms Subserve Feedback and Feedforward Influences among Human Visual Cortical Areas. *Neuron*, *89*(2), 384-397. https://doi.org/10.1016/j.neuron.2015.12.018

Muller, L., Chavane, F., Reynolds, J., & Sejnowski, T. J. (2018). Cortical travelling waves : Mechanisms and computational principles. *Nature Reviews Neuroscience*, *19*(5), Article 5. https://doi.org/10.1038/nrn.2018.20

Newson, J. J., & Thiagarajan, T. C. (2019). EEG Frequency Bands in Psychiatric Disorders : A Review of Resting State Studies. *Frontiers in Human Neuroscience*, *12*, 521. https://doi.org/10.3389/fnhum.2018.00521

Nunez, P. L. (1974). The brain wave equation : A model for the EEG. *Mathematical Biosciences*, *21*(3-4), 279-297. https://doi.org/10.1016/0025-5564(74)90020-0

Nunez, P. L. (2000). Toward a quantitative description of large-scale neocortical dynamic function and EEG. *Behavioral and Brain Sciences*, *23*(3), 371-398. https://doi.org/10.1017/S0140525X00003253

Pang (庞兆阳), Z., Alamia, A., & VanRullen, R. (2020). Turning the Stimulus On and Off Changes the Direction of α Traveling Waves. *eNeuro*, *7*(6), ENEURO.0218-20.2020. https://doi.org/10.1523/ENEURO.0218-20.2020

Plomp, G., Roinishvili, M., Chkonia, E., Kapanadze, G., Kereselidze, M., Brand, A., & Herzog, M. H. (2013). Electrophysiological Evidence for Ventral Stream Deficits in Schizophrenia Patients. *Schizophrenia Bulletin*, *39*(3), 547-554. https://doi.org/10.1093/schbul/sbr175

Powers, A. R., Mathys, C., & Corlett, P. R. (2017). Pavlovian conditioning–induced hallucinations result from overweighting of perceptual priors. *Science*, *357*(6351), 596-600. https://doi.org/10.1126/science.aan3458

Rao, R. P. N., & Ballard, D. H. (1999). Predictive coding in the visual cortex : A functional interpretation of some extra-classical receptive-field effects. *Nature Neuroscience*, *2*(1), Article 1. https://doi.org/10.1038/4580

Roach, B. J., & Mathalon, D. H. (2008). Event-Related EEG Time-Frequency Analysis : An Overview of Measures and An Analysis of Early Gamma Band Phase Locking in Schizophrenia. *Schizophrenia Bulletin*, *34*(5), 907-926. https://doi.org/10.1093/schbul/sbn093

Samaha, J., Bauer, P., Cimaroli, S., & Postle, B. R. (2015). Top-down control of the phase of alpha-band oscillations as a mechanism for temporal prediction. *Proceedings of the National Academy of Sciences*, *112*(27), 8439-8444. https://doi.org/10.1073/pnas.1503686112

Sterzer, P., Adams, R. A., Fletcher, P., Frith, C., Lawrie, S. M., Muckli, L., Petrovic, P., Uhlhaas, P., Voss, M., & Corlett, P. R. (2018). The Predictive Coding Account of Psychosis. *Biological Psychiatry*, *84*(9), 634-643. https://doi.org/10.1016/j.biopsych.2018.05.015

Stuke, H., Weilnhammer, V. A., Sterzer, P., & Schmack, K. (2019). Delusion Proneness is Linked to a Reduced Usage of Prior Beliefs in Perceptual Decisions. *Schizophrenia Bulletin*, *45*(1), 80-86. https://doi.org/10.1093/schbul/sbx189

Uhlhaas, P. J., Linden, D. E. J., Singer, W., Haenschel, C., Lindner, M., Maurer, K., & Rodriguez, E. (2006). Dysfunctional Long-Range Coordination of Neural Activity during Gestalt Perception in Schizophrenia. *The Journal of Neuroscience*, *26*(31), 8168-8175. https://doi.org/10.1523/JNEUROSCI.2002-06.2006

Uhlhaas, P. J., & Singer, W. (2006). Neural Synchrony in Brain Disorders : Relevance for Cognitive Dysfunctions and Pathophysiology. *Neuron*, *52*(1), 155-168. https://doi.org/10.1016/j.neuron.2006.09.020

Uhlhaas, P. J., & Singer, W. (2010). Abnormal neural oscillations and synchrony in schizophrenia. *Nature Reviews Neuroscience*, *11*(2), Article 2. https://doi.org/10.1038/nrn2774

Uhlhaas, P. J., & Singer, W. (2013). High-frequency oscillations and the neurobiology of schizophrenia. *Dialogues in Clinical Neuroscience*, *15*(3), 301-313. https://doi.org/10.31887/DCNS.2013.15.3/puhlhaas

van Pelt, S., Heil, L., Kwisthout, J., Ondobaka, S., van Rooij, I., & Bekkering, H. (2016). Beta- and gamma-band activity reflect predictive coding in the processing of causal events. *Social Cognitive and Affective Neuroscience*, *11*(6), 973-980. https://doi.org/10.1093/scan/nsw017

Venables, N. C., Bernat, E. M., & Sponheim, S. R. (2009). Genetic and Disorder-Specific Aspects of Resting State EEG Abnormalities in Schizophrenia. *Schizophrenia Bulletin*, *35*(4), 826-839. https://doi.org/10.1093/schbul/sbn021

Vezoli, J., Vinck, M., Bosman, C. A., Bastos, A. M., Lewis, C. M., Kennedy, H., & Fries, P. (2021). Brain rhythms define distinct interaction networks with differential dependence on anatomy. *Neuron*, *109*(23), 3862-3878.

Wacongne, C. (2016). A predictive coding account of MMN reduction in schizophrenia. *Biological Psychology*, *116*, 68-74. https://doi.org/10.1016/j.biopsycho.2015.10.011

Weilnhammer, V., Röd, L., Eckert, A.-L., Stuke, H., Heinz, A., & Sterzer, P. (2020). Psychotic Experiences in Schizophrenia and Sensitivity to Sensory Evidence. *Schizophrenia Bulletin*, *46*(4), 927-936. https://doi.org/10.1093/schbul/sbaa003

Zhang, Z. G., Hu, L., Hung, Y. S., Mouraux, A., & Iannetti, G. D. (2012). Gamma-Band Oscillations in the Primary Somatosensory Cortex—A Direct and Obligatory Correlate of Subjective Pain Intensity. *Journal of Neuroscience*, *32*(22), 7429-7438. https://doi.org/10.1523/JNEUROSCI.5877-11.2012

Chapter 6. Do we really measure what we think we are measuring?

Dario Gordillo, [1,4] Janir Ramos da Cruz, [1,2,3] Dana Moreno, [1] Simona Garobbio, [1] and Michael H. Herzog [1]

[1]Laboratory of Psychophysics, Brain Mind Institute, School of Life Sciences, École Polytechnique Fédérale de Lausanne (EPFL), CH-1015 Lausanne, Switzerland

[2]Institute for Systems and Robotics – Lisboa (LARSyS), Department of Bioengineering, Instituto Superior Técnico, Universidade de Lisboa, 1049-001 Lisbon, Portugal

[3]Wyss Center for Bio and Neuroengineering, CH-1202 Geneva, Switzerland

Postprint of the article published in *iScience*

Full citation: Gordillo, D., da Cruz, J. R., Moreno, D., Garobbio, S., & Herzog, M. H. (2023). Do we really measure what we think we are measuring? iScience, 26, 106017. https://doi.org/10.1016/j.isci.2023.106017

Detailed personal contribution: I conceptualized the project, and performed statistical and EEG analyses. I wrote and revised the article with the collaboration of the other authors.

Highlights

- Many tests in science are assumed to measure the same phenomena
- EEG features showing significant effects do not strongly correlate with each other
- Cognitive tasks are only poorly predicted by EEG features
- A significant result may tell less of a research question than believed

Summary

Tests used in the empirical sciences are often (implicitly) assumed to be representative of a given research question in the sense that similar tests should lead to similar results. Here, we

show that this assumption is not always valid. We illustrate our argument with the example of resting-state electroencephalogram (EEG). We used multiple analysis methods, contrary to typical EEG studies where one analysis method is used. We found, first, that many EEG features correlated significantly with cognitive tasks. However, these EEG features correlated weakly with each other. Similarly, in a second analysis, we found that many EEG features were significantly different in older compared to younger participants. When we compared these EEG features pairwise, we did not find strong correlations. In addition, EEG features predicted cognitive tasks poorly as shown by cross-validated regression analysis. We discuss several explanations of these results.

Introduction

Representative paradigms with elaborated tests are crucial in all empirical sciences. In the brain sciences, neuroimaging methods are used to investigate mechanisms underlying cognition and perception. Typically, a link between a neuroimaging feature (e.g., brain volume, connectivity) and a cognitive function of interest is declared if the chosen test delivers a significant result (after accounting for confounding variables). There is often the implicit assumption that the significant neuroimaging feature is representative of the neural mechanism under investigation. Here, we explicitly tested this assumption with the example of resting-state electroencephalogram (EEG).

In resting-state studies, EEG is recorded for around 5 min during which participants do nothing else than rest quietly. Signal processing methods are applied to quantify spatial and/or temporal characteristics of spontaneous brain activity. The outcomes of the analysis methods, i.e., EEG features, are interpreted to reflect brain processes linked to certain aspects of perception and cognition. For example, activity in the alpha and theta bands has been linked to memory and executive functions,[1,2,3] alpha-band activity to visual perception,[4,5] temporal autocorrelations of alpha-band oscillations and EEG microstates dynamics to reaction times,[6,7] connectivity features and alpha activity to intellectual abilities,[8,9,10] just to give a few examples. Similarly, EEG features reveal abnormalities in patients with schizophrenia,[11,12,13,14,15] depression,[16,17,18,19] and healthy older adults,[20,21,22,23] among others.

Each of these findings indicates a significant link between a given EEG feature and an aspect of cognition or a disease. In this respect, this approach has been very successful. Yet, these results provoke the questions of how the different EEG features relate to each other and how representative they are of the underlying mechanisms. For example, one might expect different EEG features, recorded from the same patients, to correlate with each other if they are supposed to point to the same aspect of the disease.

Here, we analyzed data from resting-state EEG recordings and a battery of cognitive tests. To obtain a comprehensive set of neurophysiological features, we applied widely used analysis methods to the same EEG data, including time-domain, frequency-domain, connectivity, and nonlinear dynamical analysis methods both in the electrode and source spaces. We extracted 175 EEG features. From the battery of cognitive tests, we obtained 12 cognitive variables describing several cognitive aspects. We correlated each EEG feature with each cognitive variable using methods that permitted us to examine linear and nonlinear relationships. Next, we correlated the features revealing significant correlations with the same cognitive variable using univariate and multivariate correlation methods. This comparison allowed us to investigate whether the features, showing a significant correlation with one of the cognitive variables, point to a common mechanism. In a second project, we conducted group comparisons between younger and older adults using each EEG feature. A significant group difference would indicate that the EEG features tap into important age-related changes in brain processing. To test whether the features showing group differences target common age-related aspects, we correlated the EEG features revealing significant group differences. Furthermore, we used principal component analysis to assess the latent dimensions of multiple EEG features showing significant correlations to a cognitive variable and significant group differences between younger and older adults. As a complementary analysis, we evaluated cross-validated regression models using each EEG feature to predict the cognitive variables. Importantly, we did not want to elaborate on any particular relationship between an EEG feature and cognitive ability or an EEG feature and aging. We were interested in how significant results from single analyses relate to each other.

Results

We analyzed data from the publicly available LEMON database.[24] This database includes resting-state EEG recordings and a battery of cognitive tasks. The sample used for the present study consisted of 201 participants, 138 younger adults (mean age = 25.43, SD = 3.39, 42 females) and 63 older adults (mean age = 67.66, SD = 4.79, 31 females). Using multiple analysis methods, we obtained 175 EEG features from the resting-state EEG recordings. The EEG features can be composed either of 61, 80, or 4 variables, corresponding to the number of electrodes, brain regions, or microstate parameters, respectively. From the battery of 6 cognitive tests, we obtained 12 cognitive variables. Details are shown in experimental model and subject details.

Correlations between EEG features and cognitive variables

We computed Spearman and distance correlations between each EEG feature and cognitive variable. Thus, for each age group and correlation type, we performed 2100 (175∗12) analyses. With this evaluation, we sought to identify the EEG features reflective of a neural process linked to each cognitive ability. Next, the EEG features showing a significant correlation to a cognitive variable were pairwise correlated either using Spearman or distance correlations and multivariate distance correlations. Strong correlations between EEG features would suggest that the features point to the same mechanism representative of the cognitive aspect under study. In younger adults, 109 analyses were significant using Spearman correlations and 121 using distance correlations (after correction for multiple comparisons for each pair of EEG feature and cognitive variable). For most cognitive variables, we found more than one EEG feature showing a significant correlation (Figure 1A). The correlations between these EEG features were weak in most of the cases. Similar results were found using multivariate distance correlations ($\sqrt{|\mathcal{R}_n^*|}$), which permitted us to correlate EEG features considering all the variables, i.e., electrodes, brain regions, or microstate parameters (Figure 1B). Results for older adults were similar and are presented in Figure S1.

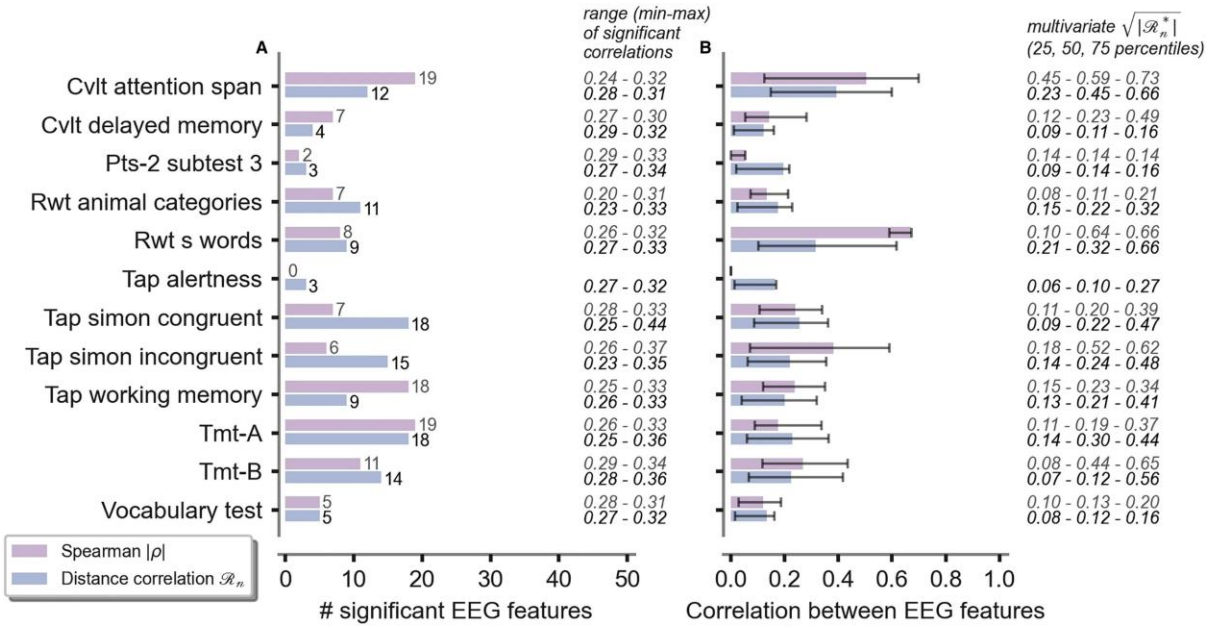

Figure 1. Result of the correlation analysis in younger adults. (A) EEG features with significant correlations to cognitive variables. On the right side of the panel, we indicate the range (min-max) of the magnitudes of the significant correlations (see correlations between EEG features and cognitive variables in quantification and statistical analysis). (B) Median (confidence interval: 25th and 75th percentiles) Spearman and distance correlations between the EEG features showing a significant correlation with the same cognitive variable. On the right side of the panel, we indicate the 25th, 50th, and 75th percentiles of the multivariate distance correlations ($\sqrt{|\mathcal{R}_n^*|}$; ranging from 0 to 1) between the EEG features (with all its variables) showing a significant correlation with the same cognitive variables.

For instance, for younger adults, both the life time statistics of the amplitude envelopes in the theta band (life time theta) and the node strength of delta connectivity measured in the electrode space using phase locking value (node str e-plv delta) correlated significantly with the working memory variable obtained from the test of attentional performance (Tap working memory; ρ_{max} = -0.28 and ρ_{max} = 0.29, respectively). However, life time theta and node str e-plv delta did not correlate strongly with each other (ρ = -0.11; $\sqrt{|\mathcal{R}_n^*|} = 0.07$; Figure 2). Similarly, using distance correlations, both the occurrence of microstate class C (microstate C) and the betweenness centrality of gamma connectivity measured in the electrode space using weighted phase lag index (betw cen e-wpli gamma) showed significant correlations with the module A variable of the trail making test (Tmt-A; $\mathcal{R}_{n\,max}$ = 0.25 and $\mathcal{R}_{n\,max}$ = 0.36, respectively). However, the two EEG features only weakly correlate with each other ($\mathcal{R}_n$ = 0.15; $\sqrt{|\mathcal{R}_n^*|} =$ 0.01; Figure 3). ρ_{max} and $\mathcal{R}_{n\,max}$ denote the maximum significant Spearman or distance correlation (among all the electrodes, brain regions, or microstate parameters) of the EEG feature with the cognitive variable.

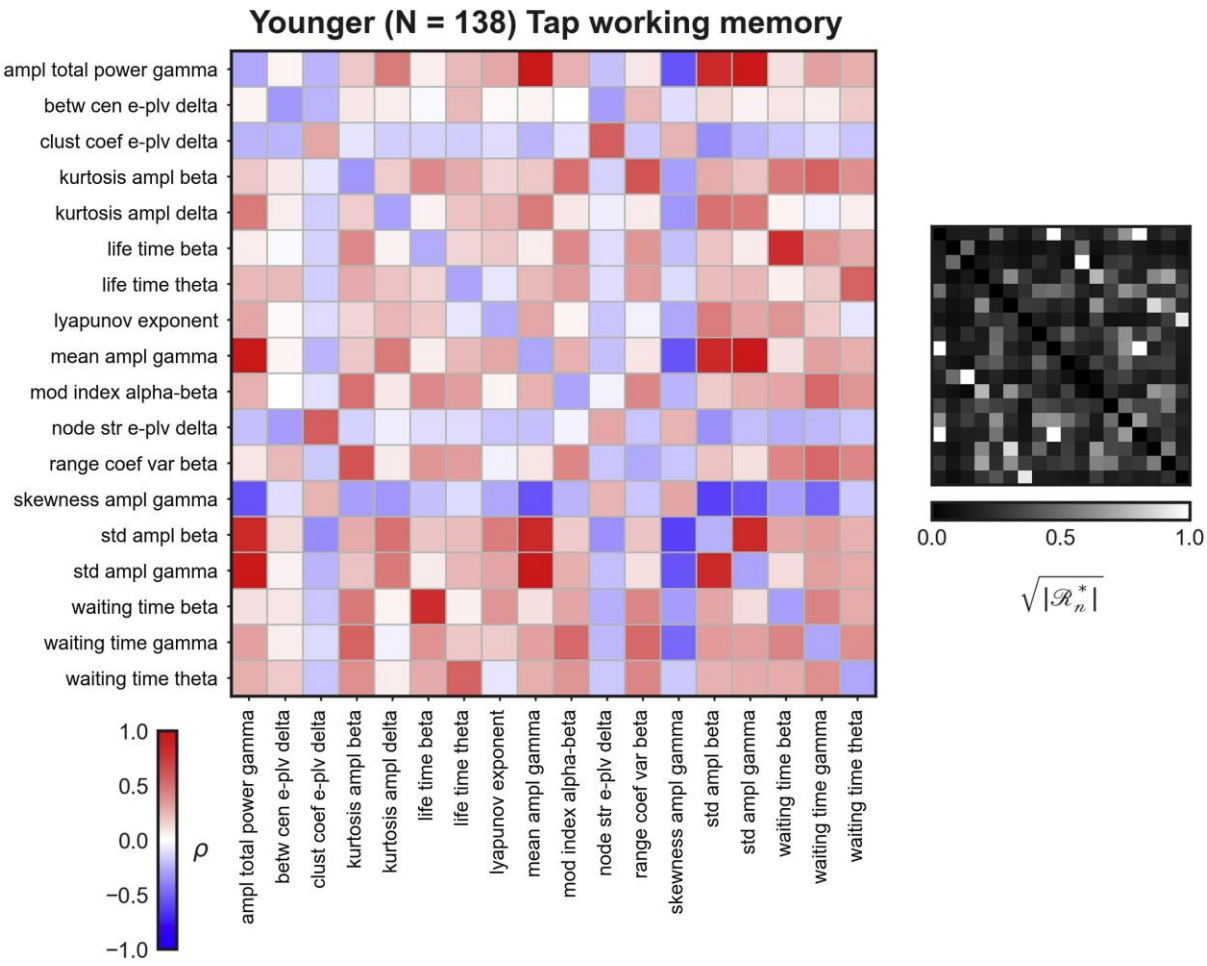

Figure 2. Spearman correlations between the EEG features that correlated significantly with the Tap working memory variable in younger adults. The main diagonal has the ρmax (maximum Spearman rho) of the electrode or brain region showing the largest significant correlation to the cognitive variable. On the right side, we show the pairwise multivariate distance correlations between the EEG features (with all its variables).

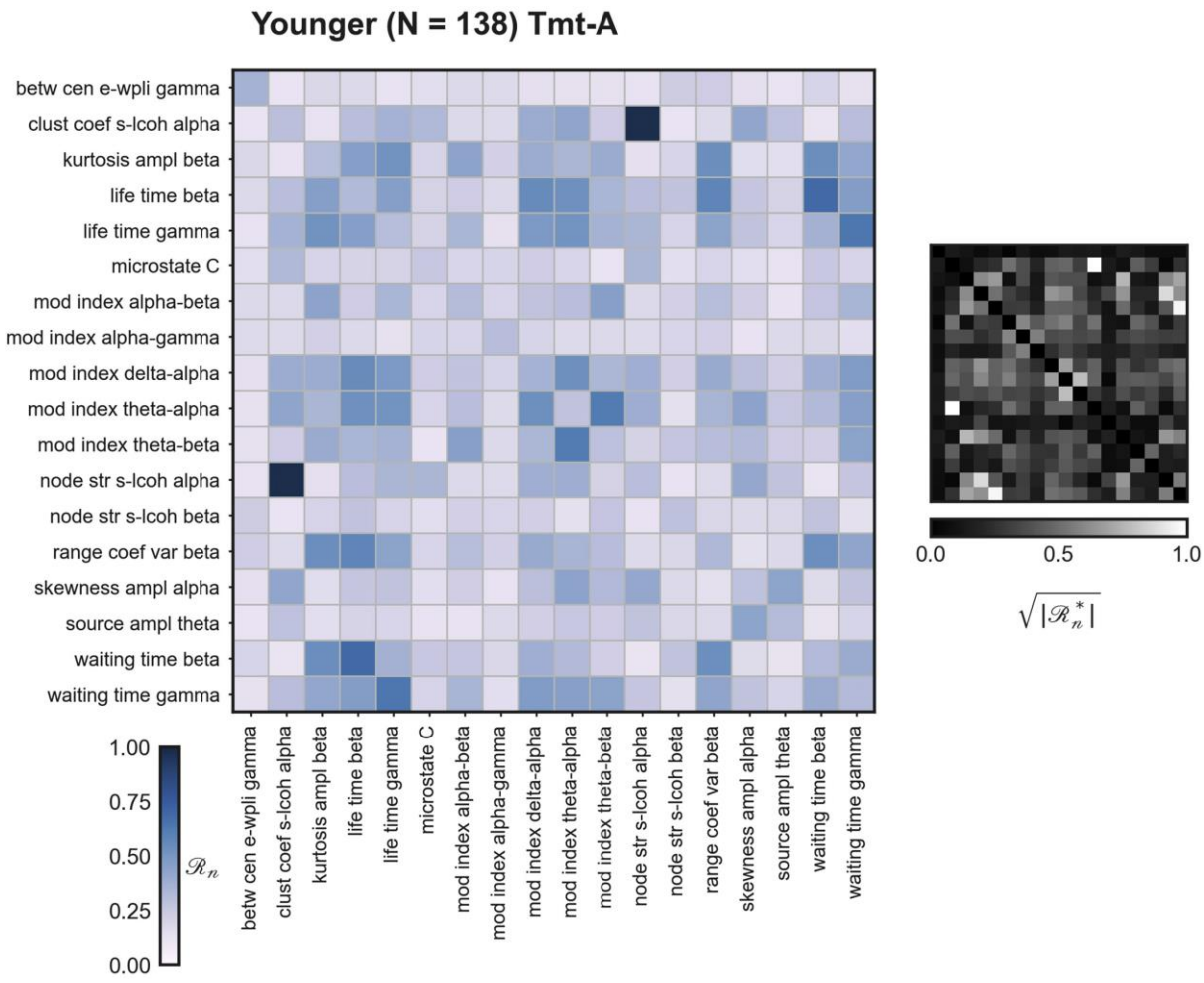

Figure 3. Distance correlations between the EEG features that correlated significantly with the Tmt-A variable in younger adults. The main diagonal contains the $\mathcal{R}_{n\,max}$ (maximum distance correlation) of the electrode, brain region, or microstate parameter showing the largest significant correlation to the cognitive variable. On the right side, we show the pairwise multivariate distance correlations between the EEG features.

While the correlations between EEG features were generally low (Figure 1B), some EEG features obtained from different analysis methods were highly correlated with each other. For example, in younger adults, both the Hjorth activity parameter (hjorth activity) and the standard deviation of the amplitude envelopes in the beta band (std ampl beta) showed significant correlations with the attention span module of the Cvlt (Cvlt attention span; ρ_{max} = 0.28 and ρ_{max} = 0.30, respectively). The two EEG features correlated strongly with each other (ρ = 0.84; $\sqrt{|\mathcal{R}_n^*|}$ = 0.77). Similarly, using distance correlations, the animal categories variable of the Rwt test (Rwt animal categories) correlated significantly with the occurrence of microstate class B (microstate B; $\mathcal{R}_{n\,max}$ = 0.27) and with the clustering coefficient of alpha connectivity measured in the electrode space using weighted phase lag index (clust coef e-wpli alpha; $\mathcal{R}_{n\,max}$ = 0.28). The EEG features microstate B and clust coef e-wpli alpha exhibit a

moderate correlation with each other ($\mathcal{R}_n$ = 0.41; $\sqrt{|\mathcal{R}_n^*|}$ = 0.35). All pairs of EEG feature and cognitive variable that showed significant results are presented in Figure 4.

Next, we used a principal component analysis (PCA) to examine whether EEG features, showing a significant correlation with a cognitive variable, can be grouped into a set of latent variables. Then, we used the EEG latent variables in a multiple regression model to predict the cognitive scores (see dimensionality reduction and multiple regression in quantification and statistical analysis). We found that a small number of EEG latent variables tended to explain a considerable amount of the variance of the EEG features that had a significant correlation (Spearman or distance correlation) with a cognitive variable (see Figures S5–S10). For instance, in younger adults, we applied PCA on the 18 EEG features that showed a significant Spearman correlation to the Tap working memory scores in younger adults (Figure 2). The first principal component explained 31.99% of the variance of the 18 EEG features. The first three principal components explained 57.61% of the variance of the 18 EEG features (Figure S6). Results are similar across cognitive variables. The proportion of variance explained by the first principal components of the EEG features showing a Spearman correlation to a cognitive variable ranged from 29.32% (Rwt animal categories; 7 EEG features) to 62.83% (Rwt s words; 8 EEG features; median across cognitive variables: 44.15%). For EEG features showing a significant distance correlation to a cognitive variable, the variance explained by the first principal components ranged from 27.81% (Rwt animal categories; 11 EEG features) to 58.64% (Rwt s words; 9 EEG features; median across cognitive variables: 33.90%).

Finally, we investigated whether a combination of EEG latent variables explains the cognitive variables better than a single latent variable. Thus, we asked whether various uncorrelated EEG features carry complementary information of the cognitive variables. To this end, we computed a multiple regression model. First, we used only the first PC as the predictor variable and then added, one by one, more PCs to the model (up to the third PC, i.e., three predictors). To compare models with different numbers of predictor variables, we used adjusted-R^2 to measure the goodness of fit. The analysis was performed for younger and older adults separately. For the EEG features showing a significant Spearman correlation with a cognitive variable in younger adults, the adjusted-R^2 values ranged from 0.00 (Pts 2 subtest 3) to 0.22 (Tmt-B) using only the first principal component in the regression model (median adjusted-R^2 across cognitive variables: 0.15), and from 0.11 (*Cvlt attention span*) to 0.32 (Cvlt delayed

memory) using the first three principal components (median adjusted-R^2 across cognitive variables: 0.21; Table S2). For EEG features showing a significant distance correlation, in younger adults, the adjusted-R^2 values ranged from 0.07 (Tap alertness) to 0.20 (Tmt-B) using only the first principal component in the regression model (median adjusted-R^2 across cognitive variables: 0.12), and from 0.09 (Tap alertness) to 0.22 (Rwt animal categories) using the first three principal components (median adjusted-R^2 across cognitive variables: 0.14; Table S4). Results for older adults are presented in Table S3 and Table S5. Importantly, the estimates of predictive performance were not obtained using cross-validation. As such, results should be taken with caution.

Interim conclusions: There are significant correlations between cognitive variables and EEG features obtained with different analysis methods, including connectivity, spectral power, and microstate methods. Classically, studies in the field investigate the relationship between one EEG feature and one cognitive variable in great detail with the tacit assumption that the EEG feature is representative of a proposed brain mechanism. However, we found that even though various EEG features show a significant correlation with a cognitive variable, these EEG features usually do not strongly correlate with each other. We found that a set of latent dimensions composed of multiple EEG features may explain some cognitive variables better than a single latent dimension. Yet, this was not the case for most cognitive variables. Hence, one cannot take it for granted that an EEG feature is representative of the research question at hand just because there is a significant correlation between the feature and a cognitive or another variable. We are not claiming that studies based on single correlations cannot provide meaningful information about brain mechanisms. We are just pointing out that a significant result does not guarantee it. We examine this notion further in the general discussion.

Prediction of cognitive variables using EEG features

The features studied in EEG research are hypothesized to reflect neurophysiological processes involved in cognitive function. Therefore, we would expect that EEG features predict cognitive scores adequately. In this section, to test for predictive ability, we go beyond correlations and used cross-validated machine learning (ML) models. Thus, we tested the ability of single EEG features to predict each cognitive variable in an out-of-sample manner. This approach has several advantages. First, ML models handle multivariate predictors very well. Neuroimaging

data are often composed of information from several brain regions or electrodes, and thus, multivariate methods provide a compact way to use all the information. Second, models can be evaluated using cross-validation, where different parts of the data are used to train and test the models, providing a rigorous test for the generalizability of results. We tested two models, namely ridge models, which are sensitive to linear relationships between predictors and predicted variables, and random forest models, which detect nonlinear relationships.

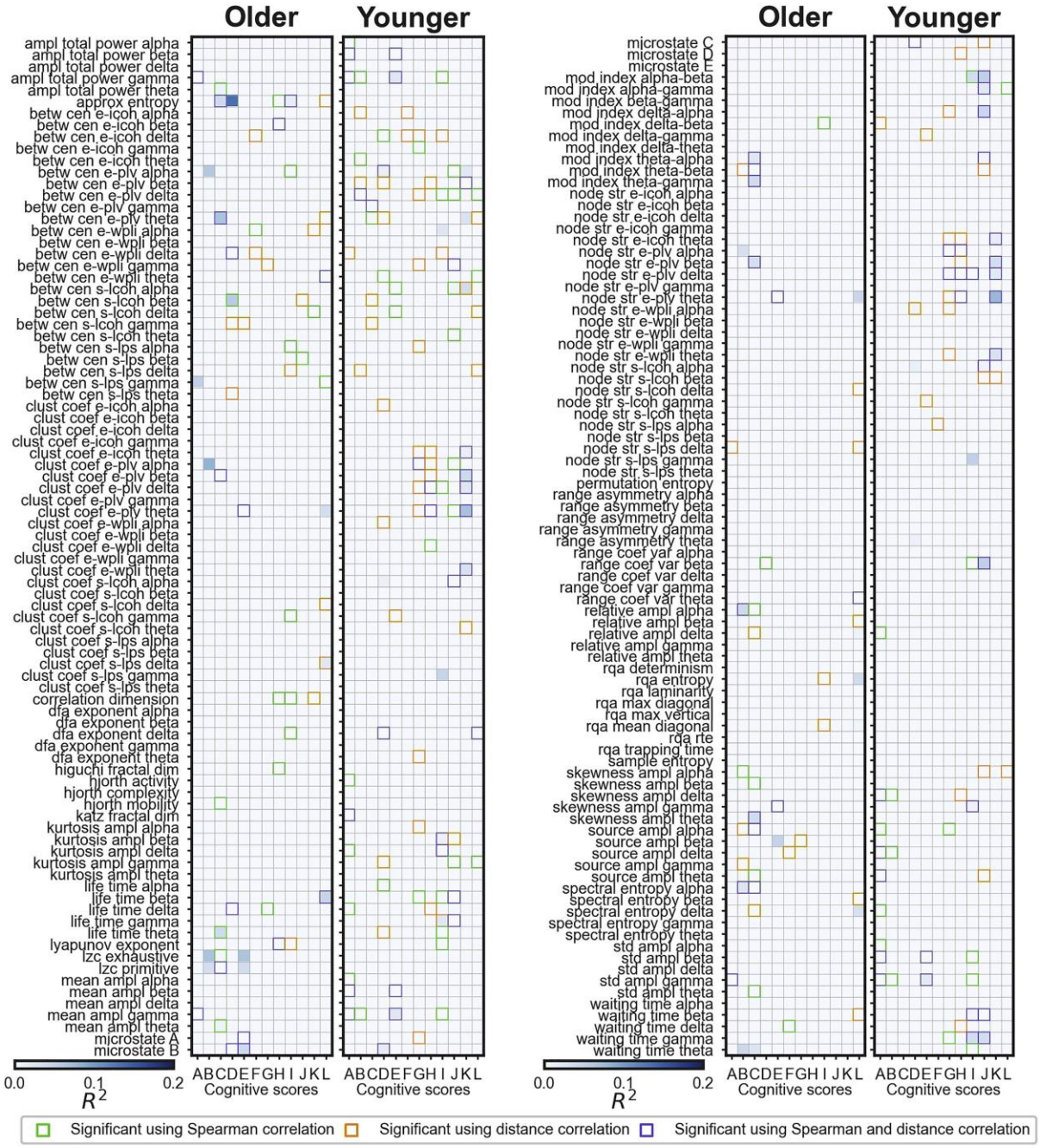

Figure 4. Prediction of cognitive variables using EEG features. Cross-validated R^2 is shown (median R^2 across 50 iterations). A ridge regression model was built for each pair of EEG feature and cognitive variable. Abbreviations: A = Cvlt attention span, B = Cvlt delayed memory, C = Pts-2 subtest 3, D = Rwt animal categories, E = Rwt s words, F = Tap alertness, G = Tap simon congruent, H = Tap simon incongruent, I = Tap working memory, J = Tmt-A, K = Tmt-B, L = Vocabulary test. Green and orange squares indicate that Spearman and distance correlation analyses were significant, respectively. Purple squares indicate that both Spearman and distance correlations were significant for the same EEG and cognitive variable pair. Colormap limits are set between 0 and 0.2. Negative R^2 values are shown as zero.

In total, 2100 (175∗12) models were built using one EEG feature and one cognitive variable for each ML model (ridge or random forest) and age group (younger and older). Predictive performance was estimated using the coefficient of determination (R^2). Models were trained using cross-validation on 67% of the data and tested on the left-out 33%. We repeated the entire procedure 50 times, with different allocations of participants in the train and test sets, and obtained the median predictive performance (see cross-validated prediction of cognitive variables using EEG features in quantification and statistical analysis). Note that R^2 calculations (using the sums of squares formula and not the squared correlation) can result in negative values when the model prediction on data not used in model training is less accurate than it would be by just predicting the mean value of the data.[25,26] For younger adults, the 25th, 50th, and 75th percentiles of the 2100 (175∗12) R^2 values obtained using ridge regression were 0.00, 0.00, and 0.03 for the training data and −0.04, −0.03, and −0.02 for the testing data (Figure 4). For the random forest regression models, the 25th, 50th, and 75th percentiles of the R^2 values were 0.65, 0.74, and 0.78 for the training data, and −0.14, −0.10, and −0.06 for the testing data. For older adults, the 25th, 50th, and 75th percentiles of the R2 values obtained using ridge regression were 0.00, 0.00, and 0.06 for the training data and −0.09, −0.06, and −0.04 for the testing data. For random forest regression models, the 25th, 50th, and 75th percentiles of the R^2 values were 0.80, 0.82, and 0.83 for the training data, and −0.24, −0.16, and −0.10 for the testing data. See Data S2 to S5 for detailed results.

Interim conclusions: Predictions play a crucial role in science. With this analysis, we set out to assess the ability of EEG features to predict cognitive variables. We used cross-validated prediction models. There is a hypothesized relationship between neurophysiological features at rest and cognitive performance. Thus, if EEG features truly reflect core aspects of cognitive functioning, one might expect EEG to predict cognitive performance well. Surprisingly, we found generally weak predictive performance using two different regression models. Hence,

there is the possibility that we might need to rethink to what extent neurophysiological features obtained from resting-state recordings truly have a clear-cut link to behavioral measures. Another option is that the relationships might be less strong than often implicitly thought. We like to stress that our results provide only a general overview of brain-behavior predictive success and are only related to resting-state EEG features.

Group comparisons of the EEG features between younger and older adults

Classically, case-control studies using EEG are set out to identify neurophysiological processes differing in two groups (e.g., patients and controls, younger and older adults). The tacit assumption is that a significant result shows that an EEG feature under study points, for example, to a cause of a disease. In this analysis, we examined differences between older and younger adults. Each of the 175 EEG features was subjected to group comparisons between older and younger adults. 108 out of the 175 EEG features (61.71%) contained at least one variable showing significant group differences between older and younger adults, indicating that important age-related effects are detected. The absolute effect sizes (r; ranging from 0 to 1) of the representative variables ranged between 0.18 (microstate E) and 0.58 (spectral entropy beta), corresponding to small to large effect sizes.[27] The 25th, 50th, and 75th percentiles of the absolute significant effect sizes (one value per significant EEG feature) were 0.26, 0.31, and 0.42, respectively. For 56 out of the 108 EEG features showing significant group differences, the effects were positive, namely, older adults showed higher values than younger adults and the opposite was the case for the remaining 52 EEG features (Figure 5).

Older adults showed significantly decreased node strength in theta connectivity measured in the source space using lagged phase synchronization (node str s-lps theta; r = -0.31), increased long-range temporal correlations in the delta band (dfa exponent delta; r = 0.29), as well as longer mean duration of the microstate class A (microstate A; r = 0.50), to name a few. Group differences were also observed in EEG features in the different frequency bands, for instance, older adults showed reduced spectral entropy in the delta band (spectral entropy delta; r = -0.41), reduced spectral amplitudes in the theta band in the source space (source ampl theta; r = -0.40), reduced node strength in alpha connectivity measured in the source space using lagged phase synchronization (node str s-lps alpha; r = -0.25), increased waiting time statistics of the amplitude envelopes in the beta band (waiting time beta; r = 0.33), and increased node

strength in gamma connectivity measured in the electrode space using phase locking value (node str e-plv gamma; r = 0.26).

Interim conclusions: We identified various EEG features that showed group differences in older compared to younger participants. The effect sizes of the group differences ranged from small to large, with a median significant effect size of r = 0.31. Hence, these features point to age-related changes in brain processing. There is the question of whether the EEG features, showing clear-cut group differences, point to the same neurophysiological mechanism differing in older participants.

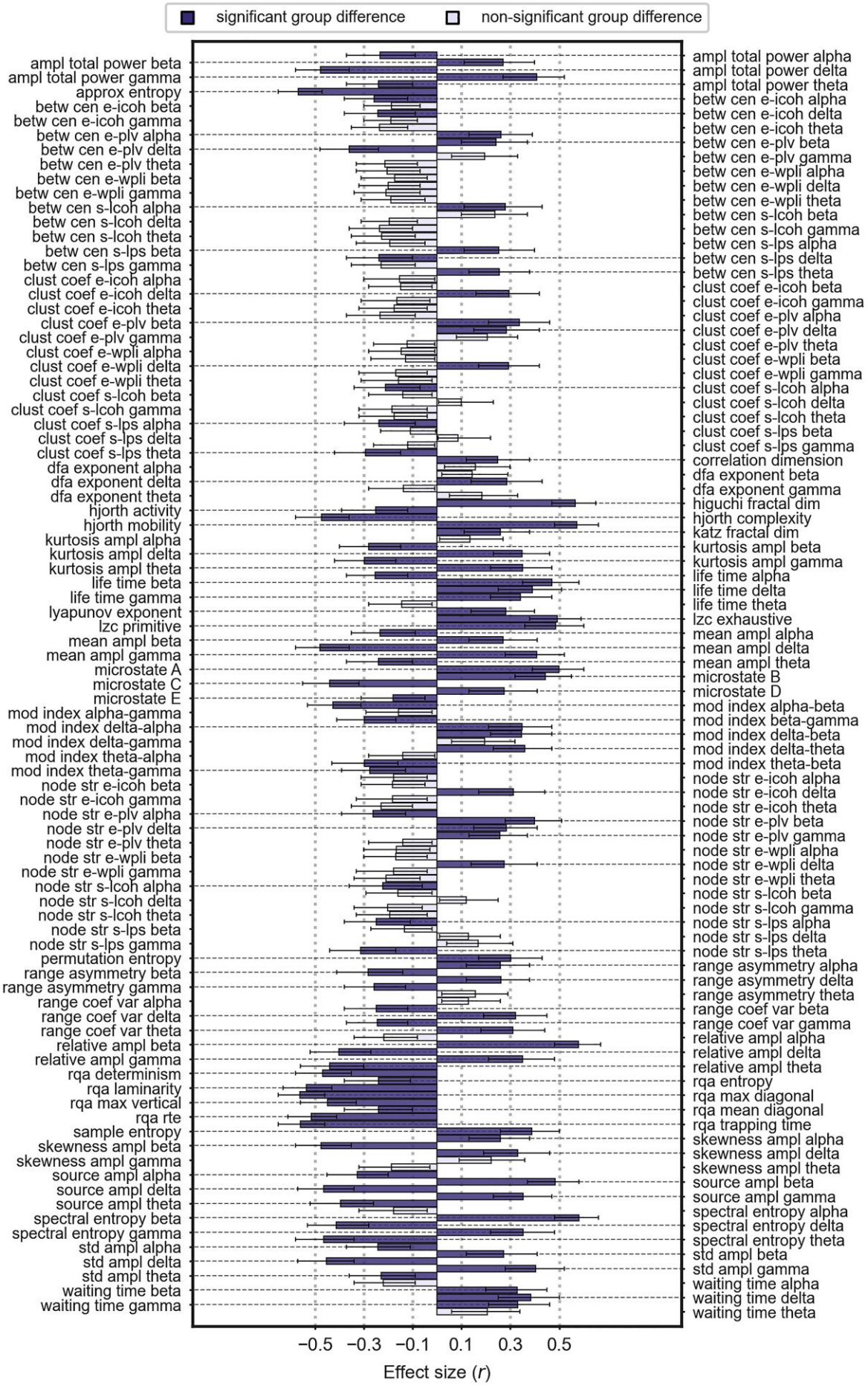
significant group difference
non-significant group difference
ampl total power beta
ampl total power gamma
approx entropy
betw cen e-icoh beta
betw cen e-icoh gamma
betw cen e-plv alpha
betw cen e-plv delta
betw cen e-plv theta
betw cen e-wpli beta
betw cen e-wpli gamma
betw cen s-lcoh alpha
betw cen s-lcoh delta
betw cen s-lcoh theta
betw cen s-lps beta
betw cen s-lps gamma
clust coef e-icoh alpha
clust coef e-icoh delta
clust coef e-icoh theta
clust coef e-plv beta
clust coef e-plv gamma
clust coef e-wpli alpha
clust coef e-wpli delta
clust coef e-wpli theta
clust coef s-lcoh beta
clust coef s-lcoh gamma
clust coef s-lps alpha
clust coef s-lps delta
clust coef s-lps theta
dfa exponent alpha
dfa exponent delta
dfa exponent theta
hjorth activity
hjorth mobility
kurtosis ampl alpha
kurtosis ampl delta
kurtosis ampl theta
life time beta
life time gamma
lyapunov exponent
lzc primitive
mean ampl beta
mean ampl gamma
microstate A
microstate C
microstate E
mod index alpha-gamma
mod index delta-alpha
mod index delta-gamma
mod index theta-alpha
mod index theta-gamma
node str e-icoh beta
node str e-icoh gamma
node str e-plv alpha
node str e-plv delta
node str e-plv theta
node str e-wpli beta
node str e-wpli gamma
node str s-lcoh alpha
node str s-lcoh delta
node str s-lcoh theta
node str s-lps beta
node str s-lps gamma
permutation entropy
range asymmetry beta
range asymmetry gamma
range coef var alpha
range coef var delta
range coef var theta
relative ampl beta
relative ampl gamma
rqa determinism
rqa laminarity
rqa max vertical
rqa rte
sample entropy
skewness ampl beta
skewness ampl gamma
source ampl alpha
source ampl delta
source ampl theta
spectral entropy beta
spectral entropy gamma
std ampl alpha
std ampl delta
std ampl theta
waiting time beta
waiting time gamma
ampl total power alpha
ampl total power delta
ampl total power theta
betw cen e-icoh alpha
betw cen e-icoh delta
betw cen e-icoh theta
betw cen e-plv beta
betw cen e-plv gamma
betw cen e-wpli alpha
betw cen e-wpli delta
betw cen e-wpli theta
betw cen s-lcoh beta
betw cen s-lcoh gamma
betw cen s-lps alpha
betw cen s-lps delta
betw cen s-lps theta
clust coef e-icoh beta
clust coef e-icoh gamma
clust coef e-plv alpha
clust coef e-plv delta
clust coef e-plv theta
clust coef e-wpli beta
clust coef e-wpli gamma
clust coef s-lcoh alpha
clust coef s-lcoh delta
clust coef s-lcoh theta
clust coef s-lps beta
clust coef s-lps gamma
correlation dimension
dfa exponent beta
dfa exponent gamma
higuchi fractal dim
hjorth complexity
katz fractal dim
kurtosis ampl beta
kurtosis ampl gamma
life time alpha
life time delta
life time theta
lzc exhaustive
mean ampl alpha
mean ampl delta
mean ampl theta
microstate B
microstate D
mod index alpha-beta
mod index beta-gamma
mod index delta-beta
mod index delta-theta
mod index theta-beta
node str e-icoh alpha
node str e-icoh delta
node str e-icoh theta
node str e-plv beta
node str e-plv gamma
node str e-wpli alpha
node str e-wpli delta
node str e-wpli theta
node str s-lcoh beta
node str s-lcoh gamma
node str s-lps alpha
node str s-lps delta
node str s-lps theta
range asymmetry alpha
range asymmetry delta
range asymmetry theta
range coef var beta
range coef var gamma
relative ampl alpha
relative ampl delta
relative ampl theta
rqa entropy
rqa max diagonal
rqa mean diagonal
rqa trapping time
skewness ampl alpha
skewness ampl delta
skewness ampl theta
source ampl beta
source ampl gamma
spectral entropy alpha
spectral entropy delta
spectral entropy theta
std ampl beta
std ampl gamma
waiting time alpha
waiting time delta
waiting time theta
−0.5
−0.3
−0.1
0.1
0.3
0.5
Effect size (r)

Figure 5. Effect size and confidence intervals of the group differences between younger and older adults for each of the 175 EEG features. Negative effect sizes indicate that older adults had significantly reduced values compared to younger adults. Black dotted horizontal lines serve as a guide to the labels of the EEG features showing significant group differences.

Correlations between EEG features showing age-related differences

In the previous analysis, we found 108 EEG features showing differences in older compared to younger participants. In this section, by pairwise correlating these EEG features, we ask whether the targeted brain processes point to a common mechanism underlying age-related differences. We calculated Spearman correlations between the representative variables (i.e., showing the largest group effect) of the 108 EEG features showing group differences (Figure 6). We found that 41.74% of the correlation values were significant for younger adults and 33.77% for older adults (without correction for multiple comparisons). Since significance depends on the sample size, we focus on the magnitudes of the pairwise correlations. The 25^{th}, 50^{th}, and 75^{th} percentiles of the magnitudes of the 5778 ($108*107/2$) correlation values were 0.06, 0.13, and 0.29, for younger adults and 0.08, 0.17, and 0.31, for older adults.

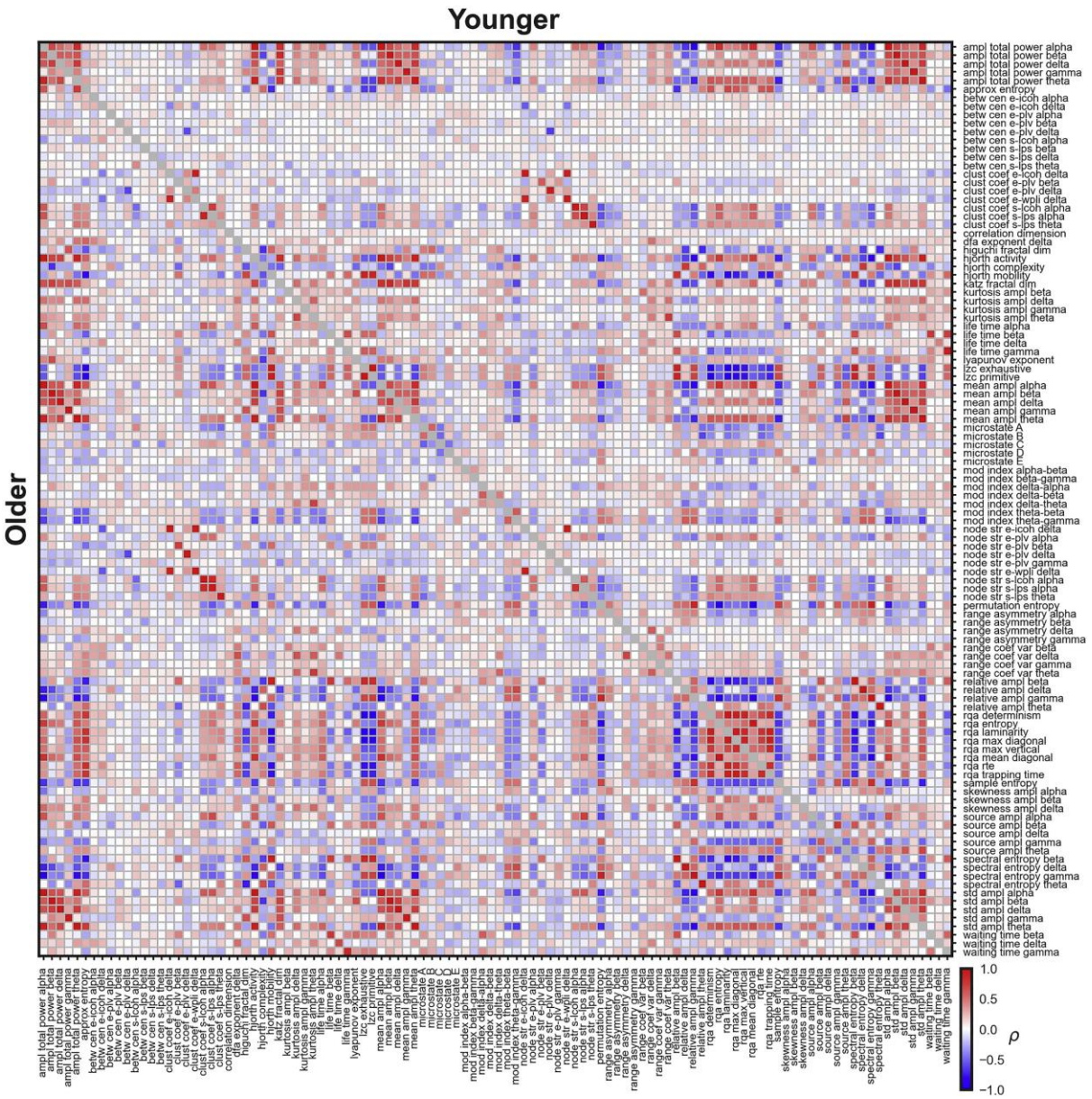

Figure 6. Spearman correlations between the 108 EEG features that showed a significant group difference between younger and older adults. The *ρ* correlations belonging to younger and older adults are presented in the upper and lower triangular parts of the matrix, respectively. To calculate the correlations, from each EEG feature, we selected the electrode, brain region, or microstate parameter showing the biggest effect size in the group comparisons between older and younger adults. See Figure S2 for the results using multivariate distance correlations.

Importantly, since the choice of EEG reference may influence the results,[28] we obtained zero-referenced EEG features and compared them to those with average reference and current source density (CSD; for connectivity features in the electrode space), which were the ones used in the previous analyses. We found a very good agreement between average/CSD and zero-referenced EEG features, as quantified by intraclass correlations (ICC) and distance

correlations (see comparison between EEG reference choices in quantification and statistical analysis). For younger adults, the 25th, 50th, and 75th percentiles of the ICC values between average/CSD and zero-referenced EEG features were 0.57, 0.92, and 0.97 (ICC ranges from 0 to 1), while for older adults, the percentile values were 0.65, 0.93, and 0.97, suggesting that the choice of reference does not affect the results. For younger adults, the 140 distance correlation values between average/CSD and zero-referenced EEG features were 0.79, 0.98, and 0.99, while for older adults, the distance correlations were 0.81, 0.99, and 1, for the 25th, 50th, and 75th percentiles. While for most EEG features the ICC and distance correlation values were high, network EEG features, in particular, betweenness centrality features showed rather low ICCs (see Data S6). However, this did not change the relationship between EEG features (see: Figures S3 and S4). For zero-referenced EEG features, the pairwise correlations between the 140 EEG features (see Data S6) in younger adults were 0.09, 0.19, and 0.36, whereas in older adults the pairwise correlations were 0.11, 0.17, and 0.33, for the 25th, 50th, and 75th percentiles. For average/CSD EEG features, the correlations were 0.10, 0.20, and 0.38 for younger adults, and 0.12, 0.20, and 0.35 for older adults (25th, 50th, and 75th percentiles of the multivariate distance correlation).

EEG features may be more adequately summarized considering the whole set of electrodes, brain regions, or microstate parameters. Hence, in addition to the previous univariate correlation assessment, we calculated multivariate distance correlations, which allowed us to compare EEG features using all their variables (Figure S2). The results are similar. For younger adults, the magnitudes of the multivariate distance correlations ($\sqrt{|\mathcal{R}_n^*|}$) were 0.12, 0.23, and 0.41, whereas for older adults the magnitudes were 0.12, 0.21, and 0.38, for the 25th, 50th, and 75th percentiles. In younger adults, 58.54% of the multivariate distance correlations were significant, whereas 53.01% were significant for older adults (without correction for multiple comparisons).

Furthermore, to investigate whether the EEG features showing a group difference between older and younger participants can be grouped into a set of latent variables, we used PCA on the representative variables (i.e., the variables showing the largest group difference between older and younger participants) of the 108 EEG features. For older adults, the first PC explained 24.01% of the variance of the EEG features. The second and third PCs explained 13.47% and 7.54%, respectively (Figure S11). The first PC consists essentially of EEG features obtained from

nonlinear dynamical and entropy analysis methods (e.g., rqa trapping time, lzc primitive, and permutation entropy). The second PC is mainly composed of beta and delta band features (e.g., mean ampl beta, node str e-plv delta, and relative ampl delta) and also nonlinear dynamical features (e.g., katz fractal dim and lyapunov exponent). The third PC contains mainly temporal and connectivity EEG features (e.g., microstate D, node str e-plv alpha, and life time delta). These latent dimensions could be interesting for future investigations of age-related differences in neurophysiology.

Most of the strong correlations were found between EEG features obtained from very similar methods. For example, the node strength and the clustering coefficient of delta connectivity estimated in the electrode space using the imaginary part of coherence (node str e-icoh delta and clust coef e-icoh delta, respectively) showed strong correlations with each other (ρ = 0.97, $\sqrt{|\mathcal{R}_n^*|}$= 0.99 and ρ = 0.97, $\sqrt{|\mathcal{R}_n^*|}$ = 1 in younger and older adults, respectively). Similarly, EEG features obtained using recurrence quantification analysis, including determinism (rqa determinism) and laminarity (rqa laminarity), were strongly correlated (ρ = 0.99, $\sqrt{|\mathcal{R}_n^*|}$ = 0.98 and ρ = 0.99, $\sqrt{|\mathcal{R}_n^*|}$ = 1 in younger and older adults, respectively). The life-time and waiting-time statistics of the amplitude envelopes in the gamma band (life time gamma and waiting time gamma) showed also strong positive correlations (ρ = 0.91, $\sqrt{|\mathcal{R}_n^*|}$ = 0.97 and ρ = 0.83, $\sqrt{|\mathcal{R}_n^*|}$ = 0.98 in younger and older adults, respectively), to name a few examples.

Interim conclusions: Identifying brain mechanisms underlying cognition or perception is crucial in the brain sciences. Our analysis showed that various EEG features, all showing group differences in older compared to younger adults, mainly correlate weakly with each other. While there are strong correlations between similar methods, for example, between entropy and nonlinear measures, these features did not correlate, for instance, with EEG microstates, connectivity, or autocorrelation features. Hence, while the EEG features point to meaningful brain processes showing clear-cut group differences, they do not point to a general neurophysiological deficit in older compared to younger adults. The main conclusion from this analysis, as well as the previous ones, is that statistically significant effects might explain much less of the research question than it is often implicitly assumed.

Discussion

Science relies on tests targeting the crucial aspects of a research field. Classically, these tests show a significant group difference between an intervention and a control condition, between a case and a control group, or strong correlations to real-world or experimental outcomes. Then, in-depth studies are carried out to describe the test in great detail in order to understand the causes of the observed effects. It usually is assumed that these tests are representative of the interrogated mechanisms in the sense that other tests supposed to target the same mechanism should strongly correlate with each other. Here, we have shown that this rationale might not always hold. To exemplify our argument, we analyzed a publicly available database containing resting-state EEG recordings and performance scores from a battery of cognitive tests of older and younger adults.[24]

We extracted 175 EEG features from the EEG recordings and 12 cognitive variables from the battery of cognitive tests. To identify the associations between EEG features and cognitive variables, we correlated each EEG feature with each cognitive variable using Spearman and distance correlations. For younger adults, Spearman correlations were significant for 109 analyses, while 121 analyses were significant using distance correlations. For older adults, Spearman correlations were significant for 57 analyses and distance correlations for 60 (Figure S1). Then, we correlated the EEG features that showed a significant correlation with a cognitive variable (Figure 1). Surprisingly, the correlations were weak in most cases, suggesting that not all the EEG features are representative of the investigated cognitive variable. Using PCA, we found that a set of latent dimensions composed of multiple EEG features may explain some cognitive variables better than a single latent dimension. Next, we found 108 EEG features revealing a significant group difference between older and younger participants. These features also did not show strong correlations, even though they showed clear-cut group effects. Using cross-validated regression analysis, we found very weak evidence that EEG features are adequate predictors of the cognitive variables suggesting that it may be possible that the link between a cognitive aspect and an EEG feature is less informative than believed.

How can these results be explained? There are at least five possibilities. First, EEG features might have low test-retest reliability. Even though there are significant correlations with the cognitive tasks, the low test-retest reliability may have led to weak correlations between EEG

features (cf.[29]). While here we do not have a measure of test-retest, certain EEG features have shown adequate reliabilities in previous studies.[30,31,32,33,34,35] Second, there might be clear-cut group differences but the variance in the groups is low. In this case, one would not expect high correlations, the so-called reliability paradox.[36] However, variance, for example, was rather high in the older participants in our study. Third, the EEG features do not reflect the intended brain aspects well. For instance, the EEG features may point to nonlinear brain mechanisms. Yet, some of the EEG analysis methods are linear and as such, they might miss nonlinear patterns. Hence, the correlations between EEG features might be misled by the linear methods. Fourth, the EEG features target a common mechanism and, to a substantial amount, also target-unspecific, i.e., idiosyncratic, aspects, which have little to do with the targeted mechanism but contribute to the large inter-individual variability. For example, some EEG features might be sensitive to fatigue,[37] whereas others are not. Hence, if substantial parts of the variance correspond to such target-unspecific aspects and different EEG features tap into different target-unspecific aspects, the correlations may be low. Fifth, each EEG feature targets a different aspect of a highly heterogeneous, multifactorial mechanism. Previous research indicates that this scenario might be true in certain instances. For example, by combining different resting-state or evoked EEG features, previous studies have improved classification between groups or experimental conditions.[38,39,40,41,42,43] Similarly, previous studies have reported that a combination of EEG features allowed a better characterization of certain brain processes.[44,45,46] Our results using PCA also show evidence that, for some cognitive variables, latent dimensions of EEG features might be more informative than single features. All these studies suggest that combining measures and features from the same paradigms might offer new insights into complex processes.

In our analysis, significant results came with *small* to *medium* effect sizes in the range from 0.20 to 0.37 ($|\rho|$) in the correlation analysis, and with *small* to *large* effect sizes in the range of 0.18 to 0.58 ($|r|$) in the case-control analyses according to Cohen[27] and from *typical* (0.2 - 0.3) to *relatively large* (> 0.3) according to Gignac and Szodorai.[47] However, even for "large" effect sizes, there is a large proportion of unexplained variance. For example, for an of $r = 0.5$, the unexplained variance is 75%, and a Cohen's d of 0.8 corresponds to a discriminability of 65% only (for the optimal decision criterion, i.e., hits = correct rejections). A good discriminability of 90% corresponds to a $d = 2.5$. Hence, the question is where does all the

dominant noise come from? In an optimistic scenario, it comes from measurement noise. For example, EEG is a relatively noisy technique (e.g., electrode misplacement, volume conduction). Thus, the true effects might be larger. The pessimistic scenario is that noise is low and inter-individual variability is high, i.e., there are multiple factors and each paradigm taps into one, or a nonlinear combination of all of them plus a large amount of target-unspecific variance. This large amount of unexplained variance could account for why one may obtain both significant group differences and low correlations. Hence, even if clear-cut effects are found, this does not guarantee that a paradigm represents the intended aspects well. Therefore when a test leads to a significant result, one needs to ask how representative the test is for the research question at hand. Particularly in complex systems where everything is correlated with everything to some degree, there can be many tests, which show significant but negligible effects.

Our impression is that the above considerations have been overlooked and hold true in many other research areas. As an example, in schizophrenia research, several studies have found atypical patterns in several resting-state EEG features, which are thereon studied in detail and linked to the crucial aspects of the disease. Here, again, the tacit assumption is that the EEG feature under study taps into the common and representative aspects of the disease, and for that reason, they should correlate with similar features. However, we have shown that this is not always the case. In a previous EEG study, we extracted 194 EEG features from the resting-state recordings of 121 patients with schizophrenia and 75 healthy controls. We found that 69 out of the 194 EEG features showed a significant group difference between patients with schizophrenia and healthy controls. However, the features showed mainly weak correlations with each other, questioning to what extent a single EEG feature is representative of the disease.[48] In another example, in vision research, weak correlations have been found between performances in various visual tasks in older and younger adults.[49,50,51,52] Visual illusions also correlate weakly,[53,54] suggesting that the underlying visual functions cannot be explained using only one visual paradigm. Similarly, four visual tasks assumed to capture visual magnocellular stream function showed weak relationships with each other.[55] The authors concluded that none of these tasks is a general measure of magnocellular function, as was assumed. Eisenberg et al.[56] showed that several questionnaires and cognitive tasks thought to point to the same

psychological construct correlate weakly with each other and predict real-world outcomes poorly. The authors concluded that the construct lacks coherence.

Most natural sciences face severe crises. The brain sciences are among the fields hard-hit. First, many studies are underpowered and/or subject to questionable research practices. False positives are the consequence.[57,58,59] Second, even if the very same data are used, different analysis tools can lead to different results. This problem becomes more severe with complex analysis pipelines and more degrees of freedom.[60,61,62] Third, the uncontrolled use of open data for hypothesis testing can increase false positives.[63,64,65] Fourth, here, we have shown that there is one additional problem. Studies may have been conducted perfectly with clear-cut, significant results. Still, the studies may not target the mechanism assumed or they are less representative of the research question than believed. Overall, our results show that single measurements, even with "large" effect sizes, may be less meaningful than thought. To what extent the above-mentioned scenarios hold must be shown for each study individually.

Limitations of the study

One of the main limitations of our study is that resting-state EEG and behavior were not measured simultaneously. Hence, whether there are causal links between EEG features and cognitive variables is not clear-cut. The evoked EEG features show a more direct link to the temporal aspects of cognitive processing, and thus stronger brain-behavior relationships might be expected. As such, our results and interpretations of the weak correlations between EEG and cognition do not concern evoked EEG paradigms. Furthermore, there are at least two limitations that should be considered when interpreting the results from our prediction analysis. First, our sample size is small for a reliable assessment of predictive ability.[66] Second, we do not have an independent dataset to test our predictive models. We tried to account for these limitations using a repeated train-test split procedure, which produces unbiased estimates of predictive ability for small sample sizes. Nonetheless, larger sample sizes and independent datasets are needed. Finally, we do not have a measure of the test-retest reliability of the EEG features. Hence, EEG features with poor reliabilities may mislead the correlations. While our results show that similar EEG features correlate strongly with each other (resembling test-retest), measuring and accounting for reliability, e.g., using disattenuated correlations, will tell about the "true" correlations between EEG features.

Star methods

Key resources table

REAGENT or RESOURCE	SOURCE	IDENTIFIER
Biological samples		
EEG and cognitive data	Leipzig Study for Mind-Body-Emotion Interactions	https://doi.org/10.1038/sdata.2018.308
Software and algorithms		
MATLAB	https://matlab.mathworks.com/	Version R2020b
Python	https://www.python.org/	Version 3.6
R Studio	https://www.r-project.org/	Version 4.0.1
Cartool	https://sites.google.com/site/cartoolcommunity	Version 3.8
LORETA	https://www.uzh.ch/keyinst/loreta	Version v20200414
Other		
Scripts for data processing	Github repository	https://github.com/dgl59311/stats_eegfeatures

Resource availability

Lead contact

Further information and requests for resources should be directed to and will be fulfilled by the lead contact: Dario Gordillo

Materials availability

The study did not generate new materials

Data and code availability

- This paper analyzes existing, publicly available data. These accession numbers for the datasets are listed in the key resources table.
- All original code has been deposited at Github and is publicly available as of the date of publication. DOIs are listed in the key resources table.
- Any additional information required to reanalyze the data reported in this paper is available from the lead contact upon request.

Experimental model and subject details

Data from 227 participants were collected in Leipzig, Germany, as part of the Leipzig Study for Mind-Brain-Body Interactions (LEMON[24]). The sample comprises data from two age groups, 153 younger adults (between 20 and 35 years old) and 74 older adults (between 59 and 77 years old). Participants underwent a physiological and psychological screening at the Day Clinic for Cognitive Neurology of the University Clinic Leipzig and the Max Planck Institute for Human Cognitive and Brain Sciences. Written informed consent was provided by all the participants before data collection. Study protocols were in accordance with the Declaration of Helsinki and were approved by the ethics committee of the University of Leipzig (reference number 154/13-ff).

The data were made publicly available. In the present study, only data from participants that had resting-state EEG recordings were analyzed. Preprocessed resting-state EEG recordings were available for 203 participants (https://ftp.gwdg.de/pub/misc/MPI-Leipzig_Mind-Brain-Body-LEMON/EEG_MPILMBB_LEMON/). We excluded two participants (sub-010276, and sub-010277) due to differences in the sampling rate. The final sample used for the present study consisted of 201 participants, 138 younger adults (mean age = 25.43, SD = 3.39, 42 females), and 63 older adults (mean age = 67.66, SD = 4.79, 31 females).

Method details

EEG collection and preprocessing

EEG was recorded using a 62-channel active electrode ActiCAP system (Brain Products GmbH, Germany) placed according to a 10-10 system arrangement with the FCz electrode as the reference. The ground was placed on the sternum. Impedances of the electrodes were kept below 5 kΩ. EEG signals were band-pass filtered online between 0.015 Hz and 1 kHz. Data were digitized with a sampling rate of 2500 Hz. During recording, participants alternated between eyes-closed and eyes-open conditions, after 1 min. A 16-min recording was obtained for each participant. Following data acquisition, signals were band-pass filtered between 1 and 45 Hz (eighth order, Butterworth filter). Data were downsampled to 250 Hz.

Further offline preprocessing consisted of the rejection of artifactual channels and segments following a visual inspection. The dimensionality of the data was reduced using principal

component analysis (PCA). The PCs (N ≥ 30) allowing to explain 95% of the total variance were retained. Other physiological artifacts, such as eye movements, blinks, or heartbeats, were identified using independent component analysis and removed. Finally, the retained components were back-projected to the electrode space. Further details on data acquisition and preprocessing are available in.[24]

In the present study, we used 8-min blocks corresponding to the eyes-closed condition segments. Missing electrodes were interpolated using spherical spline interpolation in EEGLAB[67] to fit the same 61-channel montage for all participants. Then, the recordings were re-referenced to the average and down-sampled to 125 Hz.

Cognitive assessment

In total, participants performed six cognitive tests. The data were made publicly available by the LEMON study (https://ftp.gwdg.de/pub/misc/MPI-Leipzig_Mind-Brain-Body-LEMON/Behavioural_Data_MPILMBB_LEMON/Cognitive_Test_Battery_LEMON/). From the six cognitive tests, we extracted 12 variables. The tests and the extracted variables are described below. More details can be found in the documentation of the database.

California verbal learning task

The California Verbal Learning Task (CVLT) measures memory processes and verbal learning capacity.[68] Participants listened to a 16-word list (list A) over five trials. The words belonged to four different semantic categories. After each trial, participants were asked to recall as many words from list A as they could. Then, another 16-word list (list B) was presented as an interference list, which had to be recalled right after its presentation, and had to be followed by a recall of list A. After a delay of 20 min, participants were asked to recall the words from list A, with or without semantic category cues. Based on Donders,[69] and Mahjoory and colleagues,[70] we extracted two scores: attention and delayed-memory scores. The attention score was calculated by adding up the number of words that were correctly recalled after hearing list A for the first time and the number of correctly recalled words from list B. The delayed memory score was calculated by adding the number of correctly recalled words from list A after listening to list B, and the number of correctly recalled words from list A after the 20-min delay, with and without cues.

Test of attentional performance

The Test of Attentional Performance (TAP) consists of three modules that assess different aspects of attention.[71] In the first module, participants had to press a button as soon as a cross appeared on the screen. Two conditions were tested: with and without a pre-stimulus audio signal. The alertness score was estimated from this module as the reaction time averaged across the two conditions. The second module corresponded to the Simon task. In the Simon task, participants had to press a left or right button to indicate the direction of an arrow appearing on the left or the right side of the screen. Congruent (i.e., the direction of the arrow matched its location) and incongruent (e.g., left-pointing arrow on the right side of the screen) trials were presented. The average reaction times (RT) and the percentage correct (PC) were recorded and combined into a rate correct score (i.e., RT/PC.[72] We extracted two scores from this module, given by the rate correct score for the congruent and incongruent trials of the Simon task. In the third module, participants were presented (serially) with numbers from 1 to 9, and they had to press a button whenever the current number was the same as the second to last number (2-back task). We extracted a working memory score from this module, given by the percentage of correct matches.

Trail making test

The Trail Making Test (TMT) measures cognitive flexibility.[73] In module A, participants had to connect digits from 1 to 25 in ascending order. In module B, 13 numbers and 12 letters had to be alternately connected in their numerical and alphabetical order (e.g., 1-A-2-B-3-C- …). We extracted two scores from the TMT given by the inverse efficiency score (i.e., Task completion time/PC) for modules A and B.

Vocabulary test

The Vocabulary Test (VT) measures verbal intelligence and language comprehension.[74] Participants had to identify a target word among five distracting words. There were 42 trials. We extracted one score from the VT, given by the number of correctly identified target words over all the trials (VT-score).

Performance testing system-2 Subtest 3

The Subtest 3 of the Performance Testing System-2 (Pts-2) assesses logical deductive thinking.[75] For 3 min, 40 rows of eight symbols were presented to the participants. For each

row, participants had to identify the symbol that did not follow the logical rule. We extracted one score from the Pts-2, given by the total number of correctly identified symbols.

Regensburger word fluency test

The Regensburger Word Fluency Test (Rwt) measures verbal fluency.[76] The Rwt test consisted of two modules. In the first module, for 2 min, participants had to list as many words starting with the letter "S" as they could. In the second module, participants had to list words representing animals, for 2 min. We extracted two scores from the Rwt, given the total number of correct words in each module.

EEG features extraction

Using time-domain, frequency-domain, nonlinear, and connectivity analysis methods, we extracted 175 features from the resting-state EEG signals. For some analysis methods, we filtered the EEG signals into five frequency bands: delta (1–4 Hz), theta (4–8 Hz), alpha (8–13 Hz), beta (13–30 Hz), and gamma (30–45 Hz). The dimensionality of the analysis outcomes (i.e., EEG features) depended on the analysis method. For instance, for each participant, we obtained either 61 or 80 variables if the analyses were conducted in the electrode or source space, respectively, or 4 variables for EEG features extracted using microstates analysis. Hence, each EEG feature is always composed of more than one variable. We described the analysis methods below. The list of all the EEG features extracted is available in Data S1.

Statistics of amplitude envelopes

For each frequency band, we calculated five statistical descriptors of the distribution of the signal. Amplitude envelopes were extracted using Hilbert transform. The descriptors were: mean and standard deviation of the amplitude envelopes, kurtosis, skewness, and total power of the signals. First, EEG signals were divided into non-overlapping 4-s segments and filtered into five frequency bands. Then, the statistical descriptors were calculated for the amplitude envelope values of each electrode, at each time segment. The average across time segments was used for further analyses. The analyses were conducted in the electrode space. We obtained 25 EEG features from these analyses (Features: 1–5, 68–72, 81–85, 151–155, 166–170; in Data S1).

Spectral amplitudes

To estimate spectral amplitudes, first, EEG signals were divided into non-overlapping 4-s segments. For each electrode time series, at each time segment, we used Fourier analysis to obtain the frequency amplitudes. Relative spectral amplitudes were defined for each frequency band, as the ratio between the sum of the squared Fourier coefficients within the bounds of the frequency band of interest (e.g., within 1–4 Hz, for the delta band), and the squared Fourier coefficients of the full-band signal. The average across time segments was used for further analyses. This analysis was conducted in the electrode space. We obtained five EEG features from this analysis (Features: 137–141; in Data S1).

In addition, we estimated the current source amplitudes for each frequency band using the software LORETA.[77] We defined 80 brain regions of interest (80; 40 per hemisphere) according to the AAL atlas (see Table S1). ROIs included gray matter voxels within a 10-mm radius of the seed. This analysis was conducted in the source space. We obtained five features from this analysis (Features: 156–160; in Data S1).

Temporal correlations

For each frequency band we calculated long-range and short-range temporal correlations of EEG oscillations. Long-range (>1 s) temporal correlations (LRTC) were calculated using detrended fluctuation analysis (DFA[78]). Short (∼< 1 s) temporal correlations were calculated using life – and waiting-time statistics.[79] For DFA, first, we extracted the amplitude envelopes from the EEG time series using Hilbert transform. The amplitude envelopes were integrated. Then, we defined 30 window sizes, varying from 3 to 50 s, distributed evenly on a logarithmic scale. The integrated signal was divided into 50% overlapping segments for each previously defined window-size. At each of these segments, the integrated signal was detrended, and the fluctuation function (i.e., variance) was obtained. The average fluctuation function across segments of each window size was calculated. The average fluctuation functions were plotted in logarithmic axes, and a line was fit. The slope of the line indicated the scaling exponent and this value was used for further analyses. To estimate short-range temporal correlations, we extracted the amplitude envelopes of the EEG time series using Hilbert transform. The median amplitude envelope was used as a threshold, which defined the onset and end of the oscillation bursts. The distributions for life and waiting times were built using the durations of all the burst

events that occurred above or below the threshold, respectively. The 95th percentile of the distributions of life and waiting times were used for further analyses. The analyses were performed in the electrode space. We obtained 15 EEG features from these analyses (Features: 58–62, 73–77, 171–175; in Data S1).

Network and connectivity measures

First, EEG functional connectivity was calculated using five connectivity algorithms. Three of these algorithms (i.e., phase locking value, imaginary part of coherence, and weighted phase lag index) were defined in the electrode space, and two (i.e., lagged coherence and lagged phase synchronization) in the source space. EEG Functional connectivity was calculated at each of the five frequency bands. Electrode connectivity analyses were performed using FieldTrip.[80] Before estimating electrode connectivity, scalp current densities were obtained from the EEG time series using the FieldTrip function ft_scalpcurrentdensity with the spline method. For source connectivity analyses, first, cortical activity was estimated with the exact low-resolution electromagnetic tomography (eLORETA) algorithm using the software LORETA. We defined 80 brain regions (40 per hemisphere) according to the AAL atlas (see Table S1). ROIs included gray matter voxels within a 10-mm radius of the seed. Then, using the Brain Connectivity Toolbox (BCT [81]), three network statistics (i.e., betweenness centrality, clustering coefficient, and node strength) were calculated from each of the connectivity matrices. The BCT functions employed were betweenness_wei, clustering_coef_wu, and strength_und. The extracted EEG features consisted of the network analysis outcomes. We obtained 45 features in the electrode space (Features: 7–21, 32–46, 101–115, in Data S1) and 30 features in the source space (Features: 22–31, 47–56, 116–125, in Data S1).

Microstates

First, for a given participant, the voltage maps at the peaks of the global field power (GFP) signal were extracted. Maps at GFP peaks have been indicated to have a higher signal-to-noise ratio, providing a more stable representation of the EEG topographies.[82] Then, a k-means clustering procedure was performed on these maps with k (i.e., the number of cluster centroids) equal to 5. GFP peak maps were then assigned to the cluster centroid to which they showed the highest spatial correlation, as long as the correlation value was above 0.5, otherwise, maps were left unassigned.

Second, a k-means clustering procedure was performed on the concatenated cluster centroids from all the participants, obtained in the previous step. The algorithm was initialized 200 times for each value of k, with k varying from 1 to 15. The optimal number of subject-level cluster centroids was selected according to a metacriterion based on seven independent indicators for optimal cluster solution.[83] Out of the 200 initializations, the cluster solution showing the highest fraction of explained variance was the one retained. The polarity of the voltage maps was always ignored. Maps were only assigned to a given microstate class if they showed a spatial correlation larger than 0.5. Finally, the cluster centroids obtained from the subject-level analysis were assigned to the EEG data of each participant, this time, not only considering the GFP peaks but all the data. Voltage maps showing a correlation below 0.5 to any of the cluster centroids were left unassigned. Temporal smoothing (Besag factor = 10 and window half size = 2) was applied to avoid the interruption of quasi-stable segments.[84] Segments equal to or smaller than three samples were rejected. For each microstate class, we extracted four temporal statistics namely the global explained variance, mean duration, time coverage, and frequency of occurrence. Microstates analysis was performed using the software Cartool version 3.8.[85] We obtained five EEG features from this analysis (Features: 86–90, in Data S1).

Entropy and complexity measures

We quantified the complexity of EEG signals using five different methods: approximate entropy, sample entropy, spectral entropy, permutation entropy, and Lempel-Ziv complexity. First, we divided the EEG signals into non-overlapping 4-s segments. Approximate,[86] permutation,[87] and sample[88] entropies were calculated for the full-band EEG signals, using an embedding dimension value of three. Approximate entropy was computed using the function approximateEntropy from the Predictive Maintenance Toolbox for MATLAB. Permutation entropy was calculated based on Unakafova.[89] Sample entropy was computed using the code provided by Martínez-Cagigal.[90] The time delay to estimate approximate and permutation entropies was set to one. Lempel-Ziv complexity was calculated from the full-band EEG time series,[91] using the code provided by Thai.[92] Spectral entropy was calculated for each frequency band, and it was defined as the Shannon's entropy of the ratio between the normalized power spectral density (PSD) within the frequency band bounds (e.g., within 1–4 Hz, for the delta band), and the full-band EEG signal. All calculations were performed at each time segment, and the average across segments was used for further analyses. The analyses were conducted in

the electrode space. We obtained 10 EEG features from these analyses (Features: 6, 79, 80, 126, 150, 161–165, in Data S1).

Nonlinear dynamical measures

Before obtaining nonlinear dynamical features, the EEG signals were divided into non-overlapping 4-s segments. To obtain recurrence quantification analysis (RQA) features, first, for each electrode time series at each segment, we built recurrence plots and extracted eight RQA features using the CRP toolbox for MATLAB.[93] The RQA features were: determinism, entropy, laminarity, maximal diagonal line length, maximal vertical line length, mean diagonal line length, recurrence times entropy, and trapping time. Recurrence plots were constructed using a fixed radius allowing a 10% recurrence rate. The Lyapunov exponent[94] and correlation dimension[95] were obtained using the functions lyapunovExponent, and correlationDimension, available in the Predictive Maintenance Toolbox for MATLAB. We also calculated the Higuchi's,[96] and Katz's[97] fractal dimensions using the code provided by Monge-Álvarez.[98] The kmax parameter in Higuchi's fractal dimension calculation was set to 25. All nonlinear dynamical features were obtained from the full-band EEG signals. For RQA measures, correlation dimension, and Lyapunov exponent, the embedding parameters (time delay and embedding dimension) were calculated using the function phaseSpaceReconstruction from the Predictive Maintenance Toolbox in MATLAB. The analyses were conducted in the electrode space. We obtained 12 EEG features from these analyses (Features: 57, 63, 67, 78, 142–149, in Data S1)

Phase-amplitude coupling

EEG features describing cross-frequency (CF) interactions via phase-amplitude coupling were obtained using the modulation index.[99] First, EEG time series were divided into non-overlapping 4-s segments and were filtered into the five frequency bands. For each band-pass filtered electrode time series, at each segment, the amplitude envelope and the instantaneous phase were extracted using the Hilbert transform. Then, we defined ten different CF interactions, these were between delta phase-theta amplitude, delta phase-alpha amplitude, delta phase-beta amplitude, delta phase-gamma amplitude, theta phase-alpha amplitude, theta phase-beta amplitude, theta phase-gamma amplitude, alpha phase-beta amplitude, alpha phase-gamma amplitude, and beta phase-gamma amplitude. For each CF interaction, we

obtained the corresponding phase and amplitude time series (e.g., phase time series in the theta band and amplitude time series in the gamma band for theta phase-gamma amplitude). Then, the phase values were binned into 18 values (from −180 to 180°) and the mean amplitude value (of the modulated frequency) over each bin was calculated. Hence, we obtained the mean amplitude value of the modulated frequency, for each phase value of the phase-modulating frequency. The Kullback-Leibler (KL) divergence indicated whether the amplitude values are uniformly distributed according to the phase values (i.e., no phase-amplitude coupling). The KL divergence was calculated for each of the ten cross-frequency interactions, and the average value across time segments was used for further analyses. The analysis was conducted in the electrode space. We obtained ten EEG features from this analysis (Features: 91–100, in Data S1).

Time-domain amplitude features

Peak-to-peak amplitude asymmetry and coefficient of variation were calculated for each frequency band using range-EEG analysis.[100] Range features were obtained using the code provided by Toole and Boylan.[101] We also obtained the Hjorth parameters activity, mobility, and complexity from the full band EEG time series.[102] First, we divided the EEG time series into non-overlapping 4-s segments. Then, we calculated the time-domain amplitude features for each time segment and electrode signal. The average across segments was used for further analyses. The analyses were conducted in the electrode space. We obtained 13 EEG features from these analyses (Features: 64–66, 127–136, in Data S1).

Quantification and statistical analysis

Correlations between EEG features and cognitive variables

This section describes the analysis behind the results presented in the correlations between EEG features and cognitive variables subsection in results. To investigate the associations between the 175 EEG features and the 12 cognitive variables, we calculated Spearman correlations and distance correlations. Hence, we conducted 2100 correlation analyses (175∗12; for each correlation metric) for older and younger adults separately, because of the large age differences between the samples (see experimental model and subject details). Four older adults had missing values in some cognitive variables (sub-010044 in Tap alertness, sub-010047 in Tmt-A, sub-010050 in Tap working memory and Tap simon incongruent, and sub-

010099 in Rwt s words and Rwt animal categories). These participants were only excluded in the analyses where the EEG features were correlated with the variables in which they had missing values. These participants were included for the rest of the correlation analyses.

For each pair of EEG feature (with all its electrodes, brain regions, or microstate parameters) and cognitive variable (e.g., approximate entropy and Tmt-A), we calculated Spearman correlation coefficients and distance correlations. EEG features can have a different number of variables, depending on whether the analysis method was conducted in the electrode space, source space, or using microstates analysis (see method details). Thus, for EEG features obtained in the electrode space (e.g., approximate entropy) we obtained 61 correlations to one cognitive variable (each electrode was correlated with the cognitive variable). For EEG features in the source space (e.g., source spectral amplitude in the alpha band, source ampl alpha) we obtained 80 correlations and 4 correlations for each microstate class. The p values of the correlations were corrected using False Discovery Rate (FDR[103]) with an error rate of 5%. The p values of the distance correlations were obtained using 1000 repetitions of a bootstrapping procedure and corrected with FDR. We used the distance_corr function implemented in the pingouin 0.5.1 package for Python.[104]

Next, to evaluate whether EEG features showing significant correlations with the same cognitive variable relate to each other, we calculated Spearman or distance correlations between these EEG features, depending on the method used in the previous step (i.e., either Spearman or distance correlation). From each EEG feature showing a significant correlation to a cognitive variable, we took the electrode, brain region, or microstate parameter showing the highest correlation to be the representative variable for that EEG feature in the analysis. The EEG features revealing a significant correlation to the cognitive variables were also compared using multivariate distance correlations,[105] which considered all the variables of the EEG features (see correlations between EEG features showing age-related differences section below).

Dimensionality reduction and multiple regression

This section describes the analysis behind the results presented in the correlations between EEG features and cognitive variables subsection in results. We analyzed the EEG features that showed a significant correlation to a cognitive variable using principal component analysis

(PCA). Importantly, EEG and cognitive variables were log-transformed to improve normality using the function PowerTransformer from scikit-learn. For example, for the Tap working memory variable, we found 18 EEG features showing a significant correlation. We took one variable from each of these 18 EEG features (the one showing the largest correlation to the Tap working memory variable) and used a PCA. We calculated the proportion of explained variance. This analysis was performed for each cognitive variable and age group separately.

Then, to understand whether the set of latent variables obtained using PCA can explain the cognitive variables, we used multiple regression. We used the function OLS from the statsmodels 0.13.2 package for Python.[106] We obtained the latent variables from the EEG features that showed a significant correlation to a cognitive variable. Each EEG feature contributed with one variable (i.e., electrode, brain region, or microstate parameter), which was the one showing the highest correlation to the corresponding cognitive variable. We generated a regression model, first, using the first PC of the EEG data, and then, we added PCs one by one, up to the third PC (i.e., model 1: PC1, model 2: PC1 and PC2, model 3: PC1, PC2, and PC3). To quantify predictive performance, we used adjusted- R^2. In this analysis, we did not use cross-validation to calculate adjusted-R^2 values.

Cross-validated prediction of cognitive variables using EEG features

This section describes the analysis behind the results presented in the prediction of cognitive variables using EEG features subsection in results. We investigated how well the EEG features predicted the cognitive variables using ridge regression and nonlinear random forest regression. We used the Scikit-learn 1.0.2 package for Python.[26] For each pair of EEG feature (with all its electrodes, brain regions, or microstate parameters) and cognitive variable, prediction performance was calculated using 50 repetitions of a train-test split procedure. The predictive performance was calculated using the coefficient of determination R^2. First, 33% of the data were left out for validation (testing set) and the remaining 67% of the data (training set) were used for model optimization. For linear ridge models, before training the model we applied a power transform to the data to improve normality using the PowerTransformer function. The amount of penalization λ (100 values from 10^{-3} to 10^{5} on an evenly spaced logarithmic scale) was selected using cross-validation with the efficient leave-one-out method implemented in the function RidgeCV. For random forest models, we used the function

RandomForestRegressor. The parameters of the random forest models were selected using a grid search procedure with 3-fold cross-validation as implemented in the GridSearchCV function. We used 100 estimators and adjusted the tree-depth considering the values 4, 6, 8, or no constraint, and also adjusted the maximum number of features using log2, sqrt, or auto as options. The model with the parameters giving the best performance in the training set was applied to the testing set. The prediction performance R^2 was calculated using the function r2_score. The R2 values were aggregated for each of the 50 repetitions of the procedure and the median predictive performance was reported. The analysis was conducted for the sample of older and younger adults separately.

Group comparisons of EEG features between older and younger adults

This section describes the analysis behind the results presented in the Group comparisons of the EEG features between younger and older adults subsection in results. We conducted group comparisons between older and younger adults using each of the 175 EEG features. For each variable (61 electrodes, 80 brain regions, or 4 microstate parameters) of a given EEG feature, we conducted a Mann-Whitney test using the function wilcox_test from R Studio version 4.0.1 [107] and the package coin 1.4_2.[108] The p values and effect size r-values (with bootstrap confidence intervals) were obtained using the R Studio package rstatix 0.7.0.[109] The p values were corrected for multiple comparisons using FDR with an error rate of 5%, within each EEG feature.

Correlations between EEG features showing age-related differences

This section describes the analysis behind the results presented in the correlations between EEG features showing age-related differences subsection in results. First, for each EEG feature that contained at least one variable showing a significant difference between younger and older adults (after correcting for multiple comparisons), we selected the variable (i.e., the electrode, brain region, or microstate parameter) with the largest effect size to be the representative variable for that feature for the correlation analysis. For each age group separately, we computed pairwise Spearman correlations between these variables.

Second, to consider not only one but all variables of the EEG features revealing significant group differences, we used an unbiased multivariate distance correlation test for independence in high dimensions.[105] In high dimensions, the original distance correlation

statistic (used in the correlation between EEG features and cognitive variables section) increases even under independence. The absolute unbiased estimate accounts for the bias in high dimensions and thus can provide an effect size of the relationship between two EEG features with all its variables (electrodes, brain regions, or microstate parameters) ranging from 0 to 1. We reported the square root of the absolute unbiased distance correlation ($\sqrt{|\mathcal{R}_n^*|}$) because the unbiased distance correlation approximates the population squared distance correlation. The effect sizes and p values were obtained using the function dcorT.test from the R Studio package energy 1.7_10.[110]

Comparison between EEG reference choices

To investigate the effect of the EEG reference choice on our results, we re-analyzed the EEG data using zero-reference as implemented in the REST toolbox.[111] We obtained 140 EEG features (not considering source space EEG features) with this reference choice. These zero-referenced EEG features were compared to average or current source density CSD (for electrode connectivity features) referenced EEG features, which were the ones used in the main analyses, using intraclass correlations and distance correlations. For the comparison, we used the intraclass correlation with an absolute agreement (ICC2; to account for mean differences across references) as implemented in the function intraclass_corr from the pingouin 0.5.1 package for Python. Since EEG features have different numbers of variables (i.e., electrodes or microstate parameters), we calculated the ICC2 values for each variable of each EEG feature. For example, for the EEG feature microstate A, we obtained 4 ICC2 values (for global explained variance, mean duration, time coverage, and frequency of occurrence).

Furthermore, to examine whether the choice of reference affects the correlations between EEG features, we pairwise correlated the 140 EEG features obtained with zero reference using multivariate distance correlations, for younger and older adults separately.

Acknowledgments

This work was funded by the National Centre of Competence in Research (NCCR) Synapsy financed by the Swiss National Science Foundation under grant 51NF40-185897. We acknowledge all the contributors to the Leipzig Study for Mind-Body-Emotion Interactions.

Author contributions

Conceptualization, M.H.H., D.G., and J.R.C.; Methodology, D.G., J.R.C., and D.M.; Investigation, D.G. and S.G.; Writing – Original Draft, D.G., M.H.H., J.R.C., and S.G.; Writing- Review & Editing, D.G. and M.H.H.; Supervision, M.H.H.

Declaration of interests

The authors declare no competing interests.

References

1. Finnigan, S., and Robertson, I.H. (2011). Resting EEG theta power correlates with cognitive performance in healthy older adults. Psychophysiology *48*, 1083–1087. 10.1111/j.1469-8986.2010.01173.x.
2. Klimesch, W., Vogt, F., and Doppelmayr, M. (1999). Interindividual differences in alpha and theta power reflect memory performance. Intelligence *27*, 347–362. 10.1016/S0160-2896(99)00027-6.
3. Clark, C.R., Veltmeyer, M.D., Hamilton, R.J., Simms, E., Paul, R., Hermens, D., and Gordon, E. (2004). Spontaneous alpha peak frequency predicts working memory performance across the age span. Int. J. Psychophysiol. *53*, 1–9. 10.1016/j.ijpsycho.2003.12.011.
4. Chen, L., Wu, B., Qiao, C., and Liu, D.-Q. (2020). Resting EEG in alpha band predicts individual differences in visual size perception. Brain Cogn. *145*, 105625. 10.1016/j.bandc.2020.105625.
5. Rogala, J., Kublik, E., Krauz, R., and Wróbel, A. (2020). Resting-state EEG activity predicts frontoparietal network reconfiguration and improved attentional performance. Sci. Rep. *10*, 5064. 10.1038/s41598-020-61866-7.
6. Irrmischer, M., Poil, S.-S., Mansvelder, H.D., Intra, F.S., and Linkenkaer-Hansen, K. (2018). Strong long-range temporal correlations of beta/gamma oscillations are associated with poor sustained visual attention performance. Eur. J. Neurosci. *48*, 2674–2683. 10.1111/ejn.13672.
7. Zanesco, A.P., King, B.G., Skwara, A.C., and Saron, C.D. (2020). Within and between-person correlates of the temporal dynamics of resting EEG microstates. NeuroImage *211*, 116631. 10.1016/j.neuroimage.2020.116631.
8. Doppelmayr, M., Klimesch, W., Stadler, W., Pöllhuber, D., and Heine, C. (2002). EEG alpha power and intelligence. Intelligence *30*, 289–302. 10.1016/S0160-2896(01)00101-5.
9. Thatcher, R.W., North, D., and Biver, C. (2005). EEG and intelligence: Relations between EEG coherence, EEG phase delay and power. Clin. Neurophysiol. *116*, 2129–2141. 10.1016/j.clinph.2005.04.026.
10. Zakharov, I., Tabueva, A., Adamovich, T., Kovas, Y., and Malykh, S. (2020). Alpha Band Resting-State EEG Connectivity Is Associated With Non-verbal Intelligence. Front. Hum. Neurosci. *14*, 10. 10.3389/fnhum.2020.00010.
11. da Cruz, J.R., Favrod, O., Roinishvili, M., Chkonia, E., Brand, A., Mohr, C., Figueiredo, P., and Herzog, M.H. (2020). EEG microstates are a candidate endophenotype for schizophrenia. Nat. Commun. *11*, 3089. 10.1038/s41467-020-16914-1.

12. Di Lorenzo, G., Daverio, A., Ferrentino, F., Santarnecchi, E., Ciabattini, F., Monaco, L., Lisi, G., Barone, Y., Di Lorenzo, C., Niolu, C., et al. (2015). Altered resting-state EEG source functional connectivity in schizophrenia: the effect of illness duration. Front. Hum. Neurosci. *9*. 10.3389/fnhum.2015.00234.

13. Nikulin, V.V., Jönsson, E.G., and Brismar, T. (2012). Attenuation of long-range temporal correlations in the amplitude dynamics of alpha and beta neuronal oscillations in patients with schizophrenia. NeuroImage *61*, 162–169. 10.1016/j.neuroimage.2012.03.008.

14. Rieger, K., Diaz Hernandez, L., Baenninger, A., and Koenig, T. (2016). 15 Years of Microstate Research in Schizophrenia – Where Are We? A Meta-Analysis. Front. Psychiatry *7*. 10.3389/fpsyt.2016.00022.

15. Sponheim, S.R., Clementz, B.A., Iacono, W.G., and Beiser, M. (2000). Clinical and biological concomitants of resting state EEG power abnormalities in schizophrenia. Biol. Psychiatry *48*, 1088–1097. 10.1016/S0006-3223(00)00907-0.

16. Fingelkurts, A.A., Fingelkurts, A.A., Rytsälä, H., Suominen, K., Isometsä, E., and Kähkönen, S. (2007). Impaired functional connectivity at EEG alpha and theta frequency bands in major depression. Hum. Brain Mapp. *28*, 247–261. 10.1002/hbm.20275.

17. Jaworska, N., Blier, P., Fusee, W., and Knott, V. (2012). Alpha power, alpha asymmetry and anterior cingulate cortex activity in depressed males and females. J. Psychiatr. Res. *46*, 1483–1491. 10.1016/j.jpsychires.2012.08.003.

18. Murphy, M., Whitton, A.E., Deccy, S., Ironside, M.L., Rutherford, A., Beltzer, M., Sacchet, M., and Pizzagalli, D.A. (2020). Abnormalities in electroencephalographic microstates are state and trait markers of major depressive disorder. Neuropsychopharmacology *45*, 2030–2037. 10.1038/s41386-020-0749-1.

19. Shim, M., Im, C.-H., Kim, Y.-W., and Lee, S.-H. (2018). Altered cortical functional network in major depressive disorder: A resting-state electroencephalogram study. NeuroImage Clin. *19*, 1000–1007. 10.1016/j.nicl.2018.06.012.

20. Babiloni, C., Binetti, G., Cassarino, A., Dal Forno, G., Del Percio, C., Ferreri, F., Ferri, R., Frisoni, G., Galderisi, S., Hirata, K., et al. (2006). Sources of cortical rhythms in adults during physiological aging: A multicentric EEG study. Hum. Brain Mapp. *27*, 162–172. 10.1002/hbm.20175.

21. Kumral, D., Şansal, F., Cesnaite, E., Mahjoory, K., Al, E., Gaebler, M., Nikulin, V.V., and Villringer, A. (2020). BOLD and EEG signal variability at rest differently relate to aging in the human brain. NeuroImage *207*, 116373. 10.1016/j.neuroimage.2019.116373.

22. Scally, B., Burke, M.R., Bunce, D., and Delvenne, J.-F. (2018). Resting-state EEG power and connectivity are associated with alpha peak frequency slowing in healthy aging. Neurobiol. Aging *71*, 149–155. 10.1016/j.neurobiolaging.2018.07.004.

23. Zappasodi, F., Marzetti, L., Olejarczyk, E., Tecchio, F., and Pizzella, V. (2015). Age-Related Changes in Electroencephalographic Signal Complexity. PLOS ONE *10*, e0141995. 10.1371/journal.pone.0141995.

24. Babayan, A., Erbey, M., Kumral, D., Reinelt, J.D., Reiter, A.M.F., Röbbig, J., Schaare, H.L., Uhlig, M., Anwander, A., Bazin, P.-L., et al. (2019). A mind-brain-body dataset of MRI, EEG, cognition, emotion, and peripheral physiology in young and old adults. Sci. Data *6*, 180308. 10.1038/sdata.2018.308.

25. Alexander, D.L.J., Tropsha, A., and Winkler, D.A. (2015). Beware of R^2 : Simple, Unambiguous Assessment of the Prediction Accuracy of QSAR and QSPR Models. J. Chem. Inf. Model. *55*, 1316–1322. 10.1021/acs.jcim.5b00206.

26. Pedregosa, F., Varoquaux, G., Gramfort, A., Michel, V., Thirion, B., Grisel, O., Blondel, M., Prettenhofer, P., Weiss, R., Dubourg, V., et al. (2011). Scikit-learn: Machine Learning in Python. J. Mach. Learn. Res. *12*, 2825–2830.

27. Cohen, J. (1988). Statistical power analysis for the behavioral sciences 2nd ed. (L. Erlbaum Associates).

28. Qin, Y., Xu, P., and Yao, D. (2010). A comparative study of different references for EEG default mode network: The use of the infinity reference. Clin. Neurophysiol. *121*, 1981–1991. 10.1016/j.clinph.2010.03.056.

29. Loken, E., and Gelman, A. (2017). Measurement error and the replication crisis. Science *355*, 584–585. 10.1126/science.aal3618.

30. Gudmundsson, S., Runarsson, T.P., Sigurdsson, S., Eiriksdottir, G., and Johnsen, K. (2007). Reliability of quantitative EEG features. Clin. Neurophysiol. *118*, 2162–2171. 10.1016/j.clinph.2007.06.018.

31. Haartsen, R., van der Velde, B., Jones, E.J.H., Johnson, M.H., and Kemner, C. (2020). Using multiple short epochs optimises the stability of infant EEG connectivity parameters. Sci. Rep. *10*, 12703. 10.1038/s41598-020-68981-5.

32. Khanna, A., Pascual-Leone, A., and Farzan, F. (2014). Reliability of Resting-State Microstate Features in Electroencephalography. PLoS ONE *9*, e114163. 10.1371/journal.pone.0114163.

33. Kondacs, A., and Szabó, M. (1999). Long-term intra-individual variability of the background EEG in normals. Clin. Neurophysiol. *110*, 1708–1716. 10.1016/S1388-2457(99)00122-4.

34. Nikulin, V.V., and Brismar, T. (2004). Long-range temporal correlations in alpha and beta oscillations: effect of arousal level and test–retest reliability. Clin. Neurophysiol. *115*, 1896–1908. 10.1016/j.clinph.2004.03.019.

35. Velde, B., Haartsen, R., and Kemner, C. (2019). Test-retest reliability of EEG network characteristics in infants. Brain Behav. *9*, e01269. 10.1002/brb3.1269.

36. Hedge, C., Powell, G., and Sumner, P. (2018). The reliability paradox: Why robust cognitive tasks do not produce reliable individual differences. Behav. Res. Methods *50*, 1166–1186. 10.3758/s13428-017-0935-1.

37. Meisel, C., Bailey, K., Achermann, P., and Plenz, D. (2017). Decline of long-range temporal correlations in the human brain during sustained wakefulness. Sci. Rep. *7*, 11825. 10.1038/s41598-017-12140-w.

38. Abel, J.H., Badgeley, M.A., Meschede-Krasa, B., Schamberg, G., Garwood, I.C., Lecamwasam, K., Chakravarty, S., Zhou, D.W., Keating, M., Purdon, P.L., et al. (2021). Machine learning of EEG spectra classifies unconsciousness during GABAergic anesthesia. PLOS ONE *16*, e0246165. 10.1371/journal.pone.0246165.

39. Al Zoubi, O., Ki Wong, C., Kuplicki, R.T., Yeh, H., Mayeli, A., Refai, H., Paulus, M., and Bodurka, J. (2018). Predicting Age From Brain EEG Signals—A Machine Learning Approach. Front. Aging Neurosci. *10*, 184. 10.3389/fnagi.2018.00184.

40. Imperatori, L.S., Cataldi, J., Betta, M., Ricciardi, E., Ince, R.A.A., Siclari, F., and Bernardi, G. (2021). Cross-participant prediction of vigilance stages through the combined use of wPLI and wSMI EEG functional connectivity metrics. Sleep *44*, zsaa247. 10.1093/sleep/zsaa247.

41. Price, G.W., Michie, P.T., Johnston, J., Innes-Brown, H., Kent, A., Clissa, P., and Jablensky, A.V. (2006). A Multivariate Electrophysiological Endophenotype, from a Unitary Cohort, Shows Greater Research Utility than Any Single Feature in the Western Australian Family Study of Schizophrenia. Biol. Psychiatry *60*, 1–10. 10.1016/j.biopsych.2005.09.010.

42. Sitt, J.D., King, J.-R., El Karoui, I., Rohaut, B., Faugeras, F., Gramfort, A., Cohen, L., Sigman, M., Dehaene, S., and Naccache, L. (2014). Large scale screening of neural signatures of consciousness in patients in a vegetative or minimally conscious state. Brain *137*, 2258–2270. 10.1093/brain/awu141.

43. Wolff, A., Di Giovanni, D.A., Gómez-Pilar, J., Nakao, T., Huang, Z., Longtin, A., and Northoff, G. (2019). The temporal signature of self: Temporal measures of resting-state EEG predict self-consciousness. Hum. Brain Mapp. *40*, 789–803. 10.1002/hbm.24412.

44. Hatz, F., Hardmeier, M., Bousleiman, H., Rüegg, S., Schindler, C., and Fuhr, P. (2016). Reliability of Functional Connectivity of Electroencephalography Applying Microstate-Segmented Versus Classical Calculation of Phase Lag Index. Brain Connect. *6*, 461–469. 10.1089/brain.2015.0368.

45. Hülsemann, M.J., Naumann, E., and Rasch, B. (2019). Quantification of Phase-Amplitude Coupling in Neuronal Oscillations: Comparison of Phase-Locking Value, Mean Vector Length, Modulation Index, and Generalized-Linear-Modeling-Cross-Frequency-Coupling. Front. Neurosci. *13*, 573. 10.3389/fnins.2019.00573.

46. Imperatori, L.S., Betta, M., Cecchetti, L., Canales-Johnson, A., Ricciardi, E., Siclari, F., Pietrini, P., Chennu, S., and Bernardi, G. (2019). EEG functional connectivity metrics wPLI and wSMI account for distinct types of brain functional interactions. Sci. Rep. *9*, 8894. 10.1038/s41598-019-45289-7.

47. Gignac, G.E., and Szodorai, E.T. (2016). Effect size guidelines for individual differences researchers. Personal. Individ. Differ. *102*, 74–78. 10.1016/j.paid.2016.06.069.

48. Gordillo, D., da Cruz, J.R., Chkonia, E., Lin, W.-H., Favrod, O., Brand, A., Figueiredo, P., Roinishvili, M., and Herzog, M.H. (2022). The EEG multiverse of schizophrenia. Cereb. Cortex, bhac309. 10.1093/cercor/bhac309.

49. Bosten, J.M., Goodbourn, P.T., Bargary, G., Verhallen, R.J., Lawrance-Owen, A.J., Hogg, R.E., and Mollon, J.D. (2017). An exploratory factor analysis of visual performance in a large population. Vision Res. *141*, 303–316. 10.1016/j.visres.2017.02.005.

50. Cappe, C., Clarke, A., Mohr, C., and Herzog, M.H. (2014). Is there a common factor for vision? J. Vis. *14*, 4–4. 10.1167/14.8.4.

51. Garobbio, S., Pilz, K.S., Kunchulia, M., and Herzog, M.H. (2022). No Common Factor Underlying Decline of Visual Abilities in Mild Cognitive Impairment. Exp. Aging Res., 1–18. 10.1080/0361073X.2022.2094660.

52. Shaqiri, A., Pilz, K.S., Cretenoud, A.F., Neumann, K., Clarke, A., Kunchulia, M., and Herzog, M.H. (2019). No evidence for a common factor underlying visual abilities in healthy older people. Dev. Psychol. *55*, 1775–1787. 10.1037/dev0000740.

53. Cretenoud, A.F., Karimpur, H., Grzeczkowski, L., Francis, G., Hamburger, K., and Herzog, M.H. (2019). Factors underlying visual illusions are illusion-specific but not feature-specific. J. Vis. *19*, 12. 10.1167/19.14.12.

54. Grzeczkowski, L., Clarke, A.M., Francis, G., Mast, F.W., and Herzog, M.H. (2017). About individual differences in vision. Vision Res. *141*, 282–292. 10.1016/j.visres.2016.10.006.

55. Goodbourn, P.T., Bosten, J.M., Hogg, R.E., Bargary, G., Lawrance-Owen, A.J., and Mollon, J.D. (2012). Do different 'magnocellular tasks' probe the same neural substrate? Proc. R. Soc. B Biol. Sci. *279*, 4263–4271. 10.1098/rspb.2012.1430.

56. Eisenberg, I.W., Bissett, P.G., Zeynep Enkavi, A., Li, J., MacKinnon, D.P., Marsch, L.A., and Poldrack, R.A. (2019). Uncovering the structure of self-regulation through data-driven ontology discovery. Nat. Commun. *10*, 2319. 10.1038/s41467-019-10301-1.

57. Francis, G. (2012). Publication bias and the failure of replication in experimental psychology. Psychon. Bull. Rev. *19*, 975–991. 10.3758/s13423-012-0322-y.

58. Simonsohn, U., Nelson, L.D., and Simmons, J.P. (2014). P-curve: A key to the file-drawer. J. Exp. Psychol. Gen. *143*, 534–547. 10.1037/a0033242.

59. Yarkoni, T. (2009). Big Correlations in Little Studies: Inflated fMRI Correlations Reflect Low Statistical Power—Commentary on Vul et al. (2009). Perspect. Psychol. Sci. *4*, 294–298. 10.1111/j.1745-6924.2009.01127.x.

60. Botvinik-Nezer, R., Holzmeister, F., Camerer, C.F., Dreber, A., Huber, J., Johannesson, M., Kirchler, M., Iwanir, R., Mumford, J.A., Adcock, R.A., et al. (2020). Variability in the analysis of a single neuroimaging dataset by many teams. Nature *582*, 84–88. 10.1038/s41586-020-2314-9.

61. Carp, J. (2012). On the Plurality of (Methodological) Worlds: Estimating the Analytic Flexibility of fMRI Experiments. Front. Neurosci. *6*. 10.3389/fnins.2012.00149.

62. Silberzahn, R., Uhlmann, E.L., Martin, D.P., Anselmi, P., Aust, F., Awtrey, E., Bahník, Š., Bai, F., Bannard, C., Bonnier, E., et al. (2018). Many Analysts, One Data Set: Making Transparent How Variations in Analytic Choices Affect Results. Adv. Methods Pract. Psychol. Sci. *1*, 337–356. 10.1177/2515245917747646.

63. Aharoni, E., and Rosset, S. (2014). Generalized α -investing: definitions, optimality results and application to public databases. J. R. Stat. Soc. Ser. B Stat. Methodol. *76*, 771–794. 10.1111/rssb.12048.

64. Thompson, W.H., Wright, J., Bissett, P.G., and Poldrack, R.A. (2020). Dataset decay and the problem of sequential analyses on open datasets. eLife *9*, e53498. 10.7554/eLife.53498.

65. Weston, S.J., Ritchie, S.J., Rohrer, J.M., and Przybylski, A.K. (2019). Recommendations for Increasing the Transparency of Analysis of Preexisting Data Sets. Adv. Methods Pract. Psychol. Sci. *2*, 214–227. 10.1177/2515245919848684.

66. Poldrack, R.A., Huckins, G., and Varoquaux, G. (2020). Establishment of Best Practices for Evidence for Prediction: A Review. JAMA Psychiatry *77*, 534. 10.1001/jamapsychiatry.2019.3671.

67. Delorme, A., and Makeig, S. (2004). EEGLAB: an open source toolbox for analysis of single-trial EEG dynamics including independent component analysis. J. Neurosci. Methods *134*, 9–21. 10.1016/j.jneumeth.2003.10.009.

68. Niemann, H., Sturm, W., Thöne-Otto, A.I., and Willmes, K. (2008). CVLT California Verbal Learning Test. German adaptation. Manual (Pearson).

69. Donders, J. (2008). A Confirmatory Factor Analysis of the California Verbal Learning Test—Second Edition (CVLT-II) in the Standardization Sample. Assessment *15*, 123–131. 10.1177/1073191107310926.

70. Mahjoory, K., Cesnaite, E., Hohlefeld, F.U., Villringer, A., and Nikulin, V.V. (2019). Power and temporal dynamics of alpha oscillations at rest differentiate cognitive performance involving sustained and phasic cognitive control. NeuroImage *188*, 135–144. 10.1016/j.neuroimage.2018.12.001.

71. Zimmermann, P., and Fimm, B. (2012). Testbatterie zur Aufmerksamkeitsprüfung Version 2.3.1. (Psytest).

72. Vandierendonck, A. (2018). Further Tests of the Utility of Integrated Speed-Accuracy Measures in Task Switching. J. Cogn. *1*, 8. 10.5334/joc.6.

73. Reitan, R.M., and Wolfson, D. (1993). The Halstead-Reitan neuropsychological test battery theory and clinical interpretation (Neuropsychology Press).

74. Schmidt, K.-H., and Metzler, P. (1992). Wortschatztest : WST (Beltz).

75. Kreuzpointner, L., Lukesch, H., and Horn, W. (2013). Leistungsprüfsystem 2 LPS-2 (Hogrefe).

76. Aschenbrenner, S., Lange, K.W., and Tucha, O. (2000). RWT : Regensburger Wortflüssigkeits-Test (Hogrefe).

77. Pascual-Marqui, R.D., Lehmann, D., Koukkou, M., Kochi, K., Anderer, P., Saletu, B., Tanaka, H., Hirata, K., John, E.R., Prichep, L., et al. (2011). Assessing interactions in the brain with exact low-resolution electromagnetic tomography. Philos. Trans. R. Soc. Math. Phys. Eng. Sci. *369*, 3768–3784. 10.1098/rsta.2011.0081.

78. Hardstone, R., Poil, S.-S., Schiavone, G., Jansen, R., Nikulin, V.V., Mansvelder, H.D., and Linkenkaer-Hansen, K. (2012). Detrended Fluctuation Analysis: A Scale-Free View on Neuronal Oscillations. Front. Physiol. *3*. 10.3389/fphys.2012.00450.

79. Montez, T., Poil, S.-S., Jones, B.F., Manshanden, I., Verbunt, J.P.A., van Dijk, B.W., Brussaard, A.B., van Ooyen, A., Stam, C.J., Scheltens, P., et al. (2009). Altered temporal correlations in parietal alpha and prefrontal theta oscillations in early-stage Alzheimer disease. Proc. Natl. Acad. Sci. *106*, 1614–1619. 10.1073/pnas.0811699106.

80. Oostenveld, R., Fries, P., Maris, E., and Schoffelen, J.-M. (2011). FieldTrip: Open Source Software for Advanced Analysis of MEG, EEG, and Invasive Electrophysiological Data. Comput. Intell. Neurosci. *2011*, 1–9. 10.1155/2011/156869.

81. Rubinov, M., and Sporns, O. (2010). Complex network measures of brain connectivity: Uses and interpretations. NeuroImage *52*, 1059–1069. 10.1016/j.neuroimage.2009.10.003.

82. Koenig, T., Prichep, L., Lehmann, D., Sosa, P.V., Braeker, E., Kleinlogel, H., Isenhart, R., and John, E.R. (2002). Millisecond by Millisecond, Year by Year: Normative EEG Microstates and Developmental Stages. NeuroImage *16*, 41–48. 10.1006/nimg.2002.1070.

83. Custo, A., Van De Ville, D., Wells, W.M., Tomescu, M.I., Brunet, D., and Michel, C.M. (2017). Electroencephalographic Resting-State Networks: Source Localization of Microstates. Brain Connect. *7*, 671–682. 10.1089/brain.2016.0476.

84. Pascual-Marqui, R.D., Michel, C.M., and Lehmann, D. (1995). Segmentation of brain electrical activity into microstates: model estimation and validation. IEEE Trans. Biomed. Eng. *42*, 658–665. 10.1109/10.391164.

85. Brunet, D., Murray, M.M., and Michel, C.M. (2011). Spatiotemporal Analysis of Multichannel EEG: CARTOOL. Comput. Intell. Neurosci. *2011*, 1–15. 10.1155/2011/813870.

86. Pincus, S.M. (1991). Approximate entropy as a measure of system complexity. Proc. Natl. Acad. Sci. *88*, 2297–2301. 10.1073/pnas.88.6.2297.

87. Bandt, C., and Pompe, B. (2002). Permutation Entropy: A Natural Complexity Measure for Time Series. Phys. Rev. Lett. *88*, 174102. 10.1103/PhysRevLett.88.174102.

88. Richman, J.S., and Moorman, J.R. (2000). Physiological time-series analysis using approximate entropy and sample entropy. Am. J. Physiol.-Heart Circ. Physiol. *278*, H2039–H2049. 10.1152/ajpheart.2000.278.6.H2039.

89. Unakafova, V., and Keller, K. (2013). Efficiently Measuring Complexity on the Basis of Real-World Data. Entropy *15*, 4392–4415. 10.3390/e15104392.

90. Martínez-Cagigal, V. Sample Entropy. https://ch.mathworks.com/matlabcentral/fileexchange/69381-sample-entropy.

91. Lempel, A., and Ziv, J. (1976). On the Complexity of Finite Sequences. IEEE Trans. Inf. Theory *22*, 75–81. 10.1109/TIT.1976.1055501.

92. Thai, Q. calc_lz_complexity. https://ch.mathworks.com/matlabcentral/fileexchange/38211-calc_lz_complexity.

93. Marwan, N., Carmenromano, M., Thiel, M., and Kurths, J. (2007). Recurrence plots for the analysis of complex systems. Phys. Rep. *438*, 237–329. 10.1016/j.physrep.2006.11.001.

94. Rosenstein, M.T., Collins, J.J., and De Luca, C.J. (1993). A practical method for calculating largest Lyapunov exponents from small data sets. Phys. Nonlinear Phenom. *65*, 117–134. 10.1016/0167-2789(93)90009-P.

95. Theiler, J. (1987). Efficient algorithm for estimating the correlation dimension from a set of discrete points. Phys. Rev. A *36*, 4456–4462. 10.1103/PhysRevA.36.4456.

96. Higuchi, T. (1988). Approach to an irregular time series on the basis of the fractal theory. Phys. Nonlinear Phenom. *31*, 277–283. 10.1016/0167-2789(88)90081-4.

97. Katz, M.J. (1988). Fractals and the analysis of waveforms. Comput. Biol. Med. *18*, 145–156. 10.1016/0010-4825(88)90041-8.

98. Monge-Álvarez, J. Higuchi and Katz fractal dimension measures. https://ch.mathworks.com/matlabcentral/fileexchange/50290-higuchi-and-katz-fractal-dimension-measures.

99. Tort, A.B.L., Komorowski, R., Eichenbaum, H., and Kopell, N. (2010). Measuring Phase-Amplitude Coupling Between Neuronal Oscillations of Different Frequencies. J. Neurophysiol. *104*, 1195–1210. 10.1152/jn.00106.2010.

100. O'Reilly, D., Navakatikyan, M.A., Filip, M., Greene, D., and Van Marter, L.J. (2012). Peak-to-peak amplitude in neonatal brain monitoring of premature infants. Clin. Neurophysiol. *123*, 2139–2153. 10.1016/j.clinph.2012.02.087.

101. Toole, J.M.O., and Boylan, G.B. (2017). NEURAL: quantitative features for newborn EEG using Matlab. ArXiv170405694 Phys. Q-Bio Stat.

102. Hjorth, B. (1970). EEG analysis based on time domain properties. Electroencephalogr. Clin. Neurophysiol. *29*, 306–310. 10.1016/0013-4694(70)90143-4.

103. Benjamini, Y., and Hochberg, Y. (1995). Controlling the False Discovery Rate: A Practical and Powerful Approach to Multiple Testing. J. R. Stat. Soc. Ser. B Methodol. *57*, 289–300. 10.1111/j.2517-6161.1995.tb02031.x.

104. Vallat, R. (2018). Pingouin: statistics in Python. J. Open Source Softw. *3*, 1026. 10.21105/joss.01026.

105. Székely, G.J., and Rizzo, M.L. (2013). The distance correlation t -test of independence in high dimension. J. Multivar. Anal. *117*, 193–213. 10.1016/j.jmva.2013.02.012.

106. Seabold, S., and Perktold, J. (2010). Statsmodels: Econometric and statistical modeling with python. In 9th Python in Science Conference.

107. RStudio Team (2020). RStudio: Integrated Development Environment for R.

108. Hothorn, T., Hornik, K., Wiel, M.A. van de, and Zeileis, A. (2008). Implementing a Class of Permutation Tests: The coin Package. J. Stat. Softw. *28*. 10.18637/jss.v028.i08.

109. Kassambara, A. (2021). rstatix: Pipe-Friendly Framework for Basic Statistical Tests.

110. Rizzo, M., and Székely, G. (2022). energy: E-Statistics: Multivariate Inference via the Energy of Data.

111. Dong, L., Li, F., Liu, Q., Wen, X., Lai, Y., Xu, P., and Yao, D. (2017). MATLAB Toolboxes for Reference Electrode Standardization Technique (REST) of Scalp EEG. Front. Neurosci. *11*, 601. 10.3389/fnins.2017.00601.

Chapter 7. General Discussion

7.1. Contextual effects and predictive coding

Contextual vision studies in schizophrenia have yielded contradicting findings (King et al., 2017; Notredame et al., 2014; Silverstein & Keane, 2011b), which might be due to the heterogeneity of schizophrenia, but also to the idiosyncrasy of the paradigms. For example, some paradigms might require stronger attention than others. Since patients with schizophrenia often suffer from impairments in attentional processes (Chkonia, Roinishvili, Herzog, et al., 2010), there might be differences between controls and patients in some paradigms due to attentional rather than contextual processing deficits. Furthermore, schizophrenia might affect different patients differently. Therefore, comparing results from different patient samples is not as accurate as comparing the same patient sample using different experimental methods. In Chapter 4, we tested the very same patients and controls using two variants of an (un)crowding paradigm. Importantly, (un)crowding allows to investigate both faciliating and deteriorating contextual effects which may serve as an assessment of lower attention (e.g., if only deteriorating effects are found).

We found that the same patients showed intact processing in one of the variants of the paradigm (Experiment 1), whereas clear-cut contextual vision impairments were found in the other variant (Experiment 2). These results suggest that mixed results might also be provoked by differences in the spatial arrangements of the stimuli and experimental design. Notably, our results also question whether there is a *general* abnormal mechanism for contextual vision in schizophrenia, since if there is a general deficit this should be evident across paradigms. Our results cannot be explained by deficits in attention (Braff, 1993; Chkonia, Roinishvili, Herzog, et al., 2010) or target enhancement (Herzog et al., 2013), since patients did not exhibit lower performance in all the conditions. Further research is needed to investigate which other factors might be involved in the paradigms and how much they contribute to contextual visual processing.

Importantly, our results are consistent with previous findings indicating that patients may successfully perform complex visual tasks in a qualitatively intact manner, while still

demonstrating a main deficit, manifested as lower overall performance (Brand et al., 2005; Roinishvili et al., 2015; Schütze et al., 2007). This was observed particularly for the crowding conditions. However, in the uncrowding conditions, we found that patients had both qualitative and quantitative deficits in Experiment 2, yet uncrowding was intact in Experiment 1. What provokes these discrepancies will need to be clarified in future studies. Evaluating individual differences might be important in future studies to determine to what extent better performance in the *target-only* condition results in better performance for (un)crowding conditions, or whether visual acuity contributes to our results. Previous studies have shown that differences in visual acuity might strongly bias results in patients with schizophrenia for contrast paradigms (Bi et al., 2023). Controlling for these variables might however require larger samples, which is another limitation of our study. Altogether, we suggest that claims about abnormal mechanisms in schizophrenia should be supported by multiple paradigms.

Importantly, mixed results are expected in the absence of publication bias, i.e., the tendency to publish only positive results. Whether mixed results exist to the extent given the power of the individual studies (i.e., whether results are *more mixed* than expected) needs to be addressed through systematic meta-analyses. Our results suggest that such analyses might benefit from including studies matched by experimental design, and even stimuli properties and setups to the extent that is possible since these factors might influence the results. Furthermore, since some of the contextual effects might be more (or less) pronounced depending on whether patients are stable or in acute states (Keane et al., 2013; Silverstein et al., 2013), matching studies by the state of the patients will lead to more robust results. Moreover, chronicity might also need to be considered as a confounding factor. For example, brain structural abnormalities are less pronounced in first-episode psychosis patients compared to patients with a longer illness duration (Zhao et al., 2022).

Differences in visual processing paradigms in schizophrenia have been conceptualized within the framework of predictive coding (PC). Specifically, it has been proposed that sensory inputs and prior information are abnormally combined in patients, leading to aberrant perception (Adams et al., 2013; Sterzer et al., 2018). In Chapter 5, I presented a neurophysiological study of PC in schizophrenia using the method of oscillatory traveling waves. A notable advantage of this neurophysiological approach is its systematic evaluation of the different components involved in PC, such as prediction errors and prior precisions (Alamia & VanRullen, 2019; Arnal

& Giraud, 2012; Friston, 2019). This approach contrasts with behavioral paradigms where generally the outcome of the entire PC process is measured.

PC processes have been proposed to occur at multiple levels in a hierarchy composed of several priors (Corlett et al., 2019; Sterzer et al., 2018). Alterations at different levels in this hierarchy may give rise to different phenomena, ranging from basic sensory impairments (for alterations at lower levels) to more complex symptoms (for alterations at higher levels) in schizophrenia. The results presented in Chapter 5 are well in line with this view, as we found evidence suggesting alterations at plausibly different prior levels in schizophrenia. Patients with schizophrenia exhibited higher alpha-band backward traveling waves (TW) during resting-state, suggesting higher precision in priors located at hierarchically-higher levels of PC processes. Conversely, results using visual backward masking data showed higher forward (bottom-up, mirroring prediction errors) TW, suggesting that priors located at lower levels of PC processes exhibit less precision in patients compared to controls. This latter effect only arose when there were visual stimuli, indicating that this specific alteration might become evident when sensory information needs to be processed.

Importantly, while TW is a versatile tool that allows to investigate distinct components of PC processes, the link to priors is still premature. While there is computational evidence that TW might be a plausible mechanism for PC processing (Alamia & VanRullen, 2019), whether this is implemented in the brain in a way that is measurable through EEG has received to now only experimental support, e.g., through pharmacological intervention studies (Alamia et al., 2020). Further studies involving intra-cranial recordings, or neuroimaging methods exceeding the resolution of EEG, combined with rigorous biophysical modeling might help establish a more direct link between TW and priors in schizophrenia. Furthermore, alpha-band modulations have been shown to reflect attentional effects (Compton et al., 2019), and therefore decreased attention in the patients might be a plausible explanation for the differences observed in visual backward masking. However, we did not find differences for one of the control conditions in the task where there was no visual processing involved (Supplementary Information Chapter 5). Therefore, attentional effects might not strongly impact our resutls.

There is the question of to what extent these different levels of predictive processing are related. Recent experimental evidence in healthy subjects has revealed weak correlations between bistable visual illusions, pareidolias, and self-reports of hallucinations, which may to

some extent tap into different PC levels, suggesting that alterations at different stages of PC might be independent (Lhotka et al., 2023). However, in our TW analysis, we found evidence for a correlation between alterations at lower and higher level priors. Thus, further research employing several paradigms targeting explicitly those different levels of predictive processing is necessary to assess the relation among these levels and, most importantly, how they contribute to the pathophysiology of schizophrenia.

Schizophrenia, however, is much more than visual dysfunctions and psychotic symptoms. Patients often suffer from impairments in working memory (Meyer-Lindenberg et al., 2001) and attention (Chkonia, Roinishvili, Herzog, et al., 2010), which significantly affect their quality of life (Eack & Newhill, 2007; Green et al., 2015). These deficits might potentially not be explained by predictive processing mechanisms. Moreover, hallucinations and perceptual alterations are common in other disorders, such as Alzheimer's disease (El Haj et al., 2017), or bipolar disorder (Baethge et al., 2005), questioning the specificity of predictive processing abnormalities for schizophrenia. While predictive coding provides an appealing model for interpreting experimental findings, its ability to account for the heterogeneity of schizophrenia is severely limited.

7.2. On the complexity of schizophrenia

Schizophrenia has been studied for more than a century, yet its underlying causes remain an enigma. One reason could be that the complexity of the disorder has strongly been underestimated. Traditionally, schizophrenia research has focused on single deficits. However, experimental work has uncovered a wide array of deficits associated with schizophrenia, suggesting that there might be several impaired mechanisms. Hence, the classic approach in schizophrenia research might need to be accompanied by new approaches aiming to address this heterogeneity. Analyzing the relationship between multiple paradigms might offer a comprehensive understanding of the complexity of the illness. In Chapter 2, we took a step forward in this direction by employing a *multiverse* approach, analyzing a broad spectrum of neurophysiological features in patients with schizophrenia.

Our study revealed that despite significant group differences between patients and controls, with effect sizes ranging from medium to large, 69 EEG features were not highly correlated

with each other in patients. These results suggest that even if a significant result is found, this might not necessarily indicate that this result points to a *general* abnormal mechanism in schizophrenia. However, our study has limitations. For instance, while in our group comparison analysis we used ANCOVAs to control for demographical differences, since groups were not initially matched by Gender or education, the influence of these variables might still be underestimated (Miller & Chapman, 2001). Therefore, our results might still be influenced by demographical and also other variables related for instance nicotine consumption, among many others. However, notably correlations between patients and controls were largely similar (***Figure 1***), suggesting that if there are influences of confounding factors, this might not have strong effects on the correlations between EEG features.

However, there might be other plausible explanations for the low correlations between EEG features. For instance, the EEG features might have low test-retest reliabilities, which reduces the *true* pairwise correlations. Test retests are crucial for correlation analyses, and not having a measure of reliability is a severe limitation of our study. However, some of the features that we employed have shown adequate reliabilities in previous studies (Gudmundsson et al., 2007; Haartsen et al., 2020; Khanna et al., 2014; Kondacs & Szabó, 1999; Nikulin & Brismar, 2004). Furthermore, we found that some features obtained from similar methods are highly correlated, resembling to some extent test-retests. However, a rigorous test-retest assessment, with two recording sessions, is crucial for interpretability.

Another possible explanation for the low correlations is that while the features might be targeting the same general aspects of schizophrenia they are also sensitive to other *target-unspecific* aspects, such as comorbidities, among many others. Therefore, if *target-unspecific* aspects significantly contribute to the variance, and EEG features are sensitive to different aspects, correlations will be low. In a more complex scenario, schizophrenia may be a highly heterogeneous disorder at the neurophysiological level, with each feature pointing to roughly independent factors.

In Chapter 3, we aimed to investigate some of the aforementioned scenarios through a longitudinal assessment of EEG features. Our preliminary findings indicate that several EEG features exhibit remarkable long-term stability. This is particularly noteworthy considering that the measurements were spaced, on average, 4 years apart. Therefore, the influence of measurement error and *target-unspecific* variance might be smaller in these stable features.

Importantly, the benchmarks that we used for poor, and excellent reliability provided by Cicchetti (1994) are rather optimistic, e.g., compared to Koo & Li. (2016) where excellent reliabilities are considered those > 0.9 instead of > 0.75. However, our study goes beyond testing reliability only due to measurement error but rather probes long-term fluctuations, since the time differences between recordings were much larger than in classic test-retest studies. Importantly, longitudinal assessments might require different analyses than reliability assessments, which are often performed after a few days, or even hours. For example, the choice of the ICC function, and also to what extent stability is not influenced by signal preprocessing or illness chronicity will need to be rigorously accounted for to establish stability of EEG features more robustly. Furthermore, we made different analytical decisions in Chapter 2, compared to Chapter 1, to increase signal-to-noise ratios. However, a direct comparison between the two studies will be important to see the extent to which these decisions improved the correlations. While this comparison cannot be done directly, since the bounds and number of frequency bands are different in the two studies, there might be other means to compare SNR in the two studies. For instance, frequency bands at the re-test might be defined for all the samples based on the mean alpha peak frequency (instead of defining the frequency bands for each subject based on their peak), which will allow us to compare the features using reliability or correlation analyses.

If these stable EEG features, indeed, reflect distinct factors, this could provide valuable insights into the complexity of schizophrenia and might open new avenues for inquiry. There might be several explanations for schizophrenia in this multifactorial scenario. For instance, schizophrenia may be an additive disorder, where having more deficits leads to more severe symptoms or genetic risk. Polygenic risk scores (PRS) could be an example since a summary of several variants was shown to explain more variance than single variants (Ripke et al., 2014). Alternatively, it is possible that having one or a few pronounced deficits leads to more severe symptoms or heightened risk for schizophrenia. This scenario is supported by recent findings indicating that a few rare variants confer a much higher risk than common variants (Singh et al., 2022). Hence, a small number of features might have a high explanatory power. In a more complex scenario, only certain combinations of deficits provoke schizophrenia. This latter scenario would pose significant challenges in discovering the key mechanisms of schizophrenia since all potential contributing factors would need to be considered. Notably, these scenarios

may need to be addressed through a *shallow rooting* approach, as several deficits might need to be examined.

Importantly, in our correlation analyses, we included EEG features showing significant group differences between patients and controls, which however were not always associated with *large* effect sizes. Studies in other domains such as cognition have yielded both higher effect sizes and also higher correlations in patients (Dickinson et al., 2011), suggesting that cognitive paradigms might overcome the explanatory power of neurophysiological features (Kahn & Keefe, 2013; Mesholam-Gately et al., 2009). Other studies involving reading abilities (Revheim et al., 2014) and eye movements (Benson et al., 2012; St Clair et al., 2022) also have been associated with effect sizes larger than in many neurophysiological studies. Therefore, it is plausible that some domains might be more promising to elucidate the underlying mechanisms of schizophrenia. Notably, these results might be promising in the sense that potentially combining such paradigms associated with larger effect sizes, might even lead to larger group differences between groups.

7.3. Variability is the rule

In the complex sciences, every branch relies on tests assumed to target the key aspects of the field. Typically, these tests reveal a significant group difference between an intervention and a control condition or effectively predict other variables under study. Then, numerous subsequent studies are conducted with these tests to uncover underlying mechanisms. There is an unstated assumption that the test being employed represents a key aspect of the research field. However, recent experimental work, as well as results presented in this thesis, indicate that this assumption may not necessarily hold, as a wide array of measures aimed to target similar mechanisms do not strongly correlate with each other (i.e., construct validity is poor). Where does the variance of these measures come from? Measurement error is a potential candidate. However, as mentioned earlier, behavioral paradigms and EEG measurements often had adequate reliabilities. This, however, does not necessarily mean that signal-to-noise ratios are adequate for the research questions and extensive efforts are being made on this front with an emphasis on developing new technologies and also more adequate methods in human neuroscience (Nebe et al., 2023).

On a more speculative note, there are at least three explanations for high stabilities and low correlations. The first explanation is that the underlying mechanisms being targeted are highly complex, involving several factors. If this scenario holds, *shallow rooting* approaches combining different test outcomes may aid in enhancing explanatory power. We found evidence supporting this scenario in Chapter 6, where latent dimensions exhibited higher explanatory power compared to single features in some cases. Other studies support this scenario too (Abel et al., 2021; Al Zoubi et al., 2018; Giuliani et al., 2023; Imperatori et al., 2021; Price et al., 2006; Sitt et al., 2014; Wolff et al., 2019). Notably, within this complex scenario, there are several nuances depending on the target mechanism and research question (as illustrated in the last paragraph of the previous section). Thus, tailored methodologies are necessary.

A second explanation could be that the paradigms or brain measurements might be less specific than assumed, meaning that while the intended mechanisms might indeed be targeted, many other factors might be targeted too. Hence, tests might be less explanatory of the target mechanism than assumed. The results presented in Chapter 4 point to some extent in this direction showing that even with paradigms targeting ostensibly the same target function, results might be conflicting. Besides other mechanisms, recent work suggests that paradigms and brain measurements may capture highly specific traits of participants of aspects related to data recordings (Greene et al., 2022). *Deep rooting* approaches might be necessary to thoroughly investigate the factors contributing to the variance of a specific measurement, while *shallow rooting* ones may help reveal how much variance of the mechanism is shared across different measurements.

Third, variability may stem from genuine differences between individuals, namely roughly each individual might exhibit distinct traits for brain processing. Here, a more individualized approach will be necessary, systematically examining and identifying which specific traits represent better each individual. In the best-case scenario, a small number of clusters may emerge, composed of subjects exhibiting similar processing patterns. Tailored methodologies will be required to investigate mechanisms within these hypothetical clusters. There are examples that this scenario might hold in some cases. For instance, clustering analysis in patients with psychotic symptoms has provided evidence for three clusters of psychosis patients showing distinct brain profiles (Clementz et al., 2016). In a more complex scenario, there are no clusters and every individual demonstrates highly specific traits. Relying on

average statistics will be insufficient if this scenario holds and new approaches that prioritize the analysis of individual data over average responses will become crucial. Determining the extent to which the scenarios described above hold will necessitate a combination of *deep* and *shallow* rooting approaches.

7.4. Future work

One of the advantages of the traveling wave analysis presented in Chapter 5, was its ability to assess different components of predictive processing, which is generally challenging with only behavioral paradigms. To gain further insights into different levels of predictive processing, employing batteries of visual paradigms combined with EEG in patients with schizophrenia and healthy controls may be helpful. The paradigms may encompass a range of tasks from basic visual illusions and visual crowding to motion and scene perception. Recent work in this direction has successfully probed PC processes through relatively simple EEG paradigms (Chen et al., 2023). Traveling waves can be one of the analyses, yet not the only one. Directed connectivities, e.g., based on Granger causality, could also potentially be employed to identify signatures of predictive processing. Notably, the analyses will need to systematically examine different frequency bands, as there is evidence that feedback and feedforward brain processing may occur through distinct frequency channels (Bastos et al., 2015). Using magnetoencephalography, for example, may provide more detailed information both about oscillations (e.g., in the gamma-band range), and the responsible brain areas, compared to EEG.

To gain further insights into the complexity of neurophysiology in schizophrenia, it will be critical to investigate the mechanisms targeted by the features showing adequate stabilities. For instance, some of the features might reflect aspects related to information processing, whereas others might tap into genetic risks. Hence, analyzing to what extent the features predict cognitive performance in a range of sensory and cognitive tasks, or whether they correlate with genetic risk, e.g., measured with polygenic risk scores, will provide further insights. Further individual differences assessments using these stable features, for example, through fingerprinting analyses, can provide insights into the extent to which these features can distinguish individuals in a population, and whether they reflect specific traits of their

cognitive or perceptual functioning (Van De Ville et al., 2021). All these assessments go hand in hand with the development and utilization of multivariate methods, such as partial least squares or canonical correlation analysis, which may help identify relationships between sets of brain features and sets of behavior variables, instead of univariate correlations.

Analyzing EEG features in different populations can also yield novel insights. For instance, investigating whether the EEG features are also different in unaffected siblings of patients with schizophrenia compared to controls will inform about genetic underpinnings. Importantly, this research has the potential to shed light on which features could be incorporated into batteries designed to detect individuals at risk for developing psychosis. Significant efforts are dedicated to changing the paradigm in psychiatry research towards a more preventive approach (Salazar De Pablo et al., 2021; Uhlhaas et al., 2023). Relatedly, a notable advantage is that resting-state EEG can be collected rapidly, enhancing its potential for applications in clinical settings. Hence, advancements might have critical implications for schizophrenia research.

We speculated on possible scenarios of complexity in schizophrenia (e.g., in Section 7.2). Many of these speculations are empirical, and as such there are ways to address them. One possible analysis would involve correlating symptom scores with a summary measure of the EEG features in patients. Furthermore, polygenic risk scores could be correlated with this summary measure to determine whether deficits in more features predict a higher risk for schizophrenia. Furthermore, nonlinear methods for dimensionality reduction could be employed on the stable EEG features, to determine clusters of features that may not be effectively revealed by classic linear methods such as PCA. It will be important to employ only the EEG features showing high reliabilities, and it is more certain that they might be less influenced by idiosyncratic aspects and measurement error. The overarching goal of these studies would be to systematically assess different potential scenarios of complexity in schizophrenia.

Finally, simulation studies could offer valuable insights into the central problems discussed in this thesis. This meta-scientific approach might provide insights into the causes of the low correlations. There are several examples of how this approach can help comprehend very general aspects of science (Thompson et al., 2020; Ulrich & Miller, 2020; Wang & De Boeck, 2022). By employing simple linear models that incorporate factors such as a *target*, *measurement error*, and *bias* we could run systematic simulations to better understand the impact of these factors on correlations. Moreover, proposing underlying data models, some of

which may involve nonlinearities or interactions, might allow us to identify which model best aligns with real-world observations. Exploring synthetic models in this manner offers flexibility and expands the scope for inquiry.

Supplementary Information Chapter 2

A supplementary information file containing 13 Supplementary Tables, Supplementary Methods, and Supplementary results is available at the publisher's website: https://academic.oup.com/cercor/article/33/7/3816/6677568

Supplementary Information Chapter 4

Supplemental Tables Parameter estimates

Table 1. Estimates from the linear mixed-effects model of Exp1. with each configuration and group as predictors (no interaction between the two predictors) and individual observers as random intercepts.

Fixed Effects	β estimate	β standard error	t-value
(Intercept)	1.832	0.2222	8.274
1 sq – 7 sq	-1.062	0.204	-5.217
1 sq – 35 sq	-1.942	0.204	-9.544
1 sq – square(sq)&star(st)	0.825	0.204	4.054
1 sq – sq&st repeated	-0.318	0.204	-1.565
1 sq – sq&st random	0.703	0.204	3.453
Groups	0.216	0.252	0.998

Table 2. Estimates from the linear mixed-effects model in Line condition of Exp2. with the stimulus duration and groups as predictors (no interaction between the two predictors) and individual observers as random intercepts.

Fixed Effects	β estimate	β standard error	t-value
(Intercept)	3.557	0.294	12.109
Stimulus duration	-0.221	0.029	-7.510
Groups	0.795	0.362	2.198

Table 3. Estimates from the linear mixed-effects model in Cuboid condition of Exp2. with the stimulus duration, groups, and interaction as predictors and individual observers as random intercepts.

Fixed Effects	β estimate	β standard error	t-value
(Intercept)	5.183	0.375	13.814
Stimulus duration	-0.558	0.061	-9.140
Groups	-0.558	0.532	-1.052
Interaction	0.259	0.086	2.997

Supplementary Information Chapter 5

Supplementary figure 1

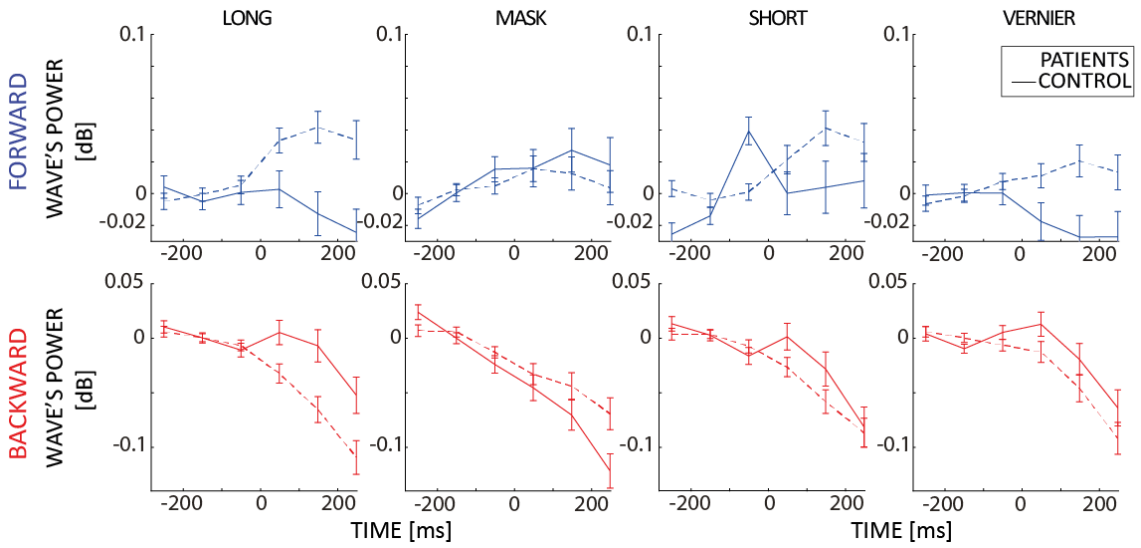

Figure S1 – Differences in alpha-band traveling waves between patients and control in the visual dataset task. Each row represents a different condition. As in the main figures, each subplot shows the mean values and standard errors for the patient (dashed lines) and the control groups (solid lines) before and after the onset of the stimulus at 0ms.

Supplementary Information Chapter 6

Further information is available at the publisher's website: https://www.sciencedirect.com/science/article/pii/S2589004223000949

Supplementary Tables

Table S1. Brain regions and coordinates for source space analysis. Related to STAR methods

x	y	z	Left hemisphere	x	y	z	Right hemisphere
-5	55	-5	LMedialOrbitofrontalCortex	5	50	-5	RMedialOrbitofrontalCortex
-30	50	-10	LMiddleOrbitofrontalCortex	30	55	-10	RMiddleOrbitofrontalCortex
-5	50	30	LSuperiorFrontalGyrusMedialPart	10	50	30	RSuperiorFrontalGyrusMedialPart
-20	50	-15	LSuperiorFrontalGyrusOrbitalPart	15	50	-15	RSuperiorFrontalGyrusOrbitalPart
-5	35	15	LAnteriorCingulateCortex	5	35	15	RAnteriorCingulateCortex
-35	35	35	LMiddleFrontalGyrus	35	35	35	RMiddleFrontalGyrus
-20	35	40	LSuperiorFrontalGyrus	20	30	45	RSuperiorFrontalGyrus
-5	35	-20	LGyrusRectus	5	35	-20	RGyrusRectus
-35	30	-10	LInferiorFrontalGyrusOrbitalPart	40	30	-10	RInferiorFrontalGyrusOrbitalPart
-45	30	15	LInferiorFrontalGyrusParsTriangularis	45	30	15	RInferiorFrontalGyrusParsTriangularis
-50	15	20	LInferiorFrontalOperculum	50	15	20	RInferiorFrontalOperculum
-5	15	-10	LOlfactoryGyrus	5	15	-10	ROlfactoryGyrus
-35	15	-35	LTemporalPoleMiddleTemporalGyrus	45	15	-30	RTemporalPoleMiddleTemporalGyrus
-40	15	-20	LTemporalPoleSuperiorTemporalGyrus	45	15	-15	RTemporalPoleSuperiorTemporalGyrus
-40	10	0	LInsula	40	10	0	RInsula
-5	5	60	LSupplementaryMotorArea	10	0	60	RSupplementaryMotorArea
-40	-5	50	LPrecentralGyrus	40	-10	50	RPrecentralGyrus
-50	-10	15	LRolandicOperculum	50	-5	15	RRolandicOperculum
-5	-15	40	LMiddleCingulateCortex	5	-10	40	RMiddleCingulateCortex
-20	-15	-20	LParahippocampalGyrus	20	-15	-20	RParahippocampalGyrus
-45	-20	10	LHeschlGyrus	45	-15	10	RHeschlGyrus
-25	-20	-10	LHippocampus	25	-20	-10	RHippocampus
-55	-20	5	LSuperiorTemporalGyrus	55	-20	5	RSuperiorTemporalGyrus
-5	-25	70	LParacentralLobule	5	-30	70	RParacentralLobule
-45	-25	50	LPostcentralGyrus	40	-25	55	RPostcentralGyrus
-50	-30	-25	LInferiorTemporalGyrus	55	-30	-20	RInferiorTemporalGyrus
-55	-35	30	LSupramarginalGyrus	55	-30	35	RSupramarginalGyrus
-55	-35	0	LMiddleTemporalGyrus	55	-35	0	RMiddleTemporalGyrus
-30	-40	-20	LFusiformGyrus	35	-40	-20	RFusiformGyrus
-5	-45	25	LPosteriorCingulateCortex	5	-45	20	RPosteriorCingulateCortex
-45	-45	45	LInferiorParietalLobule	45	-45	50	RInferiorParietalLobule
-10	-55	50	LPrecuneus	10	-55	45	RPrecuneus
-25	-60	60	LSuperiorParietalLobule	25	-60	60	RSuperiorParietalLobule
-45	-65	40	LAngularGyrus	40	-60	40	RAngularGyrus
-15	-70	-5	LLingualGyrus	15	-65	-5	RLingualGyrus
-10	-80	10	LCalcarineSulcus	15	-75	10	RCalcarineSulcus
-5	-80	25	LCuneus	15	-80	30	RCuneus
-35	-80	-10	LInferiorOccipitalGyrus	35	-80	-10	RInferiorOccipitalGyrus
-30	-80	15	LMiddleOccipitalGyrus	35	-85	20	RMiddleOccipitalGyrus
-20	-85	30	LSuperiorOccipitalGyrus	20	-80	30	RSuperiorOccipitalGyrus

Table S2. Adjusted R^2 of in-sample principal component regression for younger adults using the EEG features showing a significant Spearman correlation to the cognitive variables. Related to STAR methods

Abbreviations: A = Cvlt attention span, B = Cvlt delayed memory, C = Pts-2 subtest 3, D = Rwt animal categories, E = Rwt s words, F = Tap alertness, G = Tap simon congruent, H = Tap simon incongruent, I = Tap working memory, J = Tmt-A, K = Tmt-B, L = Vocabulary test

	A	B	C	D	E	G	H	I	J	K	L	median
PC 1	0.09	0.05	-0.01	0.15	0.1	0.11	0.15	0.17	0.21	0.22	0.18	0.15
PC 1-2	0.09	0.11	0.17	0.26	0.1	0.11	0.14	0.18	0.2	0.23	0.19	0.17
PC 1-3	0.11	0.32		0.26	0.22	0.13	0.14	0.21	0.27	0.22	0.18	0.21
PC 1-4	0.14	0.32		0.25	0.24	0.12	0.14	0.21	0.35	0.25	0.18	0.22
PC 1-5	0.14	0.32		0.25	0.24	0.12	0.14	0.23	0.34	0.25	0.18	0.23
PC 1-6	0.13	0.32		0.25	0.24	0.13	0.14	0.23	0.36	0.25		0.24
PC 1-7	0.16	0.33		0.24	0.28	0.12		0.22	0.35	0.24		0.24
PC 1-8	0.15				0.28			0.22	0.35	0.24		0.24
PC 1-9	0.16							0.23	0.35	0.24		0.23
PC 1-10	0.17							0.25	0.36	0.23		0.24
PC 1-11	0.16							0.25	0.36	0.23		0.24
PC 1-12	0.15							0.24	0.35			0.24
PC 1-13	0.16							0.24	0.35			0.24
PC 1-14	0.16							0.23	0.35			0.23
PC 1-15	0.16							0.27	0.37			0.27
PC 1-16	0.15							0.29	0.36			0.29
PC 1-17	0.16							0.29	0.36			0.29
PC 1-18	0.16							0.29	0.36			0.29
PC 1-19	0.16								0.36			0.26

Table S3. Adjusted R^2 of in-sample principal component regression for older adults using the EEG features showing a significant Spearman correlation to the cognitive variables. Related to STAR methods

Abbreviations: A = Cvlt attention span, B = Cvlt delayed memory, C = Pts-2 subtest 3, D = Rwt animal categories, E = Rwt s words, F = Tap alertness, G = Tap simon congruent, H = Tap simon incongruent, I = Tap working memory, J = Tmt-A, K = Tmt-B, L = Vocabulary test

	A	B	C	D	E	F	H	I	L	median
PC 1	0.15	0.21	0.24	0.37	0.23	0.26	0.41	0.47	0.41	0.26
PC 1-2	0.14	0.22	0.33	0.36	0.22	0.25	0.45	0.46	0.46	0.33
PC 1-3	0.13	0.2	0.33	0.38	0.23		0.47	0.45	0.46	0.35
PC 1-4			0.32	0.37	0.22		0.46	0.44	0.45	0.41
PC 1-5			0.33	0.39	0.22		0.46	0.43		0.39
PC 1-6			0.35					0.42		0.39
PC 1-7			0.35					0.44		0.39
PC 1-8			0.35							0.35
PC 1-9			0.35							0.35
PC 1-10			0.34							0.34
PC 1-11			0.33							0.33
PC 1-12			0.33							0.33
PC 1-13			0.32							0.32
PC 1-14			0.31							0.31
PC 1-15			0.35							0.35
PC 1-16			0.34							0.34
PC 1-17			0.33							0.33
PC 1-18			0.31							0.31

PC 1-19			0.34							0.34
PC 1-20			0.33							0.33

Table S4. Adjusted $\boldsymbol{R^2}$of in-sample principal component regression for younger adults using the EEG features showing a significant distance correlation to the cognitive variables. Related to STAR methods

Abbreviations: A = Cvlt attention span, B = Cvlt delayed memory, C = Pts-2 subtest 3, D = Rwt animal categories, E = Rwt s words, F = Tap alertness, G = Tap simon congruent, H = Tap simon incongruent, I = Tap working memory, J = Tmt-A, K = Tmt-B, L = Vocabulary test

	A	**B**	**C**	**D**	**E**	**F**	**G**	**H**	**I**	**J**	**K**	**L**	**median**
PC 1	0.11	0.17	0.11	0.11	0.11	0.07	0.12	0.09	0.14	0.18	0.2	0.14	0.12
PC 1-2	0.13	0.17	0.11	0.22	0.11	0.09	0.11	0.14	0.14	0.17	0.21	0.14	0.14
PC 1-3	0.15	0.18	0.11	0.22	0.13	0.09	0.11	0.14	0.15	0.17	0.21	0.13	0.14
PC 1-4	0.15	0.2		0.22	0.14		0.13	0.14	0.18	0.18	0.26	0.13	0.16
PC 1-5	0.15			0.21	0.14		0.14	0.13	0.18	0.22	0.25	0.14	0.15
PC 1-6	0.14			0.21	0.13		0.13	0.2	0.2	0.23	0.25		0.2
PC 1-7	0.14			0.22	0.12		0.17	0.19	0.19	0.26	0.25		0.19
PC 1-8	0.13			0.21	0.16		0.17	0.19	0.19	0.25	0.25		0.19
PC 1-9	0.13			0.21	0.16		0.21	0.18	0.19	0.25	0.26		0.2
PC 1-10	0.12			0.2			0.21	0.18		0.26	0.25		0.2
PC 1-11	0.13			0.2			0.27	0.17		0.26	0.25		0.22
PC 1-12	0.14						0.26	0.17		0.26	0.25		0.25
PC 1-13							0.29	0.16		0.26	0.25		0.25
PC 1-14							0.29	0.16		0.25	0.26		0.26
PC 1-15							0.28	0.16		0.24			0.24
PC 1-16							0.28			0.24			0.26
PC 1-17							0.29			0.24			0.27
PC 1-18							0.3			0.24			0.27

Table S5. Adjusted $\boldsymbol{R^2}$of in-sample principal component regression for older adults using the EEG features showing a significant distance correlation to the cognitive variables. Related to STAR methods

Abbreviations: A = Cvlt attention span, B = Cvlt delayed memory, C = Pts-2 subtest 3, D = Rwt animal categories, E = Rwt s words, F = Tap alertness, G = Tap simon congruent, H = Tap simon incongruent, I = Tap working memory, J = Tmt-A, K = Tmt-B, L = Vocabulary test

	A	**B**	**C**	**D**	**E**	**F**	**G**	**H**	**I**	**K**	**L**	**median**
PC 1	0.18	0.14	0.24	0.31	0.24	0.2	0.08	0.13	0.13	0.22	0.13	0.18
PC 1-2	0.27	0.23	0.34	0.4	0.26	0.2	0.07	0.15	0.15	0.21	0.29	0.23
PC 1-3	0.26	0.28	0.37	0.44	0.25	0.19			0.22		0.34	0.27
PC 1-4	0.25	0.27	0.36	0.43	0.23				0.34		0.42	0.34
PC 1-5		0.29	0.38	0.47	0.23				0.32		0.44	0.35
PC 1-6			0.37		0.23						0.43	0.37
PC 1-7			0.36								0.46	0.41
PC 1-8			0.35								0.45	0.4
PC 1-9			0.34								0.45	0.39
PC 1-10			0.33								0.44	0.38
PC 1-11			0.34								0.43	0.39
PC 1-12			0.34								0.42	0.38
PC 1-13			0.33									0.33

Supplementary Figures

Figure S1. Result of the correlation analysis in older adults. Related to Figure 1.

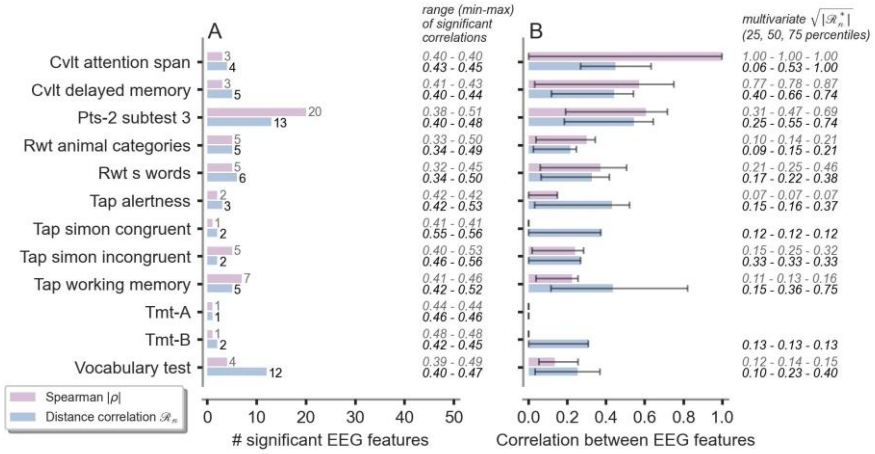

A) EEG features with significant correlations to cognitive variables. On the right side of the panel, we indicate the range (min-max) of the magnitudes of the significant correlations of the EEG features with cognitive variables (see ***Quantification and statistical analysis***). B) Median (confidence interval: 25th and 75th percentiles) Spearman and distance correlations between the EEG features showing a significant correlation with the same cognitive variable. On the right side of the panel, we indicate the 25th, 50th, and 75th percentiles of the multivariate distance correlations ($\left|\sqrt{\mathcal{R}_n^*}\right|$; ranging from 0 to 1) between the EEG features showing a significant correlation with the same cognitive variables (see ***Method details***).

Figure S2. Multivariate distance correlations between the 108 EEG features showing significant group differences between older and younger adults. Related to Figure 6.

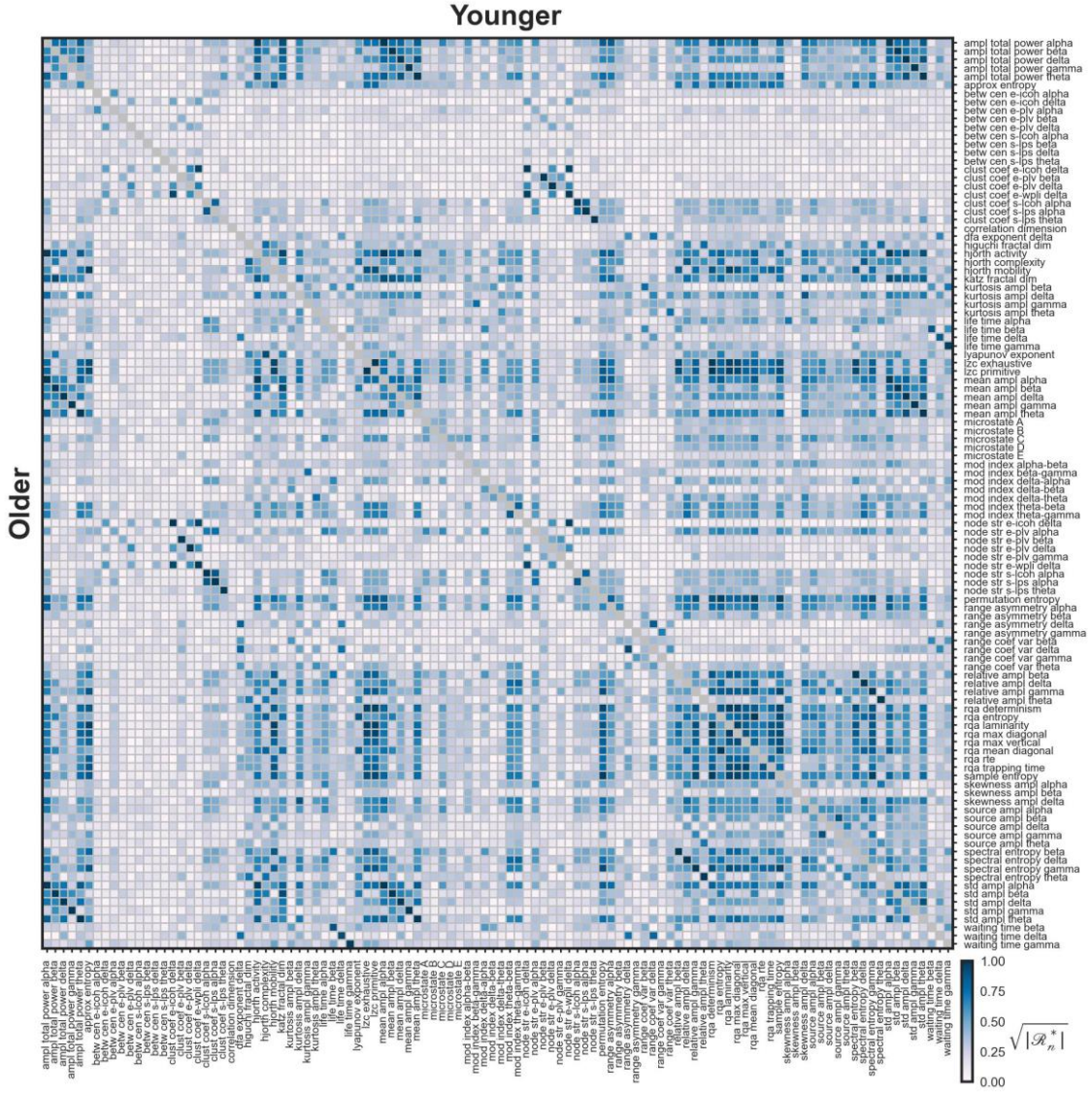

Figure S3. Multivariate distance correlations between EEG features obtained using average/CSD reference and zero reference for younger adults. Related to Figure 6.

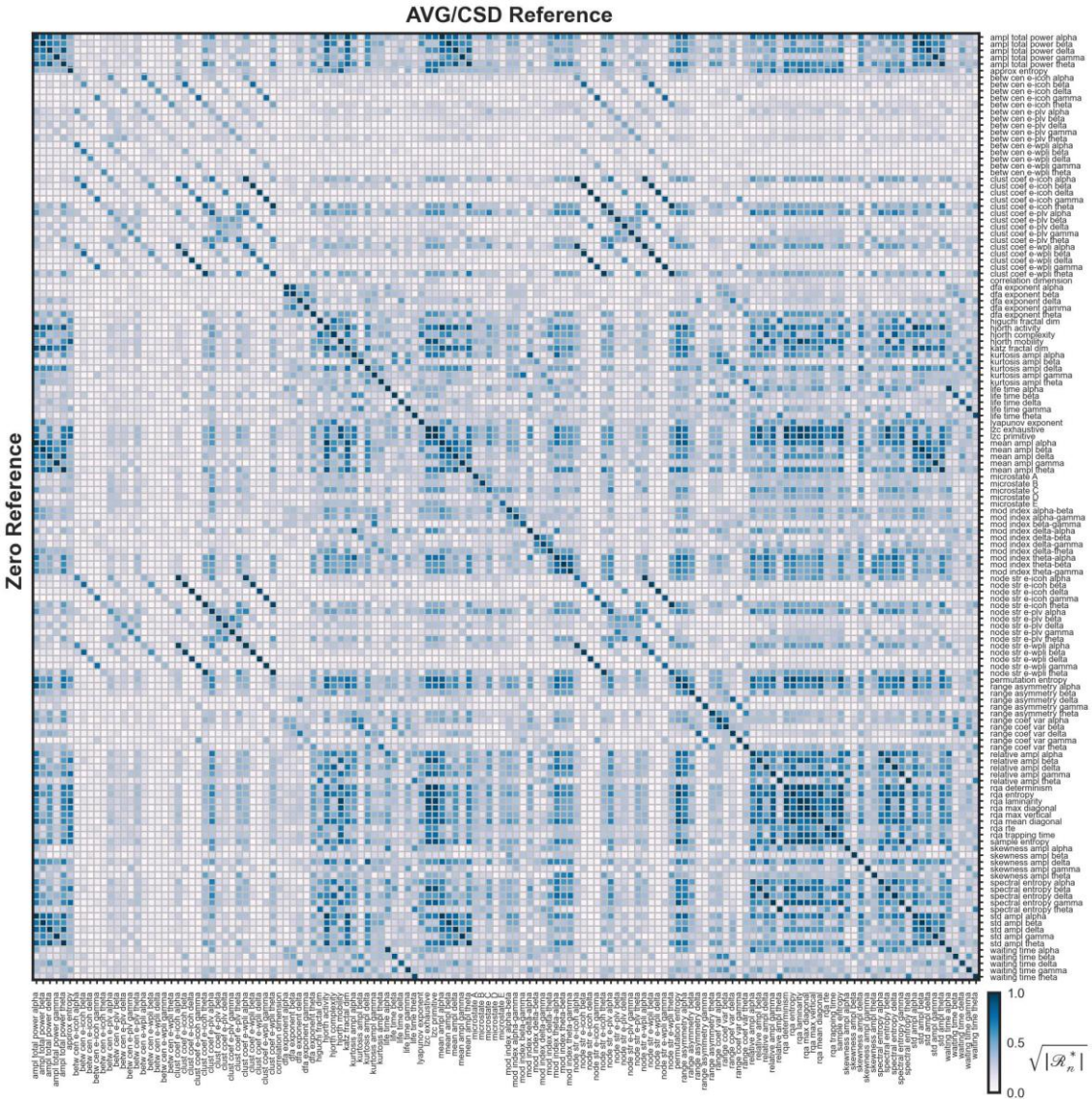

Figure S4. Multivariate distance correlations between EEG features obtained using average/CSD reference and zero reference for older adults. Related to Figure 6.

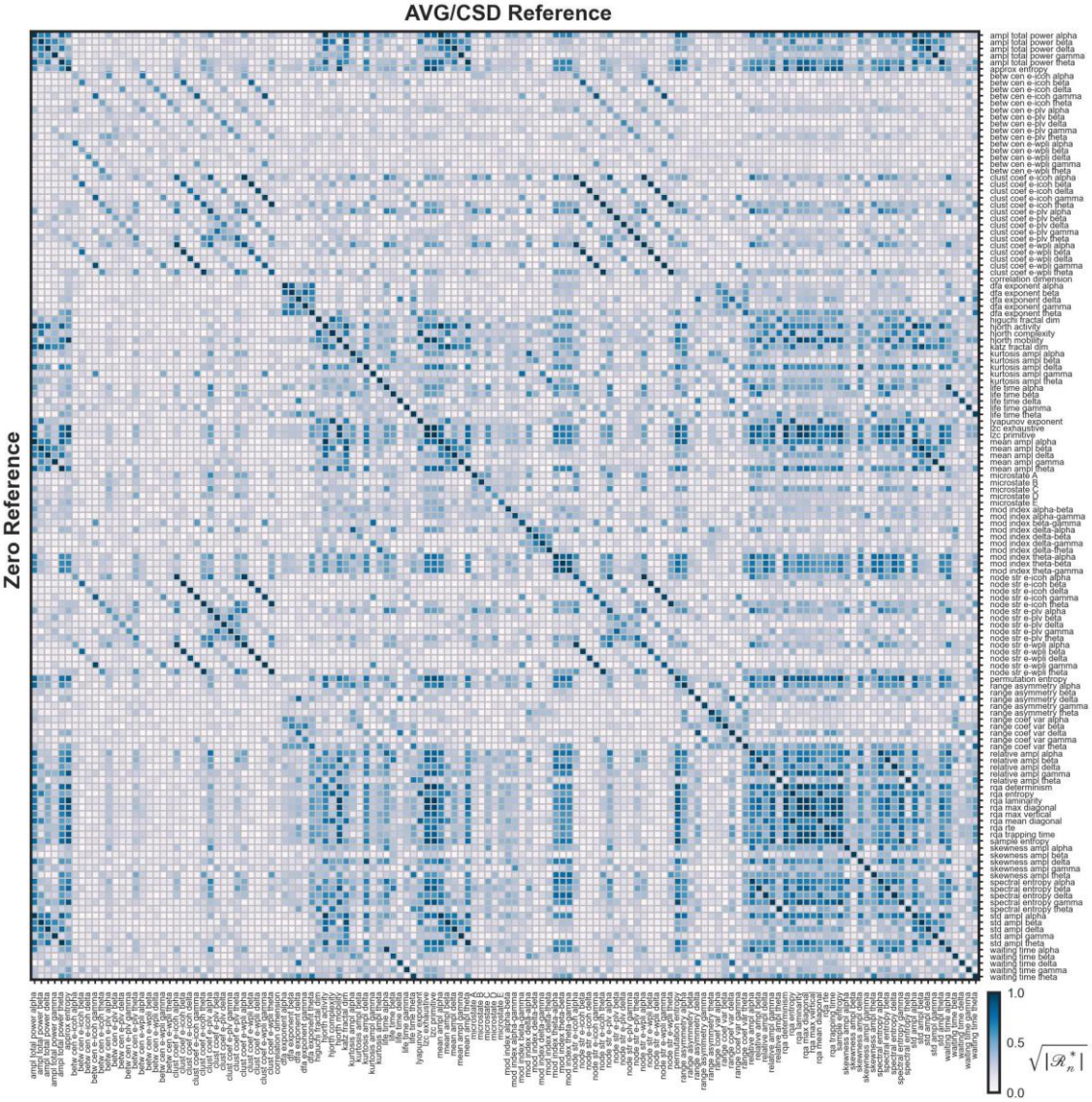

Figure S5. Principal components obtained from the EEG features showing a significant Spearman correlation to *Cvlt attention span*, *Cvlt delayed memory*, *Rwt animal categories*, and *Rwt s words* for younger adults. Related to STAR methods.

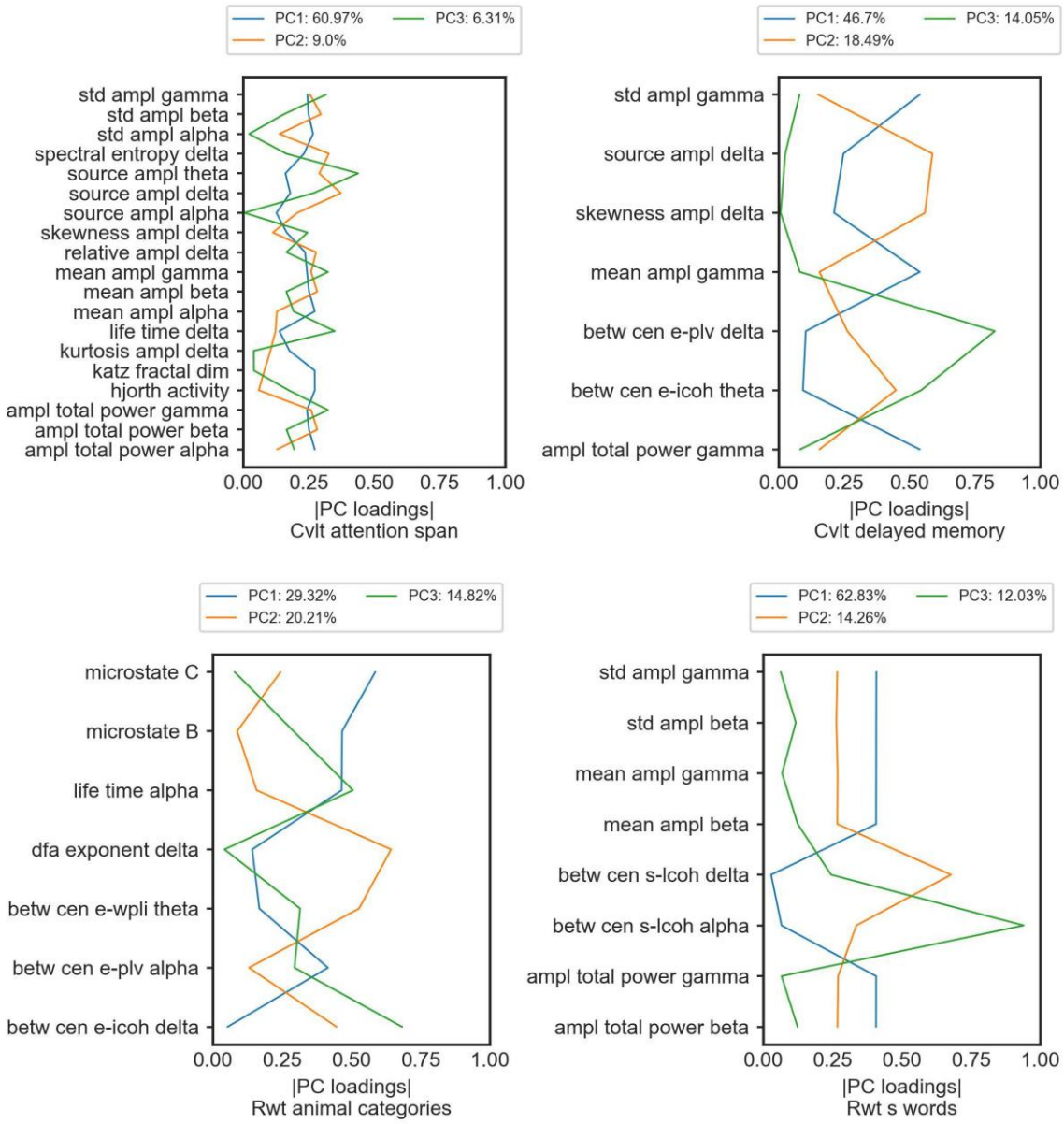

Figure S6. Principal components obtained from the EEG features showing a significant Spearman correlation to *Tap simon congruent*, *Tap simon incongruent*, *Tap working memory*, and *Tmt-A*, for younger adults. Related to STAR methods.

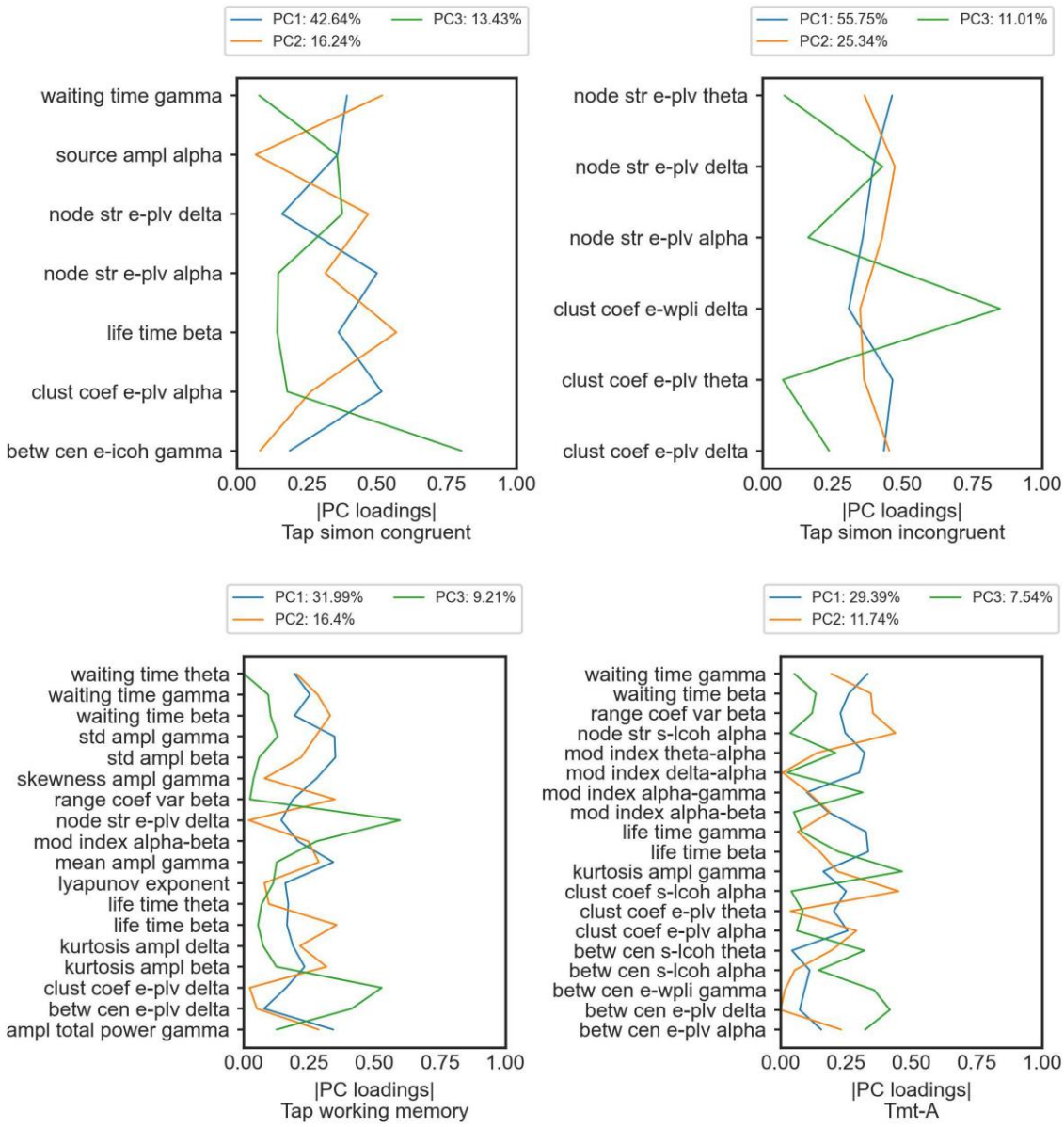

Figure S7. Principal components obtained from the EEG features showing a significant Spearman correlation to *Tmt-B*, and *Vocabulary test* for younger adults. Related to STAR methods.

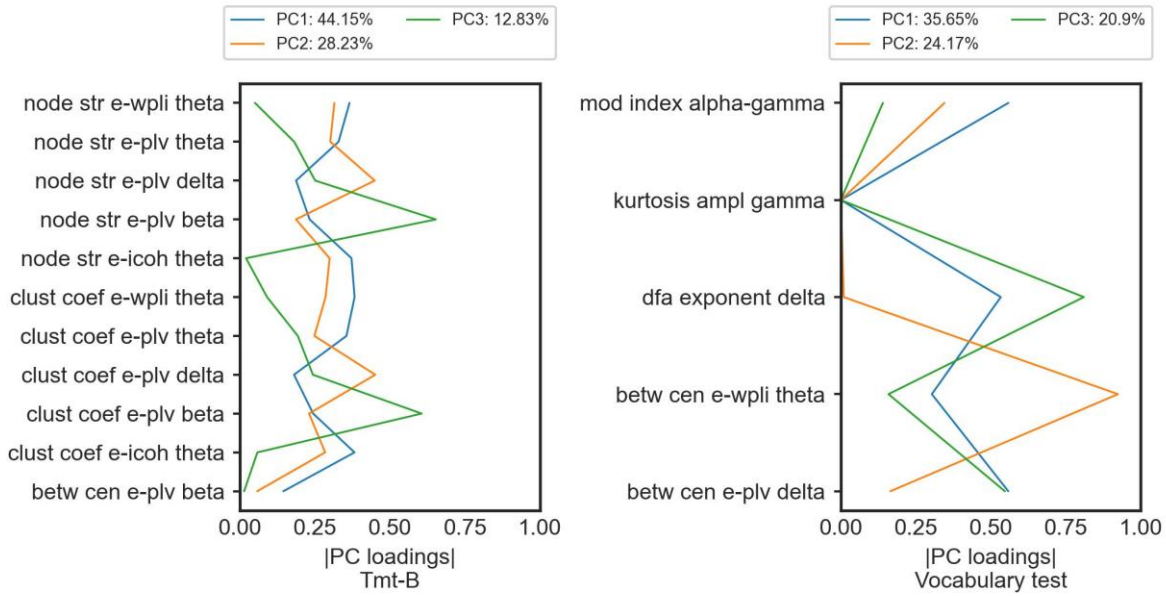

Figure S8. Principal components obtained from the EEG features showing a significant distance correlation to *Cvlt attention span*, *Cvlt delayed memory*, *Pts-2 subtest 3*, and *Rwt animal categories*, for younger adults. Related to STAR methods.

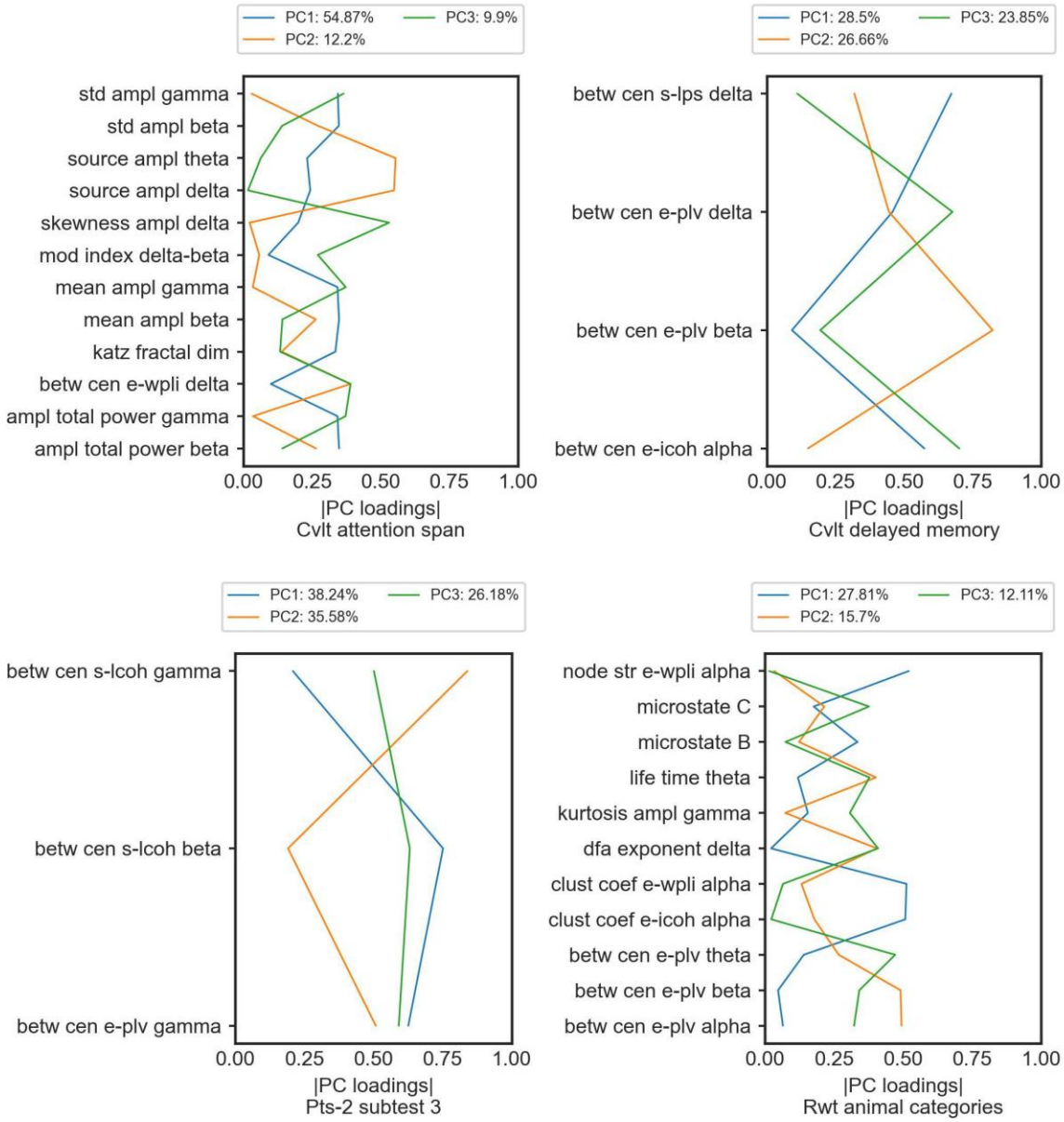

Figure S9. Principal components obtained from the EEG features showing a significant distance correlation to *Rwt s words*, *Tap alertness*, *Tap simon congruent*, and *Tap simon incongruent* for younger adults. Related to STAR methods.

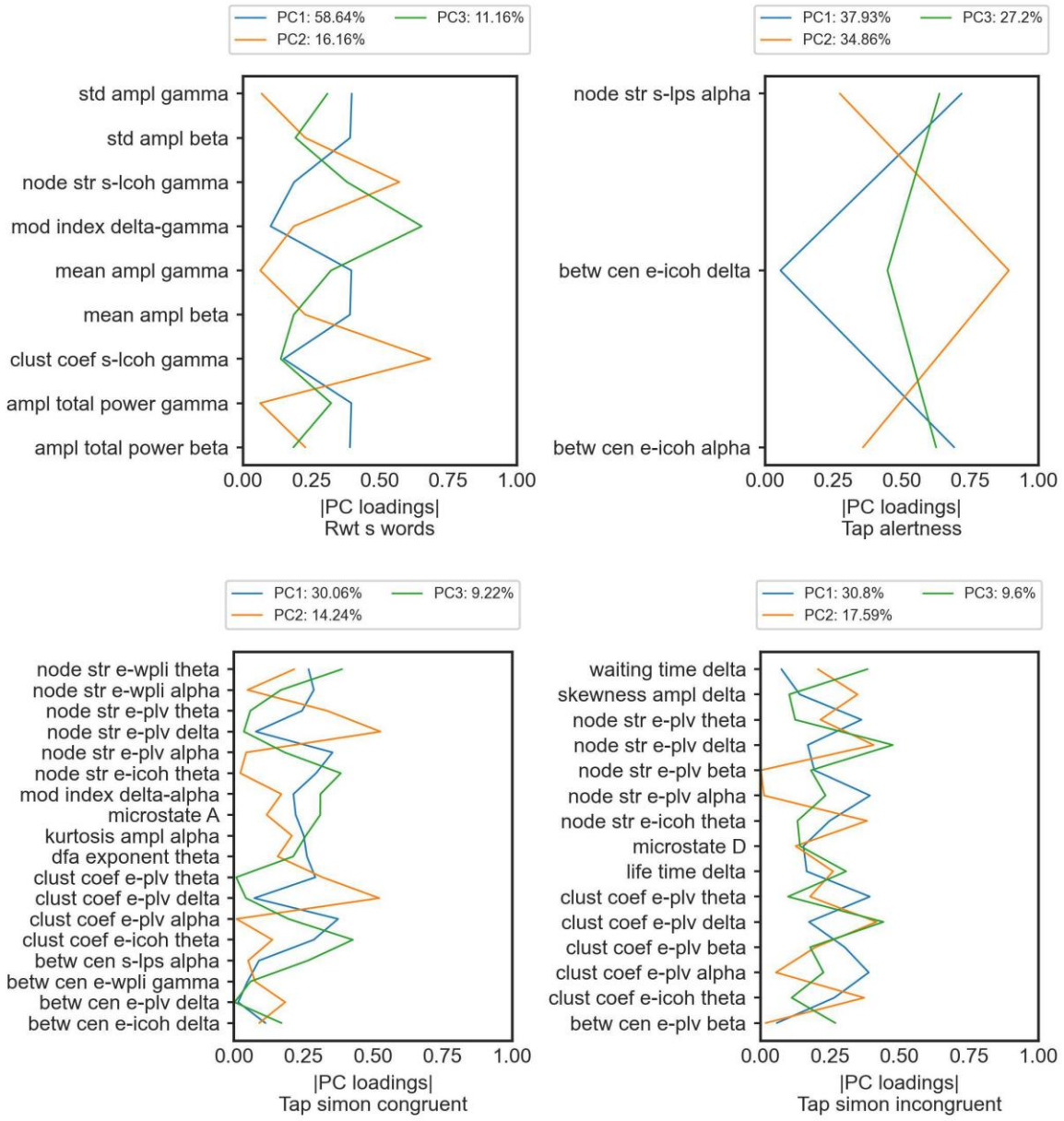

Figure S10. Principal components obtained from the EEG features showing a significant distance correlation to *Tap working memory*, *Tmt-A*, *Tmt-B*, and *Vocabulary test*, for younger adults. Related to STAR methods.

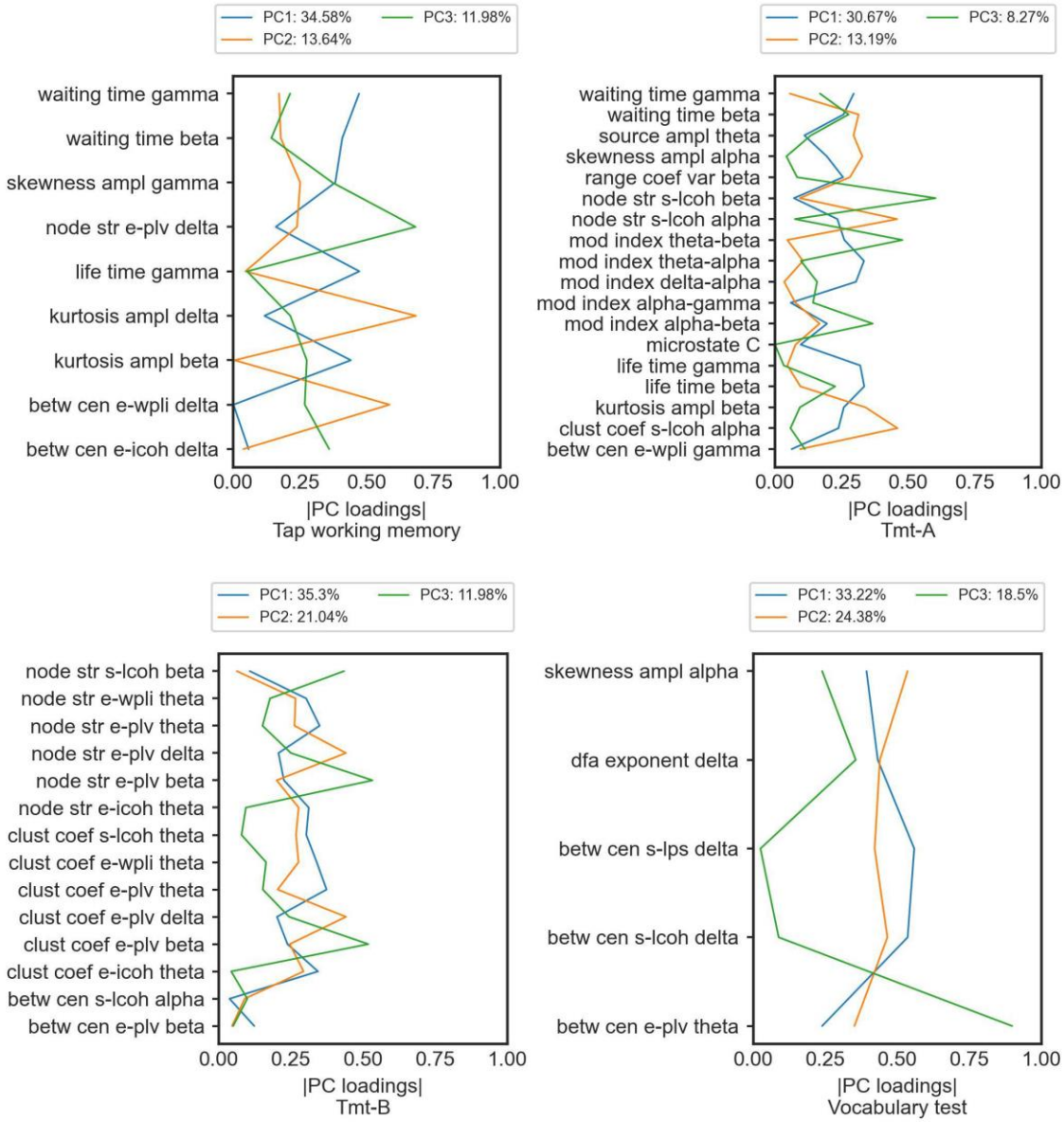

Figure S11. Principal components obtained from the EEG features showing a significant difference between younger and older adults (using the variables from older participants). Related to Figure 6.

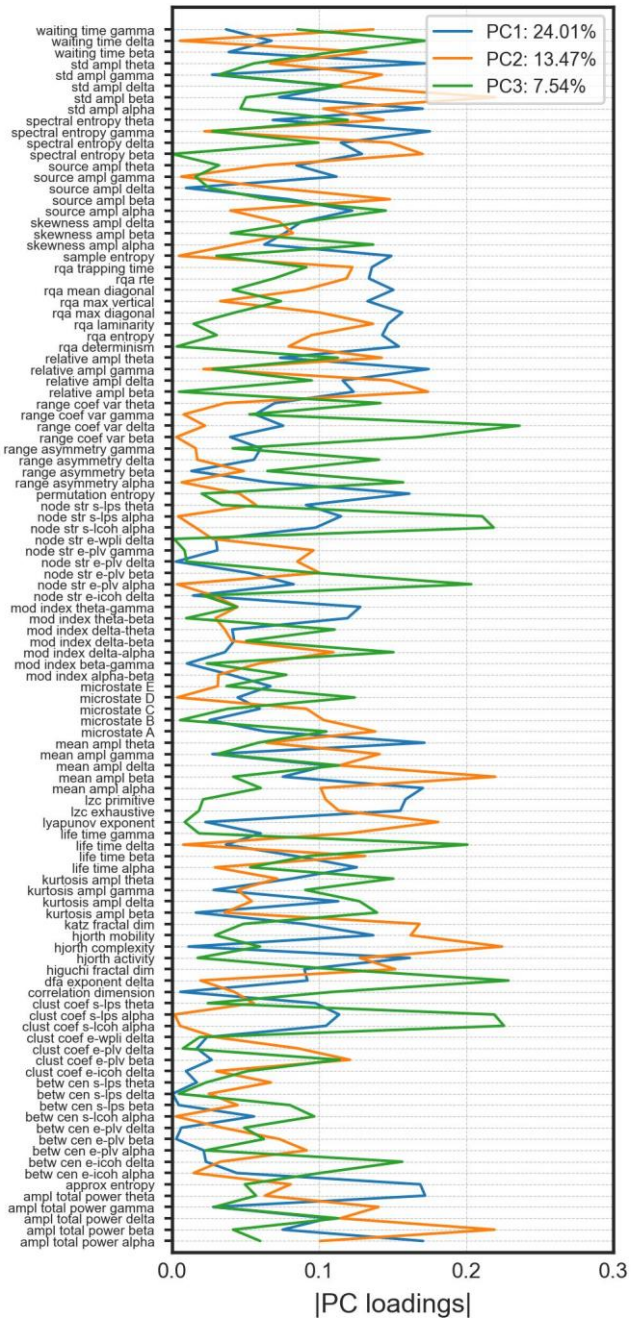

Bibliography

Abel, J. H., Badgeley, M. A., Meschede-Krasa, B., Schamberg, G., Garwood, I. C., Lecamwasam, K., Chakravarty, S., Zhou, D. W., Keating, M., Purdon, P. L., & Brown, E. N. (2021). Machine learning of EEG spectra classifies unconsciousness during GABAergic anesthesia. *PLOS ONE*, *16*(5), e0246165. https://doi.org/10.1371/journal.pone.0246165

Adams, R. A., Stephan, K. E., Brown, H. R., Frith, C. D., & Friston, K. J. (2013). The Computational Anatomy of Psychosis. *Frontiers in Psychiatry*, *4*. https://doi.org/10.3389/fpsyt.2013.00047

Al Zoubi, O., Ki Wong, C., Kuplicki, R. T., Yeh, H., Mayeli, A., Refai, H., Paulus, M., & Bodurka, J. (2018). Predicting Age From Brain EEG Signals—A Machine Learning Approach. *Frontiers in Aging Neuroscience*, *10*, 184. https://doi.org/10.3389/fnagi.2018.00184

Alamia, A., Timmermann, C., Nutt, D. J., VanRullen, R., & Carhart-Harris, R. L. (2020). DMT alters cortical travelling waves. *eLife*, *9*, e59784. https://doi.org/10.7554/eLife.59784

Alamia, A., & VanRullen, R. (2019). Alpha oscillations and traveling waves: Signatures of predictive coding? *PLOS Biology*, *17*(10), e3000487. https://doi.org/10.1371/journal.pbio.3000487

Allen, A. J., Griss, M. E., Folley, B. S., Hawkins, K. A., & Pearlson, G. D. (2009). Endophenotypes in schizophrenia: A selective review. *Schizophrenia Research*, *109*(1–3), 24–37. https://doi.org/10.1016/j.schres.2009.01.016

Arnal, L. H., & Giraud, A.-L. (2012). Cortical oscillations and sensory predictions. *Trends in Cognitive Sciences*, *16*(7), 390–398. https://doi.org/10.1016/j.tics.2012.05.003

Baethge, C., Baldessarini, R. J., Freudenthal, K., Streeruwitz, A., Bauer, M., & Bschor, T. (2005). Hallucinations in bipolar disorder: Characteristics and comparison to unipolar depression and schizophrenia. *Bipolar Disorders*, *7*(2), 136–145. https://doi.org/10.1111/j.1399-5618.2004.00175.x

Barch, D. M., & Ceaser, A. (2012). Cognition in schizophrenia: Core psychological and neural mechanisms. *Trends in Cognitive Sciences*, *16*(1), 27–34. https://doi.org/10.1016/j.tics.2011.11.015

Bastos, A. M., Vezoli, J., Bosman, C. A., Schoffelen, J.-M., Oostenveld, R., Dowdall, J. R., De Weerd, P., Kennedy, H., & Fries, P. (2015). Visual Areas Exert Feedforward and Feedback Influences through Distinct Frequency Channels. *Neuron*, *85*(2), 390–401. https://doi.org/10.1016/j.neuron.2014.12.018

Benson, P. J., Beedie, S. A., Shephard, E., Giegling, I., Rujescu, D., & St. Clair, D. (2012). Simple Viewing Tests Can Detect Eye Movement Abnormalities That Distinguish Schizophrenia Cases from Controls with Exceptional Accuracy. *Biological Psychiatry*, *72*(9), 716–724. https://doi.org/10.1016/j.biopsych.2012.04.019

Bi, H., Abrham, Y., Butler, P. D., Hu, B., & Keane, B. P. (2023). When do contrast sensitivity deficits (or enhancements) depend on spatial frequency? Two ways to avoid spurious interactions. *European Journal of Neuroscience*, *57*(2), 351–359. https://doi.org/10.1111/ejn.15887

Bosten, J. M., Goodbourn, P. T., Bargary, G., Verhallen, R. J., Lawrance-Owen, A. J., Hogg, R. E., & Mollon, J. D. (2017). An exploratory factor analysis of visual performance in a large population. *Vision Research*, *141*, 303–316. https://doi.org/10.1016/j.visres.2017.02.005

Braff, D. L. (1993). Information Processing and Attention Dysfunctions in Schizophrenia. *Schizophrenia Bulletin*, *19*(2), 233–259. https://doi.org/10.1093/schbul/19.2.233

Braff, D. L., Freedman, R., Schork, N. J., & Gottesman, I. I. (2006). Deconstructing Schizophrenia: An Overview of the Use of Endophenotypes in Order to Understand a Complex Disorder. *Schizophrenia Bulletin*, *33*(1), 21–32. https://doi.org/10.1093/schbul/sbl049

Braff, D. L., Light, G. A., & Swerdlow, N. R. (2007). Prepulse Inhibition and P50 Suppression Are Both Deficient but not Correlated in Schizophrenia Patients. *Biological Psychiatry*, *61*(10), 1204–1207. https://doi.org/10.1016/j.biopsych.2006.08.015

Brand, A., Kopmann, S., Marbach, S., Heinze, M., & Herzog, M. H. (2005). Intact and deficient feature fusion in schizophrenia. *European Archives of Psychiatry and Clinical Neuroscience*, *255*(6), 413–418. https://doi.org/10.1007/s00406-005-0590-x

Burmeister, M., McInnis, M. G., & Zöllner, S. (2008). Psychiatric genetics: Progress amid controversy. *Nature Reviews Genetics*, *9*(7), 527–540. https://doi.org/10.1038/nrg2381

Cappe, C., Clarke, A., Mohr, C., & Herzog, M. H. (2014). Is there a common factor for vision? *Journal of Vision*, *14*(8), 4–4. https://doi.org/10.1167/14.8.4

Chen, L., Cichy, R. M., & Kaiser, D. (2023). Alpha-frequency feedback to early visual cortex orchestrates coherent naturalistic vision. *Science Advances*, *9*(45), eadi2321. https://doi.org/10.1126/sciadv.adi2321

Chen, Y., Norton, D., & Ongur, D. (2008). Altered Center-Surround Motion Inhibition in Schizophrenia. *Biological Psychiatry*, *64*(1), 74–77. https://doi.org/10.1016/j.biopsych.2007.11.017

Chkonia, E., Roinishvili, M., Herzog, M. H., & Brand, A. (2010). First-order relatives of schizophrenic patients are not impaired in the Continuous Performance Test. *Journal of Clinical and Experimental Neuropsychology*, *32*(5), 481–486. https://doi.org/10.1080/13803390903201777

Chkonia, E., Roinishvili, M., Makhatadze, N., Tsverava, L., Stroux, A., Neumann, K., Herzog, M. H., & Brand, A. (2010). The Shine-Through Masking Paradigm Is a Potential Endophenotype of Schizophrenia. *PLoS ONE*, *5*(12), e14268. https://doi.org/10.1371/journal.pone.0014268

Cicchetti, D. V. (1994). Guidelines, criteria, and rules of thumb for evaluating normed and standardized assessment instruments in psychology. *Psychological Assessment*, *6*(4), 284–290. https://doi.org/10.1037/1040-3590.6.4.284

Clementz, B. A., Sweeney, J. A., Hamm, J. P., Ivleva, E. I., Ethridge, L. E., Pearlson, G. D., Keshavan, M. S., & Tamminga, C. A. (2016). Identification of Distinct Psychosis Biotypes Using Brain-Based Biomarkers. *American Journal of Psychiatry*, *173*(4), 373–384. https://doi.org/10.1176/appi.ajp.2015.14091200

Cohen, J. (1988). *Statistical power analysis for the behavioral sciences* (2nd ed). L. Erlbaum Associates.

Colombo, M., & Seriès, P. (2012). Bayes in the Brain—On Bayesian Modelling in Neuroscience. *The British Journal for the Philosophy of Science*, *63*(3), 697–723. https://doi.org/10.1093/bjps/axr043

Compton, R. J., Gearinger, D., & Wild, H. (2019). The wandering mind oscillates: EEG alpha power is enhanced during moments of mind-wandering. *Cognitive, Affective, & Behavioral Neuroscience*, *19*(5), 1184–1191. https://doi.org/10.3758/s13415-019-00745-9

Corlett, P. R., Frith, C. D., & Fletcher, P. C. (2009). From drugs to deprivation: A Bayesian framework for understanding models of psychosis. *Psychopharmacology*, *206*(4), 515–530. https://doi.org/10.1007/s00213-009-1561-0

Corlett, P. R., Horga, G., Fletcher, P. C., Alderson-Day, B., Schmack, K., & Powers, A. R. (2019). Hallucinations and Strong Priors. *Trends in Cognitive Sciences*, *23*(2), 114–127. https://doi.org/10.1016/j.tics.2018.12.001

Cortes-Briones, J. A., Tapia-Rivas, N. I., D'Souza, D. C., & Estevez, P. A. (2022). Going deep into schizophrenia with artificial intelligence. *Schizophrenia Research*, *245*, 122–140. https://doi.org/10.1016/j.schres.2021.05.018

Cretenoud, A. F., Karimpur, H., Grzeczkowski, L., Francis, G., Hamburger, K., & Herzog, M. H. (2019). Factors underlying visual illusions are illusion-specific but not feature-specific. *Journal of Vision*, *19*(14), 12. https://doi.org/10.1167/19.14.12

Cullen, A. E., Holmes, S., Pollak, T. A., Blackman, G., Joyce, D. W., Kempton, M. J., Murray, R. M., McGuire, P., & Mondelli, V. (2019). Associations Between Non-neurological Autoimmune Disorders and Psychosis: A Meta-analysis. *Biological Psychiatry*, *85*(1), 35–48. https://doi.org/10.1016/j.biopsych.2018.06.016

da Cruz, J. R., Favrod, O., Roinishvili, M., Chkonia, E., Brand, A., Mohr, C., Figueiredo, P., & Herzog, M. H. (2020). EEG microstates are a candidate endophenotype for schizophrenia. *Nature Communications*, *11*(1), 3089. https://doi.org/10.1038/s41467-020-16914-1

Diamond, A., Silverstein, S. M., & Keane, B. P. (2022). Visual system assessment for predicting a transition to psychosis. *Translational Psychiatry*, *12*(1), 351. https://doi.org/10.1038/s41398-022-02111-9

Dickinson, D., Goldberg, T. E., Gold, J. M., Elvevag, B., & Weinberger, D. R. (2011). Cognitive Factor Structure and Invariance in People With Schizophrenia, Their Unaffected Siblings, and Controls. *Schizophrenia Bulletin*, *37*(6), 1157–1167. https://doi.org/10.1093/schbul/sbq018

Eack, S. M., & Newhill, C. E. (2007). Psychiatric Symptoms and Quality of Life in Schizophrenia: A Meta-Analysis. *Schizophrenia Bulletin*, *33*(5), 1225–1237. https://doi.org/10.1093/schbul/sbl071

Eisenberg, I. W., Bissett, P. G., Zeynep Enkavi, A., Li, J., MacKinnon, D. P., Marsch, L. A., & Poldrack, R. A. (2019). Uncovering the structure of self-regulation through data-driven ontology discovery. *Nature Communications*, *10*(1), 2319. https://doi.org/10.1038/s41467-019-10301-1

El Haj, M., Roche, J., Jardri, R., Kapogiannis, D., Gallouj, K., & Antoine, P. (2017). Clinical and neurocognitive aspects of hallucinations in Alzheimer's disease. *Neuroscience & Biobehavioral Reviews*, *83*, 713–720. https://doi.org/10.1016/j.neubiorev.2017.02.021

Fogelson, N., Litvak, V., Peled, A., Fernandez-del-Olmo, M., & Friston, K. (2014). The functional anatomy of schizophrenia: A dynamic causal modeling study of predictive coding. *Schizophrenia Research*, *158*(1–3), 204–212. https://doi.org/10.1016/j.schres.2014.06.011

Friston, K. J. (2005). Hallucinations and perceptual inference. *Behavioral and Brain Sciences*, *28*(6), 764–766. https://doi.org/10.1017/S0140525X05290131

Friston, K. J. (2019). Waves of prediction. *PLOS Biology*, *17*(10), e3000426. https://doi.org/10.1371/journal.pbio.3000426

Garobbio, S., Kunchulia, M., & Herzog, M. H. (2024). Weak correlations between visual abilities in healthy older adults, despite long-term performance stability. *Vision Research*, *215*, 108355. https://doi.org/10.1016/j.visres.2023.108355

Garobbio, S., Pilz, K. S., Kunchulia, M., & Herzog, M. H. (2022). No Common Factor Underlying Decline of Visual Abilities in Mild Cognitive Impairment. *Experimental Aging Research*, 1–18. https://doi.org/10.1080/0361073X.2022.2094660

Gignac, G. E., & Szodorai, E. T. (2016). Effect size guidelines for individual differences researchers. *Personality and Individual Differences*, *102*, 74–78. https://doi.org/10.1016/j.paid.2016.06.069

Giuliani, L., Koutsouleris, N., Giordano, G. M., Koenig, T., Mucci, A., Perrottelli, A., Reuf, A., Altamura, M., Bellomo, A., Brugnoli, R., Corrivetti, G., Di Lorenzo, G., Girardi, P., Monteleone, P., Niolu, C., Galderisi, S., Maj, M., & Italian Network for Research on Psychoses. (2023). A multivariate approach to investigate the associations of electrophysiological indices with schizophrenia clinical and functional outcome. *European Psychiatry*, *66*(1), e46. https://doi.org/10.1192/j.eurpsy.2023.2410

Goodbourn, P. T., Bosten, J. M., Hogg, R. E., Bargary, G., Lawrance-Owen, A. J., & Mollon, J. D. (2012). Do different 'magnocellular tasks' probe the same neural substrate? *Proceedings of the Royal Society B: Biological Sciences*, *279*(1745), 4263–4271. https://doi.org/10.1098/rspb.2012.1430

Gottesman, I. I., & Gould, T. D. (2003). The Endophenotype Concept in Psychiatry: Etymology and Strategic Intentions. *American Journal of Psychiatry*, *160*(4), 636–645. https://doi.org/10.1176/appi.ajp.160.4.636

Green, M. F., Horan, W. P., & Lee, J. (2015). Social cognition in schizophrenia. *Nature Reviews Neuroscience*, *16*(10), 620–631. https://doi.org/10.1038/nrn4005

Greene, A. S., Shen, X., Noble, S., Horien, C., Hahn, C. A., Arora, J., Tokoglu, F., Spann, M. N., Carrión, C. I., Barron, D. S., Sanacora, G., Srihari, V. H., Woods, S. W., Scheinost, D., & Constable, R. T. (2022). Brain–phenotype models fail for individuals who defy sample stereotypes. *Nature*, *609*(7925), 109–118. https://doi.org/10.1038/s41586-022-05118-w

Grzeczkowski, L., Roinishvili, M., Chkonia, E., Brand, A., Mast, F. W., Herzog, M. H., & Shaqiri, A. (2018). Is the perception of illusions abnormal in schizophrenia? *Psychiatry Research*, *270*, 929–939. https://doi.org/10.1016/j.psychres.2018.10.063

Gudmundsson, S., Runarsson, T. P., Sigurdsson, S., Eiriksdottir, G., & Johnsen, K. (2007). Reliability of quantitative EEG features. *Clinical Neurophysiology*, *118*(10), 2162–2171. https://doi.org/10.1016/j.clinph.2007.06.018

Haartsen, R., van der Velde, B., Jones, E. J. H., Johnson, M. H., & Kemner, C. (2020). Using multiple short epochs optimises the stability of infant EEG connectivity parameters. *Scientific Reports*, *10*(1), 12703. https://doi.org/10.1038/s41598-020-68981-5

Herzog, M. H., Roinishvili, M., Chkonia, E., & Brand, A. (2013). Schizophrenia and visual backward masking: A general deficit of target enhancement. *Frontiers in Psychology*, *4*. https://doi.org/10.3389/fpsyg.2013.00254

Herzog, M. H., Sayim, B., Chicherov, V., & Manassi, M. (2015). Crowding, grouping, and object recognition: A matter of appearance. *Journal of Vision*, *15*(6), 5–5. https://doi.org/10.1167/15.6.5

Herzog, M. H., Thunell, E., & Ögmen, H. (2016). Putting low-level vision into global context: Why vision cannot be reduced to basic circuits. *Vision Research*, *126*, 9–18. https://doi.org/10.1016/j.visres.2015.09.009

Horváth, S., & Mirnics, K. (2014). Immune System Disturbances in Schizophrenia. *Biological Psychiatry*, *75*(4), 316–323. https://doi.org/10.1016/j.biopsych.2013.06.010

Howes, O. D., Bukala, B. R., & Beck, K. (2024). Schizophrenia: From neurochemistry to circuits, symptoms and treatments. *Nature Reviews Neurology*, *20*(1), 22–35. https://doi.org/10.1038/s41582-023-00904-0

Huang, Y., & Rao, R. P. N. (2011). Predictive coding. *WIREs Cognitive Science*, *2*(5), 580–593. https://doi.org/10.1002/wcs.142

Huys, Q. J. M., Maia, T. V., & Frank, M. J. (2016). Computational psychiatry as a bridge from neuroscience to clinical applications. *Nature Neuroscience*, *19*(3), 404–413. https://doi.org/10.1038/nn.4238

Imperatori, L. S., Cataldi, J., Betta, M., Ricciardi, E., Ince, R. A. A., Siclari, F., & Bernardi, G. (2021). Cross-participant prediction of vigilance stages through the combined use of wPLI and wSMI EEG functional connectivity metrics. *Sleep*, *44*(5), zsaa247. https://doi.org/10.1093/sleep/zsaa247

Javitt, D. C. (2009). When Doors of Perception Close: Bottom-up Models of Disrupted Cognition in Schizophrenia. *Annual Review of Clinical Psychology*, *5*(1), 249–275. https://doi.org/10.1146/annurev.clinpsy.032408.153502

Kahn, R. S., & Keefe, R. S. E. (2013). Schizophrenia Is a Cognitive Illness: Time for a Change in Focus. *JAMA Psychiatry*, *70*(10), 1107. https://doi.org/10.1001/jamapsychiatry.2013.155

Kaliuzhna, M., Stein, T., Rusch, T., Sekutowicz, M., Sterzer, P., & Seymour, K. J. (2019). No evidence for abnormal priors in early vision in schizophrenia. *Schizophrenia Research*, *210*, 245–254. https://doi.org/10.1016/j.schres.2018.12.027

Kantrowitz, J. T., Butler, P. D., Schecter, I., Silipo, G., & Javitt, D. C. (2009). Seeing the World Dimly: The Impact of Early Visual Deficits on Visual Experience in Schizophrenia. *Schizophrenia Bulletin*, *35*(6), 1085–1094. https://doi.org/10.1093/schbul/sbp100

Keane, B. P., Silverstein, S. M., Wang, Y., & Papathomas, T. V. (2013). Reduced depth inversion illusions in schizophrenia are state-specific and occur for multiple object types and viewing conditions. *Journal of Abnormal Psychology*, *122*(2), 506–512. https://doi.org/10.1037/a0032110

Kelly, S., Jahanshad, N., Zalesky, A., Kochunov, P., Agartz, I., Alloza, C., Andreassen, O. A., Arango, C., Banaj, N., Bouix, S., Bousman, C. A., Brouwer, R. M., Bruggemann, J., Bustillo, J., Cahn, W., Calhoun, V., Cannon, D., Carr, V., Catts, S., … Donohoe, G. (2018). Widespread white matter microstructural differences in schizophrenia across 4322 individuals: Results from the ENIGMA Schizophrenia DTI Working Group. *Molecular Psychiatry*, *23*(5), 1261–1269. https://doi.org/10.1038/mp.2017.170

Khanna, A., Pascual-Leone, A., & Farzan, F. (2014). Reliability of Resting-State Microstate Features in Electroencephalography. *PLoS ONE*, *9*(12), e114163. https://doi.org/10.1371/journal.pone.0114163

King, D. J., Hodgekins, J., Chouinard, P. A., Chouinard, V.-A., & Sperandio, I. (2017). A review of abnormalities in the perception of visual illusions in schizophrenia. *Psychonomic Bulletin & Review*, *24*(3), 734–751. https://doi.org/10.3758/s13423-016-1168-5

Kondacs, A., & Szabó, M. (1999). Long-term intra-individual variability of the background EEG in normals. *Clinical Neurophysiology*, *110*(10), 1708–1716. https://doi.org/10.1016/S1388-2457(99)00122-4

Koo, T. K., & Li, M. Y. (2016). A Guideline of Selecting and Reporting Intraclass Correlation Coefficients for Reliability Research. *Journal of Chiropractic Medicine*, *15*(2), 155–163. https://doi.org/10.1016/j.jcm.2016.02.012

Lhotka, M., Ischebeck, A., Helmlinger, B., & Zaretskaya, N. (2023). No common factor for illusory percepts, but a link between pareidolia and delusion tendency: A test of predictive coding theory. *Frontiers in Psychology*, *13*, 1067985. https://doi.org/10.3389/fpsyg.2022.1067985

Mesholam-Gately, R. I., Giuliano, A. J., Goff, K. P., Faraone, S. V., & Seidman, L. J. (2009). Neurocognition in first-episode schizophrenia: A meta-analytic review. *Neuropsychology*, *23*(3), 315–336. https://doi.org/10.1037/a0014708

Meyer-Lindenberg, A., Poline, J.-B., Kohn, P. D., Holt, J. L., Egan, M. F., Weinberger, D. R., & Berman, K. F. (2001). Evidence for Abnormal Cortical Functional Connectivity During Working Memory in Schizophrenia. *American Journal of Psychiatry*, *158*(11), 1809–1817. https://doi.org/10.1176/appi.ajp.158.11.1809

Miller, G. A., & Chapman, J. P. (2001). Misunderstanding analysis of covariance. *Journal of Abnormal Psychology*, *110*(1), 40–48. https://doi.org/10.1037/0021-843X.110.1.40

Nebe, S., Reutter, M., Baker, D. H., Bölte, J., Domes, G., Gamer, M., Gärtner, A., Gießing, C., Gurr, C., Hilger, K., Jawinski, P., Kulke, L., Lischke, A., Markett, S., Meier, M., Merz, C. J., Popov, T., Puhlmann, L. M., Quintana, D. S., … Feld, G. B. (2023). Enhancing precision in human neuroscience. *eLife*, *12*, e85980. https://doi.org/10.7554/eLife.85980

Nielsen, R. E., Levander, S., Kjaersdam Telléus, G., Jensen, S. O. W., Østergaard Christensen, T., & Leucht, S. (2015). Second-generation antipsychotic effect on cognition in patients with schizophrenia-a meta-analysis of randomized clinical trials. *Acta Psychiatrica Scandinavica*, *131*(3), 185–196. https://doi.org/10.1111/acps.12374

Nikulin, V. V., & Brismar, T. (2004). Long-range temporal correlations in alpha and beta oscillations: Effect of arousal level and test–retest reliability. *Clinical Neurophysiology*, *115*(8), 1896–1908. https://doi.org/10.1016/j.clinph.2004.03.019

Notredame, C.-E., Pins, D., Deneve, S., & Jardri, R. (2014). What visual illusions teach us about schizophrenia. *Frontiers in Integrative Neuroscience*, *8*. https://doi.org/10.3389/fnint.2014.00063

Pelli, D. G., & Tillman, K. A. (2008). The uncrowded window of object recognition. *Nature Neuroscience*, *11*(10), 1129–1135. https://doi.org/10.1038/nn.2187

Price, G. W., Michie, P. T., Johnston, J., Innes-Brown, H., Kent, A., Clissa, P., & Jablensky, A. V. (2006). A Multivariate Electrophysiological Endophenotype, from a Unitary Cohort, Shows Greater Research Utility than Any Single Feature in the Western Australian Family Study of Schizophrenia. *Biological Psychiatry*, *60*(1), 1–10. https://doi.org/10.1016/j.biopsych.2005.09.010

Revheim, N., Corcoran, C. M., Dias, E., Hellmann, E., Martinez, A., Butler, P. D., Lehrfeld, J. M., DiCostanzo, J., Albert, J., & Javitt, D. C. (2014). Reading Deficits in Schizophrenia and Individuals at High Clinical Risk: Relationship to Sensory Function, Course of Illness, and Psychosocial Outcome. *American Journal of Psychiatry*, *171*(9), 949–959. https://doi.org/10.1176/appi.ajp.2014.13091196

Ripke, S., Neale, B. M., Corvin, A., Walters, J. T. R., Farh, K.-H., Holmans, P. A., Lee, P., Bulik-Sullivan, B., Collier, D. A., Huang, H., Pers, T. H., Agartz, I., Agerbo, E., Albus, M., Alexander, M., Amin, F., Bacanu, S. A., Begemann, M., Belliveau Jr, R. A., … Psychosis Endophenotypes International Consortium. (2014). Biological insights from 108 schizophrenia-associated genetic loci. *Nature*, *511*(7510), Article 7510. https://doi.org/10.1038/nature13595

Robol, V., Tibber, M. S., Anderson, E. J., Bobin, T., Carlin, P., Shergill, S. S., & Dakin, S. C. (2013). Reduced Crowding and Poor Contour Detection in Schizophrenia Are Consistent with Weak Surround Inhibition. *PLoS ONE*, *8*(4), e60951. https://doi.org/10.1371/journal.pone.0060951

Roinishvili, M., Cappe, C., Shaqiri, A., Brand, A., Rürup, L., Chkonia, E., & Herzog, M. H. (2015). Crowding, grouping, and gain control in schizophrenia. *Psychiatry Research*, *226*(2–3), 441–445. https://doi.org/10.1016/j.psychres.2015.01.009

Rolls, E. T., Deco, G., Huang, C.-C., & Feng, J. (2023). Multiple cortical visual streams in humans. *Cerebral Cortex*, *33*(7), 3319–3349. https://doi.org/10.1093/cercor/bhac276

Salazar De Pablo, G., Radua, J., Pereira, J., Bonoldi, I., Arienti, V., Besana, F., Soardo, L., Cabras, A., Fortea, L., Catalan, A., Vaquerizo-Serrano, J., Coronelli, F., Kaur, S., Da Silva, J., Shin, J. I., Solmi, M., Brondino, N., Politi, P., McGuire, P., & Fusar-Poli, P. (2021). Probability of Transition to Psychosis in Individuals at Clinical High Risk: An Updated Meta-analysis. *JAMA Psychiatry*, *78*(9), 970. https://doi.org/10.1001/jamapsychiatry.2021.0830

Sanders, L. L. O., De Millas, W., Heinz, A., Kathmann, N., & Sterzer, P. (2013). Apparent motion perception in patients with paranoid schizophrenia. *European Archives of Psychiatry and Clinical Neuroscience*, *263*(3), 233–239. https://doi.org/10.1007/s00406-012-0344-5

Schütze, C., Bongard, I., Marbach, S., Brand, A., & Herzog, M. H. (2007). Collinear contextual suppression in schizophrenic patients. *Psychiatry Research*, *150*(3), 237–243. https://doi.org/10.1016/j.psychres.2006.03.021

Seidman, L. J., Hellemann, G., Nuechterlein, K. H., Greenwood, T. A., Braff, D. L., Cadenhead, K. S., Calkins, M. E., Freedman, R., Gur, R. E., Gur, R. C., Lazzeroni, L. C., Light, G. A., Olincy, A., Radant, A. D., Siever, L. J., Silverman, J. M., Sprock, J., Stone, W. S., Sugar, C., … Green, M. F. (2015). Factor structure and heritability of endophenotypes in schizophrenia: Findings from the Consortium on the Genetics of Schizophrenia (COGS-1). *Schizophrenia Research*, *163*(1–3), 73–79. https://doi.org/10.1016/j.schres.2015.01.027

Seymour, K., Stein, T., Sanders, L. L. O., Guggenmos, M., Theophil, I., & Sterzer, P. (2013). Altered Contextual Modulation of Primary Visual Cortex Responses in Schizophrenia. *Neuropsychopharmacology*, *38*(13), 2607–2612. https://doi.org/10.1038/npp.2013.168

Silverstein, S. M., & Keane, B. P. (2011a). Perceptual Organization Impairment in Schizophrenia and Associated Brain Mechanisms: Review of Research from 2005 to 2010. *Schizophrenia Bulletin*, *37*(4), 690–699. https://doi.org/10.1093/schbul/sbr052

Silverstein, S. M., & Keane, B. P. (2011b). Vision Science and Schizophrenia Research: Toward a Re-view of the Disorder Editors' Introduction to Special Section. *Schizophrenia Bulletin*, *37*(4), 681–689. https://doi.org/10.1093/schbul/sbr053

Silverstein, S. M., Keane, B. P., Wang, Y., Mikkilineni, D., Paterno, D., Papathomas, T. V., & Feigenson, K. (2013). Effects of short-term inpatient treatment on sensitivity to a size contrast illusion in first-episode psychosis and multiple-episode schizophrenia. *Frontiers in Psychology*, *4*. https://doi.org/10.3389/fpsyg.2013.00466

Singh, T., Poterba, T., Curtis, D., Akil, H., Al Eissa, M., Barchas, J. D., Bass, N., Bigdeli, T. B., Breen, G., Bromet, E. J., Buckley, P. F., Bunney, W. E., Bybjerg-Grauholm, J., Byerley, W. F., Chapman, S. B., Chen, W. J., Churchhouse, C., Craddock, N., Cusick, C. M., … Daly, M. J. (2022). Rare coding variants in ten genes confer substantial risk for schizophrenia. *Nature*, *604*(7906), Article 7906. https://doi.org/10.1038/s41586-022-04556-w

Sitt, J. D., King, J.-R., El Karoui, I., Rohaut, B., Faugeras, F., Gramfort, A., Cohen, L., Sigman, M., Dehaene, S., & Naccache, L. (2014). Large scale screening of neural signatures of consciousness in patients in a vegetative or minimally conscious state. *Brain*, *137*(8), 2258–2270. https://doi.org/10.1093/brain/awu141

So, H.-C., Chau, K.-L., Ao, F.-K., Mo, C.-H., & Sham, P.-C. (2019). Exploring shared genetic bases and causal relationships of schizophrenia and bipolar disorder with 28 cardiovascular and metabolic traits. *Psychological Medicine*, *49*(8), 1286–1298. https://doi.org/10.1017/S0033291718001812

St Clair, D., MacLennan, G., Beedie, S. A., Nouzová, E., Lemmon, H., Rujescu, D., Benson, P. J., McIntosh, A., & Nath, M. (2022). Eye Movement Patterns Can Distinguish Schizophrenia From the Major Affective Disorders and Healthy Control Subjects. *Schizophrenia Bulletin Open*, *3*(1), sgac032. https://doi.org/10.1093/schizbullopen/sgac032

Stephan, K. E., & Mathys, C. (2014). Computational approaches to psychiatry. *Current Opinion in Neurobiology*, *25*, 85–92. https://doi.org/10.1016/j.conb.2013.12.007

Sterzer, P., Adams, R. A., Fletcher, P., Frith, C., Lawrie, S. M., Muckli, L., Petrovic, P., Uhlhaas, P., Voss, M., & Corlett, P. R. (2018). The Predictive Coding Account of Psychosis. *Biological Psychiatry*, *84*(9), 634–643. https://doi.org/10.1016/j.biopsych.2018.05.015

Strawbridge, R. J., Johnston, K. J. A., Bailey, M. E. S., Baldassarre, D., Cullen, B., Eriksson, P., deFaire, U., Ferguson, A., Gigante, B., Giral, P., Graham, N., Hamsten, A., Humphries, S. E., Kurl, S., Lyall, D. M., Lyall, L. M., Pell, J. P., Pirro, M., Savonen, K., … Smith, D. J. (2021). The overlap of genetic susceptibility to schizophrenia and cardiometabolic disease can be used to identify metabolically different groups of individuals. *Scientific Reports*, *11*(1), 632. https://doi.org/10.1038/s41598-020-79964-x

Sullivan, P. F., Kendler, K. S., & Neale, M. C. (2003). Schizophrenia as a Complex Trait: Evidence From a Meta-analysis of Twin Studies. *Archives of General Psychiatry*, *60*(12), 1187. https://doi.org/10.1001/archpsyc.60.12.1187

Tandon, R., Nasrallah, H. A., & Keshavan, M. S. (2009). Schizophrenia, "just the facts" 4. Clinical features and conceptualization. *Schizophrenia Research*, *110*(1–3), 1–23. https://doi.org/10.1016/j.schres.2009.03.005

Thompson, W. H., Wright, J., Bissett, P. G., & Poldrack, R. A. (2020). Dataset decay and the problem of sequential analyses on open datasets. *eLife*, *9*, e53498. https://doi.org/10.7554/eLife.53498

Tibber, M. S., Anderson, E. J., Bobin, T., Antonova, E., Seabright, A., Wright, B., Carlin, P., Shergill, S. S., & Dakin, S. C. (2013). Visual Surround Suppression in Schizophrenia. *Frontiers in Psychology*, *4*. https://doi.org/10.3389/fpsyg.2013.00088

Trubetskoy, V., Pardiñas, A. F., Qi, T., Panagiotaropoulou, G., Awasthi, S., Bigdeli, T. B., Bryois, J., Chen, C.-Y., Dennison, C. A., Hall, L. S., Lam, M., Watanabe, K., Frei, O., Ge, T., Harwood, J. C., Koopmans, F., Magnusson, S., Richards, A. L., Sidorenko, J., … Van Os, J. (2022). Mapping genomic loci implicates genes and synaptic biology in schizophrenia. *Nature*, *604*(7906), 502–508. https://doi.org/10.1038/s41586-022-04434-5

Uhlhaas, P. J., Davey, C. G., Mehta, U. M., Shah, J., Torous, J., Allen, N. B., Avenevoli, S., Bella-Awusah, T., Chanen, A., Chen, E. Y. H., Correll, C. U., Do, K. Q., Fisher, H. L., Frangou, S., Hickie, I. B., Keshavan, M. S., Konrad, K., Lee, F. S., Liu, C. H., … Wood, S. J. (2023). Towards a youth mental health paradigm: A perspective and roadmap. *Molecular Psychiatry*, *28*(8), 3171–3181. https://doi.org/10.1038/s41380-023-02202-z

Uhlhaas, P. J., Phillips, W. A., Mitchell, G., & Silverstein, S. M. (2006). Perceptual grouping in disorganized schizophrenia. *Psychiatry Research*, *145*(2–3), 105–117. https://doi.org/10.1016/j.psychres.2005.10.016

Ulrich, R., & Miller, J. (2020). Questionable research practices may have little effect on replicability. *eLife*, *9*, e58237. https://doi.org/10.7554/eLife.58237

Van De Ville, D., Farouj, Y., Preti, M. G., Liégeois, R., & Amico, E. (2021). When makes you unique: Temporality of the human brain fingerprint. *Science Advances*, *7*(42), eabj0751. https://doi.org/10.1126/sciadv.abj0751

Van Erp, T. G. M., Hibar, D. P., Rasmussen, J. M., Glahn, D. C., Pearlson, G. D., Andreassen, O. A., Agartz, I., Westlye, L. T., Haukvik, U. K., Dale, A. M., Melle, I., Hartberg, C. B., Gruber, O., Kraemer, B., Zilles, D., Donohoe, G., Kelly, S., McDonald, C., Morris, D. W., … Turner, J. A. (2016). Subcortical brain volume abnormalities in 2028 individuals with schizophrenia and 2540 healthy controls via the ENIGMA consortium. *Molecular Psychiatry*, *21*(4), 547–553. https://doi.org/10.1038/mp.2015.63

Van Erp, T. G. M., Walton, E., Hibar, D. P., Schmaal, L., Jiang, W., Glahn, D. C., Pearlson, G. D., Yao, N., Fukunaga, M., Hashimoto, R., Okada, N., Yamamori, H., Bustillo, J. R., Clark, V. P., Agartz, I., Mueller, B. A., Cahn, W., De Zwarte, S. M. C., Hulshoff Pol, H. E., … Orhan, F. (2018). Cortical Brain Abnormalities in 4474 Individuals With Schizophrenia and 5098 Control Subjects via the Enhancing Neuro Imaging Genetics Through Meta Analysis (ENIGMA) Consortium. *Biological Psychiatry*, *84*(9), 644–654. https://doi.org/10.1016/j.biopsych.2018.04.023

Van Essen, D. C. (2003). Organization of Visual Areas in Macaque and Human Cerebral Cortex. In L. M. Chalupa & J. S. Werner (Eds.), *The Visual Neurosciences, 1* (pp. 507–521). The MIT Press. https://doi.org/10.7551/mitpress/7131.003.0038

Vilares, I., & Kording, K. (2011). Bayesian models: The structure of the world, uncertainty, behavior, and the brain. *Annals of the New York Academy of Sciences*, *1224*(1), 22–39. https://doi.org/10.1111/j.1749-6632.2011.05965.x

Wang, S., & De Boeck, P. (2022). Understanding the role of subpopulations and reliability in between-group studies. *Behavior Research Methods*. https://doi.org/10.3758/s13428-021-01700-8

Weilnhammer, V., Röd, L., Eckert, A.-L., Stuke, H., Heinz, A., & Sterzer, P. (2020). Psychotic Experiences in Schizophrenia and Sensitivity to Sensory Evidence. *Schizophrenia Bulletin*, *46*(4), 927–936. https://doi.org/10.1093/schbul/sbaa003

Wolff, A., Di Giovanni, D. A., Gómez-Pilar, J., Nakao, T., Huang, Z., Longtin, A., & Northoff, G. (2019). The temporal signature of self: Temporal measures of resting-state EEG predict self-consciousness. *Human Brain Mapping*, *40*(3), 789–803. https://doi.org/10.1002/hbm.24412

Zhao, Y., Zhang, Q., Shah, C., Li, Q., Sweeney, J. A., Li, F., & Gong, Q. (2022). Cortical Thickness Abnormalities at Different Stages of the Illness Course in Schizophrenia: A Systematic Review and Meta-analysis. *JAMA Psychiatry*, *79*(6), 560. https://doi.org/10.1001/jamapsychiatry.2022.0799

Curriculum vitae

Dario Gordillo – darioalejj10@gmail.com – (+41) 76 633 40 47

ORCID: 0000-0001-7038-7501

Education

2019 – 2024: Ph.D. in Neuroscience at École Polytechnique Fédérale de Lausanne (EPFL), Lausanne-Switzerland

2017 – 2018: M.Sc. in Brain and Cognition at Universitat Pompeu Fabra (UPF), Barcelona - Spain

2011 – 2016: B.Eng. in Acoustics at Universidad de las Américas (UDLA), Quito - Ecuador

Contributions to international conferences

Talks:

- The EEG multiverse of schizophrenia. Gordillo, D., da Cruz, J. R., Chkonia, E., Lin, W.-H., Favrod, O., Brand, A., Figueiredo, P., Roinishvili, M., & Herzog, M. H. *Schizophrenia International Research Society (SIRS)*, 2024
- Neural enhancement in vision. Gordillo, D., da Cruz, J. R., Favrod, O., Johnston, P. R., Figueiredo, P., & Herzog, M. H. *European Conference on Visual Perception (ECVP)*, 2023
- A solution to the ill-posed problem of common factors in vision. Gordillo., D, Cretenoud, A., Garobbio, S., & Herzog, M. H. *Vision Science Society (VSS)*, 2023
- The EEG multiverse of schizophrenia. Gordillo, D., da Cruz, J. R., Chkonia, E., Lin, W.-H., Favrod, O., Brand, A., Figueiredo, P., Roinishvili, M., & Herzog, M. H. World Congress of Psychiatry (WPA), 2022
- How do microstates relate to other neurophysiological features? Gordillo, D., da Cruz, J. R., & Herzog, M. H. *Microstates Conference*, 2022

Publications

Peer-reviewed:

- Gordillo, D.*, da Cruz, J. R.*, Chkonia, E., Lin, W.-H., Favrod, O., Brand, A., Figueiredo, P., Roinishvili, M., & Herzog, M. H. (2023). The EEG multiverse of schizophrenia. *Cerebral Cortex*, 33(7), 3816–3826. https://doi.org/10.1093/cercor/bhac309
- Gordillo, D., da Cruz, J. R., Moreno, D., Garobbio, S., & Herzog, M. H. (2023). Do we really measure what we think we are measuring? *iScience*, 26, 106017. https://doi.org/10.1016/j.isci.2023.106017

- Choung, O. H., Gordillo, D., Roinishvili, M., Brand, A., Herzog, M. H., & Chkonia, E. (2022). Intact and deficient contextual processing in schizophrenia patients. *Schizophrenia Research: Cognition*, 30, 100265. https://doi.org/10.1016/j.scog.2022.100265
- Jurado, C., Gordillo, D., & Moore, B. C. (2019). On the loudness of low-frequency sounds with fluctuating amplitudes. *The Journal of the Acoustical Society of America*, 146(2), 1142-1149. https://doi.org/10.1121/1.5121700
- Jurado, C., Gallegos, P., Gordillo, D., & Moore, B. C. (2017). The detailed shapes of equal loudness-level contours at low frequencies. *The Journal of the Acoustical Society of America*, 142(6), 3821-3832. https://doi.org/10.1121/1.5018428

Preprints:

- Alamia, A. *, Gordillo, D. *, Chkonia, E., Roinishvili, M., Cappe, C., & Herzog, M. H. (2023). Oscillatory traveling waves reveal predictive coding abnormalities in schizophrenia. *BioRxiv*, 2023.10.09.561490. https://doi.org/10.1101/2023.10.09.561490

* denotes equal contribution

Teaching activities

Teaching assistant at EPFL, Lausanne for:

- Understanding Statistics and Experimental Design
- Neurosciences III: Behavioral and cognitive neuroscience
- General Physics: Mechanics
- Physiology lab I

Student supervision:

- Master student supervisor at EPFL (3 students)
- Bachelor student supervisor at UDLA (2 students)

Reviewer for:

European Psychiatry, Journal of Neural Engineering

Skills and personal interests

Computer: Machine learning, statistics, and digital signal processing using Python, MATLAB, and R Studio. I have a strong background in data analysis for neuroimaging data using EEGLAB, Fieldtrip, and MNE

Languages: Spanish (Native), English (Fluent), French (Fluent)

Interests: Songwriting, audio editing/mixing, audio recording, music production, guitar/singing